



16732/P019910
Serial: A0-1700861
22 Mar 2017

MEMORANDUM

From: J.W. Mauger, CAPT
CG MSC

Reply to Dr. Jeffrey Stettler
Attn of: (202) 795-6783

To: J.D. Neubauer, CAPT
COMDT (CG-INV)

Subj: MSC TECHNICAL REVIEW AND ANALYSIS OF THE SS EL FARO, O.N. 561732

Ref: (a) Your memo 16732 of July 22, 2016

1. As requested in reference (a), the Marine Safety Center (MSC) completed technical reviews and analyses in support of the Marine Board of Investigation (MBI) investigating the sinking of the SS EL FARO and loss of her 33 crew members on October 1, 2015.
2. The MSC has completed the following technical reviews and analyses:
 - a. Stability: including review of intact and damage stability criteria, and assessment of the EL FARO against applicable criteria and criteria which would apply if the vessel were constructed in 2016.
 - b. Structures: including review of structures criteria, and review of documented structural assessments.
 - c. Hydrostatic sinking analyses of the accident voyage: including review of wind heel and flooding effects, potential downflooding through multiple feasible paths, and combined effects of wind, seas, and flooding on hydrostatics and stability.
3. The results of the requested reviews and analyses are provided in a stand-alone MSC technical report, which is included as the enclosure to this memorandum.
4. If you have any questions or need additional information, please contact Dr. Jeffrey Stettler.

#

Enclosure: MSC Technical Report: SS EL FARO Stability and Structures

**U.S. Coast Guard
Marine Safety Center**



Technical Report

**SS EL FARO
Stability and Structures**

March 22, 2017

Table of Contents

Executive Summary	3
Introduction	4
MSC Computer Model	8
Stability Test and Uncertainty Analysis	19
Trim and Stability Booklet (T&S Booklet) and Stability Software	25
Intact and Damage Stability	32
Hydrostatic Sinking Analyses	56
Ship Structures	90
Conclusions	97
References	102
Appendix A: Uncertainty Analysis of the Stability Test and Departure Condition	106
Appendix B: SOLAS Probabilistic Damage Stability Analysis	135

Executive Summary

This report documents technical reviews of the stability and structures of the SS EL FARO completed by the Marine Safety Center (MSC), as requested by the Marine Board of Investigation (MBI) in support of the investigation into the sinking of the EL FARO and loss of her 33 crew members on October 1, 2015. The report also documents forensic hydrostatic sinking analyses conducted to assess likely contributing factors to the sinking. To aid in the accomplishment of the reviews and analyses, the MSC independently generated a detailed computer model, and used this model for analyses of vessel hydrostatics, stability and strength.

Based on review of the available technical documents and independent analyses, the MSC determined that the vessel met applicable intact and damage stability and structural strength requirements, as loaded for the accident voyage which departed Jacksonville on September 29, 2015. However, it is noted that the vessel was operated very close to the maximum load line drafts, with minimal stability margin compared to the required metacentric height (GM), and with limited available freeboard and ballast capacity, leaving little flexibility for improving stability at sea if necessary due to heavy weather or flooding.

The hydrostatic sinking analyses were based on first-principles, focusing on the righting arms, including righting energy and range of stability considerations, with effects of wind heel and free surface due to the floodwater in the cargo holds included. The results were highly sensitive to estimated cargo hold permeability. The results were also highly sensitive to variation in wind speed, especially in combination with floodwater free surface and permeability. Single-compartment flooding of Hold 3 with combined wind heel due to 70-90 knot beam winds resulted in very small residual righting arms and little residual righting energy (area under the righting arm curve). This would suggest that it would be highly unlikely that the EL FARO could have survived even single compartment flooding of Hold 3, given the sea conditions with estimated 70-90 knot winds and 25-30 foot seas. Potential sources of flooding of Hold 3 and the other cargo holds were also investigated, including vulnerabilities associated with the cargo hold ventilation system openings and the emergency fire pump piping in Hold 3. Given the sea conditions and reported initial flooding through the Hold 3 scuttle, the ventilation openings would have allowed at least intermittent flooding into the cargo holds, as the vessel was subject to variable wave height on the side shell and rolled about an estimated mean heel angle of approximately 15 degrees.

As requested by the MBI, the MSC also compared the stability of the EL FARO against criteria which would apply if the vessel were constructed in 2016. In this case, the EL FARO would be required to meet minimum righting arm criteria of Part A of the International Code on Intact Stability (2008 IS Code). Based on the MSC analyses, the EL FARO, as operated and loaded for the accident voyage, would not meet the righting arm criteria of Part A of the 2008 IS Code. Additionally, the EL FARO would have been required to meet probabilistic damage stability standards of SOLAS 2009. Based on the MSC analyses, the EL FARO, as operated and loaded for the accident voyage, would not meet the SOLAS 2009 damage stability standards. In order for the EL FARO to meet the current intact and damage stability standards at the full load draft, the minimum required GM would be in the range of 5.8-6.8 feet, which is 1.5-2.5 feet greater than the GM of the actual departure loading condition of the accident voyage.

1. Introduction

1.1. Background

Reference [1] is the memorandum from the President of the Marine Board of Investigation (MBI) to the Commanding Officer of the Marine Safety Center (MSC), requesting technical assistance in support of the investigation of the sinking of the SS EL FARO (EL FARO) and loss of her 33 crew members. The memorandum requested that the MSC complete the following reviews and analyses to support the MBI:

- (1) Stability review and analysis of the EL FARO including the following primary elements:
 - a. Summary of stability criteria, including criteria applicable to the EL FARO at the time of the casualty, and criteria which would apply if the vessel were constructed or underwent a major conversion in 2016.
 - b. Review of the EL FARO inclining experiment and Stability Test Report, including calculation of an engineering estimate of the uncertainty in the vessel's KG for the lightship condition and for the accident voyage departure condition.
 - c. Review of the EL FARO Trim and Stability Booklet (T&S Booklet).
 - d. Review of the EL FARO CargoMax stability and loading software application, and the vessel operator usage as a supplement to the T&S Booklet for load planning and stability evaluation.
 - e. Review and assessment of the intact and damage stability for the accident voyage, based on the documented departure loading condition.
- (2) Structures review of the EL FARO including the following primary elements:
 - a. Summary of applicable structures criteria, whether based on class or other requirements.
 - b. Review of the documented structural assessments completed on behalf of the vessel owners and approved by the American Bureau of Shipping (ABS), including assessments for the 1992-1993 vessel lengthening, 2005-2006 deck container (LO/LO) conversion, 2007-2009 scantling and allowable bending moment reassessments, and the post-accident hull girder section modulus and buckling analysis completed by ABS in 2015.
 - c. Review of the EL FARO CargoMax stability and loading software application and vessel operator usage for hull girder strength assessment.
- (3) Hydrostatic sinking analyses for the accident voyage of the EL FARO, incorporating the following considerations:

- a. The vessel in a “dead-ship” condition (i.e. after loss of propulsion).
- b. An estimated fuel burn-off at the time of the loss of propulsion.
- c. Wind heel resulting from estimated category 3 hurricane wind speeds and gusts (modeled meteorological wind spectra provided).
- d. Down-flooding through multiple feasible paths, including ventilation intake and exhaust openings, and cargo hold access scuttle openings.
- e. Individual compartment and combined/progressive flooding through down-flooding points, considering a range of estimated cargo hold permeability values.
- f. Additional heeling moments due to potential cargo shifts of roll-on/roll-off (RO/RO) and above deck container lift-on/lift-off (LO/LO) cargo, and entrapped water on the 2nd deck.
- g. Feasibility of the installed bilge pumping system keeping up with flooding through ventilation openings or other down-flooding points.

It was also requested that the MSC reviews and analyses be documented in a stand-alone MSC report suitable for inclusion as an appendix of the formal Report of Investigation (ROI).

1.2. Approach

To provide the desired reviews and analyses, MSC has reviewed hundreds of technical documents including drawings, calculations, procedures, etc. provided by the MBI. MSC has also reviewed MBI hearing transcripts and exhibits, as well as the voyage data recorder (VDR) audio transcript. Based on the available documentation, MSC has completed the requested independent reviews and a series of independent technical analyses where appropriate, and as requested. To aid in the accomplishment of the reviews and analyses, MSC independently generated a detailed computer model for analysis of vessel hydrostatics, stability and strength.

Section 2 provides an overview of the development of the MSC computer model. Additionally comparisons of hydrostatics properties and tank properties are made between the MSC computer model and the T&S Booklet and the CargoMax loading software application.

Section 3 documents the MSC review of the 2006 stability test (inclining experiment), and provides a summary of the requested uncertainty analysis of the lightship KG (height of the center of gravity) and the GM (metacentric height) for the accident voyage departure condition derived from the stability test. The uncertainty analysis is documented in detail in Appendix A.

Section 4 documents the MSC review of the T&S Booklet and of the CargoMax stability and loading software used onboard the EL FARO and by shore-side personnel for cargo load planning and stability assessment.

Section 5 provides a primer on basic ship stability and provides a detailed summary of the intact and damage stability criteria applicable to the EL FARO at the time of the casualty, and criteria which would apply if the vessel were constructed in 2016. The MSC computer model was used to conduct an intact stability assessment of eight “benchmark” loading conditions, including departure and arrival conditions from the 1993 and 2007 T&S Booklets, a representative departure and arrival condition from August 2015, and the accident voyage departure condition and estimated condition at the time of loss of propulsion on October 1, 2015. Damage stability criteria and application are discussed and the EL FARO is assessed in comparison to applicable damage stability criteria, with detailed results provided in Appendix B.

Section 6 documents the MSC hydrostatic analyses of the sinking of the EL FARO. The hydrostatic analyses use the MSC computer model, focusing on assessment of righting arms including righting energy and range of stability considerations, in order to gain insight into the characteristics of vessel dynamics and motions due to wind heel and flooding. The effects of wind heel are addressed in detail, along with general and nuanced considerations associated with floodwater, including effects of free surface, compartment permeability, and pocketing. The potential sources of flooding of Hold 3 are discussed, using annotated photographs and drawings for reference. Analyses of an array of wind heel and flooding conditions are used to assess likely conditions leading to the capsizing and sinking of the vessel given the estimated environmental conditions, and based on insight gained through review of the VDR audio transcript.

Section 7 documents the MSC review of the ship structures, and includes a summary of the applicable structures criteria and review of documented structural assessments completed and approved by ABS. This section also provides a summary of the CargoMax usage for hull girder strength assessment.

Section 8 provides conclusions based on the reviews and analyses.

Section 9 is a listing of references, including publicly available documents as well as MBI hearing exhibits.

Appendix A provides the detailed procedure and results for the requested uncertainty analysis of the vessel’s lightship KG and GM for the accident voyage departure condition. A separate listing of references for the uncertainty analysis is provided, including publicly available documents and MBI hearing exhibits.

Appendix B provides detailed documentation of the SOLAS damage stability analysis of the EL FARO completed using the MSC GHS computer model.

1.3. Nomenclature

A listing of nomenclature used throughout the report, including abbreviations, symbols and acronyms, is provided in Table 1-1. The listing is presented alphabetically, with special symbols given at the end. For nomenclature with multiple uses or meanings, commas separate different uses.

A	Area (wind heel), area under righting arm curve	LCF	Longitudinal position of center of flotation
A	Attained index	LCG	Longitudinal position of center of gravity
a	Distance moved	LO	Lube oil (tank)
ABS	American Bureau of Shipping	LO/LO	Lift-On/Lift-Off (containers)
AP	Aft perpendicular (plane)	LT	Long ton (2,240 pounds)
ASTM	American Society for Testing and Materials	LWL	Length on the waterline
b	Intercept (linear fit)	m	Slope (linear fit)
B	Beam, center of buoyancy	M	Metacenter, bending moment
BL	Baseline (plane)	MARAD	Maritime Administration
BM	Metacentric radius	MS	Midship section (plane)
B _m	Breadth (beam at half draft)	MSC	Marine Safety Center
C	Form factor (stability), drag coefficient (wind heel)	MT1"	Moment to trim one inch
CAD	Computer Aided Design (software)	N	Number of measurement data points
C _B	Block coefficient	P	Wind pressure, port side
C _D	Coefficient of discharge (flooding)	p _i	Probability of flooding compartment i
CFR	Code of Federal Regulations	Q	Flow rate
CL	Centerline (plane)	R	Required index
CON/RO	Container / Roll On / Roll Off	ROI	Report of Investigation
Cons	Consumables (fuel, lube, fresh water)	RO/RO	Roll-On/Roll-Off (trailers, automobiles)
C _w	Waterplane coefficient	S	Starboard side, standard error
D	Depth	s _i	Probability of sinking with flooding compartment i
d	Draft (mean)	SM	Section modulus
D'	Molded depth (corrected)	SOLAS	Safety of Life at Sea (conventions)
DB	Double bottom (tank)	SVR	Steel Vessel Rules (ABS)
DT	Deep tank	T	Limiting angle (stability), roll period
F _B	Force of buoyancy	T&S	Trim and Stability (Booklet)
FO	Fuel oil (tank)	TCG	Transverse position of center of gravity
FP	Forward perpendicular (plane)	TPI	Tons per inch immersion
g	Acceleration due to gravity	U	Uncertainty
G, g	Center of gravity (ship, component)	Û	Relative (%) uncertainty
GHS	General Hydrostatics (software)	V	Volume, wind velocity
GM	Metacentric height	VCB	Vertical (height) position of center of buoyancy
GZ	Righting arm	VCG	Vertical (height) position of center of gravity (KG)
H	Arm (wind heel), hydrostatic head (height)	VDR	Voyage Data Recorder
HA	Heeling arm	W, w	Weight (ship, component)
HM	Heeling moment	WL	Waterline
IACS	International Association of Classification Societies	x,y	Independent, dependent variable
IMO	International Maritime Organization	φ	Angle of heel (same as θ)
KG	Vertical (height) position of center of gravity (VCG)	θ	Angle of heel (same as φ)
KMt	Height of the metacenter	Δ	Displacement (weight of ship)
l	Wind heeling arm (lever)	∇	Displacement volume
LBP	Length between perpendiculars	ρ	Density of water, density of air
LCB	Longitudinal position of center of buoyancy	γ	Specific weight (γ = ρg)

Table 1-1: Nomenclature.

2. MSC Computer Model

2.1. Introduction

In order to assess the hydrostatics and stability of the EL FARO, a detailed 3-dimensional computer model of the vessel was created for use with the MSC's analysis software GHS (General HydroStatics by Creative Systems, Inc.). All modeling and analyses were completed using GHS Version 15.00. No attempt was made to thoroughly investigate how the results of analyses using Version 15.00 would compare to analyses using prior versions of GHS (other than as documented in Section 5.3.3). This section describes the development of the MSC GHS computer model for use in subsequent stability analyses and hydrostatic sinking analyses.

2.2. Development of the MSC Computer Model

An original computer model was provided by Herbert-ABS Software Solutions, LLC, created using their software HECSALV, file "Faro-10.shp" [2]. The HECSALV model file was provided along with the Final Offsets document [3] and General Arrangement Drawing [4]. Initially the HECSALV model was converted into a format compatible with the GHS software, and MSC verified that the hull stations and offsets (lines) contained in the HECSALV model accurately reflected the table of offsets in the Final Offsets document. MSC found that the HECSALV model accurately reflected the table of offsets at the stations contained in the model (see Figure 2-1), but some detail was not reflected due to the selected station spacing (particularly in the bow, stern and skeg areas), which might affect the accuracy of the calculated areas and volumes in those areas. Additionally, the HECSALV model only extended to the 2nd (bulkhead) deck, which was the freeboard or watertight deck. The MSC GHS computer model extends to the main deck to include modeling of the semi-enclosed spaces above the 2nd deck. Finally, it was noted that the hull model, when imported into Rhinoceros CAD (Rhino) software and converted to a surface model, showed that with the given lines, the hull was not fair in a number of areas when rendered. This was manifested by a number of obvious visual "dents" in the rendered hull surface when viewed in Rhino. Upon further investigation, it was determined that the table of offsets in the Final Offsets document contained a number of apparent errors (perhaps due to manual errors in measuring dimensions from the original drafted lines or writing the offset numbers into the ledger, which we might now call "typographical errors"). These apparent errors in the table of offsets manifested themselves as irregularities in the surface of the hull model, and only became apparent when the model was converted and viewed in the Rhino program viewer. Rhino was used to view the model in three different ways: (1) as a series of stations, (2) as a mesh connecting stations and offset points, and (3) as a series of NURBS (Non-Uniform Rational B-Spline) surfaces created from the existing mesh nodes. In the mesh and NURBS views the irregularities in the hull surface were most apparent. It should be noted that overall these irregularities are relatively small and result in only small differences in calculated results, as will be demonstrated subsequently.

For the MSC GHS computer model, it was decided to develop a faired hull model in the Rhino software that was consistent with the Final Offsets document including the table of offsets, but also contained necessary fairing to correct for the discovered errors in the table of offsets. It was decided that this would likely better represent the "as-built" hull surface, since during the lofting

and construction process, some fairing would have taken place to provide a smooth hull surface. To begin, the original HECSALV model consisting of 28 stations (Figure 2-1) was converted to a standard CAD Drawing Exchange Format (DXF), which was imported into Rhino for further refinement. The imported 28 stations were supplemented with details from the Final Offsets document including centerline deck heights with sheer, deck camber, midship section geometry, stem profile and radii, transom profile, house deck heights, and frame locations. With these details as reference, the series of NURBS surfaces was created, and then faired.

Once the fairing was completed in Rhino (Figure 2-2), the hull model was converted into a GHS format with a larger number of stations for higher definition such that internal tanks and compartments to be added would be created with desired accuracy. To ensure accurate numerical integration with the trapezoidal integration method used in the GHS software, MSC defined both hull and compartment stations at relatively close spacing of 2-3 feet. Figure 2-3 shows the final hull lines. Note that a separate set of lines was created for the semi-enclosed 2nd Deck so that a separate compartment external to the main watertight hull could be created to allow free flood or partial flooding as desired in the hydrostatic sinking analyses, and the wind profile area could be calculated directly by the GHS software in the analyses (see Figure 2-5 and Figure 5-5). Additional hull components were added with separate sets of lines to provide accurate definition and volumes for the keel skeg, rudder, and shafting as shown, and external components were appended to the upper hull to incorporate the external volumes of the forward and aft cargo ramps and boiler casing, as shown in Figure 2-4. A shell plating thickness of 0.8 inches was added to account for an average hull plating thickness taken from the Midship Construction Drawing [5] and Shell Expansion Plans [6, 7, 8].

Once the hull model was complete, the internal tanks and compartments were modeled including definition of decks and bulkheads making up tank and compartment boundaries. Transverse bulkheads and boundaries were based on frame locations provided in the Final Offsets document. Deck heights were defined based on the Final Offsets document, including the required deck sheer (note that the Main Deck and 2nd Deck included sheer and camber and both were included in the hull model). Longitudinal bulkheads and boundaries were defined based on a number of references including the Final Offsets document, General Arrangement Drawing, Midships Construction Drawing, and Combined Bulkhead drawing [9]. For simplicity and since it is only required for wind heel area calculations, a simple deckhouse was added external to the main hull with boundaries based on the Final Offsets document and General Arrangement Drawing. Similarly, containers were added for wind heel area calculations as “sail” components in GHS, with boundaries based on the Final Offsets document, Capacity Plan [10] and the CargoMax loading computer printout for the accident voyage [11]. Figure 2-5 shows inboard profile and plan views of the MSC GHS computer model showing decks, bulkheads, compartments, tanks, deck house, and the container profile for the accident voyage.

It was noticed in the course of creating the decks and compartment boundaries that the deck heights measured from the General Arrangement Drawing [4] were significantly different compared to the Final Offsets document [3], Midship Construction Plan [5], and other structural drawings. This led MSC to conclude that there were vertical scaling errors on the General Arrangement Drawing. It appears that the errors may be associated with typographical errors instead of a constant vertical scaling factor error, as the midships deck heights fall precisely on

whole or half feet, as shown in Table 2-1. This is considered notable since the General Arrangement Drawing is an engineering drawing and as such should be correctly scaled, and in fact the drawing states a 1/16" = 1'-0" scale in the title block. Due to the noted errors, vertical dimensions were not taken from the General Arrangement Drawing for the MSC GHS computer model development. The errors in deck heights on the General Arrangement Drawing may provide an explanation for the freeboard reference discrepancies noted by the test engineers in the 2006 Stability Test Report (see Section 3 of this report).

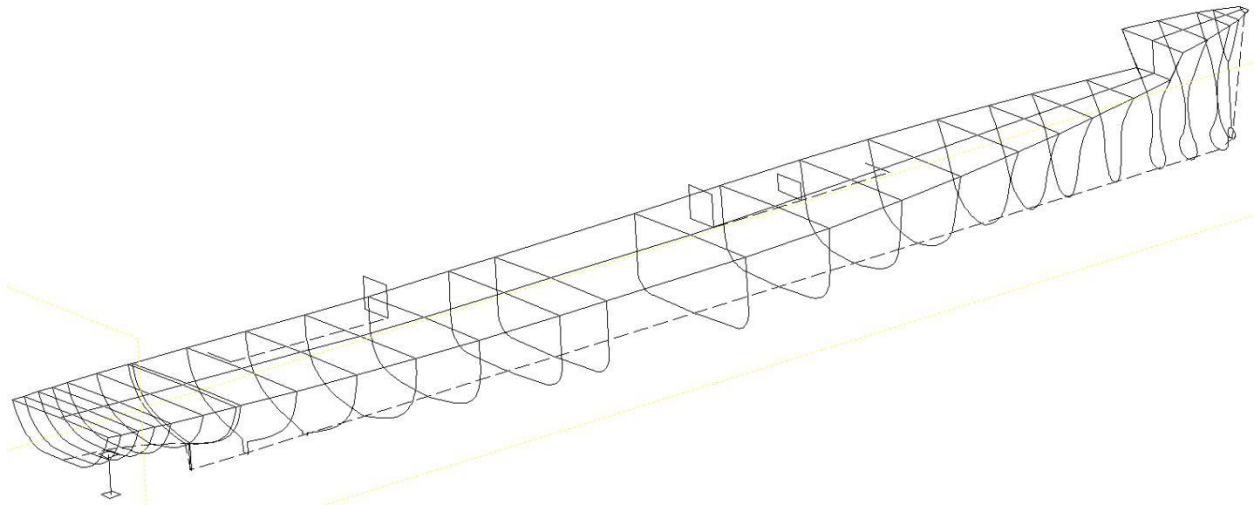


Figure 2-1: Original HECSALV computer model hull stations.

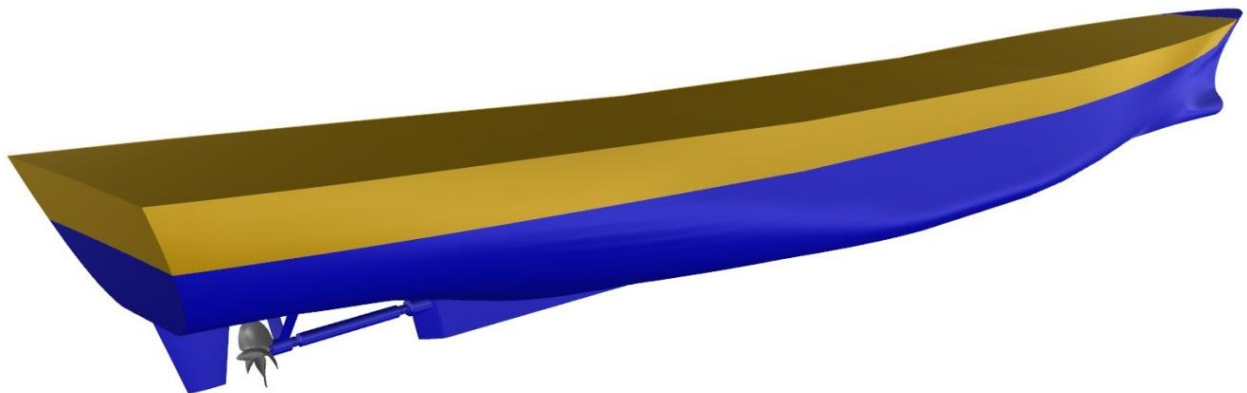


Figure 2-2: The MSC Rhino CAD surface hull model, including semi-enclosed 2nd deck.

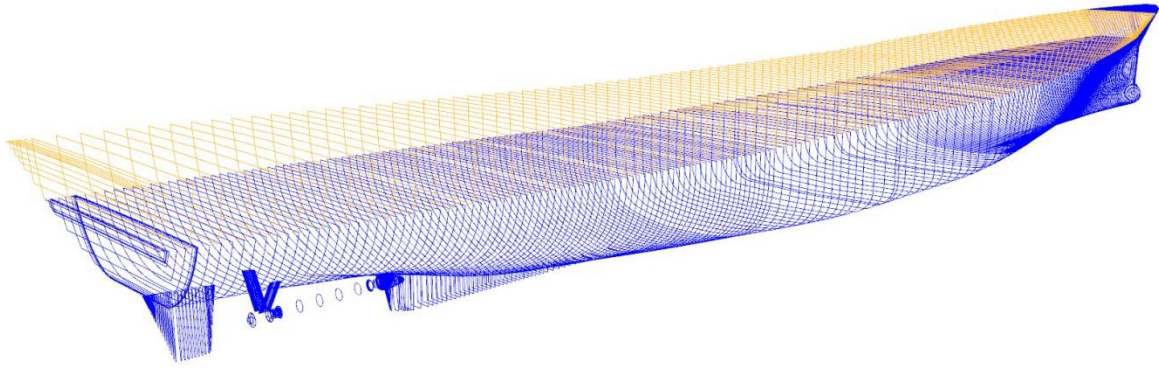


Figure 2-3: Hull stations and lines generated from the Rhino CAD surface hull model, with included lines for keel skeg, rudder and shafting, also including the semi-enclosed 2nd deck.

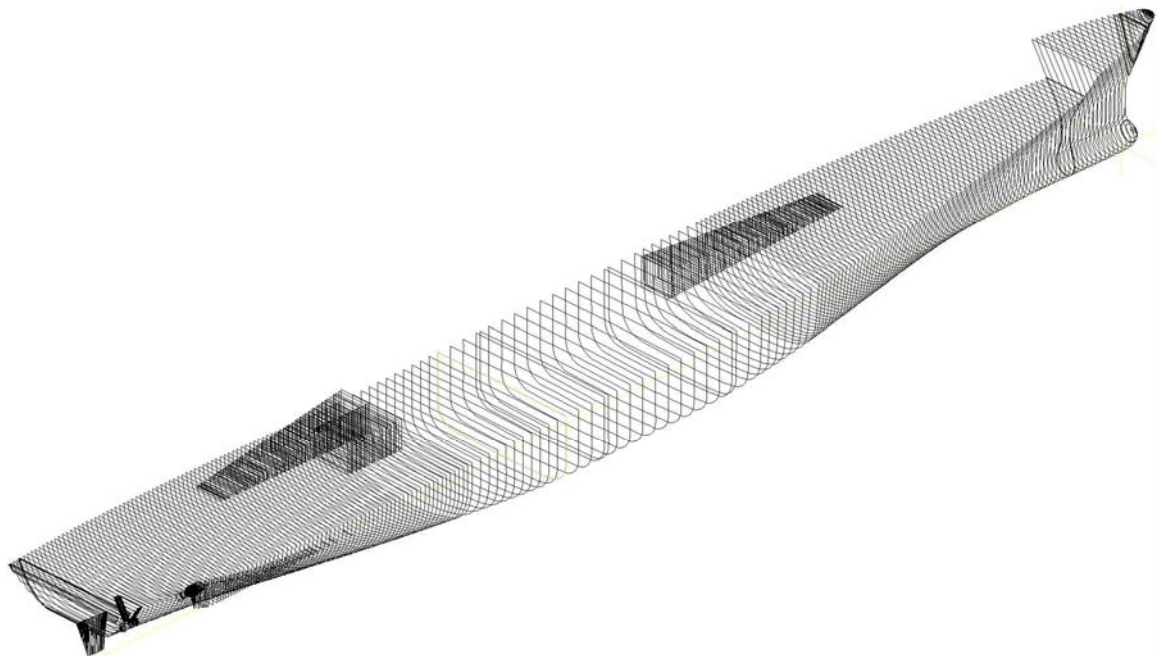


Figure 2-4: Hull stations and lines of the MSC GHS computer model, including appended forward and aft cargo ramps and boiler casing, not including the semi-enclosed 2nd deck.

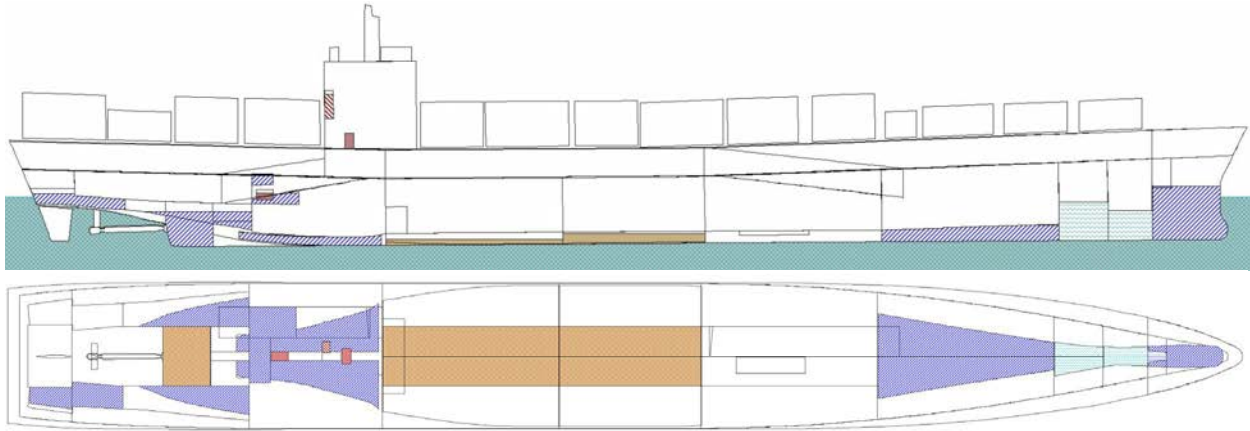


Figure 2-5: Inboard profile and plan views of the MSC GHS computer model showing decks, bulkheads, compartments, tanks, deck house, and the container profile for the accident voyage. Tanks are shown as loaded for the accident voyage.

	Final Offsets (Lines Drawing), Structural Drawings	General Arrangement Drawing
	feet above baseline	
Midships 4 th Deck (Inner Bottom)	7.50	8.00
Midships 3 rd Deck	24.14	24.50
Midships 2 nd Deck @ CL	42.64	43.50
Midships Main Deck @ CL	60.64	62.00
Transom Main Deck @ CL	67.98	70.50
Transom 2 nd Deck @ CL	49.75	50.85
Stem Main Deck @ CL	71.32	72.63
Length Between Perpendiculars (feet)	733.75	733.50
Beam, Molded (feet)	92.00	92.00
Beam, Maximum at Main Deck (feet)	105.00	105.00

Table 2-1: Comparison of deck heights and principal dimensions provided on different reference drawings.

2.3. Comparison with the T&S Booklet and CargoMax Stability Software

Table 2-2 provides key hydrostatic parameters at a nominal full load departure draft of 30.0 feet in salt water without trim or hull deflection, calculated using the MSC GHS computer model. For comparison, the values in the T&S Booklet [12] are also provided. Note that the hydrostatic tables used in the CargoMax stability software are the same as those in the T&S Booklet. Also included in the table are the calculated difference and percent difference for each parameter, using the MSC GHS computer model as the basis. To compare each to an objective quality standard, the last column provides the acceptance tolerance based on IMO MSC.1/Circ.1229, Guidelines for the Approval of Stability Instruments [13], which are identical to those in the IACS Unified Requirement L5 applied by class societies [14].

As mentioned previously, the MSC GHS computer model includes refined hull shape in the bow, stern and skeg areas. Because of the increased definition, the integrated section areas and calculated volumes are slightly greater in these areas compared to the hydrostatic table and tank tables provided in the T&S Booklet. The largest impact of this is on the moment to trim 1-inch (MT1”). For displacement the differences are relatively small, and only amount to a total difference of about 0.1% at the draft of 30.0 feet as shown in Table 2-2, but the difference increases to approximately 1% at the draft corresponding to the lightship displacement.

	MSC GHS Computer Model	T&S Booklet and CargoMax	Difference	Difference %	IMO/IACS Tolerance
Displacement (LT)	34,334	34,380	46	0.1%	2%
LCB (ft-FP)	391.2	391.2	0.0	0.0%	1% or 1.64 ft
VCB (ft-BL)	16.72	NA	NA	NA	1% or 0.164 ft
LCF (ft-FP)	427	426.6	0.4	0.1%	1% or 1.64 ft
MT1” (ft·LT/in)	5,346	5,259	87.0	1.6%	2%
KMt (ft-BL)	41.40	41.51	0.11	0.3%	1% or 0.164 ft
TPI (LT/in)	124.6	124.5	0.1	0.1%	NA

Table 2-2: Comparison of key hydrostatic properties at a nominal full load keel draft of 30.0 feet in salt water, without trim or hull deflection. Note that values for VCB are not provided in the hydrostatic table in the T&S Booklet or in CargoMax. Also included are the calculated differences and tolerances based on the IMO and IACS guidelines.

Table 2-3 provides comparison between calculated tank properties, including 100% volume and center of gravity, and maximum (slack) free surface inertia. Also included in the table are the calculated differences and tolerances based on the IMO and IACS guidelines.

The following specific comments are provided:

- (1) Tank volume and center of gravity calculations are based on an assumed “permeability” factor, which mathematically accounts for the fraction of the tank volume that can be filled with liquid, accounting for such things as internal structure, piping, and other internal components. The precise permeability factors assumed in the original calculation of the tank volumes and centers are not available in the documentation. However, for comparison, by reviewing the original HECSALV model, the permeability factors provided in the table were incorporated. The MSC GHS computer model used the same permeability factors where appropriate; however it was noted that the HECSALV model inconsistently applied permeability factors of 0.95 and 0.98 for the double bottom tanks. Based on MSC review of EL FARO structural drawings associated with the double bottom tanks [15, 16], double bottom tanks have internal transverse floor structure which would reduce the volume available for liquid. Based on this review, the MSC GHS computer model includes the consistent 0.95 permeability factor for all double bottom tanks between frames 46 and 169, as reflected in the table.

- (2) A comparison of tank volumes of the MSC GHS computer model with the T&S Booklet and CargoMax (Table 2-3) shows a large number of tanks with differences in excess of the 2% tolerance of MSC Circ. 1229 and IACS UR L5. A total of 19 tanks are in excess of the 2% tolerance. Of these 19 tanks, 8 are either small tanks (less than 2,000 ft³), are very close to the 2% tolerance, or have different assumed permeabilities. The set of tanks which stand out most is DT Aft P/S, with the T&S Booklet and CargoMax values being 20% higher than the MSC GHS computer model. These tanks are relatively simple geometrically and the difference in calculated volumes does not appear to be explainable based on difference in the station spacing and location or differences in integration techniques used. Further review of previous T&S Booklets including the 1993 T&S Booklet [17] and older T&S Booklets for sister vessels dating back to the 1970s reveals that the higher volume value of 11,286 ft³ came from the original integration of the tank volumes, probably done by hand back in the 1960s or 1970s. Based on calculation with both the MSC GHS computer model and the HECSALV model “Faro-10.shp” [2], it appears that the original volume calculation was in error. While the differences with DT Aft P/S are the most significant, similar differences are also noted with tanks DB 4 P/S and Aft Peak P/S, which are not explainable based on differences in station location and spacing, integration methods, or assumed permeability.
- (3) Transverse locations of centers of gravity (TCG) are not included in the T&S Booklet. As was common with stability booklets until recent years, the calculations contained in the sample load cases and calculation forms in the T&S Booklet account for vertical and longitudinal locations of the centers of gravity but do not account for transverse locations. This means that calculations performed in accordance with the T&S Booklet do not include static heeling effects and do not calculate static list angle. The CargoMax stability software does include transverse locations of centers of gravity of all cargo and tank weights, and does calculate vessel static list, although tank TCG values do not vary with tank level (i.e. they are given as constant). It should be noted however, that the CargoMax software applies an incorrect lightship TCG of 0.00 ft-CL, and therefore the calculation of the static list angle in CargoMax is inaccurate (see Section 3.2 of this report). The magnitude of this inaccuracy depends on the vessel loading condition and the actual metacentric height (GM). Based on MBI hearing testimony [18, 19, 20], the ship’s list calculated by CargoMax was inaccurate compared to the observed list between 2 and 3 degrees for typical full load departure conditions. For example, for the accident voyage departure condition, CargoMax calculated a list of 2.3 degrees to starboard with the assumed lightship TCG of 0.00 ft [11]; however, a simple moment calculation confirms that a lightship TCG of approximately 0.3 feet port of CL would result in the list of 0.0 degrees, as observed at departure [18]. This will be discussed in greater detail in Sections 5 and 6 of this report, as results of hydrostatic calculations using the MSC GHS computer model are provided.
- (4) The transverse locations of a number of smaller tanks (less than 5,000 ft³) are not identified correctly in the EL FARO CargoMax application. It appears that the transverse locations of these tanks were based on the original HECSALV model [2], where they were modeled as rectangular volumes placed on the centerline (i.e. TCG set

to 0.0) rather than their actual transverse locations. The largest of these tanks were the potable water and distilled water tanks. These differences introduce additional list angle error in the CargoMax calculations. For example, the 22 foot error in TCG of the distilled water tank (see Table 2-3) would introduce an error in the calculated angle of list of approximately 0.85 degrees for the accident voyage departure condition, with displacement 34,624.5 LT, GM 4.284 ft, and the distilled water tank nearly full with 100 LT of weight [11].

- (5) Longitudinal locations of centers of gravity (LCG) in the T&S Booklet and in CargoMax are constant values and do not vary with tank level. The MSC GHS computer model does include full variable tank calculation, so variable LCG and TCG are included in the MSC calculations. However, the effects of these differences on predicted drafts and trim are minimal, considering the much larger effects of the large quantity of RO/RO cargo, which was not accounted for precisely in the load plan, but placed at the centers of the holds (see Section 5 of this report).
- (6) Similar to the differences noted with tank volume calculations, review of Table 2-3 also highlights differences with calculated free surface inertias, which are used in calculation of the free surface correction to GM for stability calculations. All but one of the tanks had differences in excess of the 2% tolerance. There is no obvious reason for these differences. However, it is noted that because the moment of inertia of liquid free surface is roughly proportional to the cube of the breadth multiplied by the length of the tank, errors in transverse and length dimensions propagate to larger errors in moments of inertia (see Appendix A for a discussion of propagation of errors and uncertainty).

The IMO Circ. 1229 and IACS UR L5 tolerance comparisons included in Table 2-2 and Table 2-3 are meant to illustrate the variability of the calculated results in comparing the detailed MSC GHS computer model to the previously approved T&S Booklet and CargoMax values, and to apply an objective quality standard to the differences. However, at the time of approval of the CargoMax software application for the EL FARO by ABS [21], it was apparently determined that the tank values for the CargoMax application met the tolerance requirements since they were based on “pre-programmed data” (i.e. the previously approved T&S Booklet), and therefore met the tolerance requirements by definition.

	100% Volume (ft ³)		100% VCG (ft abv BL)		100% LCG (ft aft FP)		100% TCG (ft stbd CL)		Slack (Max) Free Surface (ft)		Permeability Factor		Volume Difference (%)	VCG Difference (%)	LCG Difference (%)	TCG Difference (ft)	FS Inertia Difference (%)	Comments/Notes
	MSC GHS	T&S & CargoMax	MSC GHS	T&S & CargoMax	MSC GHS	T&S & CargoMax	MSC GHS	CargoMax	MSC GHS	T&S & CargoMax	MSC GHS	T&S & CargoMax	Tolerance 1% or 0.164 ft	Tolerance 1% or 0.164 ft	Tolerance 1% or 0.164 ft	Tolerance 0.5% of B (0.46 ft) or 0.164 ft	Tolerance 2% 2%	
Fuel Oil																		
DB No 2A IP	12,130	12,617	3.84	3.90	370.5	370.6	-9.50	-9.62	51,265	56,290	0.95	0.98	4.0%	1.6%	0.0%	0.12	9.8%	Outer bound 19.25 ft. Double bottom permeability 0.95.
DB No 2A IS	12,130	12,617	3.84	3.90	370.5	370.6	9.50	9.62	51,265	56,290	0.95	0.98	4.0%	1.6%	0.0%	0.12	9.8%	Outer bound 19.25 ft. Double bottom permeability 0.95.
DB No 3 IP	15,047	15,312	3.85	3.90	472.0	471.6	-9.47	-9.56	63,679	69,936	0.95	0.95	1.8%	1.3%	0.1%	0.09	9.8%	Outer bound 19.25 ft.
DB No 3 IS	15,047	15,312	3.85	3.90	472.0	471.6	9.47	9.56	63,679	69,936	0.95	0.95	1.8%	1.3%	0.1%	0.09	9.8%	Outer bound 19.25 ft.
FO Sett	10,299	10,152	23.50	23.50	653.5	654.1	0.00	0.00	140,968	143,856	0.98	0.98	1.4%	0.0%	0.1%	0.00	2.0%	
Fresh Water																		
Fore Pk TK	15,431	15,029	23.53	23.68	16.8	16.7	0.00	0.00	13,922	12,934	0.98	0.98	2.6%	0.6%	0.5%	0.00	7.1%	
DT No IB S	16,973	16,996	31.22	31.40	85.1	85.2	6.73	6.74	28,167	29,121	0.98	0.98	0.1%	0.6%	0.1%	0.01	3.4%	
DB No 1 P	11,262	11,504	5.22	5.30	163.2	163.3	-7.12	-7.05	66,918	60,296	0.95	0.98	2.1%	1.5%	0.1%	0.07	9.9%	Double bottom permeability 0.95
DB No 1 S	11,262	11,504	5.22	5.30	163.2	163.3	7.12	7.05	66,918	60,296	0.95	0.98	2.1%	1.5%	0.1%	0.07	9.9%	Double bottom permeability 0.95
DB No 2 IP	14,785	15,000	3.90	4.10	269.8	269.9	-9.38	-9.48	63,617	69,936	0.95	0.95	2.1%	5.1%	0.0%	0.10	9.9%	Outer bound 19.25 ft.
DB No 2 IS	13,628	13,668	3.71	3.90	268.9	266.4	9.68	9.48	63,617	69,936	0.95	0.98	9.1%	5.1%	0.9%	0.20	9.9%	Outer bound 19.25 ft. Deduction for elevator pit.
DB No 4 P	3,932	4,291	3.94	4.50	561.6	565.1	-10.45	-10.44	50,735	62,148	0.98	0.98	9.1%	14.2%	0.6%	0.01	22.5%	
DB No 4 S	3,932	4,291	3.94	4.50	561.6	565.1	10.45	10.44	50,735	62,148	0.98	0.98	9.1%	14.2%	0.6%	0.01	22.5%	
Pot Water	2,735	2,504	42.25	41.30	607.0	606.9	2.50	0.00	27,377	26,532	0.98	NA	8.4%	2.2%	0.0%	2.50	3.1%	No variable tank data T&S Book
Dist Water	3,225	3,691	29.75	29.20	596.0	596.2	-21.63	0.00	17,617	17,280	0.98	NA	14.4%	1.8%	0.0%	21.63	1.9%	No variable tank data T&S Book
Stem T Comp	6,777	7,073	13.72	14.50	651.8	651.9	0.00	0.00	113,599	121,811	0.90	0.90	4.4%	5.7%	0.0%	0.00	7.2%	
DT Afr P	9,394	11,286	23.42	23.36	645.0	647.1	-26.06	-26.05	35,092	32,776	0.98	0.98	20.1%	0.3%	0.3%	0.01	6.6%	
DT Afr S	9,394	11,286	23.42	23.36	645.0	647.1	26.06	26.05	35,092	32,776	0.98	0.98	20.1%	0.3%	0.3%	0.01	6.6%	
Salt Water																		
DT No IA	20,211	20,091	31.13	31.40	55.2	55.1	0.00	0.00	82,110	72,148	0.98	0.98	0.6%	0.9%	0.2%	0.00	12.1%	
Afr Peak CL	28,781	29,257	28.24	28.40	711.9	710.6	0.00	0.00	362,635	353,455	0.95	0.95	1.7%	0.6%	0.2%	0.00	2.5%	
Afr Peak P	4,150	4,299	31.72	31.60	726.9	726.1	-24.52	-24.47	7,210	8,462	0.95	0.95	3.6%	0.4%	0.1%	0.05	17.4%	
Afr Peak S	4,150	4,299	31.72	31.60	726.9	726.1	24.52	24.47	7,210	8,462	0.95	0.95	3.6%	0.4%	0.1%	0.05	17.4%	
Miscellaneous																		
DT No IB P Slop	16,973	16,996	31.22	31.40	85.1	85.2	-6.73	-6.74	28,167	29,121	0.98	0.98	0.1%	0.6%	0.1%	0.01	3.4%	
Diesel Oil	679	688	89.50	87.50	564.3	564.5	-6.00	0.00	165	3,192	0.98	NA	1.3%	2.2%	0.0%	6.00	1834.5%	No variable tank data T&S Book.
LO Storage	491	616	32.50	32.00	605.7	605.7	3.50	0.00	311	NA	0.98	NA	25.6%	1.5%	0.0%	3.50	NA	No variable tank data T&S Book
LO Sump	552	484	5.54	6.00	594.8	596.1	0.00	0.00	3,689	NA	0.98	NA	12.3%	8.3%	0.2%	0.00	NA	No variable tank data T&S Book
LO Settling	631	695	32.50	32.00	605.7	605.7	-4.50	0.00	660	NA	0.98	NA	10.2%	1.5%	0.0%	4.50	NA	No variable tank data T&S Book
LO Gravity	539	450	66.00	65.00	551.5	554.8	0.00	0.00	466	NA	0.98	NA	16.5%	1.5%	0.6%	0.00	NA	No variable tank data T&S Book

Table 2-3: 100% tank volumes, centers and maximum (slack) free surface comparisons between the MSC GHS model and the T&S Book and CargoMax. Also included in the table are the calculated differences and tolerances based on the IMO and IACS guidelines.

2.4. Lightship Weight, Center of Gravity, and Distribution

In order to perform hydrostatic and stability analyses, the ship's lightship weight (displacement) and location of the center of gravity must also be known. The lightship weight and center of gravity was taken from the most recent Stability Test Report [22] which is based on the inclining experiment completed on February 12, 2006. Table 2-4 provides a summary of the lightship condition from the Stability Test Report. Note that the lightship weight of 19,943 LT includes 6,705 LT of fixed ballast in the outboard double bottom tanks. Additional discussion about the lightship weight and center of gravity, including review of the stability test and an uncertainty analysis of the lightship weight and center of gravity, are provided in Section 3 of this report. Note that the TCG of the lightship condition was incorrectly calculated in the Stability Test Report, as explained in Section 3.2.

	Lightship Condition
Displacement (LT)	19,943
KG/VCG (ft-BL)	27.82
LCG (ft-FP)	412.01
TCG (ft-CL)	0.12 port (incorrect)
Draft Aft Perp (ft)	26.65
Draft Fwd Perp (ft)	10.81
Trim (ft)	15.84 aft

Table 2-4: Lightship weight (displacement), center of gravity, drafts and trim, based on the Stability Test Report [22 (page 17)].

Based on the date of construction of the EL FARO, there was no requirement for a Loading Manual and thus, no requirement for approval of a lightship weight distribution, and none was approved. However, a Preliminary Weight Estimate was issued by JJH, Inc. (Revision A2 dated November 11, 1992) [23] which included an engineering estimate of a lightship weight distribution for the 1992-1993 conversion. Additionally, although not reviewed and approved by ABS, a lightship weight distribution was included in the CargoMax application for calculation of longitudinal bending moments and shear forces for comparison with ABS allowables.

The lightship weight distribution for the MSC GHS computer model was developed using the Preliminary Weight Estimate issued by JJH, Inc. (Revision A2 dated November 11, 1992) [23], along with estimated changes. Distributed weight for the 6,705 LT of fixed ballast was added, based on the approved Fixed Ballast Installation Drawing [24], as three trapezoidal weight distributions from 212.42 ft-FP to 528.67 ft-FP. An additional estimated 200 LT of distributed weight was added to account for the container foundations and main deck support structure which was added in the 2005-2006 conversion [25]. The estimated 713 LT spar deck structure which was removed as part of the 2005-2006 conversion [26] was accounted for in the application of the Preliminary Weight Estimate by JJH, Inc.

Figure 2-6 provides a plot of the lightship weight distribution used in the MSC GHS computer model.

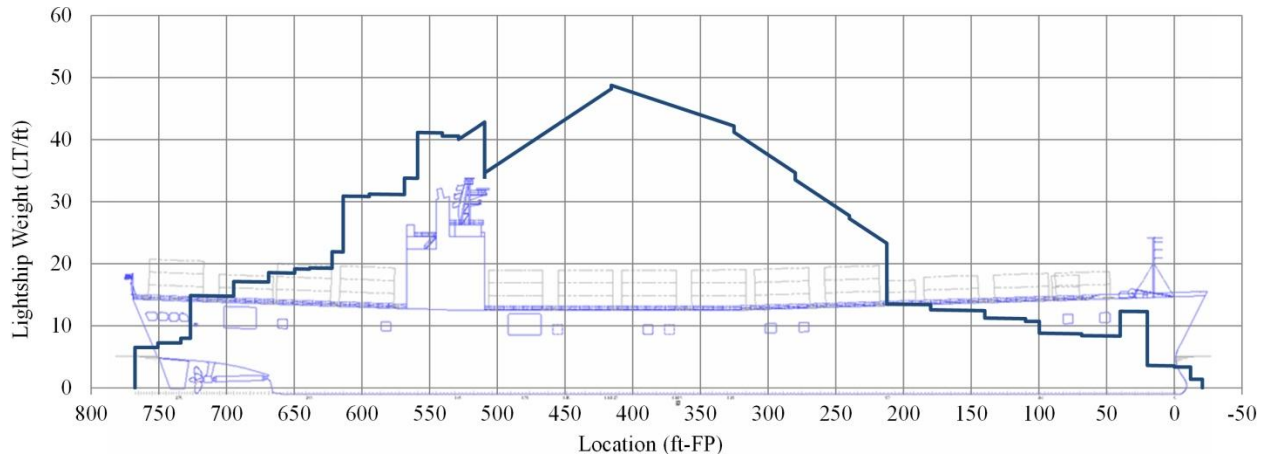


Figure 2-6: Lightship weight distribution used in the MSC GHS computer model.

2.5. Summary

This section provided an overview of the development of the MSC GHS computer model for hydrostatic and stability analyses. Additional comparisons of hydrostatics properties and tank volumes and centers of gravity between the MSC GHS computer model and the T&S Booklet and CargoMax loading software application were made, with a number of differences highlighted.

Hull hydrostatic properties compared closely, with approximately 0.1% difference in calculated displacement at the full load draft. All hydrostatic properties were within the tolerance of IMO MSC.1/Circ.1229, which has been used as an objective quality standard.

Comparison of tank volumes, centers and free surface inertia values identified discrepancies with T&S Booklet and CargoMax values. Using IMO MSC.1/Circ.1229 as an objective quality standard, 19 tanks were in excess of the 2% tolerance for volume, and 22 tanks were in excess of the 2% tolerance for maximum slack free surface inertia. Based on additional MSC review of EL FARO and sister vessel T&S Booklets going back to the 1970s, it appears that errors were made in the original tank geometry definition and/or in the original numerical integration. It also appears that these discrepancies in tank values would apply to all of the vessels of the PONCE DE LEON class.

3. Stability Test and Uncertainty Analysis

3.1. Introduction

In order to assess a vessel's hydrostatics and stability characteristics, a vessel's weight (displacement) and location of the center of gravity must be determined. For variable or deadweight loads such as cargo and onboard liquids, the weight and centers of gravity can be calculated or tabulated. However, the weight and centers of gravity of the ship's structure and other fixed weights must be experimentally determined. Upon new construction or after significant changes to the lightship are made, this is accomplished by performing a stability test, also called an inclining experiment.

For the EL FARO, a stability test was required by 46 CFR Part 170 Subpart F, Determination of Lightweight Displacement and Centers of Gravity. Standardized technical guidance for conducting a stability test is provided in ASTM F1321 (series) [27], Standard Guide for Conducting a Stability Test (Lightweight Survey and Inclining Experiment) to Determine the Light Ship Displacement and Centers of Gravity of a Vessel.

The most recent stability test for the EL FARO was completed at the Atlantic Marine Shipyard in Mobile, Alabama on February 12, 2006, following conversion for carrying LO/LO container cargo on the main deck. As required by 46 CFR 170.085, a Stability Test Procedure was submitted and approved by ABS on behalf of the USCG on February 2, 2006 [28]. After completion of the stability test, the Stability Test Report was submitted and reviewed by ABS and approved on March 22, 2006 [22], incorporating reviewing engineer's comments as well as the witnessing ABS surveyor's field notes and comments provided in the ABS Survey Report M662652 [29].

This section provides MSC review comments regarding the EL FARO Stability Test Report with ABS approval notes, along with the Stability Test Procedure and Inclining Experiment Record Sheet [30]. Additionally, as requested by the MBI, an uncertainty analysis of the stability test and departure condition of the accident voyage was completed by MSC, as documented in Appendix A of this report. Results of the uncertainty analysis are also summarized in this section.

3.2. Stability Test

As part of the reviews requested by the MBI, MSC reviewed the Stability Test Report with ABS approval notes, along with the Stability Test Procedure and Inclining Experiment Record Sheet, and provides the following comments:

- (1) The ABS approved Stability Test Procedure required that, in accordance with ASTM F1321-92 (2004), five (5) sets of freeboard and draft readings per side be taken, but draft marks may be used in lieu of specific freeboard readings only if verified and certified to approved drawings by an ABS surveyor with the vessel in drydock. As noted in the Stability Test Report, only the midship draft marks were certified by the ABS surveyor, with the fore and aft marks only "checked" by an Atlantic Marine surveyor. It was also

noted in the Stability Test Report that the reliability of the freeboard readings was in question, due to identified discrepancies between ship's drawings regarding deck heights including sheer; therefore draft marks were considered superior and freeboards were not included in definition of the fit waterline and the hydrostatic calculations by the test engineers. This effectively limited the waterline measurement to one set of three drafts (forward, midship, aft), with the draft readings taken only once at the beginning of the experiment. Although not in accordance with the ASTM F1321 guidelines, given the questions regarding accuracy of the deck height freeboard reference datum from the drawings, the use of the draft readings alone is reasonable. Further, although ships are generally built to specified construction tolerances, freeboard reference datum (deck heights), are rarely surveyed and documented to be accurate compared to ship's drawings during a typical vessel's lifetime, and therefore the practice recommended in the ASTM F1321 of using freeboard measurements with draft marks may be questionable in any case.

- (2) During the "deadweight survey" portion of the stability test, a survey of all weights to add, remove or relocate was completed to correct the "as-inclined" condition (Condition 0) to the "lightship" condition (Condition 1) by accounting for all liquids and dry items onboard [22 (pages 16-17)]. However, test engineers did not keep track of transverse center of gravity (TCG) locations for liquids and dry surveyed items and all were assigned a TCG of 0.00 feet from the centerline (ft-CL) in the Stability Test Report and the supporting calculations. Although there is no requirement in the ASTM F1321 guidelines for calculating TCG for the lightship condition, the effect of not keeping track of TCG values in the deadweight survey was that the lightship TCG calculated and presented in the summary table for the lightship (Condition 1) was incorrect.
- (3) The documentation of weights throughout the Stability Test Report did not provide sufficient significant figures for MSC to verify the supporting calculations, with weights in the report displayed only to the nearest whole long ton (LT). This applied to all inclining weights, all deadweight survey items, and the calculated results. However, based on the weight logs provided in the ABS Survey Report for the Inclining M662652 [29], it appears that this is a display issue only and calculated moments from weights and distances appear correct (to the nearest whole long ton).

The as-inclined and lightship values of displacement, centers of gravity, drafts, trim and specific gravity are provided in Table 3-1 below, based on the Stability Test Report. As noted above, the TCG of the lightship condition was incorrectly calculated in the Stability Test Report, as noted in the table.

	As-inclined (Condition 0)	Lightship (Condition 1)
Displacement (LT)	23,512	19,943
KG/VCG (ft-BL)	26.02	27.82
LCG (ft-FP)	388.08	412.01
TCG (ft-CL)	0.10 port	0.12 port (incorrect)
GMt (ft)	18.26	20.82
Draft Aft Perp (ft)	24.82	26.65
Draft Midships (ft)	22.41	Not provided
Draft Fwd Perp (ft)	20.72	10.81
Trim (ft)	4.10 aft	15.84 aft
Hog/sag (ft)	0.36 hog	Not provided
Specific Gravity	1.002	1.025

Table 3-1: As-inclined and lightship displacements, centers of gravity, drafts, trim and specific gravity, based on the Stability Test Report [22 (pages 16-17)].

3.3. Uncertainty Analysis

The MSC was requested by the MBI to review the EL FARO inclining experiment and Stability Test Report and calculate the uncertainty in the vessel's KG for the lightship condition and for the accident voyage departure condition. Appendix A of this report provides the detailed procedure and results for the requested uncertainty analysis. A summary of the results is provided in this section.

It should be noted that there is no standard accepted procedure or guidance for completing an uncertainty analysis from the results of a stability test. The procedure undertaken by the MSC is based on an application of the principles of experimental uncertainty analysis, including assessment of potential sources of measurement errors, statistical analysis, and propagation of errors. The results of the analysis are fundamentally limited based on the size and type of vessel, the stability test procedure, the type of cargo and the specific loading condition. The results obtained for the uncertainty associated with the stability test and the lightship weight and center of gravity could be considered somewhat typical of similar large deep draft vessels. The additional uncertainty associated with the vessel loading condition can vary, depending on the particular type of cargo and loading procedures.

It is often the case that vessel operators consider the calculated GM, whether calculated by hand or by stability and loading software, to be fairly precise, and then operate the vessel fairly close to the minimum required GM. It is apparent from the MBI hearing testimony [18, 19, 31, 32] that this was the case for the operation of the EL FARO, including for the accident voyage. It is important to recognize that the actual GM may not be precisely known and uncertainty in the calculated GM can exist. However, calculated uncertainty in KG or GM for an operating condition should not be used to calculate a probability that the vessel would not meet the stability criteria for that operating condition. There is currently no consideration for uncertainty in assessing a vessel's stability in accordance with U.S. or international standards, as discussed in Section 5 of this report.

As discussed in detail in Appendix A of this report, the equation for calculating the metacentric height (GM) in the as-inclined condition from the inclining experiment is [27]

$$GM = \frac{w \cdot a}{\Delta \cdot \tan\theta} = \left(\frac{w \cdot a}{\tan\theta}\right) \cdot \left(\frac{1}{\Delta}\right) \quad (3-1)$$

where w is the weight of inclining weights (LT), a is the distance inclining weights are moved (ft), $\tan\theta$ is the tangent of the angle of heel induced by the movement of inclining weights, and Δ is the vessel weight (displacement) in the as-inclined condition (LT). The first term is determined from the slope of the “best fit” line from the plot of the applied moment ($w \cdot a$) and the measured angle tangent ($\tan\theta$) for a series of sequential weight movements. Therefore, for the inclining experiment

$$GM = \left(\frac{1}{\text{slope}}\right) \cdot \left(\frac{1}{\Delta}\right) \quad (3-2)$$

The second term is determined by calculation of the displacement using the measured drafts and the hull offsets. In order to calculate the uncertainty in as-inclined GM, the uncertainty in each term must be calculated based on the experimental method, and then combined.

As developed in Appendix A, the uncertainty in as-inclined GM can be calculated

$$\left(\frac{U_{GM}}{GM}\right) = \sqrt{\left(\frac{U_{\text{slope}}}{\text{slope}}\right)^2 + \left(\frac{U_{\Delta}}{\Delta}\right)^2} \quad (3-3)$$

where U_{GM} is the uncertainty in as-inclined GM, U_{slope} is the uncertainty in slope, and U_{Δ} is the uncertainty in displacement.

For the EL FARO inclining experiment completed in 2006, each of seven steps or “trials” involved moving two or three inclining weights in sequence from port to starboard or starboard to port (initially, five weights were placed port and five weights were placed starboard). For each trial, three independent pendulums were used to measure the tangent of the induced angle. Thus there were 21 measurements of tangent (three in each of the seven trials) which could be used in the determination of the slope. A “best fit” linear slope, standard error of the slope, and 95% confidence uncertainty of the slope (U_{slope}) and other fit statistics are calculated using a linear least-squares regression method in a spreadsheet calculation.

Assessment of the uncertainty in the calculated as-inclined displacement (U_{Δ}) requires consideration of a number of independent sources of error, since the displacement is a derived quantity based on measurement of drafts, calculation of the submerged volume from the ship’s lines, and measurement of water density. This procedure is detailed in Appendix A.

Based on the Stability Test Report, the calculated value of the as-inclined GM was 18.26 ft. Based on the results of the uncertainty analysis detailed in Appendix A, the uncertainty in the as-inclined GM (U_{GM}) is 0.24 ft with a 95% confidence level. This means that there is a 95%

confidence that the true value lies within ± 0.24 ft of the calculated value, or in equation form the as-inclined GM can be written (to one decimal place)

$$GM = 18.3 \pm 0.2 \text{ ft (with 95\% confidence)}$$

Appendix A also describes calculation of uncertainties associated with the lightship KG and the KG and GM of the accident voyage. First, the as-inclined KG is calculated from the as-inclined GM by subtracting the GM from the height of the metacenter (KM), and therefore the uncertainty in the as-inclined KG accounts for the additional uncertainty in KM, which is a hydrostatic property and based on the hull offsets. The lightship KG is calculated from the as-inclined KG by adding and subtracting all of the liquid and solid weights identified during the deadweight survey portion of the stability test, and the uncertainty in the lightship KG accounts for the additional uncertainties associated with these weights and their centers of gravity. The KG for the accident voyage departure condition is calculated from the lightship KG by adding all liquid and cargo loads based on the voyage loading plan, and the uncertainty in the departure KG accounts for the additional uncertainties associated with these weights and their centers of gravity. Finally, the GM for the accident voyage is calculated by subtracting the KG from the height of the metacenter (KM), and the uncertainty in the GM for the accident voyage accounts for the additional uncertainty in the value of KM. See Appendix A for a full description of the procedure.

Table 3-2 below provides a summary of all of the key calculated uncertainties from Appendix A. The table reflects key results from the uncertainty analysis of the February 12, 2006 stability test, plus results of the additional uncertainty analysis of the lightship condition and departure condition for the accident voyage (185S).

Using the final calculated uncertainty in Table 3-2 for GM for the accident voyage departure condition, this says that there is a 95% confidence that the calculated value of GM lies within ± 0.69 ft of the true value of GM, or in equation form the departure GM can be written (to one decimal place)

$$GM = 4.3 \text{ ft} \pm 0.7 \text{ ft (with 95\% confidence)}$$

As discussed in Appendix A, the centers of gravity for LO/LO containers were calculated by default in CargoMax at the geometric center of the containers. It is recognized that most containers would likely contain cargo which would result in a center of gravity below the center of the container, and this would suggest addition of a KG-reducing (negative) bias error adjustment to the estimate of uncertainty based on the conservative calculation in CargoMax. This is estimated to be approximately a 0.2 feet reduction in KG or increase in GM for the accident voyage (see Appendix A).

With this estimated bias error adjustment applied for the accident voyage loading condition the departure GM can be written

$$GM = (4.3 + 0.2) \pm 0.7 \text{ ft} = 4.5 \pm 0.7 \text{ ft (with 95\% confidence)}$$

Parameter	Measured, calculated or nominal value with units	Uncertainty with units
Slope (tangent/moment)	$2.3460 \times 10^{-6} \text{ 1/ftLT}$	$16.68 \times 10^{-9} \text{ 1/ftLT}$
Molded vs. as-built volume (V)	849,229 ft ³	1,673 ft ³
Vessel drafts	22.45 ft	0.061 ft
Calculated molded volume (m)	849,229 ft ³	8,492 ft ³
Displacement volume (∇)	849,229 ft ³	9,126 ft ³
Specific weight, density	62.55 lb/ft ³	0.09 lb/ft ³
Vessel displacement (Δ)	23,512 LT	260 LT
As-inclined GM	18.26 ft	0.24 ft
As-inclined KG	26.02 ft	0.45 ft
Lightship KG	27.82 ft	0.72 ft
Accident voyage departure KG	37.25 ft *[-0.2 ft]	0.63 ft
Accident voyage departure GM	4.28 ft *[+0.2 ft]	0.69 ft

Table 3-2: Summary of results of the uncertainty analyses of the stability test and the loading condition for the accident voyage. All uncertainties are at the 95% confidence level. *Bracketed estimated values reflect potential bias correction, lowering KG and increasing GM due to default location of centers of gravity of LO/LO containers in CargoMax (see Appendix A).

3.4. Summary

This section documented the MSC review of the 2006 stability test (inclining experiment) and assessment of the calculations associated with determination of the lightship weight and center of gravity provided in the Stability Test Report. This section also provided a summary of the requested uncertainty analysis of the lightship KG and the GM for the accident voyage departure condition, which is documented in detail in Appendix A.

Based on the MSC uncertainty analysis of the stability test, the uncertainty in the as-inclined GM was calculated to be approximately 0.2 feet (with 95% confidence). This means that there is a 95% confidence that the true value of GM in the as-inclined condition is within ± 0.2 feet of the value calculated in the Stability Test Report. The uncertainty in the lightship KG was calculated to be approximately 0.7 feet (with 95% confidence), and the uncertainty in the GM for the accident voyage departure condition was calculated to be approximately 0.7 feet (with 95% confidence). The last statement means that there is a 95% confidence that the true value of the accident voyage GM was within ± 0.7 feet of the calculated value.

4. Trim and Stability Booklet (T&S Booklet) and Stability Software

4.1. Introduction

A stability booklet (also referred to as a trim and stability booklet) is required by 46 CFR Subchapter S, Subdivision and Stability, and must contain sufficient information to enable the master to operate the vessel in compliance with applicable regulations within the subchapter, most notably applicable intact and damage stability criteria. For the EL FARO the most recent T&S Booklet, Rev E dated February 14, 2007 [12] was approved on behalf of the U.S. Coast Guard by ABS on May 31, 2007 [33]. The stability review was completed in association with a summer load line molded draft of 30'-1-5/16" (30'-2-3/8" keel draft) corresponding to a 1966 Type "B" vessel freeboard of 12'-0-15/16" from the 2nd deck. At the time of the accident voyage, the vessel had a valid International Load Line Certificate issued by ABS on behalf of the U.S. Coast Guard on January 29, 2011 [34]. The approved load line and freeboard had not changed since the issuance of the T&S Booklet. It is noted that a stability booklet is not intended to address the assessment of vessel loading and hull strength (bending moments and hull stresses), or the assessment of cargo loading and securing. Vessel loading and hull strength assessment would be included in a vessel loading manual, if one is required; however, a loading manual was not required or provided for the EL FARO. Cargo loading and securing would be included in a vessel cargo securing manual, and the EL FARO had an ABS-approved Cargo Securing Manual [35].

Onboard stability software, also referred to as a "stability instrument", is software used to calculate the loading condition and stability of a vessel to ascertain that stability requirements specified for the ship in the stability booklet are met in an operational loading condition. For the EL FARO, the stability and loading software CargoMax was approved for onboard use by ABS on February 8, 2008 [21], as it met the requirements of the applicable ABS Steel Vessel Rules [36], IACS Unified Requirement L5 [14], and MSC.1/Circ.1229 [13]. It should be noted from the ABS approval letter [21] that the CargoMax software was reviewed and approved by ABS for use onboard the EL FARO only as a supplement to facilitate stability calculation, and not as a substitute for the approved T&S Booklet. Based on the MBI hearing testimony [18, 19, 31, 32], CargoMax was routinely used by the Tote Services, Inc. operations personnel independently of the T&S Booklet. It should also be noted from the ABS approval letter that the CargoMax software was neither reviewed nor approved for assessment of loading and hull strength (bending shear forces and moments) or for assessment of cargo loading and securing (container stack weight, tier weight and lashing requirements). However, the EL FARO CargoMax software contained features used by the Tote Services, Inc. operations personnel for these purposes and, based on MBI hearing testimony [18, 19, 20, 31, 32], was relied on for these purposes.

With the exception of recent amendments to several IMO instruments applicable to oil, chemical and gas carriers, there are no requirements for the use of onboard software for vessel stability, strength or cargo loading and securing. Under Coast Guard policy [37], the master must be provided with the capability to manually calculate stability. However, he may use whatever tools he wishes to assist him in his responsibility to ensure satisfactory stability. The Coast Guard will, upon request, verify that the onboard stability software produces nearly identical results to the approved stability booklet in a number of representative loading conditions. After

verification, the Coast Guard will recognize the software as an adjunct to the stability booklet; however, it remains incumbent upon the master to ensure the vessel is compliant with all aspects of the stability booklet.

4.2. T&S Booklet

The most recent EL FARO T&S Booklet, Rev E dated February 14, 2007 [12] was issued by Herbert Engineering Corporation and was based on the T&S Booklet, Rev 0 dated May 6, 1993, [17]. Rev 0 was applicable from the time the vessel was lengthened in 1992-1993 until the conversion in 2005-2006. Four revisions were written between 2005 and 2007, which included accounting for removal of the spar deck, addition of deck containers, container foundations and securing system, addition of permanent ballast, revision of lightship weight and center of gravity based on the 2006 stability test, and addition of variable tank data tables. Additional notes, new sample load cases, and new calculation forms were also added to reflect the conversion of the vessel to carry containers on deck (LO/LO cargo).

The most recent 2007 T&S Booklet was approved on behalf of the U.S. Coast Guard by ABS on May 31, 2007 [33], having met the requirements of 46 CFR 170.110. In addition to comments provided in Section 3 of this report applicable to the 2007 T&S Booklet, the following comments are provided:

- (1) The instructions for computation of the vessel's stability and trim on page 7 of the T&S Booklet do not appear to provide correct instructions for computation of hydrostatic properties given vessel drafts. The instructions direct that the mean draft be used to read a corresponding displacement, instead of the draft at the LCF, which must be calculated by applying a trim correction. However, it is noted that the example calculation forms provided on pages 32-35 of the T&S Booklet do provide spaces for applying the required trim corrections, although the instructions for application by the user are not clear. There are also no instructions on the proper method to correct the height of the metacenter (KM_T) for trim using the table on page 12 of the T&S Booklet.
- (2) The minimum required GM curves provided on page 16 of the T&S Booklet produced by Herbert Engineering Corporation (see Figure 4-1) were generated based upon the minimum GM required to meet the intact stability criteria of 46 CFR 170.170 (see Section 5 of this report for additional information about intact stability criteria). However, in MBI hearing testimony [38, 39, 40] it was noted that Herbert Engineering did not complete a damage stability analysis to confirm that, after the 2005-2006 conversion, the limiting criteria would remain the intact stability criteria for all loading conditions, and ABS had no records of a damage stability analysis being completed. This is important because the 2005-2006 conversion resulted in a 2-foot increase in the load line draft (28'-1-1/16" to 30'-2-3/8"), and therefore the previous damage stability analysis completed in 1993 no longer applied. In his MBI hearing testimony [38, 39], Mr. Thomas Gruber of ABS submitted results of his independent SOLAS probabilistic damage stability analysis performed in May 2016 [41], where he applied the damage stability standards which would have been applicable in 2005-2006. Mr. Gruber's analysis determined that for GM values of approximately 2.9 feet at both the load line

and partial load line drafts (30.11 and 26.02 feet), the required subdivision index of 0.60 would be attained (see Section 5.3 of this report for a more detailed discussion of damage stability assessment). This suggests that for most load conditions with 2 or more tiers of containers loaded, the limiting stability criteria would be the intact stability criteria as reflected in the T&S Booklet. However, this also means that for some load conditions with less than 2 tiers of containers loaded, the limiting stability criteria could be the damage stability criteria, and this was not reflected on the minimum required GM curves of the T&S Booklet. The MSC also performed an independent SOLAS probabilistic damage stability analysis using the MSC GHS computer model, and confirmed Mr. Gruber's basic result, with a slightly higher GM of 3.3 feet (see Section 5.3 of this report). However, it should be noted that, for the full load departure condition of the accident voyage, the limiting stability criteria would have been the intact stability criteria, which was properly reflected in the T&S Booklet and incorporated in the CargoMax stability software, since the majority of the container stacks included 3 tiers. Section 5 of this report provides additional detailed discussion of applicable intact and damage stability criteria.

MINIMUM REQUIRED GM CURVE

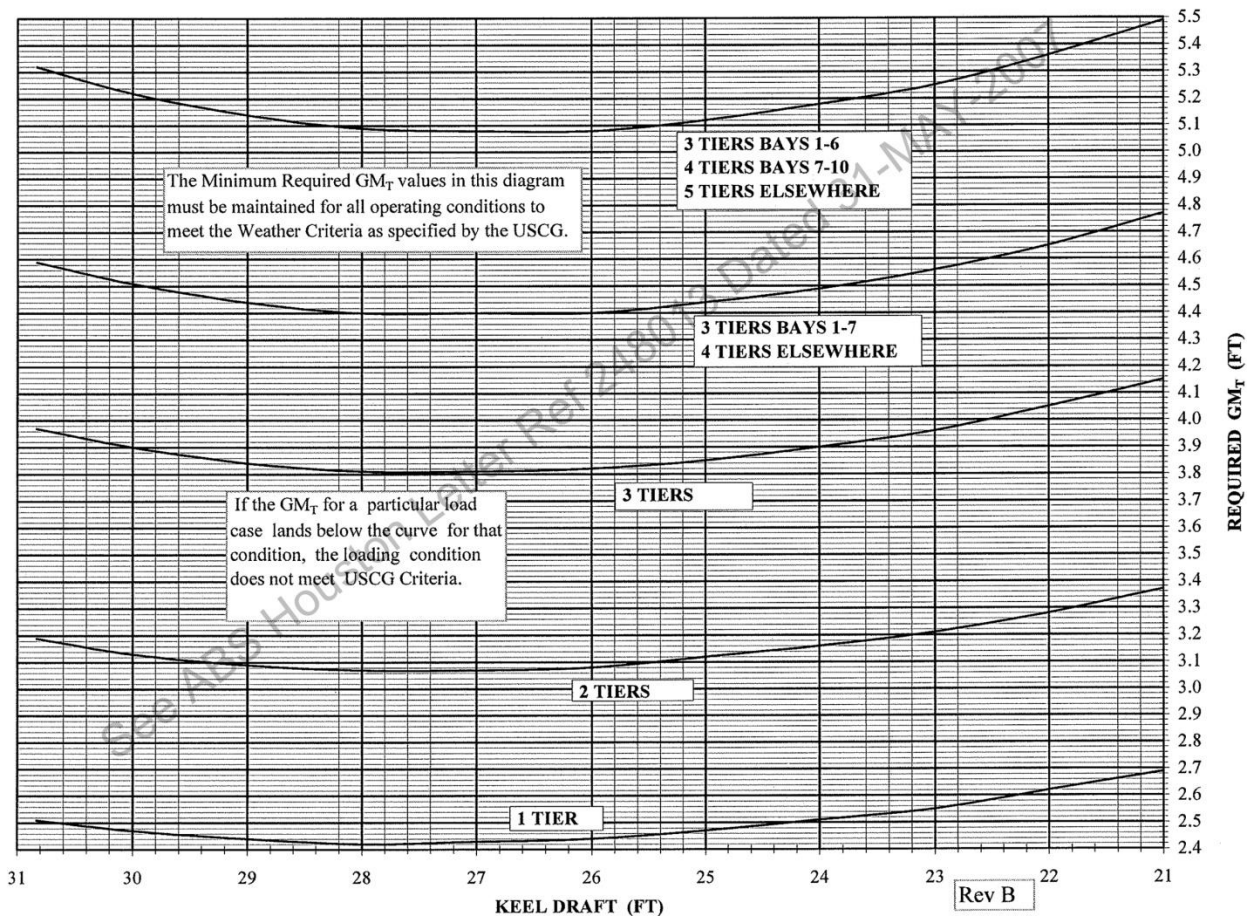


Figure 4-1: Minimum required GM curves from the 2007 T&S Booklet [12].

4.3. CargoMax Stability Software

The stability and loading software CargoMax (Herbert-ABS Software Solutions, LLC) was used onboard the EL FARO and by shore-side operations personnel for cargo load planning and stability assessment. CargoMax Version 1.21.162 dated August 31, 2007 with EL FARO ship model dated September 20, 2007 was approved for use onboard the EL FARO by ABS on February 8, 2008 [21]. However, at the time of the accident voyage, CargoMax Version 1.21.203 dated June 1, 2010 with EL FARO ship model dated June 17, 2010 was installed and being used onboard the EL FARO and by shore-side operations personnel. Based on MBI hearing testimony [38, 39] Version 1.21.203 was not specifically reviewed and approved by ABS.

In granting CargoMax approval in 2007, ABS reviewed and approved the CargoMax Vessel Information Book for the SS EL FARO, Rev 2 dated March 13, 2007 [42], and the supporting report Direct Calculation of Required GM for USCG Windheel Criteria within the CargoMax Loading Program: Implementation System and Supporting Calculations for the SS EL FARO, dated April 14, 2006 [43]. While the CargoMax for Windows User's Manual [44] is the standard reference for information about the software program, the CargoMax Vessel Information Book is the necessary companion to the User's Manual. The Vessel Information Book presents necessary ship-specific information incorporated into the EL FARO CargoMax vessel model, includes instructions for program options and custom features, and documents sample load cases comparable to those in the T&S Booklet and to be used for onboard in service verifications [42].

As stated previously, the CargoMax software was reviewed and approved by ABS for use onboard the EL FARO only as a supplement to facilitate stability calculation, and not as a substitute for the approved T&S Booklet. As such, the vessel operator was obligated to follow all operating instructions delineated in the T&S Booklet, regardless of whether or not the CargoMax software checked or warned for violations of the T&S Booklet instructions. The MSC review found that there are operating instructions in the T&S Booklet which were not followed by the operating personnel in loading the vessel using the CargoMax software for the accident voyage [11]. Specifically, it is stated in the T&S Booklet that not more than one pair of tanks assigned to each type of consumable liquid onboard the vessel shall be slack at one time. It is further stated that tanks required to be ballasted with salt water shall be immediately filled and carried pressed up at all times while such ballast is necessary, and otherwise kept pumped to minimum contents at all time. It is noted that for the accident voyage, all 5 fuel oil tanks were slack, 4 fresh water tanks were slack, and 4 of the larger salt water ballast tanks were slack. While there are checks and warnings within CargoMax to check the load line limit and the intact stability criteria, there are no warnings for T&S Booklet slack tank limitations. However, it is also noted that CargoMax does properly include all tank free surface corrections in the calculation of the vessel GM, so while this slack loading is not in accordance with the T&S Booklet and it does introduce some additional risk to the vessel, it is not an unassessed risk. In MBI hearing testimony [18, 19, 32] witnesses stated that fuel loading was normally limited to 8,200 barrels (1,825 LT) and tanks were not pressed up; the rationale given was that this would enable them to carry more cargo, but also provide enough fuel for a round trip voyage plus several days reserve.

During MSC review of the approved CargoMax Vessel Information Book for the SS EL FARO, Rev 2 dated March 13, 2007 [42] it was noted that necessary key data used to configure the CargoMax program for the EL FARO was not included; specifically documentation of the operating lightship weight and weight distribution, load line data, draft mark locations, minimum required GM tables, and allowable shear force and bending moments. Additional investigation by MSC found that the missing 15 pages were included with Rev 1 dated October 19, 2006 [45], but were apparently inadvertently omitted from the approved Rev 2 dated March 13, 2007. It is not clear if the missing pages were reviewed by ABS.

The report Direct Calculation of Required GM for USCG Windheel Criteria within the CaroMax Loading Program: Implementation System and Supporting Calculations for the SS EL FARO [43] documents required GM calculation features implemented in CargoMax which are not provided in the T&S Booklet. The calculation features in CargoMax replaced the more conservative calculation method used in the T&S Booklet in which the required GM curves were provided only for specific container stack height combinations (see Figure 4-1) without a method for interpolation or incorporation of actual container loading and wind profiles. The direct calculation method implemented in CargoMax provides a calculation of the required GM directly from the USCG criteria of 46 CFR 170.170 (see Section 5 of this report) using a calculated wind heel area based on the actual container loading profile. The report documents the calculation method and provides verification calculations and sample cases. As the calculation method provides a direct calculation of the minimum required GM based on the explicit formula provided in 46 CFR 170.170, with lateral wind area based on the actual loading condition, it meets the necessary requirements for calculation of minimum required GM.

The accuracy of the CargoMax calculations can be considered as good (or better) than the tabular form calculation performed by hand using the T&S Booklet. Fundamentally, the CargoMax model for the EL FARO consists of the same vessel data contained in the T&S Booklet, including principal dimensions, draft mark locations, hydrostatic tables, variable tank data tables including free surface, trim table, and required GM curves. The latter (required GM) may also be calculated using direct calculation of required GM as discussed previously. Otherwise, the calculations are carried out in basically the same manner. Of course, human errors may be reduced and computer precision may increase accuracy of results to some extent. For comparison, the sample load cases “full load departure” and “ballast arrival” provided in the CargoMax Vessel Information Book can be compared directly to the “homogenous full load departure” and “ballast arrival” conditions in the T&S Booklet, with the results being nearly identical, as expected.

Since the CargoMax and T&S Booklet calculations are based on the same hydrostatic tables, variable tank data tables including free surface, and other tabular vessel data, it is worthwhile comparing the results of the basic CargoMax calculation to that using the MSC GHS computer model. As discussed in Section 2 of this report, the GHS calculation implements direct calculation of all areas and volumes from the hull and tank stations and offsets using numerical integration, as opposed to the tabular data method used in CargoMax and the T&S Booklet. It would therefore be expected that the results would differ by some amount. Table 4-1 provides a summary of the results for the departure condition of the accident voyage (185S). The definition of weight for the loading condition summary was taken from the CargoMax printout [11]. The

minimum required GM was calculated using the direct calculation method using the actual wind heel area per 46 CFR 170.170 (see Figure 2-5). The calculated results are nearly identical. See Section 5 of this report for a more detailed discussion of analysis methods and stability criteria.

As discussed in Section 2.3, the CargoMax software for EL FARO applies an incorrect lightship TCG of 0.0 ft-CL, and therefore the calculation of the static list angle in CargoMax is inaccurate. From a practical perspective, using a lightship TCG of 0.00 ft-CL in the CargoMax stability software calculations led to incorrect list prediction in development of load plans using the software. This is important in that the vessel operators would have to plan for the incorrect list prediction in developing the load plan. This would be especially challenging since the amount of calculated and/or induced list would vary depending on drafts and vertical location of the center of gravity (VCG or KG), and therefore would not be a constant correction. Based on the MBI hearing testimony [18], vessel operators who used the CargoMax loading and stability software tried to anticipate the induced angle of list based upon this recognized but unquantified discrepancy in TCG.

	CargoMax	MSC GHS Computer Model
Displacement (LT)	34,625	34,516
VCG (ft-BL)	37.25	37.32
LCG (ft-FP)	402.0	401.5
Draft @ LCF (ft-K)	30.1	30.0
Trim (ft-aft)	5.8	5.6
GM uncorrected (ft)	4.69	4.60
FS correction (ft)	0.40	0.37
GM corrected (ft)	4.28	4.23
GM required (ft)	3.64	3.78
GM margin (ft)	0.64	0.45

Table 4-1: Comparison of CargoMax and MSC GHS computer model calculation results for the departure condition of the accident voyage. Drafts are above the keel (K) and GM required is calculated directly using 46 CFR 170.170.

An important note about the hydrostatics calculations regarding hull deflection should be made. Based on the calculation of bending moments for the departure condition [11], the vessel would have experienced a “hogging” hull deflection (i.e. deflected with a concave-down curvature) leading to a difference in the mean draft (average of forward and aft drafts) as compared to the actual measured midship draft. Although the calculation of the deflection based on bending moment is possible in CargoMax, it would require tabulation of structural moments of inertia at a number of frame locations, and this data was not available with the EL FARO CargoMax vessel data. However, it may be estimated that several inches of “hogging” hull deflection could be expected in the full load condition, and this is supported by reviewing historical deck logs for EL FARO Jacksonville departures over the months leading up to the accident voyage, in which forward, midship and aft draft measurements at the full load departure are documented based on crew measurement [see reference 46 for example]. The review suggests typical “hogging”

deflection on the order of 3-5 inches for full load Jacksonville departures. Based on an MSC calculation, for a midship draft near the load line of 30'-2-3/8" (the summer load line draft), the effect of 3-5 inch "hogging" hull deflection would be that the actual vessel displacement would exceed the calculated (without deflection) displacement by 300-500 LT.

4.4. Summary

This section documented the MSC review of the T&S Booklet and review of the CargoMax stability and loading software used onboard the EL FARO and by shore-side personnel for cargo load planning and stability assessment.

The CargoMax stability software used onboard the EL FARO and for load planning by shore-side personnel was neither reviewed nor approved for assessment of loading and hull strength since there was no loading manual required for the EL FARO. However, the EL FARO CargoMax software did contain features to assess hull strength, and the vessel operators relied on these features for assessment of hull girder bending moment in load planning.

The CargoMax software was neither reviewed nor approved for assessment of cargo loading and securing, including calculations required in the Cargo Securing Manual, which had been reviewed and approved by ABS. However, the EL FARO CargoMax software did contain features for assessment of cargo securing, and the vessel operators relied on these features for assessment of LO/LO container loading and securing.

With the exception of recent amendments to several IMO instruments applicable to oil, chemical and gas carriers, there are no requirements for the use of onboard software for vessel stability, strength or cargo loading and securing. Under Coast Guard policy, the master must be provided with the capability to manually calculate stability. However, he may use whatever tools he wishes to assist him in his responsibility to ensure satisfactory stability. The Coast Guard will, upon request, verify that the onboard stability software produces nearly identical results to the approved stability booklet in a number of representative loading conditions. After verification, the Coast Guard will recognize the software as an adjunct to the stability booklet; however, it remains incumbent upon the master to ensure the vessel is compliant with all aspects of the stability booklet.

5. Intact and Damage Stability

5.1. Introduction

Through proper design, loading and operation, a ship should possess enough reserve buoyancy and stability to ensure that with motion in heavy seas and even with some damage and limited flooding it will remain afloat and upright. A ship will remain afloat as long as sufficient buoyant volume exists to support the weight of the ship, its contents and limited floodwater. In order to remain upright the external forces and moments acting on a ship must be counteracted by internal forces and moments sufficient to ensure that the vessel will neither capsize nor heel to an excessive angle considering the conditions the vessel will likely encounter in service; this is ship stability. Assessment of a vessel's stability without damage is "intact stability." Assessment of a vessel's ability to withstand limited damage and flooding is "damage stability."

5.2. Intact Stability

5.2.1. Background

For a conventional ship in a seaway, external forces acting on the ship include primarily wind and wave forces exerted on the underwater and above-water surface area of the hull and any exposed structure including superstructure and above-deck cargo such as container stacks. Internal righting capacity arises from the ship's own weight and buoyant forces providing a righting moment (see Figure 5-1). As the ship is heeled by external forces, the change in the shape of the underwater volume results in a shift in the center of the underwater volume, called the center of buoyancy (B), through which the force of buoyancy (F_B) acts. As long as onboard weights do not shift, the center of gravity (G), through which the resultant weight (W) acts, remains fixed, and a righting moment is created due to the horizontal separation of the lines of action of the forces of weight and buoyancy. This horizontal separation (GZ) is referred to as a "righting arm" or a "righting lever." Depending on the location of the center of gravity and the shape of the underwater hull form, as heel angle is increased, GZ increases, achieves a maximum, and then decreases to zero as the lines of action of weight and buoyancy are again aligned. Heel beyond this point results in capsizing of the ship, and this point is often referred to as the angle of vanishing stability or simply the range of stability.

A plot of righting arms (GZ) as a function of heel angle (ϕ) is called a "righting arm curve" or "stability curve" (because this is based on a static analysis of forces and moments, it is sometimes called a "statical stability curve"). Figure 5-2 shows a righting arm curve for a notional vessel. A plot of righting moments can also be created by simple multiplication of the righting arms with the ship's weight or displacement (based on Archimedes' Principle and static equilibrium, for a floating vessel the weight and buoyant forces are equal and are referred to as the displacement). The area under a righting moment curve to a given angle is the righting energy available to restore the ship to the upright position, and the entire area under a righting moment curve is the righting energy available to resist capsizing (or conversely the energy required to capsize the vessel). For this reason the area under a righting arm curve may be used in evaluating the ability of a ship to resist capsizing. This is the case since the righting arm curve

is simply a scaled version of the righting moment curve (scaled by the displacement or weight of the vessel).

This consideration of “statical stability” as the area under the righting arm curve and available righting energy is sometimes loosely referred to as “dynamic stability” of a vessel. It should be recognized however that this does not consider true dynamics of vessel motion in a seaway, including important mass and mass moments of inertia, and synchronous roll, pitch and heave motions due to alignment of vessel natural periods or frequencies of motion with ocean wave periods or frequencies. Nevertheless, the “statical stability” view of ship stability is comparatively simple and has been used as the primary means for assessing seaworthiness of commercial and military vessels alike. However, dynamic analyses and/or model testing programs to assess true dynamics of vessel motion are often required in vessel design for critical applications or for forensic analyses.

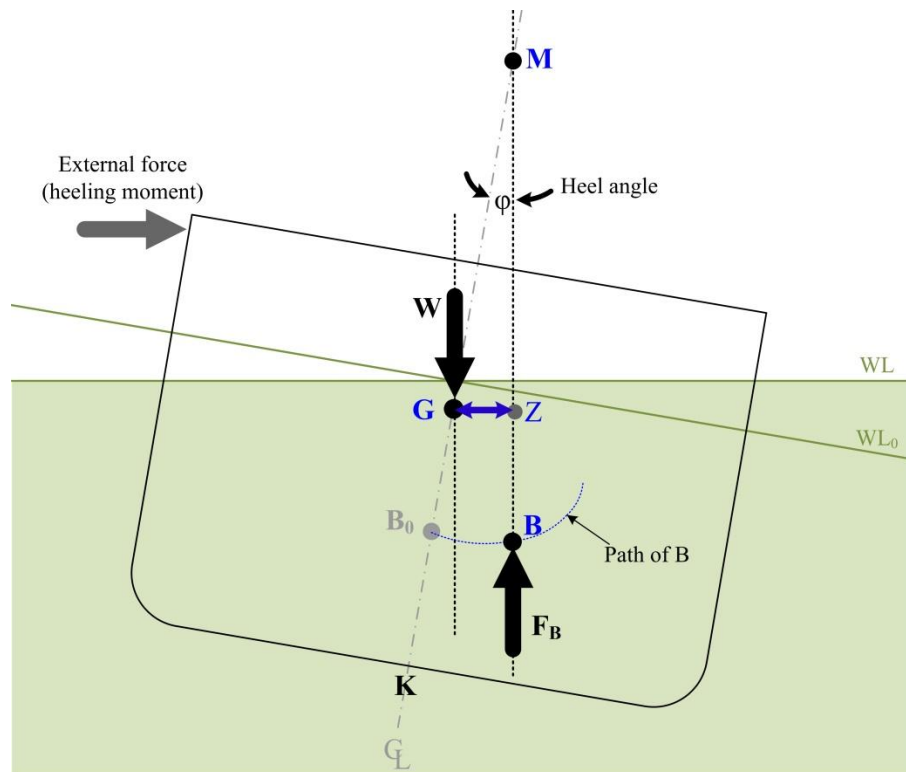


Figure 5-1: Development of righting arms (GZ) (righting moments) with vessel heel due to external forces.

Figure 5-1 includes annotation of an imaginary point through which the lines of action of the buoyant force act as the vessel is inclined through small angles of heel. This point, called the metacenter (M), is the center of the arc traveled by the path of the center of buoyancy (B) through small angles of heel (the distance from B to M is referred to as the “metacentric radius”). However, since the path of B is not a true circular arc for most vessels (other than those with circular cross sections), the metacenter is generally only applicable for small angles of heel where the path of B may be approximated by a circular arc as shown. It should be noted from Figure 5-1 that as long as the center of gravity (G) is below the metacenter (M), then the vessel would have positive righting arms for small angles of heel, and the vessel would return to an

upright condition if disturbed by a small external force. The distance from G to M is called the “metacentric height” or simply “GM,” and its magnitude is frequently used as an indicator of the initial (small angle) stability of a ship. From Figure 5-1:

$$GM = GZ/\sin\phi = GZ/\phi \text{ for small } \phi \text{ (in radians)} \tag{5-1}$$

GM is therefore the initial slope of the righting arm curve. Noting that 1 radian is equal to 57.3 degrees, GM is often annotated graphically on a righting arm curve as shown in Figure 5-2.

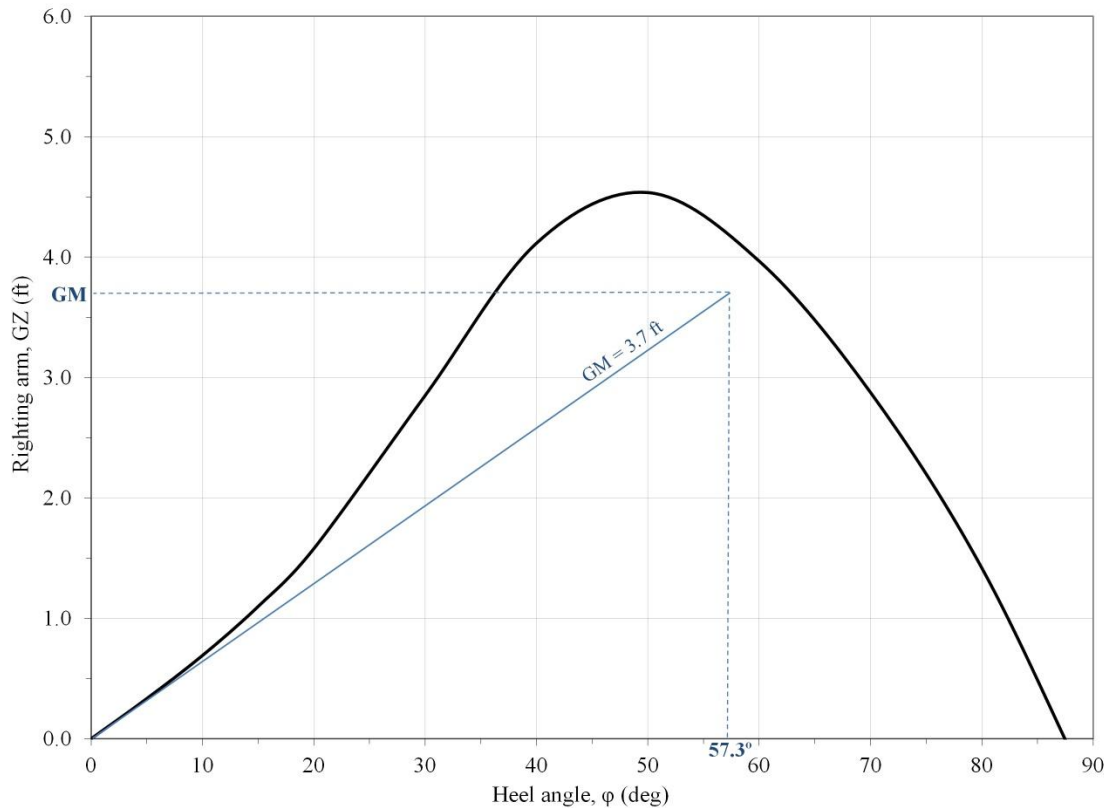


Figure 5-2: A righting arm curve for a notional vessel. GM is the initial slope of the righting arm curve.

Importantly, since GM is only the initial slope of the righting arm curve (and is only applicable for small angles), the magnitude of GM does not give an indication of the magnitude of the maximum righting arm, the angle at which the maximum occurs, the angle of vanishing stability (range of stability), or the area under the righting arm curve (righting energy). Therefore the use of GM as a stability indicator may be misleading if used by itself. However, since calculation of GM is relatively simple compared to calculation of righting arms, GM has been used extensively as a basis for evaluating stability of many types of ships, including general cargo vessels.

5.2.2. Intact Stability Criteria

A thorough discussion of intact stability, including theory and assessment criteria is provided by Moore [47]. A historical perspective of intact stability criteria applicable in the U.S., based on

GM, righting arms, righting moment and righting energy balances, including strengths and weaknesses of each method, is provided by Henrickson [48]. Additional general discussion of stability criteria applicable to U.S. flagged vessels under the U.S. Code of Federal Regulations (CFR) is provided in the U.S. Coast Guard Marine Safety Manual [37]. A historical perspective of the development of international intact stability standards through the International Maritime Organization (IMO) is provided in MSC.1/Circ. 1281 [49].

Intact stability criteria, both in the U.S. and internationally, have historically been developed based on statistical analysis of vessel casualty data. Rahola in his 1939 doctoral thesis [50] discussed the origins of the GM criteria going back to the 1920s. In the 1940s the U.S. Coast Guard refined the GM criteria based on a database using WWII “Liberty Ships” and “T2” tanker type vessels [37]. The developed GM criteria have remained mostly unchanged and are the basis for the current GM criteria specified in 46 CFR 170.170, also referred to as the “weather criteria”, as they specify minimum required GM to limit static heel angle due to a steady wind. The 170.170 weather criteria limit induced static heel due to a prescribed steady wind pressure to the lesser of 14 degrees or the angle to submerge half of the available freeboard. The applied wind heel (moment) is calculated by multiplying a prescribed wind pressure (calculated as a function of vessel length) with the projected lateral area of the vessel above the waterline and the vertical distance from the center (centroid) of the lateral area above the waterline to the center of the underwater lateral area or approximately to the one-half draft point. In equation form the minimum required GM is calculated (46 CFR 170.170):

$$GM_{required} = \frac{P \cdot A \cdot H}{\Delta \cdot \tan T} \quad (5-2)$$

where:

P = $0.005 + (L/14,200)^2$ (LT/ft²) for ocean service

L = LBP (ft)

A = projected lateral area of the vessel and deck cargo above the waterline (ft²)

H = vertical distance from the center of A to the center of the underwater lateral area or approximately half the draft (ft)

Δ = displacement (LT)

T = lesser of either 14 degrees or the angle of heel at which one-half of the freeboard to the deck edge is immersed.

The vessels used in development of the weather criteria had limited superstructure and generally carried their deadweight inside their hull envelope, typically providing a large range of stability and large righting energy, even with relatively small GM [37]. By the 1960s it was realized that some vessels could easily meet the GM weather criteria with little or no righting energy (area under the righting arm curve) and/or with very small range of stability. This became especially evident with the development of offshore supply vessels, which had larger beam-to-depth ratios producing higher GMs, but also lower freeboards causing deck edge immersion at lower angles of heel compared to conventional hulls, consequently resulting in lower range of stability and lower overall righting energy [48]. Figure 5-3 shows comparison of righting arm curves for a conventional cargo vessel and offshore supply vessel circa 1960s (reproduced from [51] with permission) illustrating the lower range of stability and righting energy of the offshore supply vessel. Following the loss of eight offshore supply vessels due to capsizing in the Gulf of

Mexico between 1956 and 1963, the Coast Guard began to apply more stringent criteria to offshore supply vessels based on Rahola’s righting arm criteria [48, 51]. Rahola published his recommended righting arm criteria as part of his doctoral thesis in 1939 [50], basing the recommended criteria on statistical analysis of casualty data from a database using coastal freighters of length 100-300 feet. In the 1960s Rahola’s recommended criteria also became the basis for newly developed international intact stability standards adopted by IMO with Resolution A.167(ES.IV) in 1968, which are the basis for the criteria specified in 46 CFR 170.173 applicable for ships under 100 meters (328 feet) in length (other than tugboats).

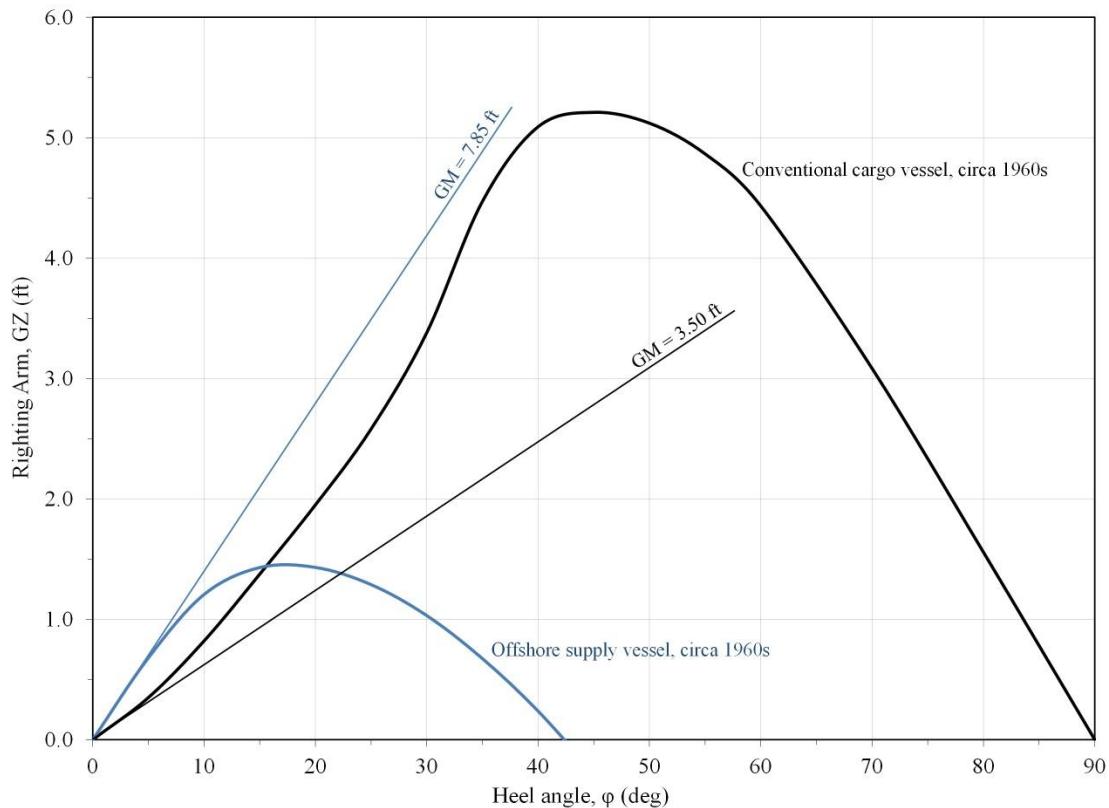


Figure 5-3: Comparison of righting arm curves for a conventional cargo vessel and offshore supply vessel circa 1960s (reproduced from [51] with permission).

Current international intact stability standards are provided in the International Code on Intact Stability, 2008 (2008 IS Code) [52]. Explanatory notes for development of the international standards are provided in the Explanatory Notes to the International Code on Intact Stability, 2008 [49]. The 2008 IS Code includes two parts: “Mandatory Criteria” (Part A) and “Recommendations for Certain Types of Ships and Additional Guidelines” (Part B).

46 CFR 170.165, which became effective in 2011, requires U.S. flagged vessels possessing certain types of international certificates (including International Load Line Certificates) to comply with the Introduction and Part A of the 2008 IS Code, unless permitted otherwise. For the special case of a vessel under the Alternate Compliance Program (ACP), the vessel must meet requirements of SOLAS and the classification society rules, with additional requirements contained in the ACP Supplement for the applicable classification society. The ACP Supplement for ABS [53] states that intact stability of cargo and passenger vessels is to comply with the

applicable parts of Subchapter S (including therefore 46 CFR 170.165, and by reference Part A of the 2008 IS Code, if applicable).

Part A of the 2008 IS Code presents minimum requirements to apply to cargo and passenger ships of 24 meters in length and over, and includes two types of intact stability criteria:

- (1) Criteria regarding righting arm (lever) curve properties (Section 2.2). These were formerly the “general criteria” originally adopted by IMO with Resolution A.167(ES.IV) in 1968, based on Rahola’s righting arm criteria. These criteria are implemented in the U.S. in 46 CFR 170.173. The following righting arm criteria are specified [52]:
 - a. The area under the righting arm curve shall not be less than 0.055 meter-radians (10.3 ft·deg) up to an angle of heel of 30 degrees, and not less than 0.09 meter-radians (16.9 ft·deg) up to an angle of heel of 40 degrees or the angle of downflooding if less than 40 degrees. Additionally the area under the righting arm curve between 30 and 40 degrees, or between 30 degrees and the angle of downflooding if less than 40 degrees, shall not be less than 0.03 meter-radians (5.6 ft·deg).
 - b. The righting arm shall be at least 0.2 meters (0.66 ft) at an angle of heel equal to or greater than 30 degrees.
 - c. The maximum righting arm shall occur at an angle of heel not less than 25 degrees.
 - d. The initial metacentric height GM shall not be less than 0.15 meters (0.49 ft).
- (2) Severe wind and rolling criteria (Section 2.3). These were formerly the “weather criteria” originally adopted by IMO with Resolution A.562(1) in 1985. The criteria were originally developed with the intent to “guarantee the safety against capsizing for a ship losing all propulsive and steering power in severe wind and waves, which is known as a dead ship” [49]. The criteria are based on an energy balance between beam wind heeling and righting moments, with roll motion also taken into account. The method is semi-empirical and based to a large extent on 1950s and 1960s Japanese data and mathematical models for steady wind, wind gusts and ship roll angle in waves. The following righting arm criteria are specified [49, 52], referring to Figure 5-4:
 - a. The ship is subjected to a steady wind pressure acting perpendicular to the ship’s centerline which results in a steady wind heeling arm (lever) l_{wl} . The angle of heel under action of the steady wind φ_0 shall not exceed 16 degrees or 80% of the angle of deck edge immersion, whichever is less.
 - b. From the resultant equilibrium angle of heel due to the steady wind φ_0 , the ship is assumed to roll due to wave action to an angle of roll φ_1 to windward

(upwind). The ship is then subjected to a gust wind of heeling arm l_{w2} . Based on energy balance, under these circumstances, the available or potential energy to resist capsizing to leeward, represented by area A_1 , shall be equal to or greater than the stored energy or work done due to the roll angle to windward, represented by area A_2 , as indicated in the figure. The upper boundary of area A_1 is the limit angle ϕ_2 , which is the lesser of 50 degrees, the angle of downflooding, or the angle of second intercept ϕ_c .

The wind heeling arms (l_{w1} and l_{w2}) are assumed constant at all angles of heel and are calculated as follows:

$$l_{w1} = \frac{P \cdot A \cdot H}{1000 \cdot g \cdot \Delta} \text{ (meters) and } l_{w2} = 1.5 \cdot l_{w1} \quad (5-3)$$

The wind pressure P is specified as 504 Pa (0.074 psi or 0.0047 ton/ft²), which is based on an assumed average wind speed of 26 m/s (50.5 knots) [49]. Area A is the projected lateral area of the ship including superstructure and deck cargo above the waterline. Vertical distance H is from the center of area A to the center of the underwater lateral area or approximately to a point one-half of the mean draft. The displacement Δ is in metric tons (1,000 kg) and the acceleration due to gravity g is 9.81 m/s². Note that this calculation is similar to the 46 CFR 170.170 “weather criteria” calculation but with different assumed wind velocity (pressure) and heel angle limits, so they do not provide for direct comparison.

The roll angle ϕ_1 is calculated as a function of several shape factors which are functions of vessel principal dimensions and coefficients of form, the height of the center of gravity (KG or VCG), and a calculated roll period based on the vessel’s calculated GM.

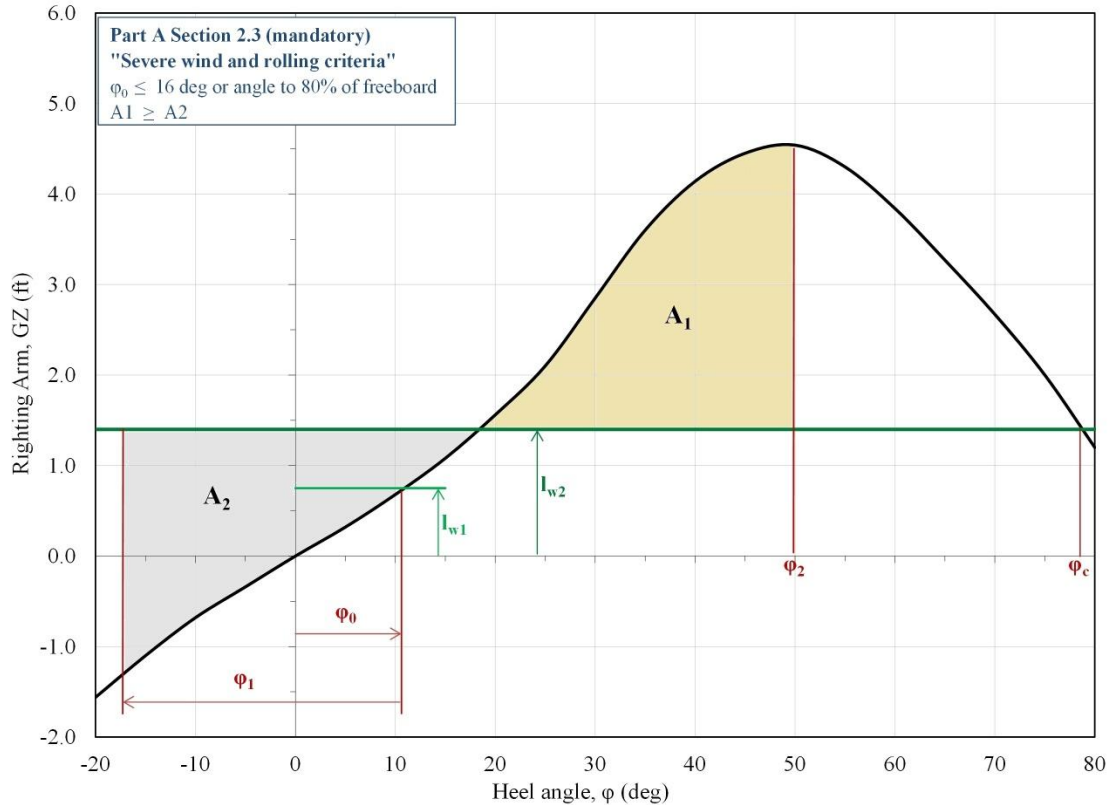


Figure 5-4: IMO severe wind and rolling criteria.

5.2.3. Intact Stability Assessment of EL FARO

5.2.3.1. GM Criteria

Based on date of construction in the 1970s and major conversion in 1992-1993, from a regulatory standpoint EL FARO was required to meet only the intact stability criteria of 46 CFR 170.170 for minimum GM. Since the GM criteria were the only applicable intact stability criteria, the operator of the EL FARO was only required to verify through calculation that the calculated GM, including a free surface effect calculated in accordance with the requirements of 46 CFR 170.285, would exceed the minimum required GM calculated in accordance with 170.170. As discussed in Section 4 of this report, the 170.170 intact stability criteria was the limiting criteria for normal full load operation of the EL FARO, since container stack heights were typically three or higher, in lieu of less restrictive damage stability criteria (although damage stability calculations were not carried out during the 2005-2006 conversion to verify this, see Section 4 of this report).

To provide an overall assessment of the intact stability of the EL FARO, eight “benchmark” loading conditions have been evaluated by the MSC using the MSC GHS computer model. These “benchmark” loading conditions are listed in Table 5-1, which provides a comparison of calculated drafts, trim, free surface correction, GM corrected, GM required, and GM margin for each of the loading conditions. The required GM is calculated using the 46 CFR 170.170 criteria, and the GM margin is the difference between GM corrected and GM required.

The following notes are applicable to all of the MSC calculations:

- (1) The 1993 T&S Booklet [17] full load departure condition is as specified on pages 26-30 and the full load arrival (10% consumables) is as specified on pages 36-40 of the T&S Booklet. The 2007 T&S Booklet [12] full load departure condition is as specified on page 32 and the full load arrival (10% consumables) is as specified on page 33 of the T&S Booklet. The voyage 178S (departed Jacksonville August 11, 2015) full load departure and arrival conditions are as specified in the CargoMax printout for voyage 178S [54] which was printed from the CargoMax load case file “EF178JX.LC” provided by Tote, Inc. It is noted that the arrival condition varies from the departure condition only by a fuel burn-off of 164 LT from each of the DB NO 3 IP and DB NO 3 IS tanks (328 LT total). The accident voyage 185S (departed Jacksonville September 29, 2015) full load departure condition is as specified in the revised CargoMax printout for voyage 185S [11]. The accident voyage estimated condition at the time of the loss of propulsion was derived from the departure condition by subtracting an estimated 240 LT of fuel burn-off, with 55 LT taken from each of the DB NO 3 IP and DB NO 3 IS (110 LT total) and 130 LT taken from the FO SETT tank used as a service tank. This estimate was based on review of the noon reports, estimated burn rates and estimated time to loss of propulsion at approximately 0600 on October 1, 2015. This is discussed in greater detail in Section 6 of this report.
- (2) For all tanks, loading in the MSC GHS computer model was specified based on the tank loading fraction (% full) provided in the reference document (T&S Booklets or CargoMax printouts). For all cargo and miscellaneous items, weights were entered with weights and centers of gravity based on the reference document. As a result of the small differences between the T&S Booklet and CargoMax and the MSC GHS computer model (see Section 2 of this report), small differences in calculated displacement, TCG and LCG are manifested. For tank free surface the GHS software was run to calculate actual free surface effect for each heel angle by direct calculation of the liquid free surface rather than using tabular look-up of free surface inertia or moment values as in the T&S Booklet and CargoMax calculations for each tank.
- (3) A correction was applied to the lightship transverse center of gravity position (TCG) to account for initial vessel list at departure, which was assumed to be zero. This was accomplished in order to correct for the lightship TCG in CargoMax as discussed in Sections 2 and 4 of this report, since it was known through testimony before the MBI that loading was accomplished to achieve a list at departure as close to zero as possible [18, 19, 20]. Based on the assumed zero departure list for voyages 178S and 185S, it was calculated that the lightship TCG should have been approximately 0.3 ft-CL to port (not 0.00 as entered into the CargoMax loading program). For the 1993 and 2007 T&S Booklet calculations, no TCG data was included so it was assumed that the vessel would be at zero list for departure, and lightship TCG was corrected to achieve the zero list for each case. Note that these small lightship TCG corrections have no effect on calculation of vessel drafts and negligible effect on calculation of GM, but are essential for proper assessment of vessel righting arms.

- (4) Wind heel areas were calculated by the GHS software based on entry of vessel profiles including specific deck cargo for each condition. For the 1993 T&S Booklet full load comparison, as the vessel did not have deck containers but included a spar deck for additional RO/RO cargo, the wind heel profile was generated assuming an average trailer height of 13'0" (including container and chassis) closely packed onto the main deck, spar deck and ramp in accordance with the cargo capacity drawings in the 1993 T&S Booklet [17]. For the 2007 T&S Booklet full load comparison, the specified uniform 3-tier profile was generated based on the Capacity Plan [10]. For the voyage 178S full load condition, a profile based on the deck container loading provided in the CargoMax printout for voyage 178S [54] was generated. For the voyage 185S (accident voyage) full load departure condition, the profile based on the deck container loading provided in the CargoMax printout for voyage 185S [11] was generated. Figure 5-5 below shows the resulting GHS model wind heel profiles for the 1993 T&S Booklet full load, 2007 T&S Booklet full load, and voyage 178S full load. The wind heel profile for the accident voyage departure condition is shown in Figure 2-5 in Section 2 of this report.

In general, the calculation results in Table 5-1 show good agreement between the original calculation source (T&S Booklet or CargoMax) and the MSC GHS computer model. Differences in free surface (FS) correction are partially due to differences in tank geometries and calculations as discussed in Section 2, but are also a manifestation of the different methods of free surface calculation. In the T&S Booklets and CargoMax program, free surface calculation is based upon tabulated tank data, while the MSC GHS computer model calculates free surface effect directly based on the actual weight shift of the liquid in the tank. For the 1993 T&S Booklet, free surface corrections are significantly higher due to the application of maximum "slack" values for all intermediate tank levels, noting variable tank data is not included in the 1993 T&S Booklet. For the 2007 T&S Booklet and CargoMax calculations, variable tank data is used, so free surface effect calculations are in closer agreement. It should also be noted that Table 5-1 provides a demonstration of some of the uncertainty in calculated GM discussed in Section 3. As can be seen by reviewing the "GM margin" column, calculated values for the MSC GHS computer model were 0.20-0.25 feet less than the CargoMax-calculated values.

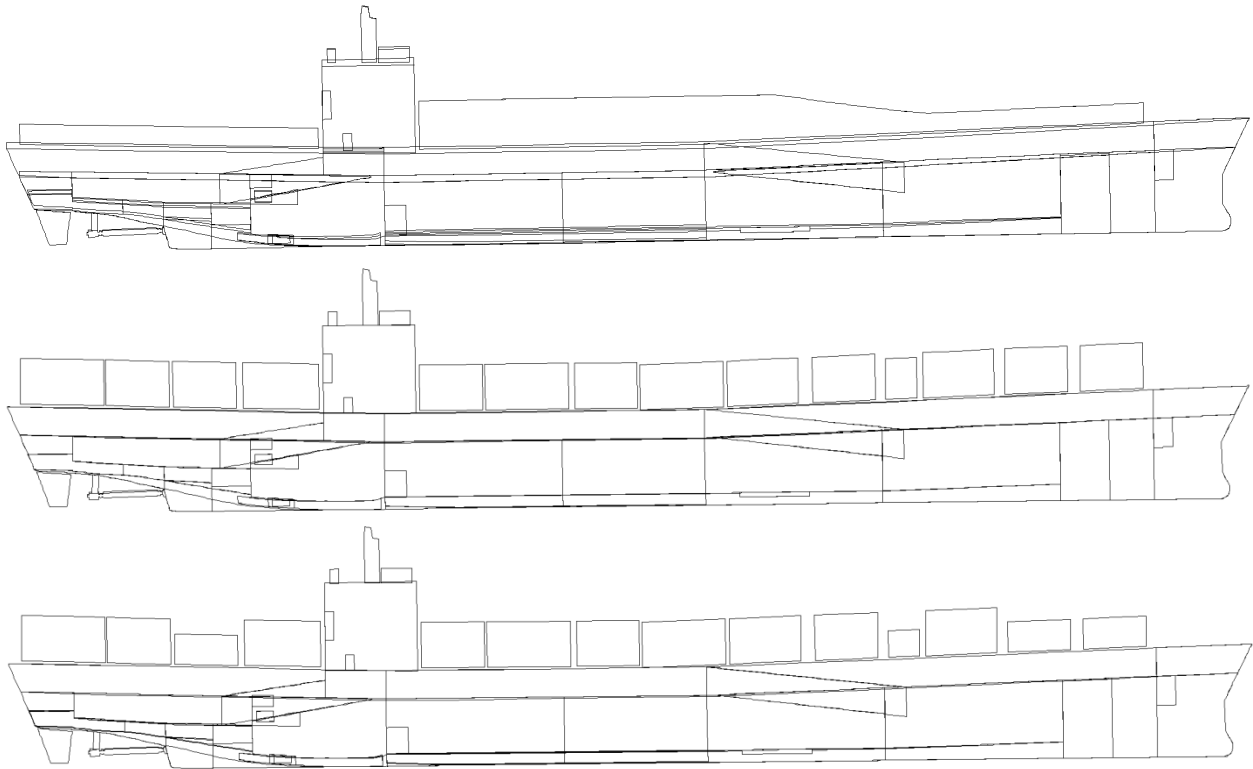


Figure 5-5: MSC GHS computer model wind heel profiles for the 1993 T&S Booklet full load, 2007 T&S Booklet full load, and voyage 178S full load.

	Calculation Source	Displacement (LT)	VCG (ft-BL)	LCG (ft-FP)	Draft at LCF (ft-BL)	Trim (ft-af)	GM Solid (ft)	F.S. Correction (ft)	GM Corrected (ft)	GM Required (ft)	GM Margin (ft)
1993 T&S Book Full Load	1993 T&S Book	31,494	36.65	397.3	28.0	5.0	4.98	0.68	4.30	3.14	1.16
	MSC GHS Model	31,394	36.71	398.1	27.9	5.3	5.51	0.36	5.15	3.35	1.80
2007 T&S Book Full Load	1993 T&S Book (10% consumables)	30,876	37.96	389.8	27.6	1.4	3.75	0.57	3.18	3.13	0.05
	MSC GHS Model	30,704	37.98	389.8	27.5	1.4	3.87	0.39	3.48	3.45	0.03
2007 T&S Book Full Load	2007 T&S Book	34,667	35.36	395.2	30.1	2.1	6.31	0.45	5.87	3.92	1.95
	MSC GHS Model	34,545	35.43	394.6	30.0	1.8	6.12	0.42	5.70	3.88	1.82
Voyage 178S Depart Jacksonville 8/11/2015	2007 T&S Book	32,930	36.70	391.0	29.0	0.7	4.98	0.53	4.45	3.84	0.61
	MSC GHS Model	32,859	36.74	390.4	28.9	0.4	4.79	0.47	4.32	3.92	0.40
Voyage 185S Accident Voyage Depart Jacksonville 9/29/2015	CargoMax	34,964	37.30	401.4	30.3	5.3	4.59	0.40	4.19	3.71	0.48
	MSC GHS Model	34,857	37.37	400.9	30.3	5.1	4.47	0.37	4.10	3.86	0.24
Depart Jacksonville 8/11/2015	CargoMax	34,636	37.61	400.7	30.1	5.1	4.32	0.40	3.92	3.68	0.24
	MSC GHS Model	34,535	37.68	400.2	30.0	4.8	4.16	0.37	3.79	3.83	-0.04
Depart Jacksonville 9/29/2015	CargoMax	34,625	37.25	402.0	30.1	5.8	4.69	0.40	4.28	3.64	0.64
	MSC GHS Model	34,516	37.32	401.5	30.0	5.6	4.60	0.37	4.23	3.78	0.45
Estimated at Loss of Propulsion (0600, 10/1/2015)	CargoMax	34,385	37.41	400.8	30.0	5.3	4.54	0.40	4.14	3.63	0.51
	MSC GHS Model	34,276	37.48	400.3	29.9	5.0	4.40	0.37	4.03	3.74	0.29

Table 5-1: Comparison of the calculated drafts, trim, free surface correction, GM corrected, GM required and GM margin for 8 benchmark loading conditions calculated manually from the T&S Books, using CargoMax, or using the MSC GHS analysis (as indicated). GM margin is the difference between GM corrected and GM required.

5.2.3.2. Righting Arm Criteria

As requested by the MBI, the intact stability of the EL FARO is also assessed in comparison to current criteria which would apply if she were constructed in 2016. If the EL FARO underwent a major conversion in 2016, she might also be required to comply with the current criteria, if it were deemed reasonable and practicable by the USCG.

Based on 46 CFR 170.165 and the ACP Supplement for ABS, since the EL FARO was issued an International Load Line Certificate, she would be required to comply with Part A of the 2008 IS Code. As discussed previously, Part A of the 2008 IS Code is the mandatory part which requires meeting two sets of criteria: (1) criteria regarding righting arm curve properties (Section 2.2 of Part A), and (2) severe wind and rolling criteria (Section 2.3 of Part A). The former is based on the Rahola criteria and is also incorporated in 46 CFR 170.173. The latter is a semi-empirical physics-based method applying an energy balance between beam wind heeling and righting moments, with roll motion also taken into account.

As discussed previously, GM is a good indicator of the initial stability for small angles of heel in response to small heeling forces and moments; however it is in general a poor indicator of overall stability, especially in response to large heeling forces and moments as might be experienced by a vessel in heavy weather where high winds and seas can be expected. The range of stability, maximum righting arm and angle, and area under the righting arm curve are the more important stability characteristics for heavy seas, and GM provides little or no insight into these characteristics. It is instructive to consider the general characteristics of the stability curve of the EL FARO prior to completing numerical assessment in comparison to the righting arm and energy criteria specified by the 2008 IS Code. Noting the previously discussed comparison of righting arm curves for a conventional cargo vessel and offshore supply vessel circa 1960s (Figure 5-3) provided by Mok and Hill [51], it is instructive to plot the righting arm curve for the EL FARO accident voyage departure condition along with these vessels, as shown in Figure 5-6. It is apparent that although the EL FARO had a GM larger than the conventional cargo vessel, the total righting energy available to resist capsizing (represented by the total area under the righting arm curve) is only a fraction of the conventional cargo vessel (16% in this illustration), and is even less than the offshore supply vessel. This is due to lower freeboards causing deck edge immersion at lower angles of heel compared to the conventional hull, resulting in lower range of stability and lower overall righting energy.

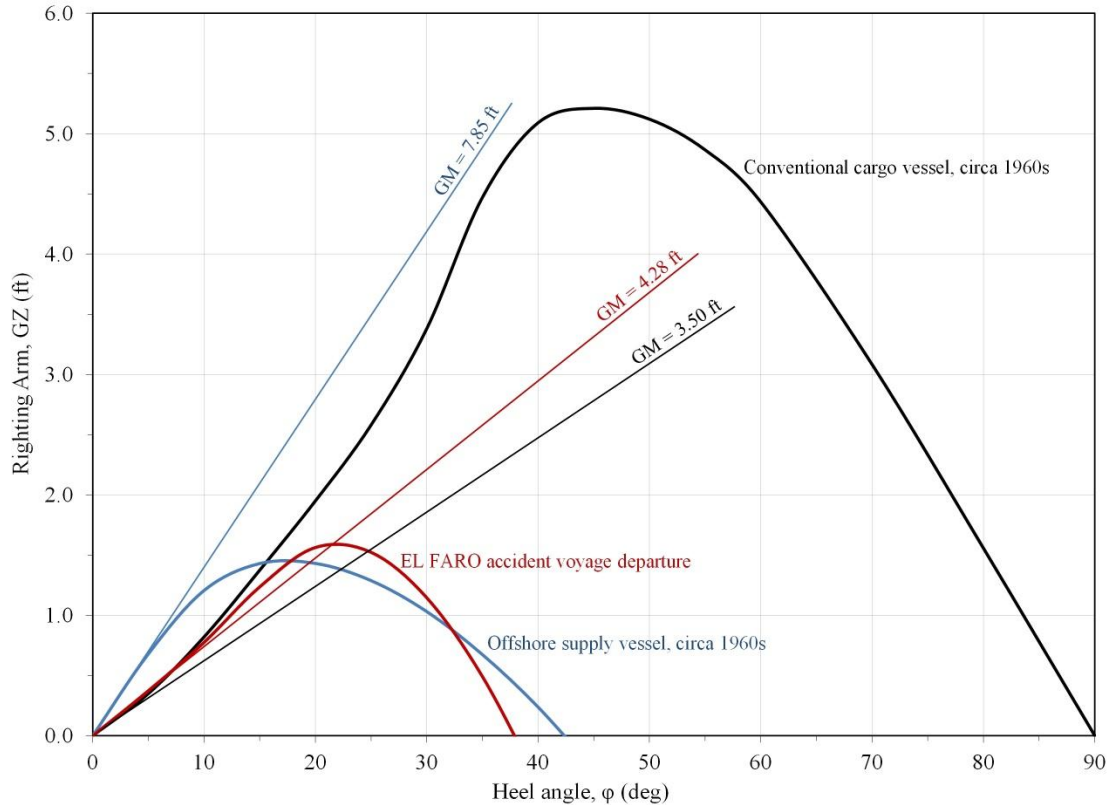


Figure 5-6: Comparison of righting arm curves for the EL FARO accident voyage departure condition with the conventional cargo vessel and offshore supply vessel from Figure 5-3.

The righting arm curves incorporated in Figure 5-3 and Figure 5-6 do not include consideration of the angles at which downflooding would occur for any of the vessels. Including downflooding angles would have the effect of truncating the righting arm curves for evaluation of the righting arm criteria. For the purposes of the evaluation of the intact stability criteria the term “downflooding” means (46 CFR 170.055) “the entry of seawater through any opening into the hull or superstructure of an undamaged vessel due to heel, trim or submergence of the vessel.” The “downflooding angle” is “the static angle from the intersection of the vessel’s centerline and the waterline in calm water to the first opening that cannot be closed weathertight and through which downflooding can occur.” The last statement is of profound importance in the consideration and analysis of the sinking of the EL FARO, as the EL FARO had large open ventilation trunks leading to the cargo holds which would have submerged at angles of heel as low as 27 degrees in the accident voyage loading condition. However, from the definition, these ventilation openings, as they could potentially be closed by means of manually-closable fire dampers, would not have been considered as providing a means of “downflooding” and therefore would not need to be considered in evaluation of the stability criteria, even under the current criteria of the 2008 IS Code. This is in apparent conflict with 46 CFR 92.15-10 which requires that fire dampers remain open at all times in port and underway (except when combating a fire) to provide positive ventilation of the vehicles holds. This will be addressed in greater detail in discussion of the sinking of the EL FARO in Section 6 of this report.

To provide an assessment of the EL FARO intact stability against current standards (i.e. if she were to be built today), the eight benchmark conditions specified in Table 5-1 were evaluated

against the mandatory criteria of Part A of the 2008 IS Code. For an initial comparison, Figure 5-7 provides the righting arm curves for the eight benchmark full load conditions, shown on one plot. Solid curves are the departure conditions and dashed curves are the arrival conditions (loss of propulsion for the accident voyage). One important observation is the reduced righting energy (area under the righting arm curve) and range of stability of the actual departure conditions 178S and 185S compared to the homogeneous full load departure conditions in the T&S Booklets. There are several reasons for this. T&S Booklet full load departure conditions were established to permit the full load arrival conditions (with 10% consumable tank loads) to meet minimum GM criteria with minimum GM margin. Consumable tank (fuel, lube and potable water) “burn-off” to the 10% level is significantly greater than what the EL FARO typically burned during the transit between Jacksonville and San Juan. Therefore, the differences between departure and arrival in the T&S Booklet cases are significantly greater than the differences for the actual voyages (here voyages 178S and 185S). As discussed previously and based upon MBI witness statements [18, 19, 31, 32], the EL FARO often departed Jacksonville loaded with cargo and consumables with GM margin around 0.5 feet in order to arrive in San Juan with GM margin around 0.25 feet. It may also be noted from Figure 5-7 that the range of stability (angle of vanishing stability) is significantly higher for both of the T&S Booklet values. This is due not only to the lower KG and increased GM at departure (reflected in the initial slope of the righting arm curves for the departure conditions) but also to the reduced drafts (increased freeboards) for the arrival condition with 10% consumables. The latter is illustrated by the reduction in draft at the LCF shown in Table 5-1 between the departure and arrival conditions for the T&S Booklet conditions.

For the righting arm curves shown in Figure 5-7, the 2008 IS Code righting arm criteria were applied, with results summarized in Table 5-2. Red (*italics*) indicates that the attained value does not meet the specific criteria and green indicates that the attained value meets the specific criteria. For the general righting arm criteria (Part A, Section 2.2), due to the relatively low range of stability, the actual operating conditions of voyage 178S and the accident voyage 185S do not meet criteria for minimum area between 30 and 40 degrees and minimum angle of maximum righting arm. All of the eight conditions meet the severe wind and rolling righting arm criteria (Part A, Section 2.3). This can be seen in greater detail in Figure 5-8, which illustrates the application of the criteria for the accident voyage (185S). In order for the EL FARO to have fully met the criteria of Part A of the 2008 IS Code at the full load draft, the minimum required GM would have been approximately 6.8 feet, which is 2.5 feet greater than the GM of the actual departure loading condition of the accident voyage.

It is noted that paragraph 2.2.3 of Part A of the 2008 IS Code provides that “alternate criteria based on an equivalent level of safety may be applied subject to the approval of the administration” if obtaining the required 25 degree angle for maximum righting arm is “not practicable.” Thus there could be permitted a relaxation of the limiting criteria for minimum angle of maximum righting arm (25 degrees), if allowed by the USCG on a case-by-case basis. In such a case the minimum required GM could be less, and could also become limited by the damage stability criteria (see Section 5.3 of this report).

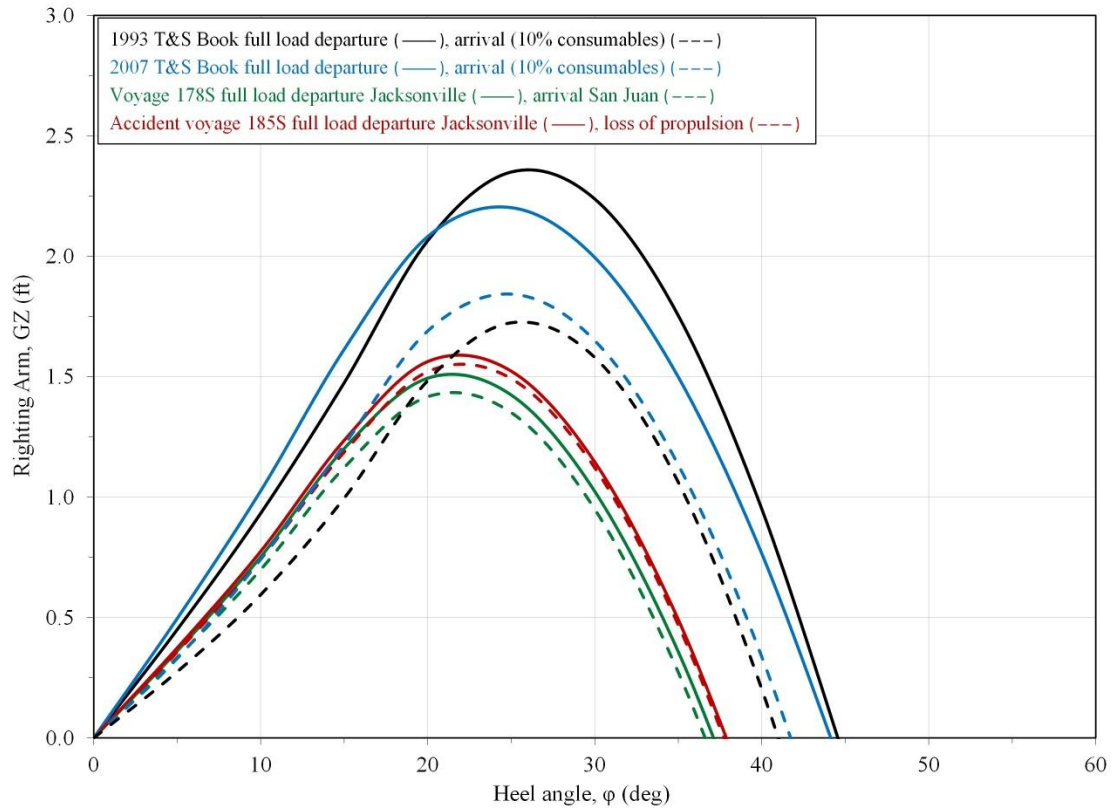


Figure 5-7: Righting arm curves for the eight benchmark full load conditions.

	Units	1993 T&S Book Full Load		2007 T&S Book Full Load		Voyage 178S Full Load Depart Jacksonville 8/11/2015		Voyage 185S Full Load Accident Voyage Depart Jacksonville 9/29/2015		Required Value
		Departure	Arrival (10% Cons.)	Departure	Arrival (10% Cons.)	Departure (Jacksonville)	Arrival (San Juan)	Departure (Jacksonville)	Estimated at Loss of Propulsion (0600, 10/1/2015)	
Part A Section 2.2 - Criteria regarding righting arm curve properties										
Area to 30 degrees	ft-deg	42.2	29.2	42.4	33.3	29.0	27.3	30.5	29.6	At least 10.3 ft-deg (0.055 m rad)
Area to 40 degrees/downflooding	ft-deg	59.2	39.1	57.0	44.1	32.3	29.7	35.1	33.9	At least 16.9 ft-deg (0.09 mrad)
Area between 30 and 40 degrees/downflooding	ft-deg	17.0	9.9	14.6	10.8	3.2	2.4	4.6	4.3	At least 5.6 ft-deg (0.03 mrad)
Maximum righting arm at 30 degrees or greater	ft	2.24	1.58	1.99	1.65	1.00	0.95	1.15	1.12	At least 0.66 ft (0.2 m)
Angle of maximum righting arm	deg	26.1	25.5	24.2	24.7	21.5	21.6	21.9	22.1	At least 25 deg
Initial GM	ft	5.15	3.47	5.70	4.31	4.10	3.79	4.23	4.03	At least 0.49 ft (0.15 m)
Part A Section 2.3 - Severe wind and rolling criteria										
Steady wind heeling arm (k_{w1})	ft	0.300	0.308	0.305	0.326	0.288	0.292	0.286	0.289	NA
Angle of static heel (ϕ_0)	deg	3.3	5.9	3.1	4.9	4.0	4.4	3.8	4.1	Not to exceed 16 deg or angle for 80% of angle to deck edge immersion
Roll angle to windward (ϕ_1)	deg	16.9	15.1	18.3	16.2	16.5	16.1	16.5	16.3	NA
Gust wind heeling arm (k_{w2})	ft	0.450	0.463	0.458	0.490	0.432	0.437	0.430	0.434	NA
Angle of 2nd intercept (ϕ_2)	deg	43.5	39.4	42.9	40.3	35.0	34.4	35.5	35.8	NA
Limit angle for area A_1 (ϕ_2)	deg	43.5	39.4	42.9	40.3	35.0	34.4	35.5	35.8	NA
Stored energy due to the roll angle to windward (Area A_2)	ft-deg	16.3	9.7	20.4	13.1	12.5	11.3	13.0	12.1	NA
Potential energy to resist capsizing to leeward (Area A_1)	ft-deg	47.3	25.2	44.2	29.8	19.6	17.4	22.1	21.0	NA
Area ratio (A_1/A_2)	ft-deg	2.9	2.6	2.2	2.3	1.6	1.5	1.7	1.7	Greater than 1

Table 5-2: Application of the 2008 IS Code criteria to the eight benchmark loading conditions. Red (italics) indicates that the attained value does not meet the specific criteria and green indicates that the attained value meets the specific criteria. The 2008 IS Code would be applicable if the EL FARO were constructed in 2016.

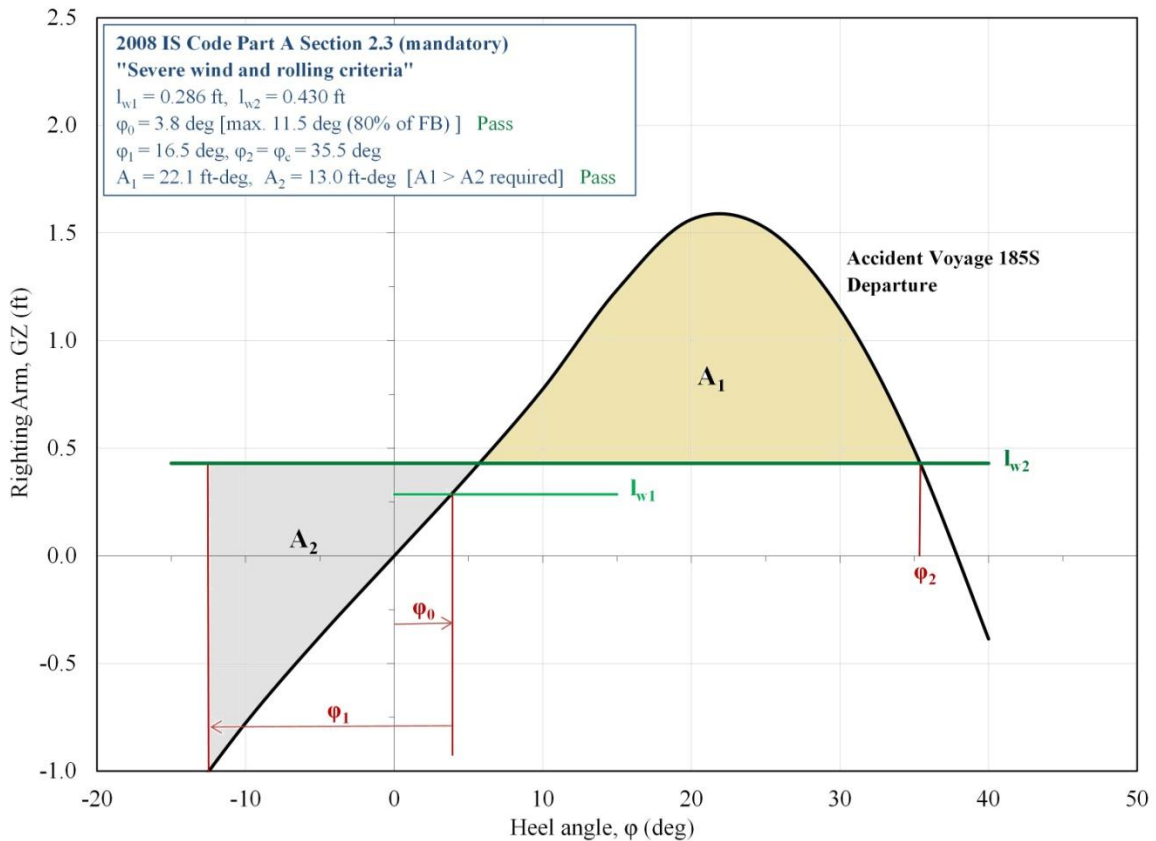
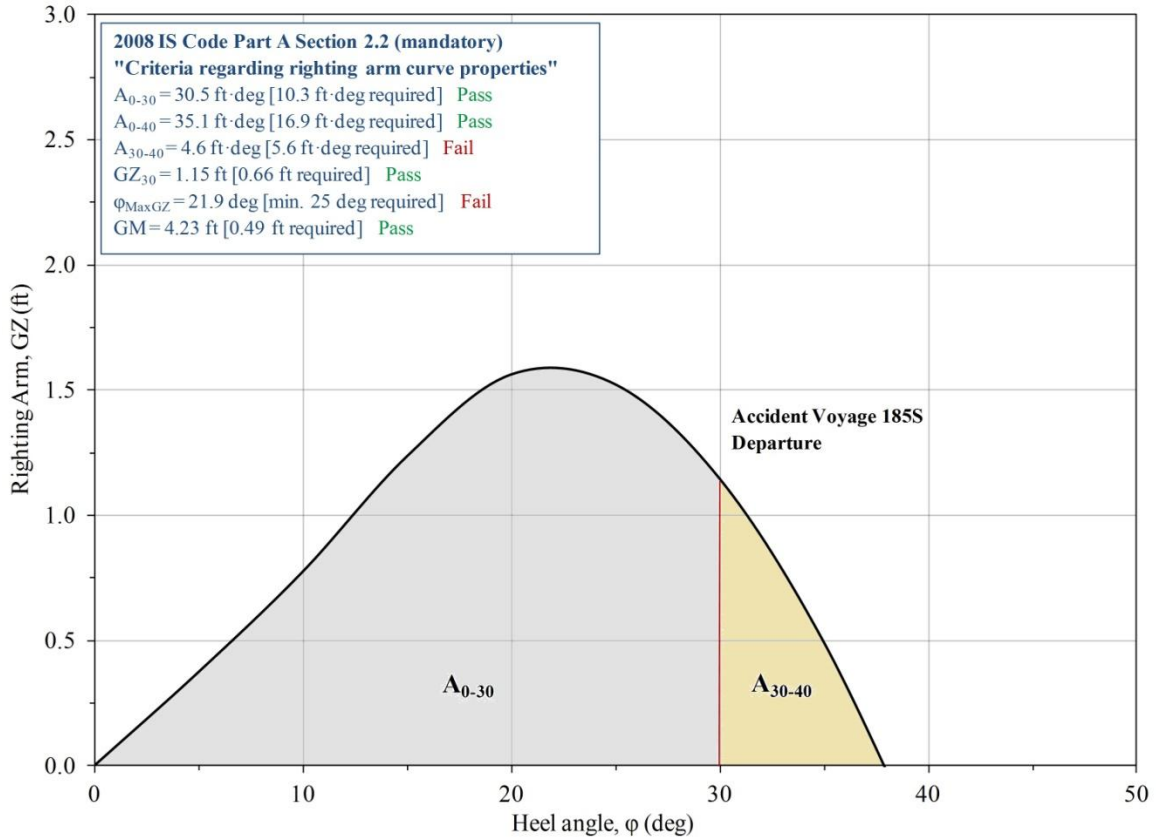


Figure 5-8: Application of 2008 IS Code righting arm criteria to the accident voyage (185S).

5.3. Damage Stability

5.3.1. Background

As stated previously, through proper design, loading and operation, a ship should possess enough reserve buoyancy and stability to ensure that with motion in heavy seas and even with some damage and limited flooding it will remain afloat and upright. Assessment of a vessel's ability to withstand limited damage and flooding is "damage stability." Requirements and regulations for ship subdivision and damage stability date back to the 1854 British Maritime Act, but recent subdivision and damage stability requirements have been primarily initiated through the International Convention for the Safety of Life at Sea (SOLAS) [55]. SOLAS conventions and amendments have been adopted internationally through IMO resolutions. Current SOLAS subdivision and stability standards applicable for dry cargo vessels including RO/RO vessels are implemented in the U.S. in 46 CFR Part 174 Subpart J.

5.3.2. Damage Stability Standards

Early damage stability standards generally consisted of single-compartment standards, which provided for maximum spacing of watertight transverse bulkheads in order to keep the ship sufficiently upright after breaching one of the main compartments [55]. One such standard was a requirement of vessels built under U.S. government subsidy or mortgage guarantee programs administered by the Maritime Administration (MARAD), the MARAD Damaged Stability Standard, also called MARAD Design Letter No. 3 [56]. Until 1992, there were no other damage stability standards applicable to dry cargo vessels such as RO/RO ships. The MARAD single-compartment standard is an example of a "deterministic" standard, in that it is based on specific damage scenarios, including specified extent and location of damage. In order to meet the standard, each damage case (single-compartment) was required to meet prescribed acceptable measures of survival, including limitations on equilibrium heel angle (15 degrees), margin line submergence, downflooding points, range of stability (20 degrees past equilibrium heel angle), GZ (4 inches), and GM (2 inches). Other "deterministic" standards were applicable to various types of vessels required surviving damage to 1, 2 or more compartments, with similar survivability measures [57].

In 1992 "probabilistic" damage stability standards became applicable to dry cargo ships over 100 meters, including RO/RO vessels, which were newly constructed or undergoing major conversions. These standards were incorporated into SOLAS 1990, Chapter II-1 Part B-1 (see [58]), with explanatory notes adopted by IMO Resolution A.684(17) [59]. These standards were subsequently modified and incorporated into SOLAS 2009 (see [60]), with explanatory notes adopted by IMO Resolution MSC.281(85) [61].

Damage survivability criteria based on probabilistic analysis are generally more complex from an application perspective, but are also generally considered to be superior for evaluating relative safety of ships exposed to damage [55]. The SOLAS probabilistic approach takes the probability of survival after a collision as a measure of a ship's safety in the damaged condition. Referring to [58], the measure of survivability is the "attained subdivision index" A. The "required subdivision index" R is a function of ship's length and determines the degree of

subdivision to be provided, through the requirement that the attained index A must be no less than the required index R. The attained index A is calculated by the summation of the products of the probabilities that each compartment or group may be flooded and the probability of survival after flooding of each compartment or group. Written in equation form:

$$A = \sum p_i s_i \quad (5-5)$$

The subscript i represents each compartment or group of compartments, p_i accounts for the probability that only the i^{th} compartment or group of compartments may be flooded, and s_i accounts for the probability of survival after flooding the i^{th} compartment or group of compartments. Calculation of factors p_i is carried out based on formulae involving the vessel's geometry and extent of damage. Calculation of factors s_i is carried out based on formulae involving vessel loading and survivability criteria. It is noted that the s_i values must be weighted according to the draft considerations to average the contributions for the deepest subdivision load line draft and the partial load line draft (as defined by SOLAS 1990). This is equivalent to calculating a separate attained index A for each draft, and then taking the average (this is the way it is implemented in the GHS software as demonstrated in Appendix B). The formulae for p_i and s_i are based on damage statistics as described in the explanatory notes [59].

One important consideration is the specification of permeability values for each compartment. A significant change was implemented in SOLAS 2009 which prescribes permeability of RO/RO spaces differently than those in SOLAS 1990. For SOLAS 1990 (which was applicable in 2005-2006), the prescribed permeability for all dry cargo spaces (including RO/RO spaces) was 0.7. For SOLAS 2009, prescribed permeability values for RO/RO spaces are 0.9 for the deepest load line and partial load line drafts, and 0.95 for the light service draft. There are, however, additional differences in the calculations which make direct comparison between results of SOLAS 1990 and SOLAS 2009 more complicated. However, Tagg [62] discusses in some detail that, in general, for RO/RO cargo ships it has been accepted that the SOLAS 2009 regulations represent a higher standard, but notes that there seems no compelling need to address the safety level of existing ships considering the limited number of ships, the limited consequences, and the rate at which the older ships are being removed from the world fleet.

5.3.3. Damage Stability Assessment of the EL FARO

There is no evidence from the documentation available to the MBI if the EL FARO (originally named PUERTO RICO, then NORTHERN LIGHTS) was built under a MARAD government subsidy, or if the loan or mortgage obligation under the subsidy was still outstanding at the time of implementation of the MARAD Damaged Stability Standard (MARAD Design Letter No. 3) in 1983 [56]. If this were the case, then the EL FARO may have been required to meet the single-compartment damage standard specified in MARAD Design Letter No. 3. There is also no documentation available to the MBI indicating that the EL FARO or any of her sister vessels were evaluated against the MARAD Damaged Stability Standard. It is worth mentioning that, from initial construction until the 1992 lengthening, there were no regulatory damage stability requirements applicable to the EL FARO. It is also of interest to note that the sister vessel EL YUNQUE, which remained in service until 2016, was never subject to regulatory damage stability requirements.

Regardless of the requirements applicable prior to 1992, when the EL FARO underwent the major conversion in 1992-1993, she was required to meet the probabilistic damage stability standard of SOLAS 1990, Chapter II-1 Part B-1. During the lengthening conversion in 1992-1993, SOLAS probabilistic damage stability analyses were completed, reviewed and approved by ABS [63], which confirmed that the limiting stability criteria were the intact (“weather” criteria) for all loading conditions. Thus the minimum required GM curves reflected in the 1993 T&S Booklet [17] were based on the USCG intact stability requirement (46 CFR 170.170).

As discussed in Section 4.2 of this report, in MBI hearing testimony [38, 39, 40] it was noted that Herbert Engineering did not complete a damage stability analysis to confirm that after the 2005-2006 conversion the limiting criteria would remain the intact stability criteria for all loading conditions, and ABS had no records of a damage stability analysis being completed. This is important since the 2005-2006 conversion resulted in a 2-foot increase in the load line draft, and therefore the previous damage stability analysis completed in 1993 no longer applied. In his MBI hearing testimony, Mr. Thomas Gruber of ABS submitted results of his independent SOLAS probabilistic damage stability analysis performed in May 2016 [41], where he applied the damage stability standards of SOLAS 1990, Chapter II-1 Part B-1, which would have been applicable in 2005-2006. Mr. Gruber’s analysis determined that for GM values of approximately 2.9 feet at both the load line and partial load line drafts (30.11 and 26.02 feet), the required subdivision index of 0.60 would be attained. This suggests that for most load conditions with 2 or more tiers of containers loaded, the limiting stability criteria would be the intact stability criteria as reflected in the T&S Booklet, but for some load conditions with less than 2 tiers of containers loaded, the limiting stability criteria could be the damage stability criteria, and this was not reflected on the minimum required GM curves of the T&S Booklet (see Figure 4-1).

As requested by the MBI, the MSC performed independent SOLAS probabilistic damage stability analyses using the MSC GHS computer model and GHS Version 15.00. Two analyses were completed:

- (1) Applying the standards of SOLAS 1990, which would have been applicable following the 2005-2006 conversion
- (2) Applying the standards of SOLAS 2009, which would be applicable if the EL FARO were constructed in 2016

Applying the SOLAS 1990 standards, analyses were run for both the deepest subdivision load line draft (30.11 feet) and the partial load line draft (26.02 feet), with the required subdivision index R calculated as 0.602. Attained indices for both drafts were averaged as discussed above, and KG was iterated until the averaged attained index A equaled the required subdivision index R . Both port and starboard damage cases were investigated, but the more limiting case was the port damage (due primarily to the port side ramps). Details of calculation results are provided in Appendix B of this report. The MSC analyses applying the SOLAS 1990 standards provided similar results to Mr. Gruber’s analysis, but with a slightly higher minimum GM value of 3.3 feet necessary to achieve the required subdivision index of 0.602. This confirms that for most load conditions with more than 2 tiers of containers loaded, the limiting stability criteria would be the

intact stability criteria as reflected in the T&S Booklet. However, for load conditions with 2 or fewer tiers of containers loaded, the limiting stability criteria could be the damage stability criteria, and this was not reflected on the minimum required GM curves of the T&S Booklet (see Figure 4-1). However, as pointed out in Section 4.2, for the full load departure condition of the accident voyage, the limiting stability criteria would have been the intact stability criteria, which was properly reflected in the T&S Booklet and incorporated in the CargoMax stability software, since the majority of the container stacks were 3 tiers.

It should be noted that the MSC calculations were performed using GHS Version 15.00 (released in January 2016), but Mr. Gruber's analysis was completed using GHS Version 8.30, which ABS would have used if they had conducted a review back in 2006 [41]. For comparison, MSC also ran the analysis using GHS Version 8.50, and calculated a minimum GM value of 3.1 feet, as compared to Mr. Gruber's calculated 2.9 feet. This small difference is considered reasonable given likely small differences in vessel models. Similarly, small differences were noted between the results obtained analyzing MSC's model using GHS Versions 15.00 and 8.50. These differences are likely indicative of small changes in the computational algorithms in the software between 2006 and 2016. See Table 5-3 for a complete comparison.

Applying the SOLAS 2009 standards, analyses were run for the deepest subdivision load line draft (30.11 feet), the partial load line draft (26.02 feet) and a light service draft (22.54 feet), with the required subdivision index R calculated as 0.674. The overall attained index was calculated as the weighted-average of the attained indices for the 3 drafts in accordance with the SOLAS 2009 standards (40% for the load line draft, 40% for the partial load draft, and 20% for the light load draft), and KG was iterated until the overall attained index A was equal to the required subdivision index R. In this case, applying the SOLAS 2009 standards, a minimum GM value of 5.8 feet would be necessary to achieve the required subdivision index of 0.674. Note that this minimum GM is greater than would be required for any loading condition based on the 46 CFR 170.170 intact stability criteria (see Figure 4-1).

The large increase in minimum (required) GM is due to the differences in the 1990 and 2009 SOLAS standards as discussed in Section 5.3.2. The most important difference is in the specified permeability for RO/RO cargo holds, increasing from 0.7 in the 1990 SOLAS standards to 0.9 and 0.95 in the 2009 SOLAS standards. This difference is an illustration of the increased level of safety provided by the 2009 SOLAS probabilistic standards discussed by Tagg [62].

A summary of the SOLAS probabilistic damage stability analyses results for the load line draft of 30.11 feet (applicable after the 2005-2006 conversion) are provided in Table 5-3 below. Note that the 2009 SOLAS standards would be applicable if the EL FARO were constructed in 2016.

Analysis	SOLAS Standard	GHS Version	Required index (R)	Required GM (feet)
ABS (Gruber) [41]	1990	8.30	0.600	2.9
MSC	1990	8.50	0.602	3.1
MSC	1990	15.00	0.602	3.3
MSC	2009	15.00	0.674	5.8

Table 5-3: SOLAS probabilistic damage stability analyses results for load line draft of 30.11 feet (applicable after the 2005-2006 conversion). Note that the SOLAS 2009 standard would be applicable if the EL FARO were constructed in 2016.

5.4. Summary

This section provided a primer on basic ship stability and comparison of the EL FARO's stability characteristics against the intact and damage stability criteria applicable to the EL FARO at the time of the casualty, and criteria which would apply if the vessel were constructed in 2016.

The MSC computer model was used to assess eight "benchmark" loading conditions defined by the MSC against intact stability criteria. The eight "benchmark" conditions included the full load departure and arrival conditions from the 1993 and 2007 T&S Booklets, a representative departure and arrival condition from August 2015 (voyage 178S), and the accident voyage (185S) departure condition and estimated condition at the time of loss of propulsion on October 1, 2015.

The eight "benchmark" loading conditions all met the applicable intact stability requirements of 46 CFR 170.170 (the GM "weather" criteria), which were applicable to the EL FARO at the time of the casualty. However, it is noted that the vessel was often operated very close to the maximum load line drafts, with minimal stability margin compared to the required GM, and little available freeboard and ballast capacity, leaving little flexibility for improving stability at sea if necessary due to heavy weather or flooding

If EL FARO were constructed in 2016, she would be required to meet the righting arm criteria of Sections 2.2 and 2.3 of Part A of the 2008 IS Code. Of the eight "benchmark" conditions, only the 1997 T&S Booklet loading conditions would meet the righting arm criteria of Section 2.2. The actual operating conditions of voyage 178S and the accident voyage 185S would not meet the criteria based on limited available area (righting energy) between 30 and 40 degrees and insufficient angle of maximum righting arm. All of the eight conditions would meet the severe wind and rolling righting arm criteria of Section 2.3. In order to fully meet the intact stability criteria of Part A of the 2008 IS Code at the full load draft, the minimum required GM would be approximately 6.8 feet, which is 2.5 feet greater than the GM of the actual departure loading condition of the accident voyage. It is noted that paragraph 2.2.3 of Part A of the 2008 IS Code provides that "alternate criteria based on an equivalent level of safety may be applied subject to the approval of the administration" if obtaining the required 25 degree angle for maximum righting arm is "not practicable." Thus there could be permitted a relaxation of the limiting criteria for minimum angle of maximum righting arm (25 degrees), if allowed by the USCG on a case-by-case basis. In such a case the minimum required GM could be less, and could also become limited by the damage stability criteria.

Despite the 2-foot increase in the load line draft resulting from the 2005-2006 conversion for carrying LO/LO containers, there was no damage stability assessment completed to verify that the EL FARO would remain limited by the intact stability criteria for all loading conditions. Damage stability assessments conducted using the applicable 1990 SOLAS probabilistic stability standards demonstrate that for load conditions with two or fewer tiers of containers, the limiting stability criteria could be the damage stability criteria instead of the intact stability criteria, and this was not reflected on the minimum required GM curves of the T&S Booklet. However, for the departure condition of the accident voyage, the limiting stability criteria was the intact stability criteria, which was properly reflected in the T&S Booklet and incorporated in the CargoMax stability software. If EL FARO were constructed in 2016, she would be required to meet the 2009 SOLAS probabilistic damage stability standards. In order to fully meet these 2009 SOLAS damage stability standards at the full load draft, the minimum required GM would be approximately 5.8 feet, which is 1.5 feet greater than the GM of the actual departure loading condition of the accident voyage.

The righting arm curves for the EL FARO are generally characterized by relatively small area (righting energy) and range of stability compared to conventional cargo vessels (see Figure 5-6). These characteristics are especially significant in consideration of limited residual righting arms and righting energy with the vessel subjected to heeling forces and moments as might be experienced in heavy weather where high winds and seas can be expected. These characteristics are significant in consideration of limited residual righting arms and righting energy when subjected to flooding.

6. Hydrostatic Sinking Analyses

6.1. Introduction

Hydrostatic sinking analyses are conducted using the MSC GHS computer model utilizing additional information provided by the MBI including estimated fuel burn-off at the time of the loss of propulsion, estimated sea state and wind conditions at the time of the loss of propulsion and sinking, details of potential downflooding and progressive flooding paths, and additional information gained through review of the VDR audio transcript [64].

The MSC analyses are based upon a first principles approach. The term “hydrostatics” is meant to limit the scope to consideration of quasi-static forces including effects of floodwater, wind, and waves. Through assessment of righting arms, including righting energy and range of stability considerations, the analyses are intended to provide some insight into characteristics of vessel dynamics and motions in a seaway. The analyses, however, do not consider true dynamics of vessel motion in a seaway, including important mass and mass moments of inertia, and synchronous roll, pitch and heave motions due to alignment of vessel natural periods or frequencies of motion with ocean wave periods or frequencies. In addition to consideration of transverse stability effects due to wind, waves and flood water, longitudinal stability effects are included accounting for vessel sinkage and trim.

6.2. Vessel Loading and Environmental Conditions

At the time of the loss of propulsion, at approximately 0610 on October 1, 2015 [64 (pp. 438-440)], approximately 240 LT of fuel would have been burned since departure from Jacksonville. This estimate is based upon review of the ship’s noon reports and typical burn rates based on previous voyages. Also, based on records of previous voyages, the crew would have replenished the fuel oil (FO) settling (service) tank from tanks FO DB 3 IP and IS (port and starboard), most likely twice a day during the 0400-0800 and 1600-2000 watches. It is unknown if the engineers actually transferred fuel on the 0400-0800 watch on the morning of October 1st, but it is considered highly unlikely due to the events unfolding, including problems with lube oil and eventual loss of propulsion [64 (pg. 338)]. For this reason it has been assumed for these analyses, that of the estimated 240 LT of fuel burned, approximately 110 LT would have been transferred from DB 3 IP and IS (55 LT each), leaving 130 LT net burn-off from the FO settling tank. The loading condition at the time of the loss of propulsion was based on this estimate.

At the time and location of the loss of propulsion and sinking, the EL FARO was in close proximity to Hurricane Joaquin. The precise wind and sea-state conditions are not known, as the nearest weather data buoy was hundreds of miles away and the ship did not have a working anemometer [64 (pg. 397)]. However, Fidele et.al. [65] provide hindcast analyses and numerical simulations, from which wind and wave conditions at the time and location of the loss of propulsion and sinking can be estimated. Estimated wind and wave conditions are summarized in Table 6-1. These wind and wave estimates were averaged based on hourly statistics from the simulations. The “significant wave height” is defined as the statistical average of the highest 1/3 of the waves measured (simulated), with height being measured from peak to trough. The

“dominant wave period” is the wave period corresponding to the maximum energy (peak of the wave spectrum), and is equal to either the swell period or wind-wave period.

Significant wave height (feet)	25-30
Dominant wave period (seconds)	10-11.5
Dominant wave direction	Northerly
Average wind speed (knots)	70-90
Dominant wind direction	Northerly

Table 6-1: Estimated wind and wave conditions based on hindcast analyses and numerical simulations by Fidele et.al. [65].

Wind and wave directions from the simulations are slightly different than those based on actual ship and storm track data provided in the NTSB Weather Group Factual Report [66], which suggests wind and waves were from the east or northeast during the final hours prior to sinking. This is illustrated in Figure 6-1 which shows the actual EL FARO track and Joaquin storm track over the morning hours on October 1, 2015 (as annotated). As can be seen on the graphic, prior to the loss of propulsion, the vessel was heading east-southeast, with winds generally off the port bow. Following the turn to port and loss of propulsion around 0600, until the sinking around 0740, the ship was drifting in a southwesterly direction. Based on hydrodynamic considerations, the ship would likely have been drifting during this time with beam to the wind and waves. Based on normal counter-clockwise storm rotation, it can be estimated that the winds were out of the northeast at 70-90 knots (sustained) between 0600 and 0740. This is consistent with the statement made by the Captain at 0710 on the VDR transcript [64 (pg. 477)].

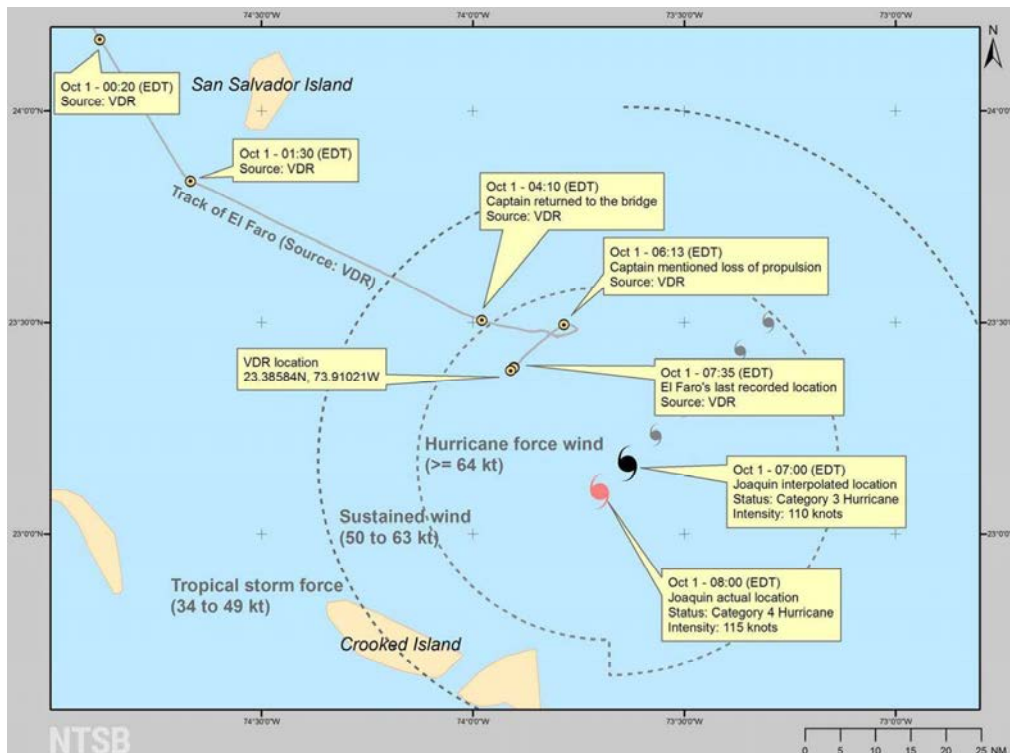


Figure 6-1: EL FARO track and Hurricane Joaquin storm track around the time of loss of propulsion and sinking. NTSB graphic.

6.3. Wind Heel

Early in the morning of October 1st the EL FARO crew discussed a noticeable list (heel angle) to starboard [64]. The crew initially believed the starboard heel to be wind-driven, being caused by the relative wind direction off the port beam as the ship headed southeast. After the turn to port and loss of propulsion around 0600, EL FARO maintained a heel to port, with wind off the starboard beam as she drifted to the southwest, as shown in Figure 6-1.

The exact magnitude of the heel during the early morning hours prior to 0518 [64 (pg. 406)] was not stated clearly in the audio transcript, but one statement which may have sounded like “eighteen degrees” was made (although the transcript notation makes this statement uncertain). It was not until the Captain prepared to call ashore that the first clear statement of a “fifteen degree list” (heel angle) was discussed at 0710 [64 (pg. 478)]. Unfortunately, nowhere in the audio transcript was the heel angle clarified further beyond this estimate and nowhere was any statement made as to the angles of dynamic roll the ship had been experiencing through the morning hours. It can only be interpreted by the Captain’s statement that the ship was experiencing a mean heel angle of about 15 degrees but was also rolling about this mean heel angle due to wave action.

The force of wind acting on the above-water surface area of a hull and any exposed structure including superstructure and above-deck cargo produces a heeling moment tending to heel the vessel from its upright equilibrium. For a steady wind (or prolonged gust) in calm water, a ship will achieve an equilibrium heel angle when the wind heeling moment is balanced by the righting moment. As discussed in Section 5 of this report, the wind heeling moment is fundamentally calculated by multiplying the wind pressure (P) with the projected lateral area of the vessel (including deck cargo) above the waterline (A) and the vertical distance from the center of the lateral area above the waterline to the center of the underwater lateral area (H). For assessment of intact stability criteria the wind pressure is prescribed based on statistical analysis of vessel casualty data as discussed in Section 5 of this report. More generally however from fluid mechanics a wind pressure is calculated from wind velocity using

$$P = C \frac{1}{2} \rho V^2 \quad (6-1)$$

where C is a dimensionless drag coefficient, ρ is the density of air and V is the wind velocity. A common calculation of P in U.S. units is based on a combined coefficient using

$$P = 0.0035 V^2 \quad (6-2)$$

with V in knots and P in lb/ft². A combined coefficient 0.004 has more commonly been used based on U.S. Navy criteria, but the slightly lower value of 0.0035 based on experimental model testing on different ship types and superstructure forms is also commonly used [47].

The desired expression for wind heeling moment (HM) as a function of heel angle ϕ is developed by considering that the effective area subject to the wind (A) and the vertical distance

(H) are both reduced approximately with the cosine of the heel angle ($\cos \varphi$), and therefore the heeling moment is

$$HM(\varphi) = PAH \cos^2 \varphi \tag{6-3}$$

Dividing the heeling moment by the displacement gives the desired expression for the heeling arm (HA). Combining, an expression in U.S. units is

$$HA(\varphi) = \frac{0.0035 V^2 AH}{2240 \Delta} \cos^2 \varphi \tag{6-4}$$

with V in knots, A in ft^2 , H in ft, Δ in LT, and HA in ft.

For a steady wind (or prolonged gust) in calm water the ship would reach an equilibrium angle where the wind heeling moment (heeling arm) is balanced by the righting moment (righting arm). The residual righting arms are then calculated by simple subtraction of the heeling arms from the righting arms at each angle φ . The residual righting energy as the vessel is heeled by the wind (i.e. the reduced energy available to resist capsizing) is the area under the residual righting arm curve. This is shown graphically in Figure 6-2, which uses the EL FARO accident voyage condition at loss of propulsion, with 80 knot beam wind. Note that this condition does not consider the effects of flooding or cargo shifting, which will be addressed subsequently.

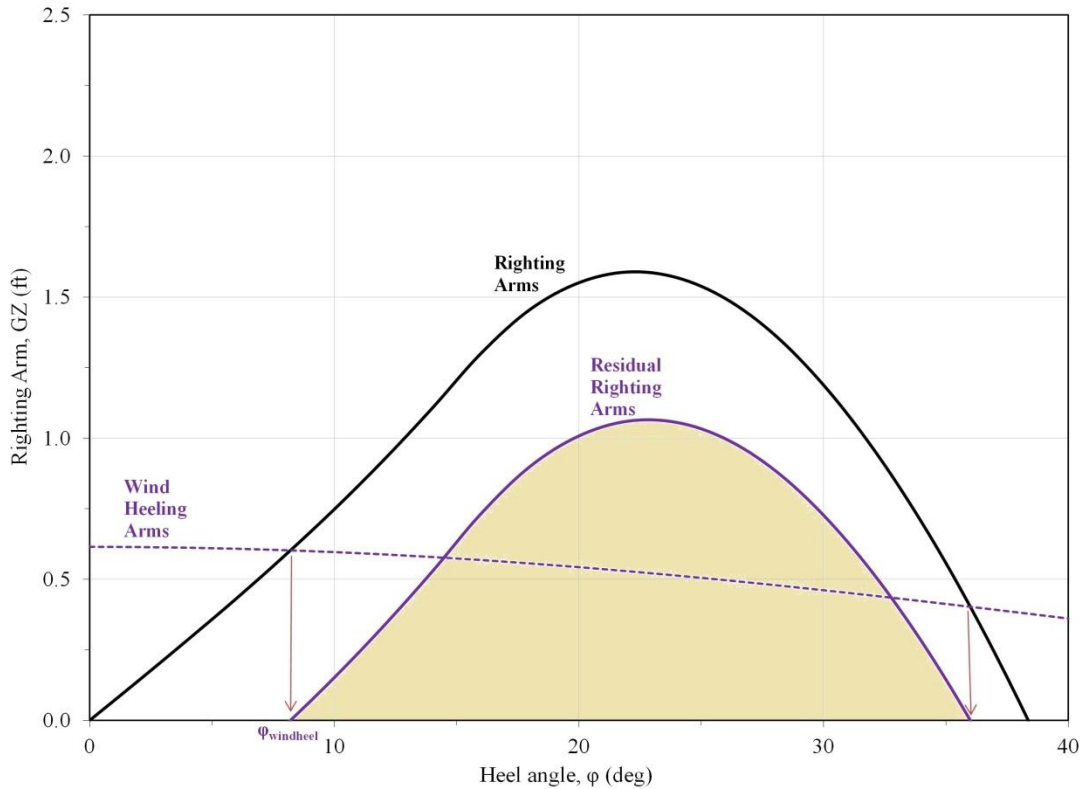


Figure 6-2: Effect of wind heeling arms on the righting arms, shown for the accident voyage condition at the time of loss of propulsion, with 80 knot beam wind (not including effects of flooding or cargo shifting). Starboard heel is shown.

Figure 6-3 provides a graphical illustration of the effects of various beam wind velocities (from 40 to 120 knots) on the righting arm curve for the accident voyage condition at the time of loss of propulsion (not including effects of flooding or cargo shifting). From the plots and based on the estimated wind conditions at the time of the loss of propulsion from 70-90 knots, it can be estimated that a wind heel angle of 7-11 degrees could be attributable to the steady beam wind alone. This does not include dynamic roll effects, as the ship would roll about the wind heel angle due to wave-driven roll motions. This also does not include the effects of flooding including the important free surface effects, as will be addressed subsequently.

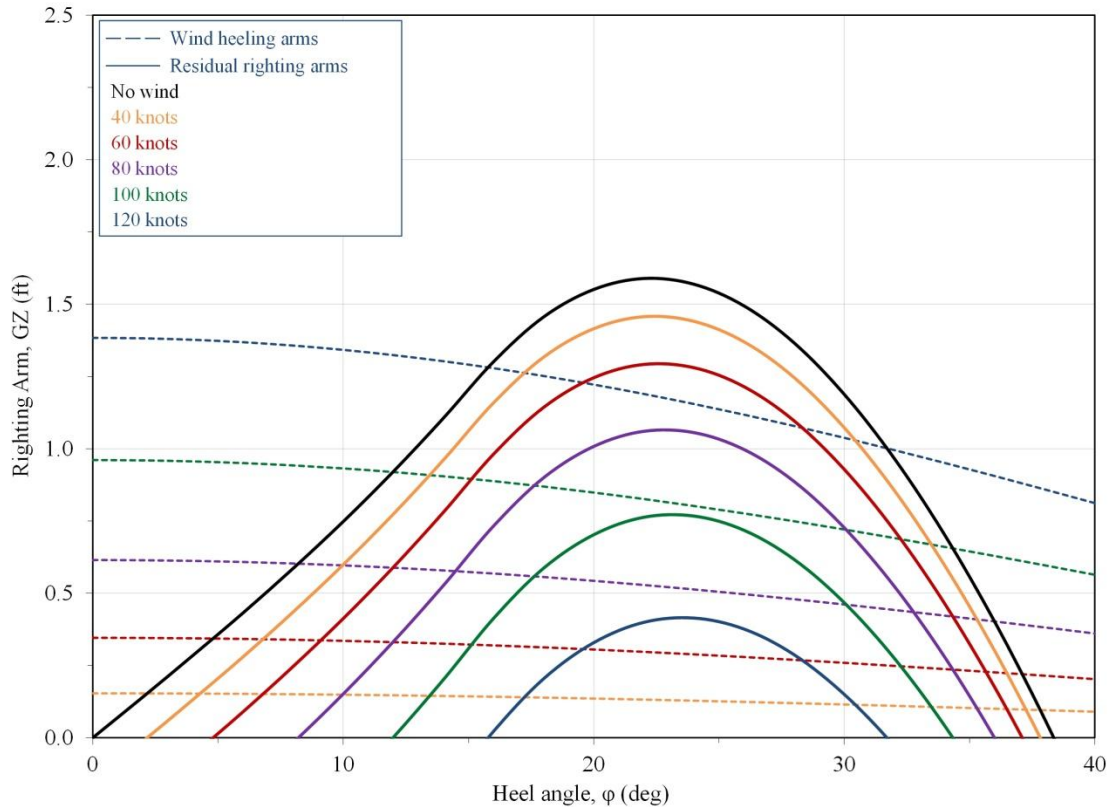


Figure 6-3: Heeling arms for beam winds from 40 to 120 knots (dashed curves) and residual righting arms (solid curves) for the accident voyage condition at the time of loss of propulsion (not including the effects of flooding or cargo shifting). Starboard heel is shown.

6.4. Flooding

6.4.1. General Effects of Flooding

From a hydrostatics, stability and trim perspective, flooding results in three primary effects. First, floodwater adds weight to the ship. The added weight increases the draft and may also cause the vessel to trim, depending on the location of the floodwater relative to the longitudinal center of flotation (LCF). If a flooded compartment is not symmetric about the centerline of the ship, the weight of the floodwater may also cause the vessel to heel. Of course, if sufficient floodwater is added to the ship to submerge additional openings in the hull, then the vessel can progressively flood and founder or sink. From a stability perspective, being below or at the

external waterline (once equalized with the sea), the weight of floodwater is low and therefore generally lowers the center of gravity of the ship (VCG) and therefore increases GM and correspondingly increases righting arms (GZ). Thus one effect of flooding is a stabilizing effect.

Second, as floodwater in compartments usually involves free surface, which is free to move as the vessel rolls and pitches (heels and trims) unless water completely floods a compartment to the overhead, there is an additional horizontal and vertical shift in the ship's center of gravity, and this is detrimental to the stability of the vessel. Specifically, the effect of the free surface is a resulting horizontal and vertical shift of the center of gravity due to the shifting of the weight of the "wedge" of liquid on the free surface, as illustrated in Figure 6-4. This resulting shifting of the ship's center of gravity (G_0G) reduces the righting arms and has the equivalent effect on the righting arms (GZ) as a virtual rise in the center of gravity (G_0G_v). This virtual rise in the ship's center of gravity is the same as the "free surface correction" (FSC) applied to GM for intact stability analysis. Free surface is always detrimental to the stability of the vessel. The horizontal component of the weight shift also results in an increase in angle of heel or trim. For flooded compartments with large free surface areas, especially those with full-beam widths such as cargo holds, the free surface effect can be significant. The free surface effect is also important for tanks carrying liquids which are neither empty nor full, and is included in the "free surface correction" discussed in previous sections of this report. A more thorough discussion of free surface effects is provided by Moore [47]. Note that as the liquid level in a compartment or tank is raised toward the overhead, the free surface effect is significantly reduced (and eventually eliminated as the compartment or tank is completely filled). This reduction in the free surface effect as the liquid level approaches the compartment or tank overhead is known as "pocketing," and is important for many conditions of flooding.

A third effect of floodwater arises if a flooded compartment is not symmetric about the centerline plane of the ship and the compartment is open to the sea (for example through a side-shell or bottom hull breach), then water is able to freely communicate with the sea, and this exacerbates the free surface effect. In the case of the EL FARO, this "free communication effect" would not have existed for flooding of the cargo holds since the cargo holds were symmetric about the ship's centerline.

The rate of flooding through an opening of a given size and shape can be estimated through calculation using principles of fluid dynamics. Calculation can be carried out for flow through an "orifice", derived from the steady form of Bernoulli's equation (see for example [67]). The pressure or head driving the flow is due to the external water pressure above the opening, and the volumetric flow rate Q (ft^3/s) can be calculated from the standard equation for flow through a "sharp-edged orifice":

$$Q = C_D A_0 \sqrt{2gH_E} \quad (6-5)$$

where A_0 is the area of the opening (ft^2), C_D is a dimensionless coefficient of discharge which depends primarily on the geometry of the opening (approximately 0.6 for flow through a sharp-edged opening), g is the acceleration due to gravity (32.2 ft/s^2), and H_E is the external hydrostatic water head (height) above the opening (ft). Figure 6-5 illustrates the geometry of the flow.

As a simple example, for a small opening of area 1 ft^2 located 1 ft below the external waterline, the calculated flow rate (Q) is approximately $4.8 \text{ ft}^3/\text{s}$, which is equivalent to 36 gal/s or $2,160 \text{ gal/min}$. Noting that the bilge pumping system on EL FARO had a capacity less than $1,000 \text{ gal/min}$, the bilge pumping system would be ineffective at keeping up with flooding through even a small opening just below the waterline.

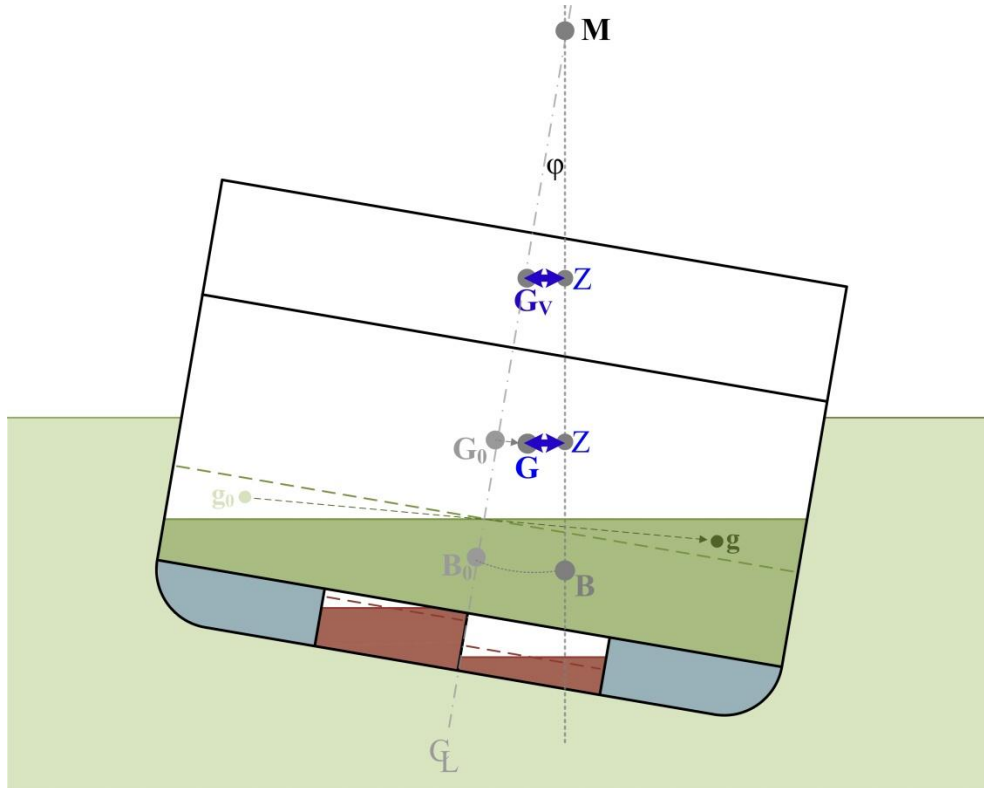


Figure 6-4: Flooding and free surface effect. Shifting of the ship's center of gravity (G_0G) has the equivalent effect on the righting arms (ZG) as a virtual rise in the center of gravity (G_0G_v).

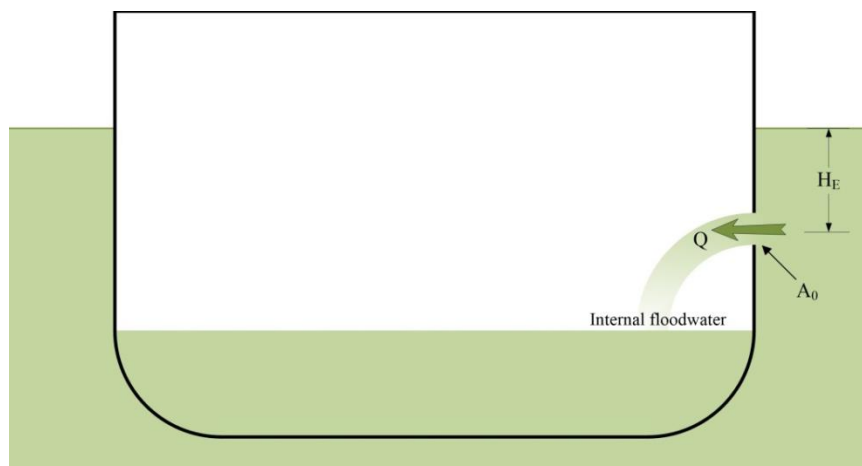


Figure 6-5: Geometry and nomenclature for the Bernoulli's equation for orifice fluid flow for calculation of flooding rate.

6.4.2. Potential Sources of Flooding

Based on the VDR audio transcript, it was not until 0543 [64 (pg. 414)] that first mention was made by the EL FARO crew that the ship might be taking on water into a cargo hold (Hold 3). Upon investigation by the Chief Mate, the initial assessment was that the source of flooding into Hold 3 was through the improperly secured personnel access scuttle on the starboard side of the 2nd deck, located at frame 163 (see Figure 6-6). This scuttle was subsequently secured, but the water level continued to rise in Hold 3 throughout the morning, indicating that there was another source or multiple sources of flooding.

During the final hour the crew attempted to identify potential sources of additional water ingress into cargo Hold 3. Based on a statement by the Chief Mate [64 (pg. 482)], the Chief Engineer identified the potential for flooding from the emergency fire pump piping, which was located on the 4th deck (tanktop, innerbottom) in the aft starboard corner of Hold 3 (see Figure 6-7). It was speculated that it may have been damaged by floating automobiles which had broken free in the lower hold. Although no visual identification of this potential source of flooding was made, the crew discussed potential methods of isolating the emergency fire pump piping from the engine room. There was no discussion on the audio transcript of closing the sea chest isolation valve with the hand-wheel remote operator from the 2nd deck starboard side (see Figure 6-6 and Figure 6-7).



Figure 6-6: Hold 3 (also called Hold D) starboard personnel access scuttle on the 2nd deck at frame 163. Note that the scuttle opening is 12 inches above the deck. The hand-wheel remote operator for the emergency fire pump sea-chest isolation valve is also shown. Screen capture from video taken aboard EL FARO September 2008 provided by Tote Inc.

Although there is no evidence suggesting a hull fracture or hull damage which may have caused additional flooding, there remains the unlikely possibility that some unspecified hull damage may have occurred and contributed to the continued flooding of Hold 3. There was no specific

discussion of hull failure on the VDR audio transcript (other than an apparent misstatement by the Captain when trying to contact his shore-based support, where he referred to a “hull breach” but then quickly corrected by stating “...a scuttle blew open during a storm” [64 (pg. 474)]). Based on review of the underwater video from the Navy Remotely Operated Vehicle (ROV), the MSC noted that the bottom of the hull is immersed in the sediment and cannot be seen in entirety, but based on what can be seen, there appears to be no visual evidence of structural damage in the amidships region of the hull. Given that the vessel was loaded in a “hogging” condition (see Section 4.3 of this report), any significant hull girder structural failure would likely have resulted in compressive buckling of the bottom plating and/or tensile fracture of the upper decks. For significant bottom plate buckling of the hull, there would likely have been some visual evidence including buckling creasing of the lower side shell above the sediment. There was no evidence of buckling creasing of the side shell or tensile fracture of the upper decks on the underwater video.



Figure 6-7: Emergency fire pump station in Hold 3, aft starboard 4th deck (tanktop, innerbottom), showing the sea chest, isolation valve, and manual remote operator on sister vessel EL YUNQUE (EL FARO similar but not identical). Inset photo shows part of the arrangement onboard EL FARO. USCG photo with Tote, Inc. photo inset.

A potential source of continued and progressive flooding was through the cargo hold ventilation system. This potential source might have been mentioned by a crew member at 0600 [64 (Pg. 428)], but it is not clear from the audio transcript if the crew recognized the potential for flooding through the ventilation system or if they ever gave any consideration to trying to limit flooding by shutting the fire dampers.

The cargo hold ventilation system consists of ventilation supply trunks with integrated supply fans and fire dampers and ducting, and ventilation exhaust trunks with integrated fire dampers and ducting. The supply and exhaust trunks for Holds 2, 2A and 3 were all similar in configuration and differed primarily in internal details and height due to the sheer of the 2nd deck, with the Hold 3 openings being the lowest and closest to the waterline due to deck sheer and vessel trim aft. Figure 6-8 shows a photograph of the EL FARO port side, highlighting the ventilation supply and exhaust hull openings for Hold 3.

Scaled drawings of sections at frames 143 and 159 showing the supply and aft exhaust arrangements are provided in Figure 6-9. The section at frame 143 shows the Hold 3 ventilation supply arrangement. The supply arrangement includes an external hull blister with side shell louvered openings, baffle plates, bellmouth, supply fan, fire damper and supply plenum. The louvered openings are forward and aft of the bellmouth, separated by the vertical baffle plates. The section at frame 159 shows the Hold 3 aft exhaust arrangement. The exhaust arrangement includes an intake plenum, a fire damper, and an exhaust trunk with a 12-ft high baffle plate and side shell louvered opening. The louvered opening is forward of the fire damper trunk, separated by the vertical baffle plate. Based on the system design, the baffle plates were intended to provide a vertical boundary to limit water from entering the cargo hold through the fire dampers. For the accident voyage, the tops of the baffle plates were approximately 25 feet above the still waterline, and they would submerge at an angle of heel of approximately 27-29 degrees.



Figure 6-8: EL FARO port side showing ventilation supply and exhaust louvered hull openings. The openings for Hold 3 are highlighted. Photo copyright Will Van Dorp, used with permission.

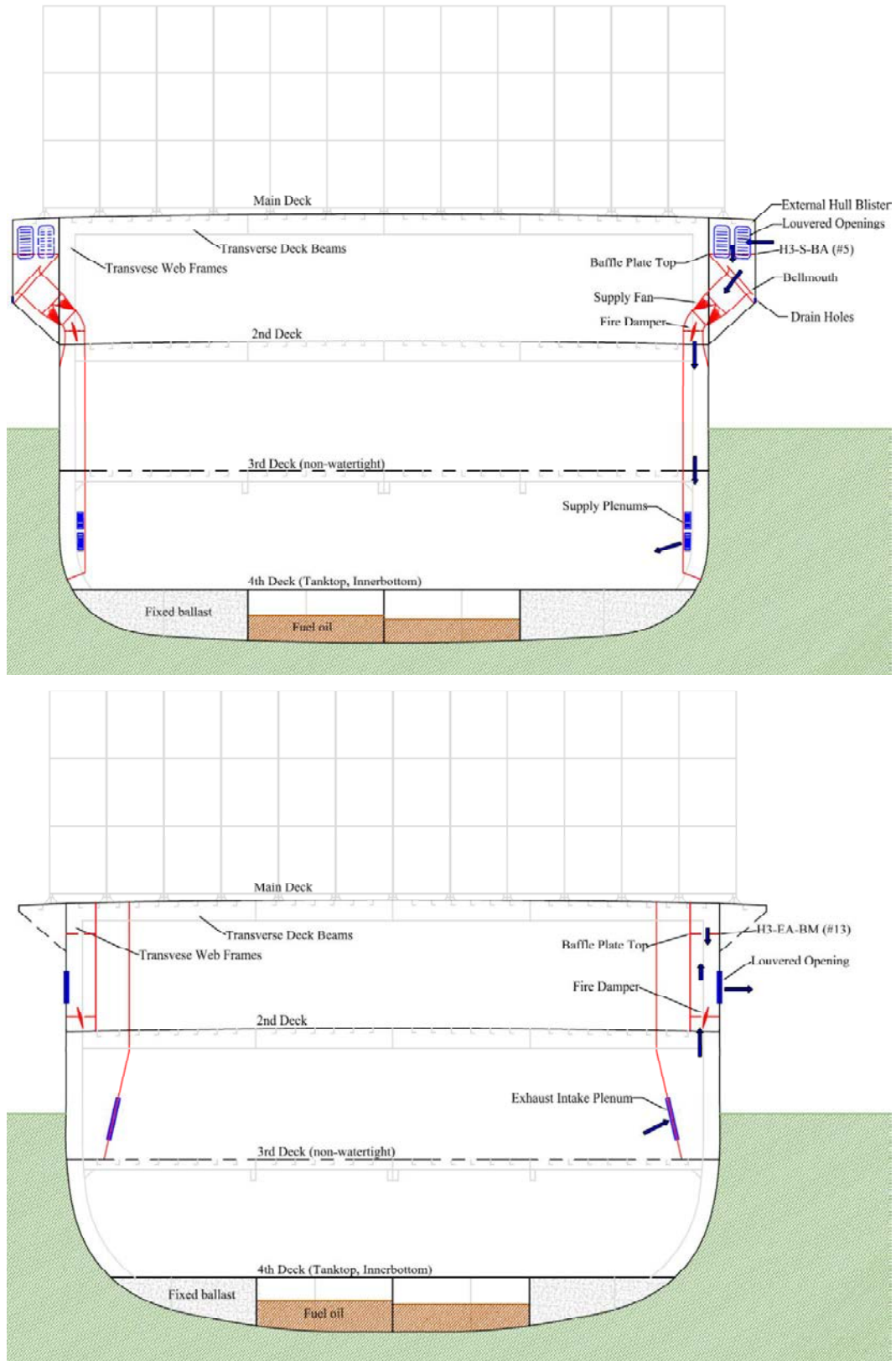


Figure 6-9: Sections at frames 143 (top) and 159 (bottom) showing Hold 3 ventilation supply and exhaust arrangements, respectively. Normal air supply and exhaust paths are shown.

Figure 6-10 through Figure 6-14 provide a series of photographs showing important components of the cargo hold ventilation system which illustrate the vulnerability of flooding through the ventilation supply and exhaust openings on the EL FARO. The ventilation system could be secured in the case of fire by manually closing the fire dampers. Otherwise the fire dampers were required to remain open at all times in port and at sea to provide positive ventilation of the vehicles holds, as required in 46 CFR 92.15-10. Based on MBI hearing testimony [19, 20, 32], crews did not close the fire dampers at sea for heavy weather. There was also no shipboard documentation in the form of a damage control plan or emergency plan which might recommend securing of the fire dampers in the case of extremely high seas to prevent flooding of the cargo holds.



Figure 6-10: Starboard ventilation louvered hull openings for Hold 3 ventilation supply and aft exhaust. Note that red paint delineates the load line (approximate full load waterline). Photo of sister vessel EL YUNQUE. USCG photo.



Figure 6-11: Hold 3 aft ventilation exhaust trunk with racking bulkhead, frames 159-162 starboard, 2nd deck. Screen capture from video taken September 2008 provided by Tote, Inc.



Figure 6-12: Hold 3 ventilation supply fan and fire damper enclosure, frames 141-144 starboard, 2nd deck. Screen capture from video taken September 2008 provided by Tote, Inc.



Figure 6-13: Ventilation supply plenums inside Hold 3, frames 141-144 port, 4th deck (tanktop, innerbottom). Photo of sister vessel EL YUNQUE. USCG photo.



Figure 6-14: Ventilation exhaust intake plenum inside Hold 3, frames 159-162 starboard, 3rd deck. Hold 3 starboard scuttle personnel access ladder and remote operator rod for the emergency fire pump suction valve (sea-chest isolation) are shown on the right. Photo of sister vessel EL YUNQUE. USCG photo.

The flooding vulnerability presented by the cargo hold ventilation system openings will be demonstrated in the subsequent analyses. To support this, various critical points (potential downflooding points) are added to the MSC GHS computer model in order to track the locations of the points relative to the still waterline, and also for annotation of righting arm curves. Table 6-2 provides specific critical points added to the MSC GHS computer model. Downflooding points were determined from the ventilation arrangement drawings [68, 69]. For the accident voyage, with the vessel at the draft and aft trim at the time of loss of propulsion, the top of the baffle plates for Hold 3 ventilation supply would submerge at an angle of heel approximately 27 degrees, and the top of the baffle plates for Hold 3 ventilation exhaust would submerge at an angle of heel of approximately 29 degrees. The significance of these downflooding points will be discussed in Section 6.6.

Critical Point Name	Short Name	Number	Longitudinal (ft-FP)	Transverse (ft-CL)	Vertical (ft-BL)
Hold 3 Access Scuttle Stbd (Coaming)	H3-SC-S	1	512.2	44.0	43.1
Downflooding Points					
Hold 1 Vent Supply (Bellmouth)	H1-S-BM	2	151.9	33.1	61.0
Hold 2 Vent Supply (Baffle)	H2-S-BA	3	274.3	47.7	55.9
Hold 2A Vent Supply (Baffle)	H2A-S-BA	4	373.3	49.0	55.2
Hold 3 Vent Supply (Baffle)	H3-S-BA	5	455.8	49.0	55.2
Hold 1 Vent Exhaust Fwd (Louver)	H1-EF-L	6	102.4	25.5	64.6
Hold 1 Vent Exhaust Aft (Louver)	H1-EA-L	7	193.2	35.5	61.5
Hold 2 Vent Exhaust Fwd (Baffle)	H2-EF-BA	8	228.9	45.2	58.6
Hold 2 Vent Exhaust Aft (Baffle)	H2-EA-BA	9	311.4	45.5	56.5
Hold 2A Vent Exhaust Fwd (Baffle)	H2A-EF-BA	10	341.7	45.7	55.9
Hold 2A Vent Exhaust Aft (Baffle)	H2A-EA-BA	11	402.2	45.8	55.9
Hold 3 Vent Exhaust Fwd (Baffle)	H3-EF-BA	12	435.2	46.0	55.9
Hold 3 Vent Exhaust Aft (Baffle)	H3-EA-BA	13	501.2	46.0	55.9

Table 6-2: Critical points (potential downflooding points) for the forward cargo holds added to the MSC GHS computer model.

6.4.3. Cargo Hold Permeability and Free Surface Pocketing Effects

An important consideration when assessing the effects of flooding is the effect of compartment permeability. This is the same effect which applies to tank volumes and free surface calculations discussed in Sections 2 and 4 of this report. Permeability is accounted for with a simple “permeability factor”, which mathematically accounts for the fraction of a compartment or tank that can be filled with liquid, accounting for such things as internal structure, piping, machinery, and any other internal components including cargo. The permeability factor therefore proportionally reduces the floodable volume (and floodwater weight) and also proportionally reduces the free surface effect. This is especially important in the case of cargo holds, where a large fraction of a compartment’s volume can be taken up with cargo. In the case of the trailered

containers and automobiles carried below decks on EL FARO, permeability should be considered widely variable in both overall fraction and uniformity through the cargo hold volumes. This is especially important with containers, which depend on the assumed watertight integrity of the containers, and their specific locations in the cargo holds. Uncertainty in estimated permeability factors can lead to significant uncertainty in the calculated results. It is therefore appropriate to consider a range of estimated values of permeability in the calculations and assess the variability in the results.

In the case of EL FARO on the accident voyage, below-deck cargo holds separated by watertight bulkheads (Holds 1, 2, 2A and 3) were loaded with a combination of automobiles, trailered containers, miscellaneous trucks and other trailered cargo, and fructose tanks [70]. In Hold 3 (also called Hold D in some of the loading documents), the 4th deck (tanktop, innerbottom) was loaded with 50 automobiles, and the 3rd deck was loaded with 15 trailered containers of 40 and 45 foot lengths. With typical automobile sizes and the deck height of the lower hold (Hold 4D) of 16.5 feet, it can be estimated that the lower hold loaded with 50 automobiles would have an overall effective permeability factor of 0.8-0.9, with a much lower value in the range of 0.6-0.7 up to the top of the automobiles and a much higher value of approximately 0.95 from the top of the automobiles to the top of the lower hold (the 3rd deck). With typical trailered container heights with chassis and deck height of the upper hold (Hold 3D) of 18.5 feet, it can be estimated that the upper hold would have an overall effective permeability factor of 0.6-0.7 if the containers are initially considered watertight, with a higher value of approximately 0.7-0.8 as the containers flood if submerged over time. Hold 2A (also called Hold C) was loaded with a similar distribution of automobiles in the lower hold (Hold 4C) and trailered containers in the upper hold (Hold 3C). Hold 2 (also called Hold B) was loaded with a combination of automobiles, trailers and fructose tanks in the lower hold (Hold 4B) and a combination of automobiles and trailers in the upper hold (Hold 3B). Hold 1 (also called Hold A) contained only fructose tanks in the lower hold (Hold 4A) and trucks and trailers in the upper hold (Hold 3A).

For these flooding analyses and assessments, a range of permeability values of 0.7-0.9 are used for illustration of the variability of results. Where there are significant impacts of permeability factor variability, the effects are discussed in detail. This is especially important for initial flooding (10-20% in the cargo holds), as the lower holds 4C and 4D were filled with automobiles, reducing the initial effective permeability.

It should be noted that this type of flooding analysis is different than the damage stability analysis performed in accordance with SOLAS requirements (refer to Section 5 of this report), where permeability factors are specified based on vessel and cargo type. Based on current SOLAS regulations [60], summer load line (full load) draft permeability factors for RO/RO spaces with containers on wheels (trailers) are prescribed as 0.9; however in earlier versions of SOLAS regulations [58], a general permeability factor for dry cargo spaces was prescribed as 0.7. This analysis incorporates this range of values.

In addition to variability of results due to variability in compartment permeability, the free surface effect is also reduced due to the effective pocketing of the floodwater in the lower cargo holds. The term “pocketing” is used to describe the reduction in free surface effect due to

interaction of the free surface with the overhead of the compartment or tank. This is important for the lower cargo holds because the 3rd deck, while essentially non-watertight (see Figure 6-9 and Figure 6-15 below), contains relatively small deck plate openings which would limit the rate of flow of water through the deck as the vessel rolls in the seaway. From a pure hydrostatics perspective the deck is considered non-watertight and the internal floodwater level would eventually equalize and rise above the deck for a given angle of heel, but due to the dynamic nature of the ship's roll motion, water would experience a partial dynamic "pocketing" effect, and therefore free surface effect would be significantly reduced in the lower cargo holds. This is illustrated in Figure 6-18 below.



Figure 6-15: Hold 3, 3rd deck, showing non-watertight openings. Photo of sister vessel EL YUNQUE. USCG photo.

6.4.4. Flooding of Hold 3

Flooding of Hold 3 would have several important effects. There would be an increase in drafts and a corresponding decrease in freeboard. Since the center of Hold 3 is aft of the LCF, aft trim would increase (i.e. aft draft would increase slightly more than forward draft). As a result of the overall reduction in freeboard and trim aft, the ventilation openings identified as potential downflooding points in Table 6-2 would move closer to the waterline. Concurrently, wind heel and roll motion due to encounter with the waves, especially after loss of propulsion when the ship would have drifted with beam to the wind and seas, would bring the ventilation openings to intermittent submergence, which would result in intermittent flooding. As Hold 3 continued to flood in this manner, eventually the ventilation openings for Hold 2A would likewise be brought to intermittent submergence as their freeboards would be reduced due to the flooding of Hold 3, the wind heel and the roll motion. This means of progressive flooding and consequences will be demonstrated subsequently.

To demonstrate the hydrostatics and stability effects of flooding Hold 3, flooding is calculated in 10% increments, from the intact condition to the level of equalization or equilibrium (i.e. until the internal level of the floodwater is equalized to the waterline external to the hull). Flooding is calculated for permeability factors 0.7, 0.8 and 0.9 to demonstrate the variability in results, as discussed previously. Figure 6-16 shows a centerline inboard profile graphic from the GHS software with Hold 3 flooded and equalized for permeability 0.8. Table 6-3 provides calculated values of displacement, floodwater weight, GM, drafts and trim, for each of the 10% flooding increments, for permeability 0.7 (the lower bound) and 0.9 (the upper bound). Figure 6-17 shows righting arm curves for each of the 10% flooding increments for permeability 0.7 (dashed curves) and 0.9 (solid curves).

One of the important conclusions that can be drawn from Table 6-3 and Figure 6-17 is the reduced righting arms and GM (slope of the righting arm curve) at the lower percentages (10% and 20%) for the higher permeability value (0.9) due to the initial free surface effect. However, as discussed previously, it is likely that due to the existence of the tightly packed automobiles in the lower holds, the effective initial permeability value would be closer to 0.6-0.7 and would only increase to an average value of approximately 0.8 as the floodwater levels increased toward the overhead of the lower hold. This is illustrated in Figure 6-18 which shows scaled drawings of the sections at frame 143 (location of the Hold 3 supply trunk) and frame 159 (location of the Hold 3 aft exhaust trunk). The loading of containers, trailers and automobiles are shown to scale and approximate position based on the Final Stow Plan [70]. The figure shows Hold 3 flooded to the 20% level, showing the effective reduction in permeability due to the automobiles, and also the impact of pocketing as the loose water hits the overhead (3rd Deck). In the figure, the flooding level at 20% and heel angle of 15 degrees are shown for example, as this was a condition which might have existed at early stages of flooding in Hold 3, based on the VDR audio transcript as previously discussed, and based on combined wind heel considerations as will be discussed. The scaled drawings in the figure also show how close the Hold 3 ventilation openings (tops of the baffle plates) would be to a still waterline with a 15 degree wind heel angle. The relative rise in water height due to waves and vessel roll motion would bring these ventilation openings to submergence, at least intermittently. This will be discussed in more detail subsequently.

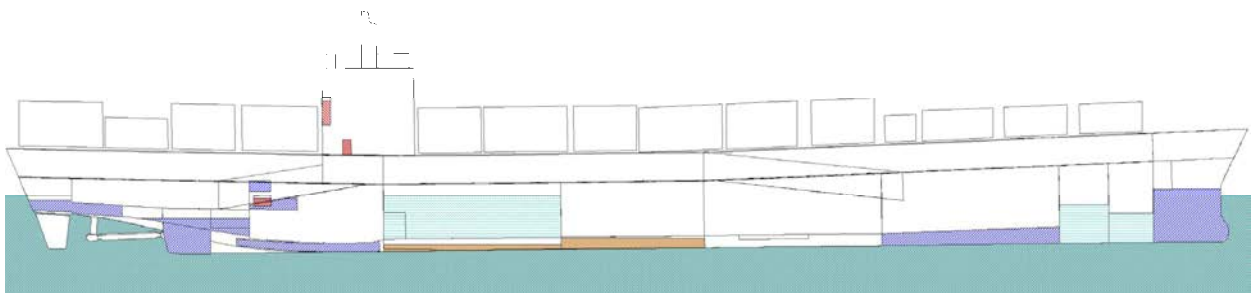


Figure 6-16: Centerline inboard profile from the GHS software showing the condition with Hold 3 flooded to equalization (i.e. flooded to the external waterline). Permeability is 0.8.

		Displacement (LT)	Total Floodwater (LT)	GM (ft)	Draft Fwd (ft-BL)	Draft Aft (ft-BL)	Trim (ft-aft)	Draft at LCF (ft-BL)
Intact Condition		34,277	0	4.03	26.9	31.9	5.0	29.9
Permeability 0.7	10%	34,970	693	0.92	27.2	32.6	5.4	30.3
	20%	35,662	1,385	1.22	27.4	33.2	5.8	30.8
	30%	36,355	2,078	1.55	27.6	33.8	6.2	31.3
	40%	37,047	2,770	1.85	27.8	34.4	6.6	31.7
	50%	37,740	3,463	2.04	28.1	35.0	6.9	32.2
	60%	38,433	4,156	2.26	28.3	35.6	7.3	32.6
	Equilibrium	39,394	5,117	2.84	28.6	36.5	7.9	33.2
Permeability 0.9	10%	35,167	890	0.05	27.2	32.8	5.6	30.5
	20%	36,058	1,781	0.46	27.5	33.5	6.0	31.1
	30%	36,948	2,671	0.89	27.8	34.3	6.5	31.7
	40%	37,839	3,562	1.29	28.1	35.1	7.0	32.2
	50%	38,730	4,453	1.56	28.4	35.9	7.5	32.8
	60%	39,620	5,343	1.84	28.7	36.6	7.9	33.4
	Equilibrium	41,173	6,896	2.61	29.2	38.0	8.8	34.3

Table 6-3: Comparison of calculated displacement, floodwater weight, GM, drafts and trim, for flooding of Hold 3 in 10% increments, for permeability 0.7 and 0.9.

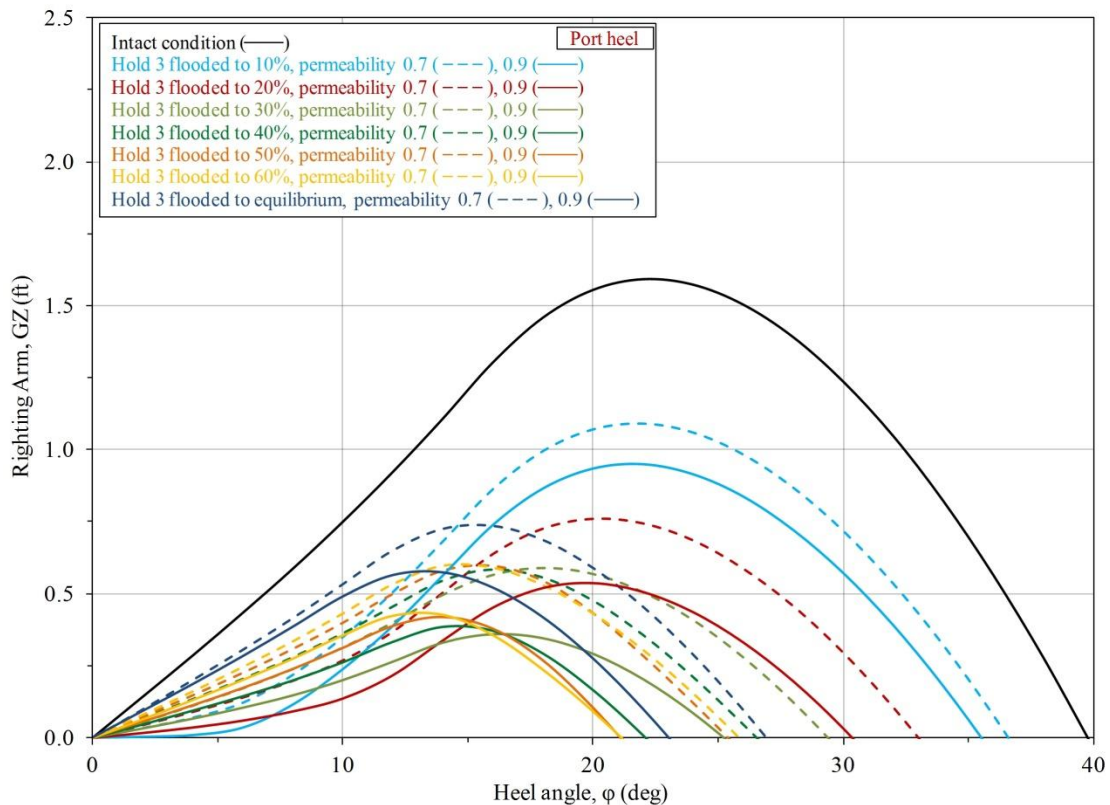


Figure 6-17: Comparison of righting arm curves for flooding of Hold 3 in 10% increments. Dashed curves are for permeability 0.7, solid curves are for permeability 0.9. Port heel is shown.

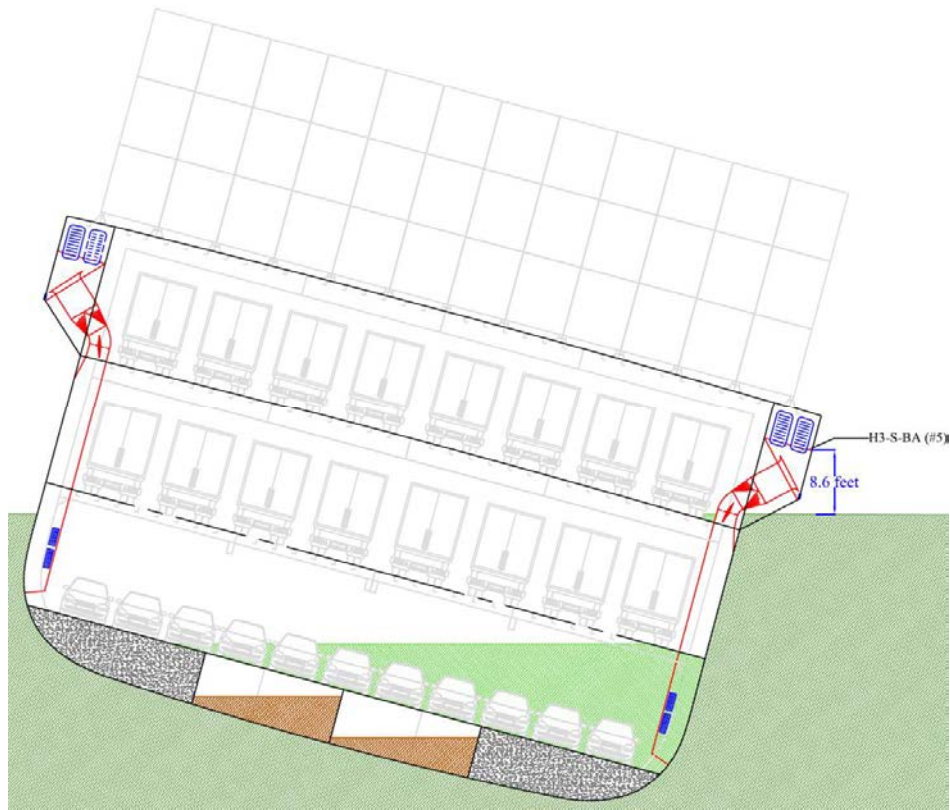


Figure 6-18: Scaled drawing of sections at frame 143 (Hold 3 ventilation supply trunk) and frame 159 (Hold 3 aft ventilation exhaust trunk), with flooding of Hold 3 to 20% with permeability 0.7 and heel angle of 15 degrees shown for example.

6.4.5. Progressive Flooding

As discussed previously, it is not clear from the VDR audio transcript when and where progressive flooding was occurring prior to the eventual capsizing of the vessel at approximately 0739 on October 1st [64 (pp. 507-508)]. However, as Hold 3 continued to flood, eventually the ventilation openings for Hold 2A would have been brought to intermittent submergence as their freeboards were reduced due to the flooding of Hold 3, in combination with the wind heel, waves and roll motion. This is illustrated in Figure 6-19, which shows a scaled drawing of the section at frame 134/22, the location of the aft ventilation exhaust trunk for Hold 2A. For a wind heel angle of 15 degrees, the waterline is shown incorporating the effect of flooding of Hold 3 to 20%. It should be noted that it is likely that Hold 2A (and perhaps also Hold 2) may have been taking on some water, at least intermittently, as the vessel rolled about a wind heel angle of 15 degrees and while Hold 3 was flooding.

In addition to the ventilation openings, it is possible that progressive flooding into Hold 2A could have also occurred through watertight door seal leakage or through leakage of the bilge pumping system check valves. Regardless of the source, at 0716 a report was made to the bridge that the Hold 2A bilge alarm had been sounding [64 (pg. 484)], suggesting that Hold 2A had been taking on some water. For illustrative purposes, the analysis is completed assuming that the progressive flooding would have occurred in sequence, once Hold 3 reached equilibrium.

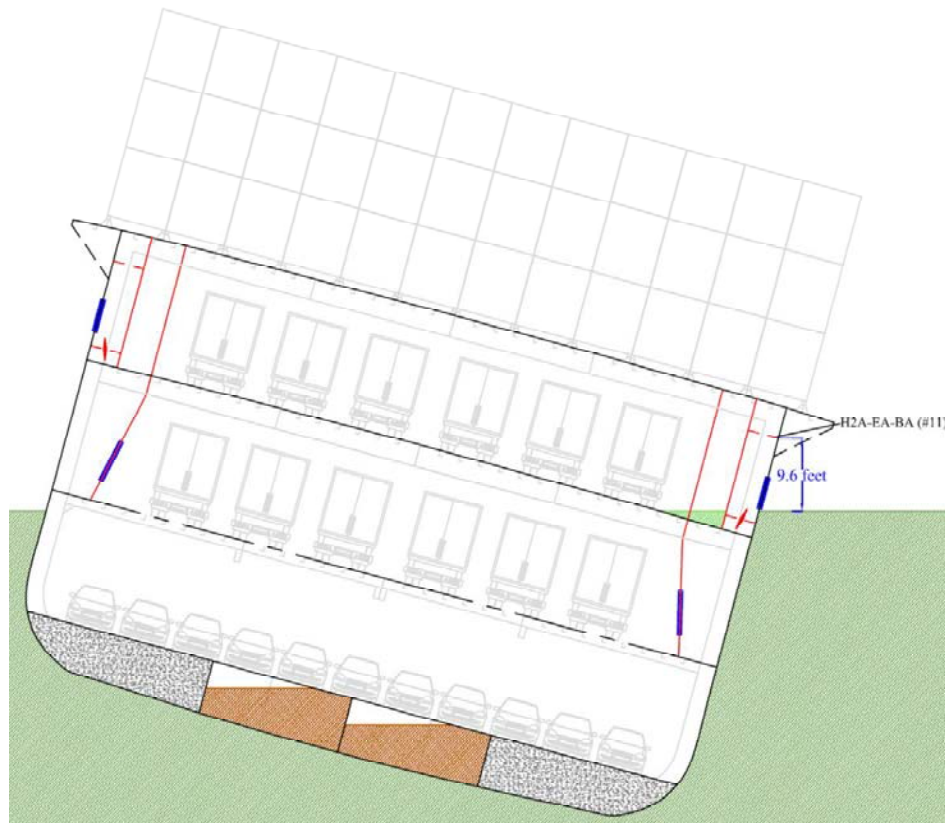


Figure 6-19: Scaled drawing of section at frame 134/22 (Hold 2A aft ventilation exhaust trunk) with still waterline resulting from flooding of Hold 3 to 20% with permeability 0.7 and heel angle of 15 degrees shown for example.

To demonstrate the hydrostatic effects of flooding Hold 2A after the flooding of Hold 3, flooding of Hold 2A is calculated in 10% increments for an average permeability value of 0.8. Figure 6-20 shows a centerline inboard profile graphic from the GHS software with Holds 3 and 2A flooded and equalized. Table 6-4 provides calculated values of displacement, floodwater weight, GM, drafts and trim, for each of the 10% flooding increments. Figure 6-21 shows righting arm curves for each of the 10% flooding increments.

As was the case with flooding of Hold 3 by itself, there is a significant reduction in GM and righting arms at lower levels of flooding (most notably 10% and 20%) due to the initial free surface effect. In fact, for the 10% level, GM and the initial righting arms are actually negative (see Figure 6-21), indicating a condition referred to as “lolling.” In this lolling condition, even without the contribution of wind heel, the vessel would not be able to remain upright but would flop to either side to a “lolling angle” (approximately 7 degrees as shown in Figure 6-21 for the 10% level). With wind heel this type of condition may only be noticeable as an apparent increase in the wind heel angle. However, as was the case for flooding of Hold 3 by itself, in reality due to the existence of the tightly packed automobiles in the lower holds, the effective permeability value would be closer to 0.6-0.7 and would only increase to an average value of 0.8 as the floodwater levels increased toward the overhead of the lower hold, so this lolling effect would also be reduced.

Comparison of Figure 6-17 and Figure 6-21 indicates a significant reduction in righting arms with flooding of Hold 3 and additional flooding of Hold 2A. While theoretically there could be sufficient residual righting energy (area under the righting arm curve) to survive flooding of these 2 compartments in calm water, with almost any significant wind heel and additional wave effects including dynamic rolling, the vessel would likely have capsized. To confirm this limitation, MSC ran a number of additional analyses with different combinations of compartment flooding. It is evident that any additional free surface effect due to the flooding of a third cargo hold would be sufficient to capsize the vessel, even in calm water.

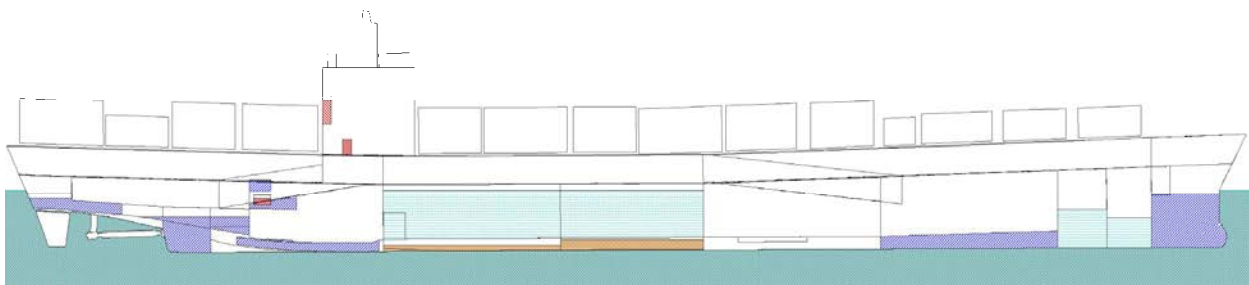


Figure 6-20: Centerline inboard profile from the GHS software showing the condition with Holds 3 and 2A flooded to equalization. Permeability is 0.8.

	Displacement (LT)	Total Floodwater (LT)	GM (ft)	Draft Fwd (ft-BL)	Draft Aft (ft-BL)	Trim (ft-aft)	Draft at LCF (ft-BL)
Hold 3 at Equilibrium	40,263	5,986	2.72	28.9	37.2	8.3	33.8
Hold 2A at 10%	41,022	6,745	-0.68	29.7	37.3	7.6	34.2
Hold 2A at 20%	41,803	7,526	-0.04	30.6	37.6	7.0	34.7
Hold 2A at 30%	42,589	8,312	0.38	31.4	38.0	6.6	35.3
Hold 2A at 40%	43,364	9,087	0.77	32.2	38.3	6.0	35.7
Hold 2A at 50%	44,138	9,861	1.09	33.0	38.5	5.5	36.2
Hold 2A at 60%	44,912	10,635	1.34	33.9	38.8	4.9	36.7
Hold 2A at 70%	45,686	11,409	1.53	34.7	39.1	4.4	37.2
Hold 2A at 80%	46,459	12,182	1.67	35.4	39.3	3.9	37.7
Hold 2A at Equilibrium	46,982	12,705	2.03	36.0	39.5	3.5	38.1

Table 6-4: Calculated displacement, floodwater weight, GM, drafts and trim, for progressive flooding of Hold 2A in 10% increments with Hold 3 flooded to equilibrium. Permeability is 0.8.

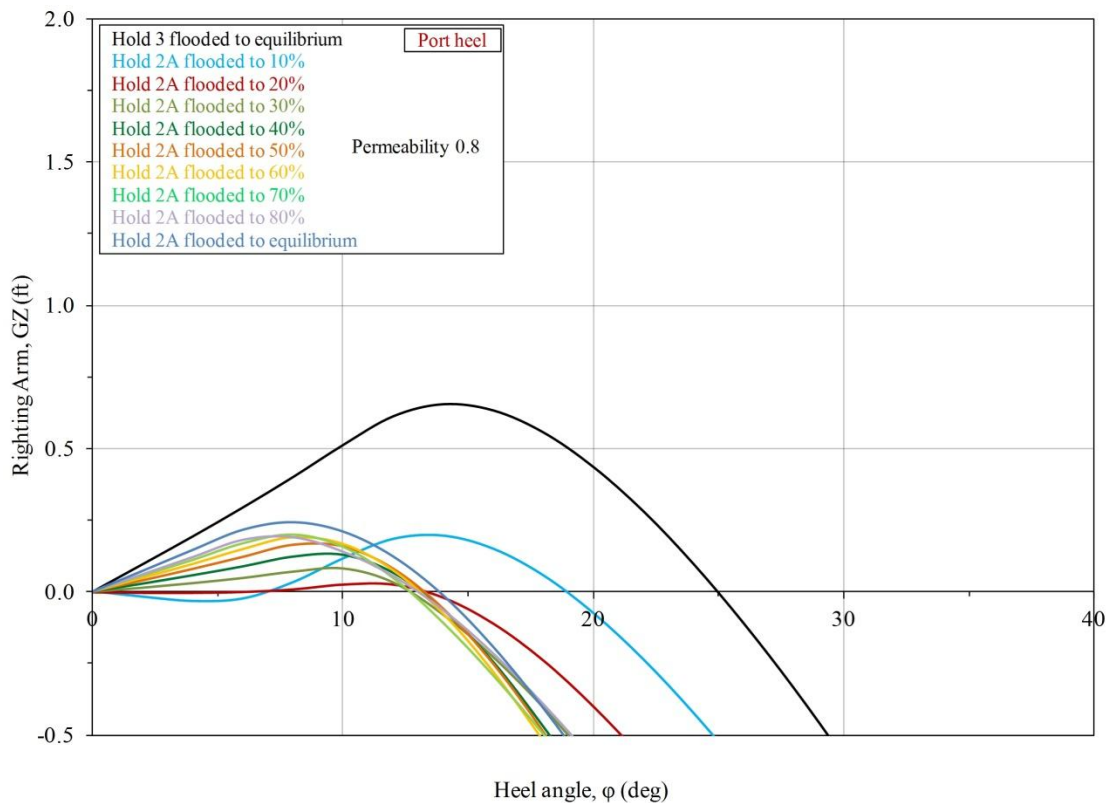


Figure 6-21: Righting arm curves for progressive flooding of Hold 2A in 10% increments with Hold 3 flooded to equilibrium. Permeability is 0.8. Port heel is shown.

6.5. Combined Effects of Wind Heel and Flooding

As illustrated in Figure 6-17 and Figure 6-21, flooding of Hold 3 and progressive flooding of Hold 2A would have left the ship with limited righting energy (area under the righting arm curve). The general effects of wind heel on the righting arm curve, including the calculation of residual righting arms and residual righting energy were discussed in Section 6.3. The combination of flooding and wind heel would have left the ship with little or no residual righting energy. Figure 6-22 shows the effects of wind heel on the righting arms with complete flooding of Hold 3 (top) and with complete flooding of Hold 3 and Hold 2A (bottom), both with average permeability of 0.8. Note that intermediate levels of flooding in either case would have reduced righting arms as shown in Figure 6-17 and Figure 6-21. One of the important conclusions that can be drawn from Figure 6-22 is that it is unlikely that the ship could survive uncontrolled flooding into even a single cargo hold with winds in excess of 70 or 80 knots, and it is unlikely that it could survive flooding of more than one cargo hold except in benign conditions with little wind and waves.

As discussed previously, for initial flooding of the lower cargo hold of Hold 3, the effective permeability factor would be closer to 0.7 up to the 20-30% flooding level. Combining these levels of flooding with permeability factor of 0.7 and wind heel in the range 70-90 knots, it can be demonstrated that a wind heel with initial flooding of Hold 3 could lead to a combined wind heel angle of approximately 15 degrees. This is illustrated in Figure 6-23, which shows wind heeling arms for 70, 80 and 90 knot winds and calculated residual righting arms, for flooding levels 10%, 20% and 30% in Hold 3, with permeability 0.7. It is clear that achieving a 15 degree heel angle as stated in the VDR transcript is possible with combined wind heel and initial flooding of Hold 3. Figure 6-24 shows the same calculation information, but shows righting arms with and without 80 knot wind for Hold 3 flooding levels 10%, 20% and 30%. It is important to recognize from these plots that the residual righting energy (area under the righting arm curves) is reduced significantly even for lower levels of flooding up to 30% when considered in combination with 80 knot beam wind. Thus, it is apparent that the vessel would have been in a vulnerable state and susceptible to capsizing even with flooding only of Hold 3, when considering the combined effects of partial flooding, wind heel and roll motion.

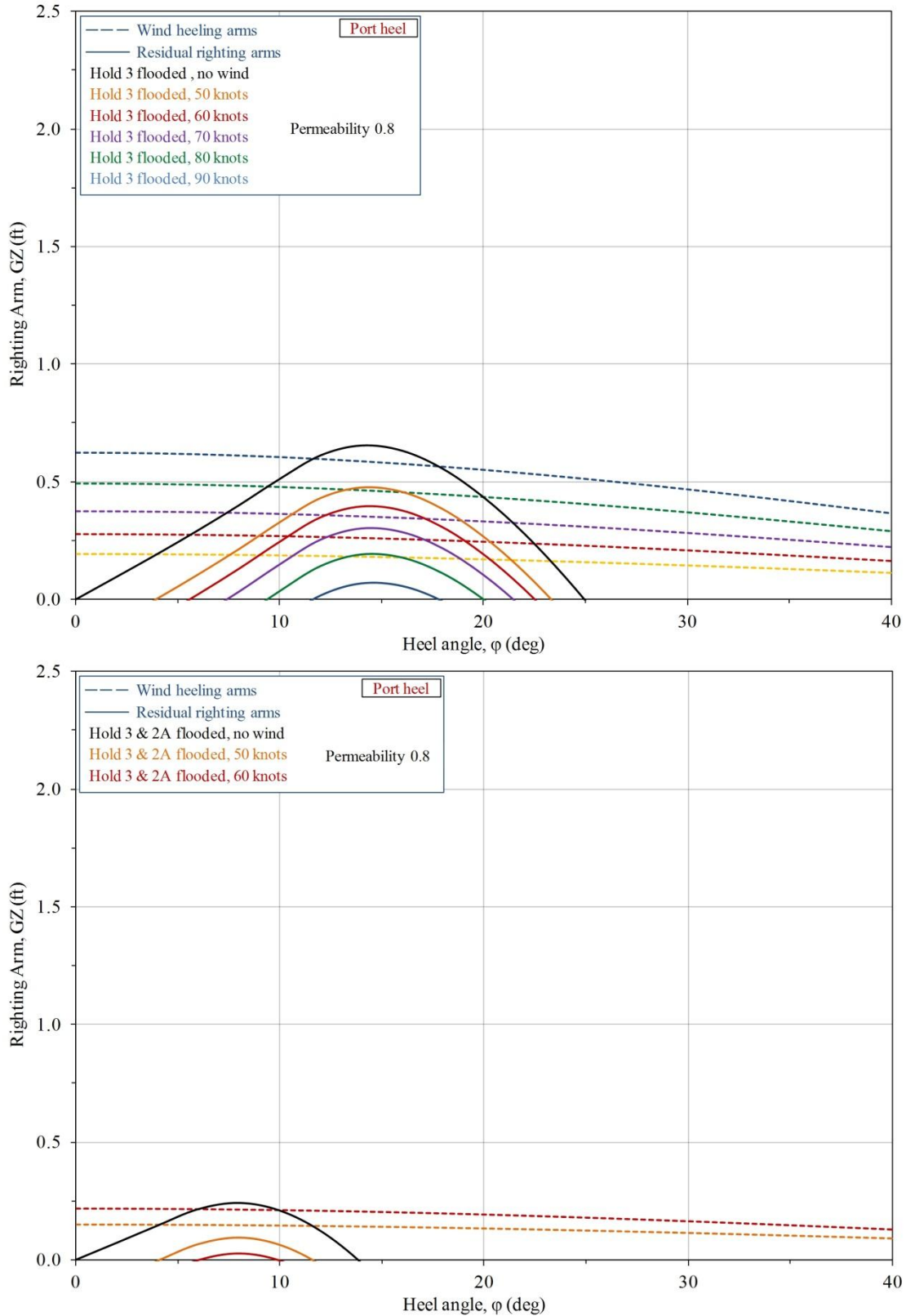


Figure 6-22: Wind heeling arms (dashed curves) and residual righting arms (solid curves) with Hold 3 flooded to equilibrium (top) and Hold 3 and Hold 2A flooded to equilibrium (bottom). Permeability is 0.8.

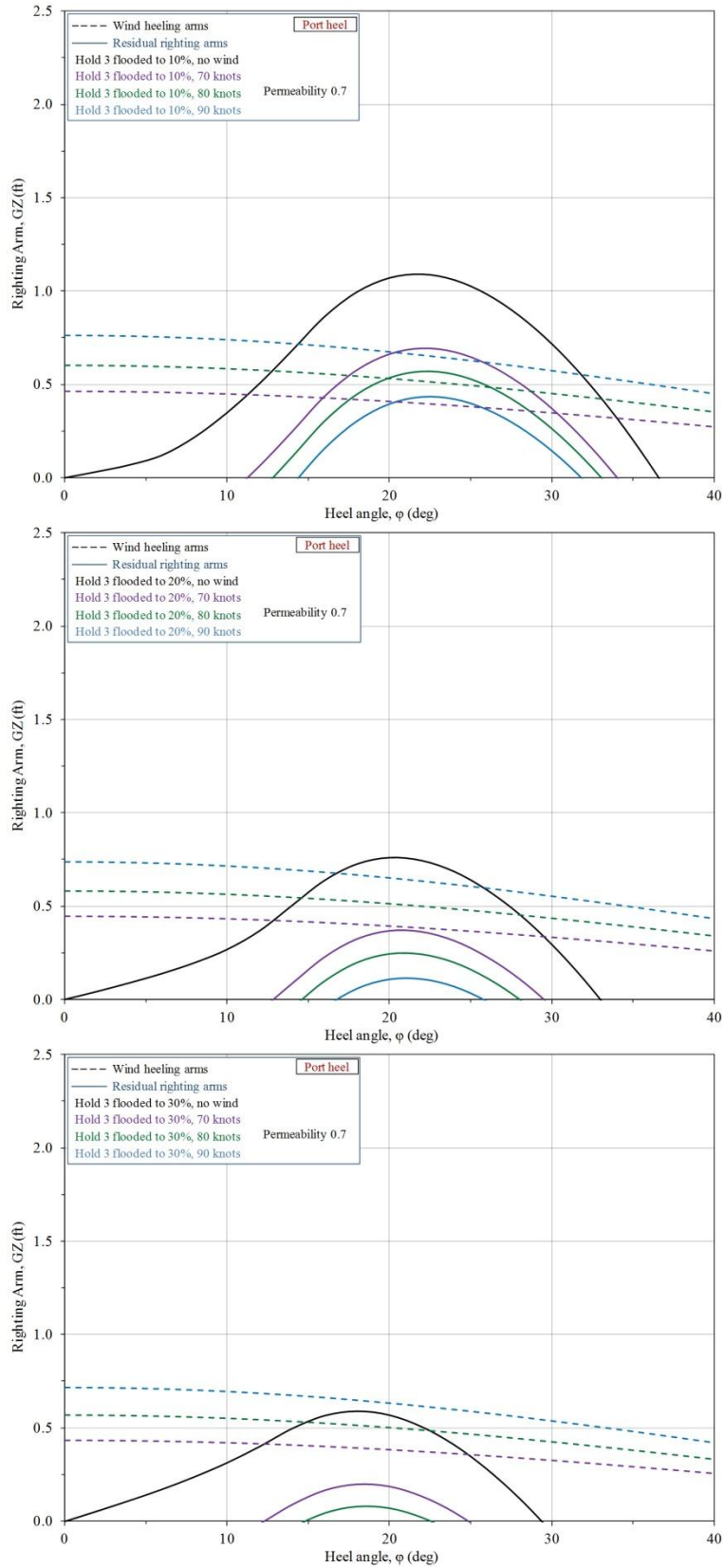


Figure 6-23: Beam wind heeling arms (dashed curves) and residual righting arms (solid curves) with Hold 3 flooded to 10% (top), 20% (middle) and 30% (bottom). Permeability is 0.7.

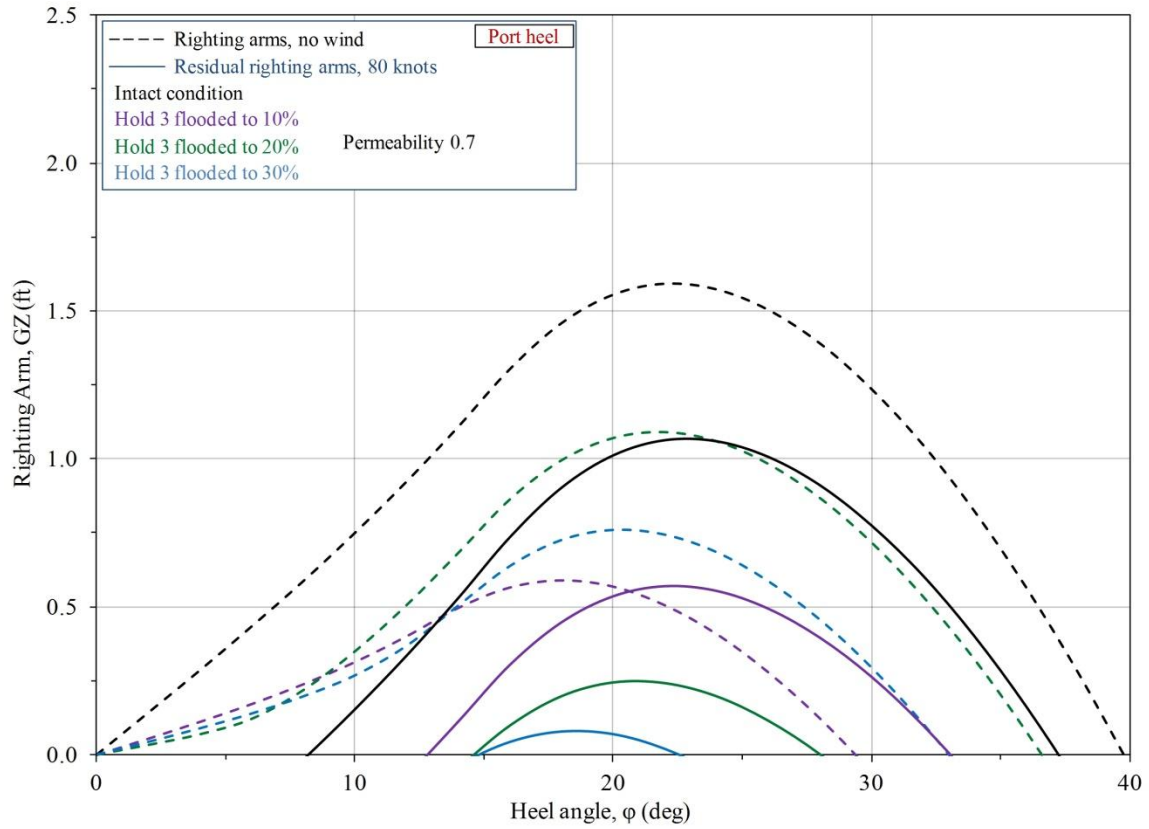


Figure 6-24: Righting arms (dashed curves) and residual righting arms (solid curves) for 80 knot beam winds with Hold 3 flooded to 10%, 20%, and 30%. Permeability is 0.7.

6.6. Downflooding

The flooding vulnerability presented by the cargo hold ventilation system was discussed in Section 6.4 and downflooding points were listed in Table 6-2. Downflooding angles for these points are tabulated and plotted on the righting arm curves for the intact condition at loss of propulsion (without flooding) and for the condition with Hold 3 flooded to 20%. Table 6-5 provides the downflooding angles for the listed points and Figure 6-25 plots downflooding points for each hold on the righting arm curves.

It was noted in Section 5.2.3.2 that including downflooding points and downflooding angles in the intact stability analysis would have the effect of truncating the righting arm curves for evaluation of the righting arm criteria. However, from the definitions based on 46 CFR 170.055, these ventilation openings, as they could potentially be closed by means of manually-closable fire dampers, would not have been considered as providing a means of “downflooding” and therefore would not need to be considered in evaluation of the stability criteria, even under the current criteria of the 2008 IS Code. This is in apparent conflict with 46 CFR 92.15-10 which requires that fire dampers remain open at all times in port and underway (except when combating a fire) to provide positive ventilation of the vehicles holds.

			Downflood Angle (deg)	
Critical Point Name	Short Name	Number	Intact Condition	Hold 3 Flooded to 20%
Hold 3 Access Scuttle Stbd (Coaming)	H3-SC-S	1	16.2	14.9
Downflooding Points				
Hold 1 Vent Supply (Bellmouth)	H1-S-BM	2	45.0	44.4
Hold 2 Vent Supply (Baffle)	H2-S-BA	3	29.6	28.9
Hold 2A Vent Supply (Baffle)	H2A-S-BA	4	27.7	26.9
Hold 3 Vent Supply (Baffle)	H3-S-BA	5	27.2	26.3
Hold 1 Vent Exhaust Fwd (Louver)	H1-EF-L	6	55.4	55.0
Hold 1 Vent Exhaust Aft (Louver)	H1-EA-L	7	43.2	42.5
Hold 2 Vent Exhaust Fwd (Baffle)	H2-EF-BA	8	33.7	33.0
Hold 2 Vent Exhaust Aft (Baffle)	H2-EA-BA	9	31.1	30.3
Hold 2A Vent Exhaust Fwd (Baffle)	H2A-EF-BA	10	30.3	29.4
Hold 2A Vent Exhaust Aft (Baffle)	H2A-EA-BA	11	29.8	28.9
Hold 3 Vent Exhaust Fwd (Baffle)	H3-EF-BA	12	29.5	28.6
Hold 3 Vent Exhaust Aft (Baffle)	H3-EA-BA	13	29.1	28.1

Table 6-5: Downflooding angles for forward cargo holds for intact condition (at loss of propulsion, without flooding) and with Hold 3 flooded to 20% with 0.7 permeability.

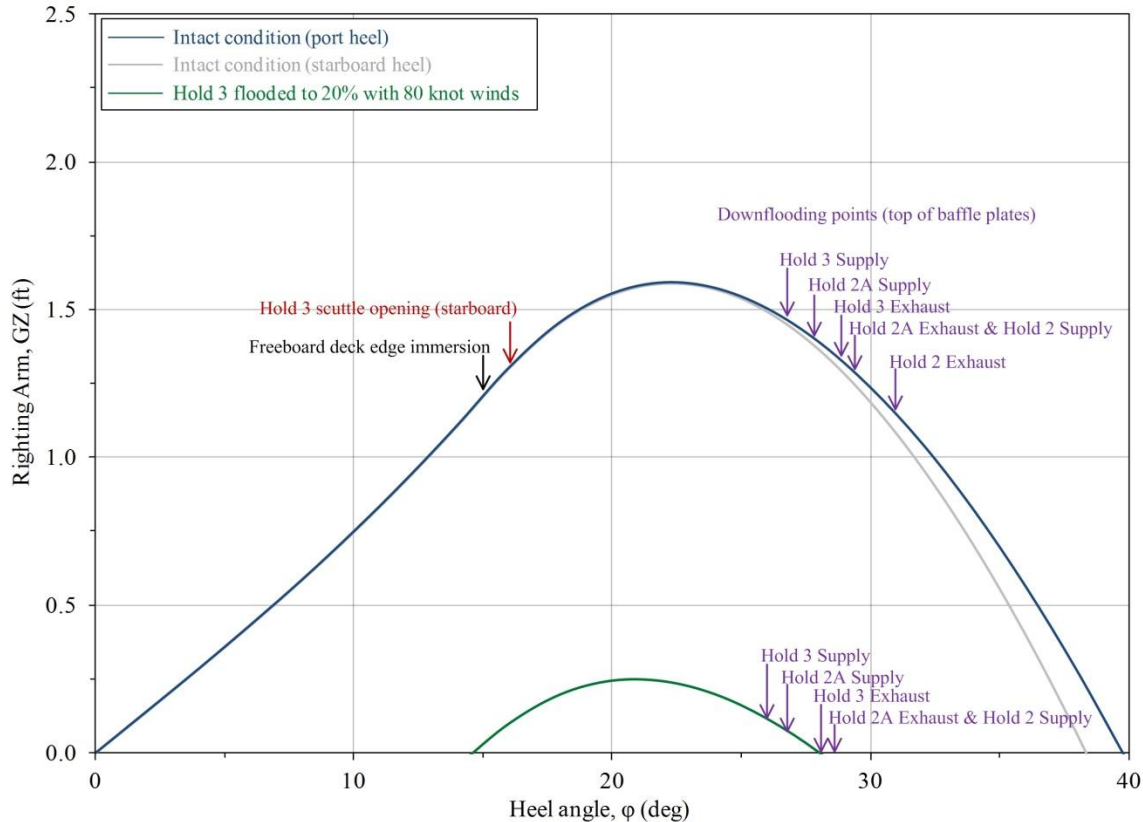


Figure 6-25: Righting arm curves with annotated downflooding angles from Table 6-5: intact condition (at loss of propulsion, without flooding) and Hold 3 flooded to 20% with 0.7 permeability and 80 knot winds.

6.7. Additional Considerations

In the foregoing analyses, no consideration was given to the impact of cargo shifting, or cargo loss. Although there was no mention specifically of large-scale cargo shift or loss until the very end of the VDR audio as the vessel slowly capsized, there was one mention of a single trailer cargo shift which was witnessed by the Chief Mate at 0436 [64 (pg. 380)] and there was some discussion of automobiles breaking free and floating in Hold 3 [64 (pg. 486)]. Cargo shifting can best be considered in this analysis as a transverse weight shift; specifically a given transverse moment which might be calculated based on shifting of a given number of trailers or containers by a given transverse distance. This is illustrated in Figure 6-26 below, which shows the effects of a transverse moment applied to the intact condition (at the loss of propulsion, not including floodwater and beam wind) and the condition with Hold 3 flooded to 20% with 80 knot beam winds. The 5,000 ft·LT transverse moment (weight multiplied by distance shifted) is shown as an example and is based on a notional shift of 20 containers of weight 25 LT each, shifting an average 10 feet. The net effect of any transverse weight shift is equivalent to a transverse shift in the ship’s center of gravity, which results in a reduction in the righting arms and a list as shown. Note that in this case, even a 5,000 ft·LT transverse weight shift produces small reductions in righting arms and small induced heel angles, when compared to large reductions in righting arms and induced heel angles due to floodwater and hurricane force beam winds as discussed

previously. However, it should be noted that even small transverse shifts in containers would exacerbate effects of floodwater and beam winds.

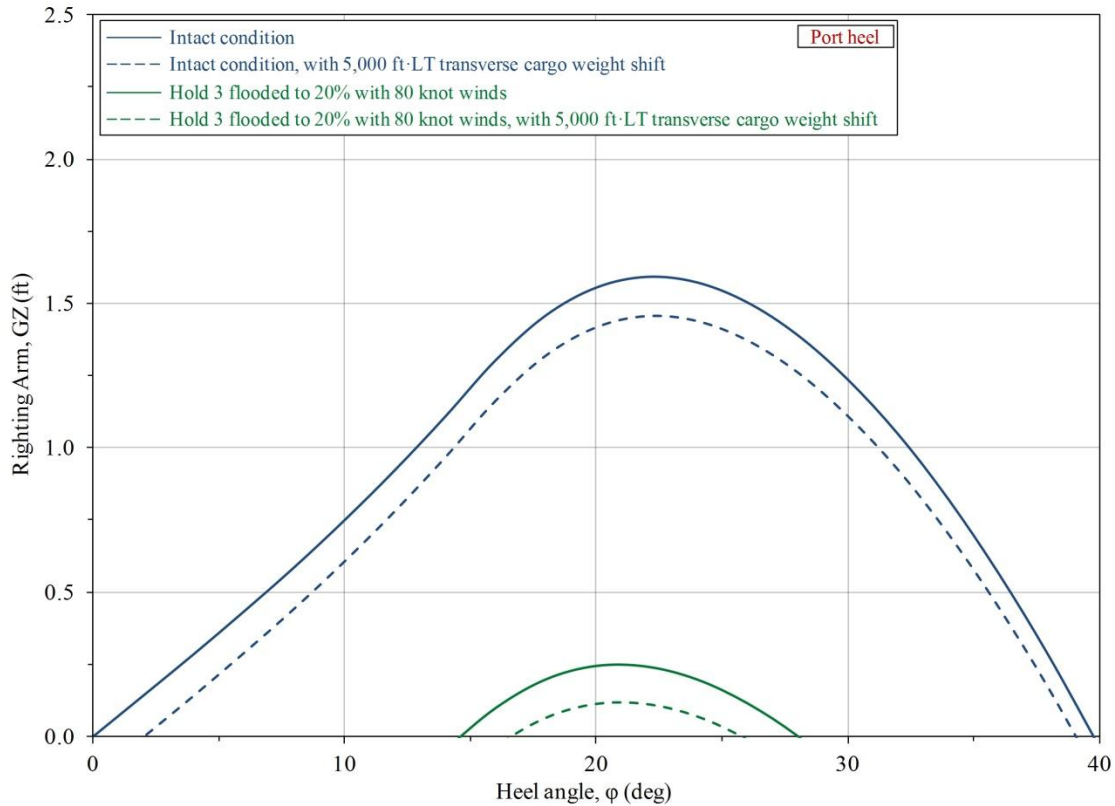


Figure 6-26: Comparison of righting arm curves with effects of transverse cargo weight shifts: intact condition (at loss of propulsion, without flooding) and Hold 3 flooded to 20% with 0.7 permeability and 80 knot winds.

The complete loss of topside containers as the vessel took heavy rolls in the seaway or while capsizing would actually lead to a temporary improvement in the stability condition of the vessel. This is the case because complete loss of topside containers would necessarily lower the ship’s center of gravity and increase righting arms, providing temporary additional righting energy and stability margin. This is illustrated in Figure 6-27, which shows for an example the potential effects of a complete loss of all containers in Bay 13 (581 LT) applied to the intact condition (at the loss of propulsion, not including floodwater and beam wind) and the condition with Hold 3 flooded to 20% with 80 knot beam winds. However, it is also feasible that entire bays of containers or sections of bays could lose structural integrity and experience partial failure or deformation and lean to one side without actually washing overboard. This has occurred on container vessels in heavy seas in recent years, including as a consequence of so-called “parametric” roll motions. In this case, the results would be similar to those of container shifting shown in Figure 6-26 for example. There was, however, no statement made by the EL FARO crew on the VDR audio transcript regarding the loss or shifting of topside containers, until just prior to vessel capsizing at 0729 when it was noted that containers were in the water [64 (pg. 498)].

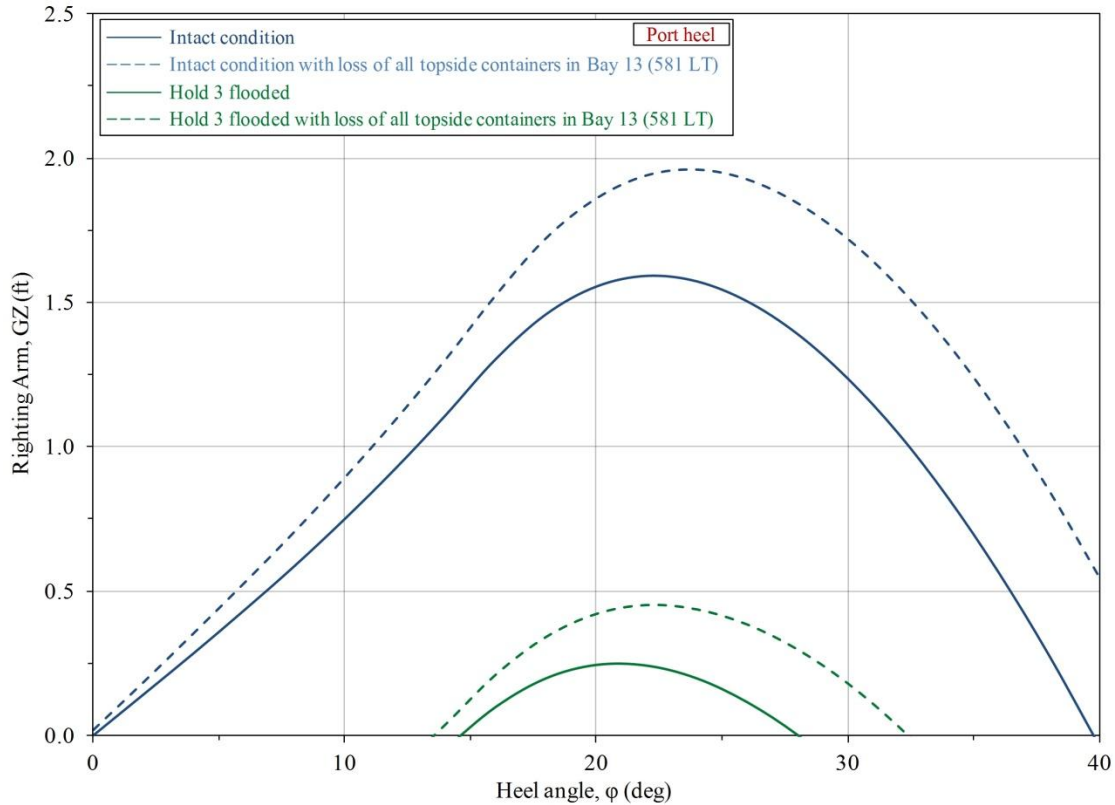


Figure 6-27: Comparison of righting arm curves with complete loss of all containers in Bay 13 for example: intact condition (at loss of propulsion, without flooding) and Hold 3 flooded to 20% with 0.7 permeability and 80 knot winds.

It was requested by the MBI to incorporate consideration of entrapped water on the 2nd Deck in the MSC analysis. This is a consideration since the 2nd Deck provides a semi-closed (semi-buoyant) free-flooding volume, allowing water to enter through limited deck openings along the side shell as the vessel rolls in the seaway. With this configuration the possibility exists for entrapment of water on the deck as the vessel rolls. Fundamentally, the hydrostatic effects of water on the 2nd Deck are included in the MSC GHS computer model and analyses, including their effects on attained static heel and the righting arm curve. For the MSC GHS computer model a separate set of lines was created for the semi-enclosed 2nd Deck, and this volume was allowed to free flood in the analysis (see Figure 2-3). However, it is noted that entrapment of water on the deck also has important dynamic effects which cannot be incorporated in a hydrostatic analysis. Specifically, entrapment of water to one side (port or starboard depending on the roll offset) would provide transverse force components on the side shell which would alter roll motions. Additionally, restriction of flow through the limited side shell openings would also provide a damping effect on the roll motion, limiting the amplitude of the roll motion. These dynamic effects could be parametrically incorporated and simulated in a dynamic analysis, but cannot be captured effectively in a hydrostatic analysis as provided.

To conclude this section, it should be noted that all of the hydrostatic sinking analyses are based on an assumption that the weight and center of gravity of the vessel and its cargo are fairly well defined based on the departure loading condition documentation. However, based on the propagation of uncertainty from the 2006 stability test (see Section 3 and Appendix A of this

report), there exists a 95% confidence that uncertainty in the height of the center of gravity (KG) is on the order of 0.7 ft for the departure condition and for the lightship condition (see Table 3-2). These uncertainties could be considered in assessing the previous analyses, or should at least be used as a reminder of the uncertainty in any calculated results. To illustrate, Figure 6-28 provides a comparison of the righting arms for the accident voyage loading condition prior to the loss of propulsion (intact condition) and with Hold 3 flooded to 20% with 80 knot beam winds, with uncertainty in calculated lightship KG included. It should be noted that these righting arm curves include the uncertainty in the lightship KG, but do not include the additional uncertainty in the cargo and tank loading and weight and free surface associated with the floodwater. The primary point in illustrating this is to highlight the significant impact that uncertainty in the assumed lightship KG has on the righting arms. Note that for all of the previous righting arm plots, significant differences would exist in the calculated angle of wind heel and residual righting energy, depending on the desired level of confidence in the results.

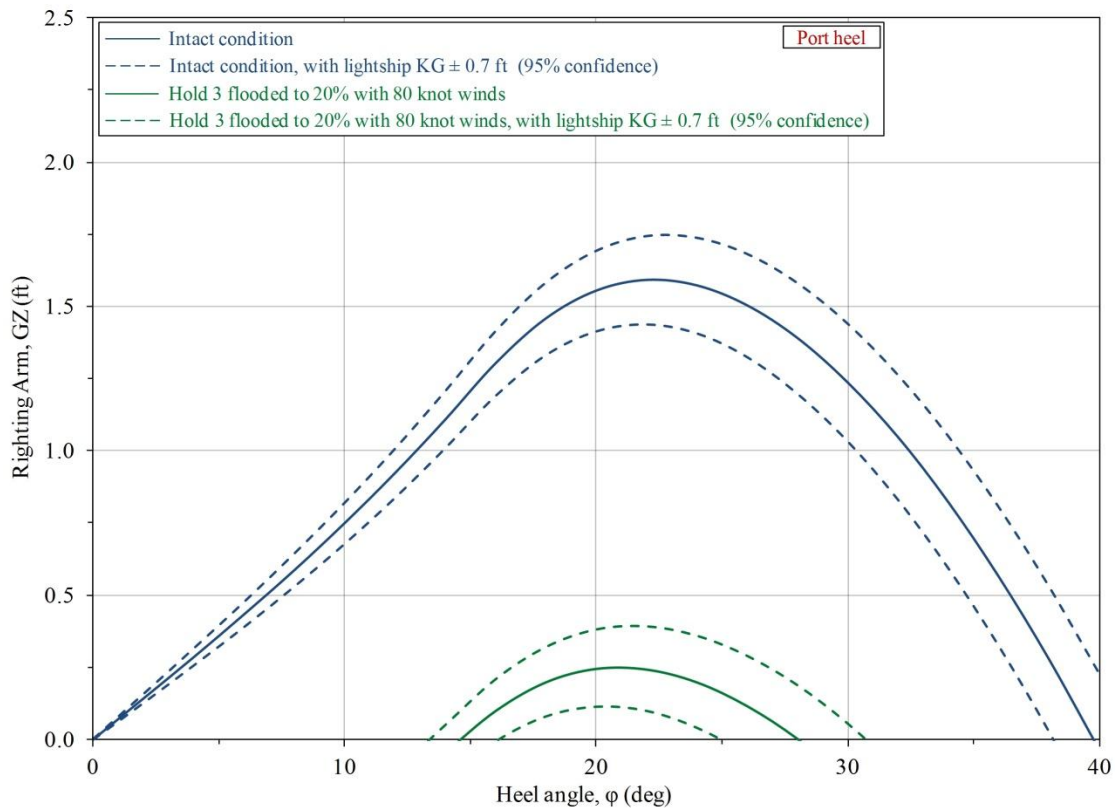


Figure 6-28: Comparison of righting arm curves with effects of uncertainty in lightship KG considered: intact condition (at loss of propulsion, without flooding) and Hold 3 flooded to 20% with 0.7 permeability and 80 knot winds.

6.8. Vessel Sinking

It can be concluded from the VDR audio transcript that the EL FARO experienced flooding of Hold 3 and was experiencing significant wind heel resulting in a mean heel angle of approximately 15 degrees. Following the loss of propulsion around 0600, the vessel would have been drifting with beam to the wind and waves, and it could be expected that the vessel would also have been rolling around the mean wind heel due to wave action. In this condition, eventually the Hold 2A ventilation supply and exhaust openings would have intermittently immersed allowing additional floodwater into Hold 2A. Additional progressive flooding could have occurred through watertight door seal leakage or leakage of the bilge pumping system check valves. Regardless of the source or sources, progressive flooding of Hold 2A was suggested by the bilge alarm as reported at 0716.

As demonstrated by the analyses, the free surface associated with the additional floodwater would likely have been sufficient to cause the vessel to capsize. However, the capsizing may have been slowed or temporarily arrested as containers on deck began to wash overboard, providing a stabilizing effect. As the vessel slowly rolled onto her port side, floodwater would have entered through the ventilation openings into all of the cargo holds and the engine room, resulting in the sinking. Due to the 6,700 tons of iron ore fixed ballast in the double bottom tanks, the vessel would have returned to an upright condition as the vessel sank.

There is one phrase in the VDR audio transcript, “bow is down” uttered by the Captain in the final minutes at 0730 [64 (pg. 499)], which might suggest that the ship was sinking by the bow. However, it may be considered that the utterance “bow is down” was likely referring to an observation through the bridge windows of the immersion of the forward main deck on the port side, which would have occurred at an angle of heel of only 20-30 degrees with Hold 3 flooded. Note that this statement was made only one minute after the 2nd Mate uttered “...containers in the water” [64 (pg. 498)], indicating that it was all happening rapidly. The interaction on the bridge between the Captain and AB-1 in the final minutes suggests that the AB-1 was stuck on the port side of the wheelhouse as the vessel was slowly capsizing to port, as the Captain yelled for him to “come up,” with the AB-1 requesting help, even requesting a ladder or a rope to assist his climb [64 (pp. 501-508)].

Based on the MSC analyses, it can be concluded that it would be highly unlikely that the vessel could have sunk by the bow, but highly likely that the vessel would have capsized. With the huge free surface effect due to the floodwater in the full-breadth cargo holds, the ship would have rolled over long before enough water entered the forward holds to put the bow down. This is illustrated by Figure 6-21 through Figure 6-24 and the text of Sections 6.4 and 6.5, as any combination of floodwater in 2 or more cargo holds would result in capsizing of the vessel. Note that the term “capsize” does not mean that the vessel completely inverted, and in fact that would be considered highly unlikely, since the deck containers would have broken free and washed overboard, and this would have temporarily improved stability (see Figure 6-27). It is considered most likely that in the final minutes, the vessel rolled on its port side due to the free surface of the floodwater and hurricane force winds, lost most or all of the deck containers (and probably most of the internal RO/RO cargo broke free and shifted), and then rapidly flooded through the cargo hold ventilation openings.

6.9. Summary

This section documented the MSC hydrostatic analyses of the sinking of the EL FARO. The hydrostatic analyses use the MSC GHS computer model, focusing on assessment of righting arms including righting energy and range of stability considerations, in order to gain insight into the characteristics of vessel dynamics and motions due to wind heel and flooding.

The effects of wind heel are addressed, along with general and nuanced considerations associated with floodwater, including effects of free surface, compartment permeability, and pocketing. The potential sources of flooding of Hold 3 are discussed, including photographs and drawings for reference of the vulnerability to flooding through the cargo hold ventilation openings, and potentially through damaged emergency fire pump piping. Potential progressive flooding paths into Hold 2A were discussed, including downflooding through the cargo hold ventilation system openings, and possibly through leakage of the watertight door seals or leakage of the bilge pumping system check valves. Analyses of an array of wind heel and flooding conditions are used to assess likely conditions leading to the capsizing and sinking of the vessel given the environmental conditions.

The analyses results were highly sensitive to variation in permeability values, and a range of permeability values was used to assess impacts of the variability on the hydrostatics and stability. The evaluation of flooding required careful consideration of compartment permeability and pocketing effects. For permeability, this included significant variability in both overall fraction and uniformity throughout the cargo holds. This is especially important when considering containers, where permeability varies significantly depending on the assumed watertight integrity and specific locations of the containers.

The analyses results were highly sensitive to variation in wind speed, especially in combination with floodwater free surface, with variability of permeability and pocketing effects considered. Single compartment flooding of Hold 3 with combined wind heel of 70-90 knot beam winds resulted in very small residual righting arms and little residual righting energy. This would suggest that it would be highly unlikely that the EL FARO could have survived even single compartment uncontrolled flooding of Hold 3, given the wind and sea conditions.

Potential sources of flooding of Hold 3 and the other cargo holds were investigated, including vulnerabilities associated with the cargo hold ventilation system. It was highlighted that the locations of the ventilation openings would likely result in at least intermittent flooding into the cargo holds, as the vessel was subject to a variable wave height on the side shell and rolled about the mean wind heel angle of around 15 degrees.

Based on the MSC analyses, regardless of the sources of flooding, the free surface associated with the floodwater in multiple cargo holds combined with hurricane force winds and seas would likely have resulted in the capsizing of the vessel. The capsizing may have been slowed or temporarily arrested as containers on deck began to wash overboard, but as the vessel slowly rolled onto her port side, floodwater would have entered through the ventilation openings into all of the cargo holds and the engine room, resulting in the sinking.

7. Ship Structures

7.1. Introduction

Sun Shipbuilding in Chester, Pennsylvania built a series of 10 RO/RO “trailerships” between 1967 and 1977. While built for several different owners, and with minor differences in configurations to accommodate different trade routes, these vessels, listed in Table 7-1, were generally known as the PONCE DE LEON class of ships. The first 7 of these ships were originally delivered as 700 foot vessels. The 8th ship, the GREAT LAND, was originally laid down as a 700 foot vessel but was lengthened to 790 feet prior to delivery. The last two ships were, from keel laying, 790 foot vessels. Four of the earlier vessels were subsequently lengthened to 790 feet with the last, EL FARO, being lengthened in 1992-1993.

Hull	Name(s)	Year Built	Length (ft)	Original Owner, Trade
647	PONCE DE LEON	1967	700/790	TTT/NPR, Puerto Rico
650	ERIC K. HOLZER	1970	700	TTT/NPR, Puerto Rico
662	LURLINE	1973	700/826	Matson, Hawaii
663	FORTALEZA	1972	700	TTT/NPR, Puerto Rico
664	MATSONIA	1973	700/713	Matson, Hawaii
666	EL TAINO (EL MORRO)	1974	700/790	PFEL, Persian Gulf
670	PUERTO RICO (NORTHERN LIGHTS, EL FARO)	1974	700/790	TTT/NPR, Puerto Rico
673	GREAT LAND	1975	790	TOTE, Alaska
674	ATLANTIC BEAR (EL YUNQUE)	1976	790	PFEL, Persian Gulf
675	WESTWARD VENTURE	1977	790	TOTE, Alaska

Table 7-1: Sun Shipbuilding PONCE DE LEON class “trailerships.”

7.1.1. Original Construction

The EL FARO, Hull 670, was built in 1974, presumably in accordance with the 1974 American Bureau of Shipping (ABS) Rules for Building and Classing Steel Vessels (SVR 1974). Notes on the EL FARO’s Midship Section Drawing [5], shown partially in Figure 7-1, indicate that the vessel’s primary structure was derived from hulls 650, 662 and 663, and was identical to hulls 664, 666 and ultimately 673.

The ship’s primary structure was arranged typically of a “shelter deck” vessel (with the semi-enclosed 2nd Deck), intended to load and stow vehicular cargo in open spaces, with minimal structural intrusions. The primary hull girder structure comprised 3 full decks (Main Deck, 2nd Deck and 3rd Deck), plus a solid floor double bottom tanktop deck (4th Deck) and shell plating.

Heavy web frames were fitted every 8 feet 3 inches, extending from the tanktop to the Main Deck, along the length of the vessel. Although not explicitly required to meet regulatory or class strength or damage stability requirements at the time of construction, watertight bulkheads, extending to the 2nd Deck, were fitted at frames 20, 46, 87, 128, 169, 200 and 246.

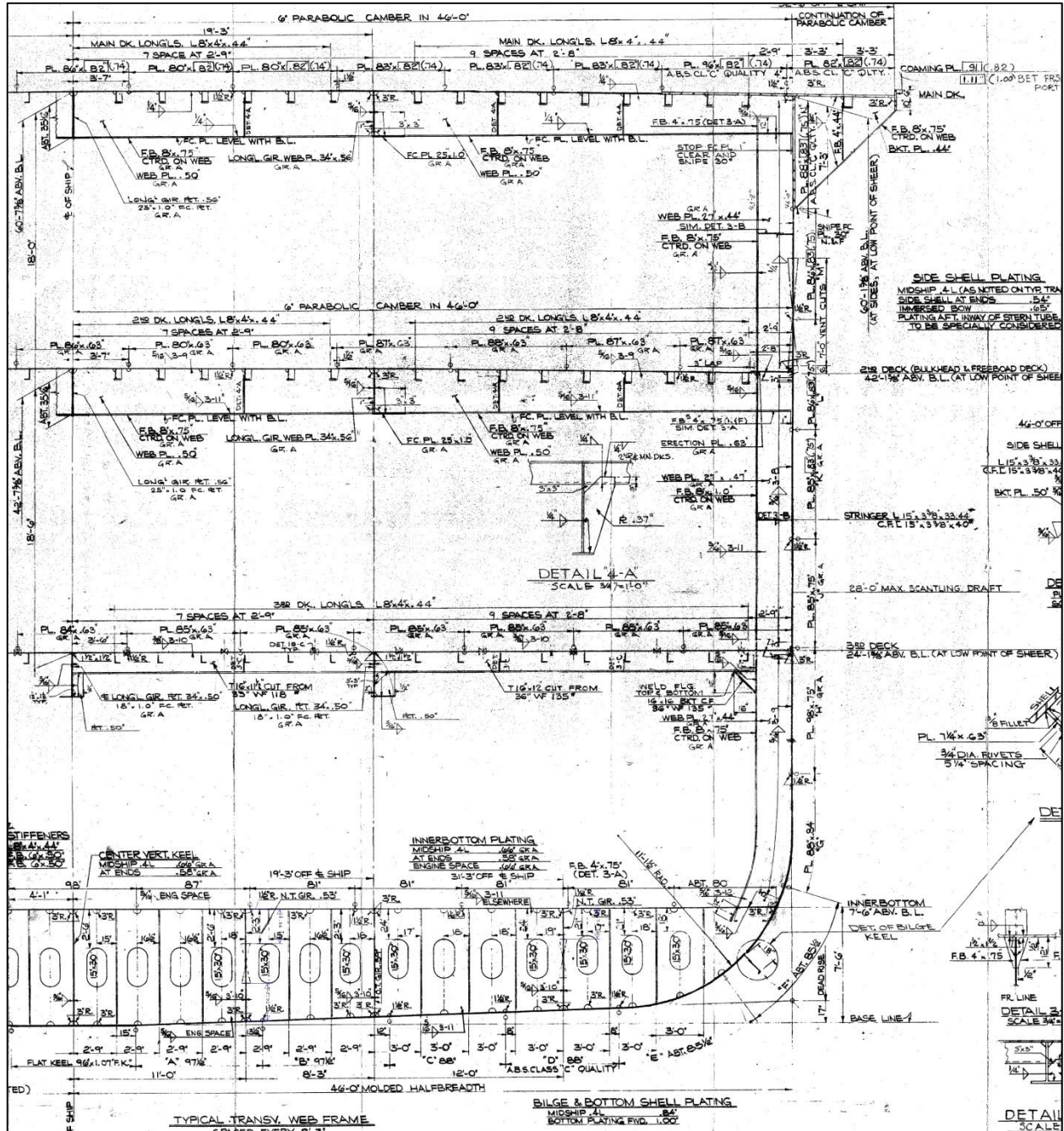


Figure 7-1: Midships Section. Taken from Sun Shipbuilding Midship Section Drawing 662-700-201, Alt E [5].

7.1.2. Significant Alterations

Although first assessed for lengthening in 1982, the EL FARO was the last of the PONCE DE LEON class of ships to be lengthened from 700 to 790 feet, and this occurred in 1992-1993. In addition to the fitting of the 90 foot mid-body section, the ship was also fit at this time with a Spar Deck above the Main Deck immediately forward of the superstructure extending from frames 128 to 162, and 1,830 LT of fixed ballast was added in double bottom tanks DB 2 P/S.

The second significant alteration to the vessel occurred in 2005-2006 with the conversion of the vessel from a pure RO/RO arrangement to a combined RO/RO and LO/LO arrangement (sometimes referred to as CON/RO). This was accomplished by removing the Spar Deck, adding container fittings to the Main Deck, adding reinforcing and supporting structure, and adding 4,875 LT of additional fixed ballast in double bottom tanks DB 2A P/S and DB 3 P/S. This would be the final significant configuration change made to the vessel.

7.2. Applicable Structural Criteria

7.2.1. Original Construction

As the continuation of a class of vessels which began construction in 1967, the EL FARO should have been built in accordance with the structural requirements of the 1974 American Bureau of Shipping (ABS) Steel Vessel Rules (1974 SVR). While there was no explicit documentation available to confirm this, a review of the information available on the Midship Section Drawing [5] does indicate that the vessel, as-built, did comply with the appropriate longitudinal strength (SVR 1974/6.3), shell plating (SVR 1974/15) and deck plating (SVR 1974/16) requirements of the 1974 SVR.

It should be noted that this class of vessels was originally designed to a maximum still water bending moment (SWBM) of 415,000 ft·LT and was constructed in accordance with the reduced plate scantling provisions of SVR 1974/15.7 and 174/16.5.10. These provisions permitted the shell plating above the deepest service draft, and exposed deck plating, to be reduced up to 10% from minimum required thickness, if they were provided with special protective coatings for corrosion control. In accordance with this allowance, and as indicated in Figure 7-2, side shell plating strakes K, L, M and N (extending from roughly 31.3 ft-BL (above baseline) up to the Main Deck), the coaming plate, and all of the vessel's Main Deck plating strakes, were all specified at 90% of the calculated scantling requirements of ABS SVR 1974/15.3 and 16.5.

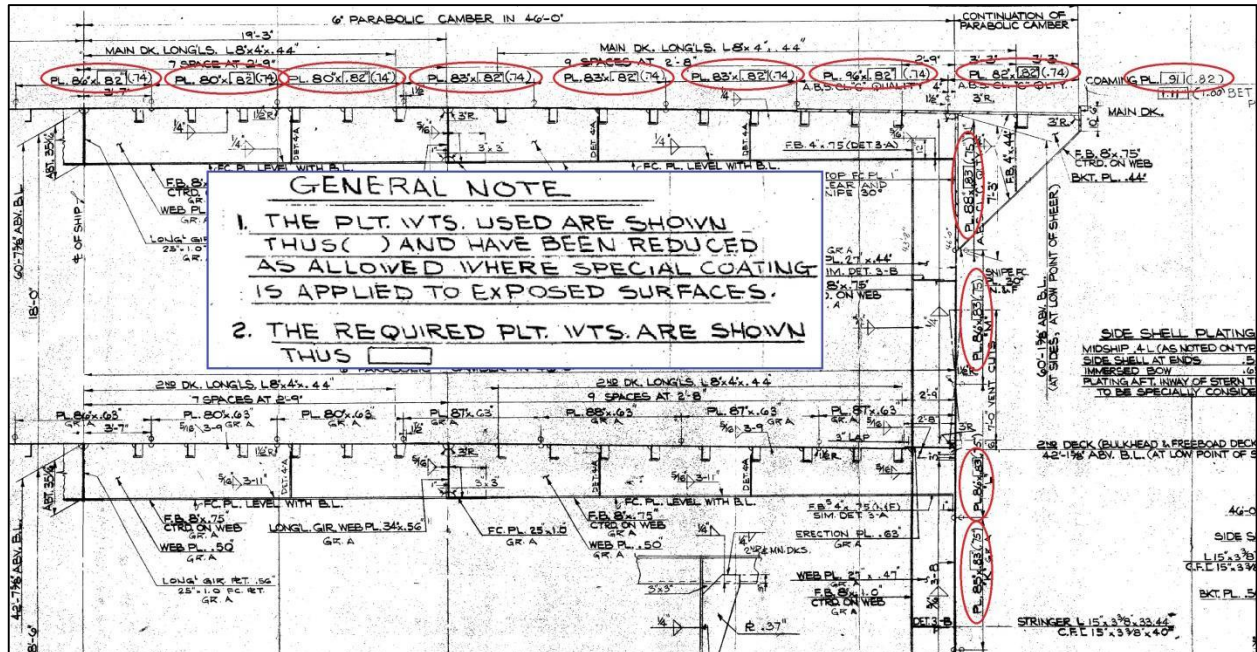


Figure 7-2: Reduced scantlings as permitted for strake plating with corrosion control coating (highlighted Midship Section Drawing [5]).

7.2.2. Lengthening Conversion (1992-1993)

As previously mentioned, the EL FARO was the fourth and final vessel of the class to be lengthened post-delivery. While several plans and structural calculations were approved by ABS for lengthening the vessel in 1982, the vessel was not actually lengthened until 10 years later in 1992-1993. Further, it is not clear what, if any, of the structural engineering performed in 1982 was used in the 1992-1993 lengthening, as the Scantling Plan [71] indicates that it was duplicated from Hull 675’s construction plans for application to EL FARO’s lengthening. As such, it is not clear what specific structural rule set was applied to the vessel for the 1992-1993 lengthening. There are, however, several aspects of the 1982 calculation package and structural plans which bear mentioning.

Of particular note, the calculation of section properties at all longitudinal locations ignored the 3rd Deck. As this deck is continuous throughout and beyond the midships 40% of the vessel’s length (0.4L), is solidly connected to the shell structure, does not appear to be arranged with expansion joints, and meets the effectiveness criteria of SVR 1982/16.5.2, it is not clear why it was ignored in calculating the section properties. This might have been an effort to artificially balance the upper and lower section properties by artificially forcing the neutral axis higher in the vessel. In any case, independent calculations performed by the MSC confirm that the vessel’s scantlings, as designed, were adequate when considering the 3rd Deck effective.

The 1982 structural calculations apply a longitudinal distribution factor to the minimum section modulus (SM) required by SVR 1982/6.3.1. It is not clear that this is appropriate, however, as SVR 1983/6.3.2c permits the Wave Induced Bending Moment (WIBM) to be modified by the distribution factor, whereas SVR 1982/6.3.2.a requires the SWBM to remain constant throughout

the midships 0.4L. As applying the distribution factor to the minimum required SM value effectively reduces both the WIBM and SWBM, this application appears to be inappropriate.

Independent calculations performed by the MSC, however, show the new midbody scantlings meeting the minimum SM requirements of SVR 1982/6.3.1 for the full design bending moment (SWBM+WIBM) and the existing structure, within the midships 0.4L of the vessel, to be adequate when applying the distribution factor to the WIBM only per SVR/6.3.2c. It should be noted that, with the lengthening of the PONCE DE LEON class vessels, the design SWBM was increased to 500,000 ft·LT due to a combination of loading and structural changes.

There is no clear indication of when or why the PONCE DE LEON class vessels received deck and bottom strapping, other than listing of the weight of bottom strapping and Main Deck doubler plates in the Preliminary Weight Estimate for the 1992-1993 conversion [23]. Whereas the original midship structural section does not reflect any kind of strapping, both the 1982 structural calculations and the 1992 scantling plans clearly indicate that the lengthened vessels were outfitted with significant strapping, both on the Main Deck and on the bottom shell. While a large portion of the deck strapping appears to be compensatory for vehicle ramp deck cutouts, a reduced amount of strapping was carried continuous through the midships portion of the vessel. The purpose of the bottom strapping is not clear but it does appear to have been carried uniformly throughout the midships portion of the vessel.

As previously mentioned, the Spar Deck between frames 128 and 162 was also added to the vessel during the lengthening in 1992-1993, and, as it was wholly located within the midships 0.4L of the vessel, it was not considered effective relative to the vessel's longitudinal strength.

7.2.3. Container Conversion (2005-2006) and Scantling Reassessments

In 2005-2006 the vessel was modified to carry containers on the Main Deck by removing the Spar Deck, reinforcing and supporting structure and adding a significant amount of additional fixed ballast. As a result of this conversion, the vessel's maximum molded draft was increased from 28.0 ft (28' 0") to 30.11 ft (30' 1-5/16").

While calculations were prepared to assess the adequacy of the tank scantlings relative to the permanent ballast installations, no structural analysis was prepared for the structural alterations or for the increase in scantling draft. Instead, the structure was accepted based upon the scantlings of the EL MORRO (Hull 666) having been accepted for a maximum molded draft of 30.75 ft (30' 9"). This was confirmed by Mr. Suresh Pisini in his MBI hearing testimony [39].

Subsequent to these alterations, a significant portion of the vessel, including the Main Deck and 2nd Deck plating, the aft peak tank and the innerbottom structure, was reassessed by ABS. While insufficient information was available for MSC to independently verify these re-assessments, ABS re-evaluated these structural elements relative to the 2007 SVR requirements and re-established corrosion allowances and minimum member thicknesses for renewal.

7.2.4. Post-Casualty Strength Analysis

After the loss of EL FARO, ABS conducted an analysis [72] of the hull girder section modulus (SM) to both the 1975 and 2015 (current) ABS class rule requirements, and also a buckling verification of the bottom shell and deck plating to the 2015 class rule requirements.

SM was evaluated amidships using as-built scantlings, amidships using scantlings from a 2011 gauging report [73], and at Frame 120 (in way of ramp openings) using the same as-gauged scantlings. Results of all three of these evaluations indicated that the EL FARO was in compliance with both 1975 and 2015 SM requirements in this regard.

ABS also evaluated buckling of the vessel in way of critical areas in both the bottom and deck structure reflecting the 2011 as-gauged scantlings and reflecting the maximum design bending moment. ABS further examined buckling stress in the bottom structure, using the as-gauged scantlings and an assumed bending moment at the time of the casualty. Results of these analyses indicated that the maximum stresses in both the bottom shell and upper deck plating were within the critical buckling limits of the 2015 class rule requirements.

With minimal differences, independent calculations performed by the MSC of these SM and buckling analyses generally confirmed these findings.

7.3. CargoMax Hull Girder Strength Assessment

As discussed in Section 2 of this report, a lightship weight distribution was created for the MSC GHS computer model, and bending moment calculations were included in assessment of the accident voyage 185S departure condition. Figure 7-3 provides a plot of the calculated still water bending moments. For comparison, bending moments calculated by CargoMax are included, along with the allowable still water bending moment.

The bending moments calculated using the MSC GHS computer model are approximately 13% higher amidships compared to the CargoMax values, but are still within the ABS allowable bending moment limits. The differences in calculated bending moments can be attributed to differences in the estimated lightship weight distribution.

As noted in Section 2 of this report, vessel loading and hull strength assessment, including lightship weight distribution and bending moment calculations, would be included in a vessel loading manual, and this would be reviewed and approved by ABS. However, based on the original date of construction, a loading manual was not required by any Coast Guard or classification society standard for EL FARO. It should also be noted from the ABS approval letter of the CargoMax software [21] that the software was neither reviewed nor approved for assessment of loading and hull strength, but it was nevertheless relied on by the Tote operations personnel for loading and hull strength assessment, based on MBI hearing testimony [18, 19, 20, 31, 32].

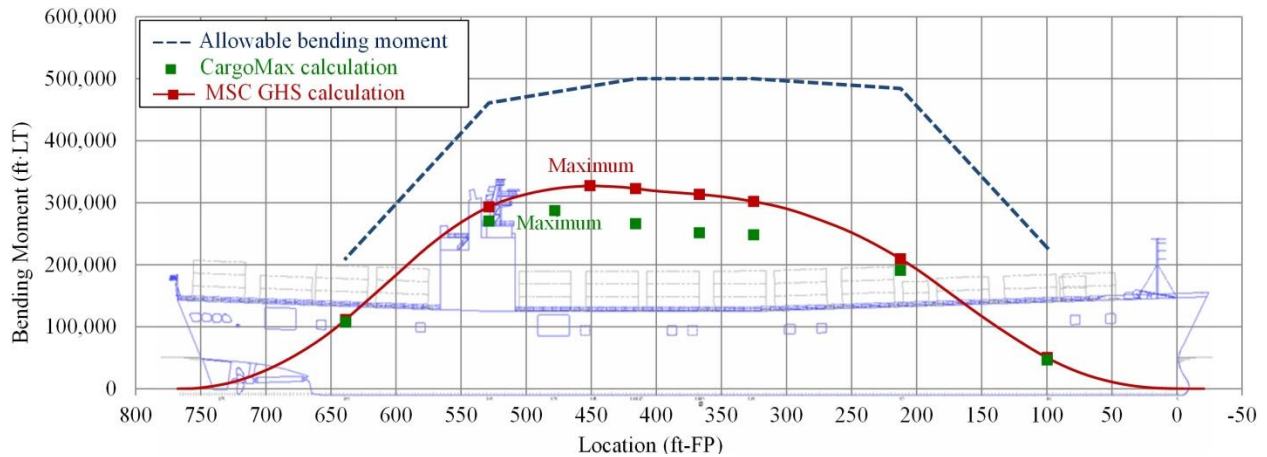


Figure 7-3: Calculated and allowable still water bending moments for the accident voyage 185S departure condition.

7.4. Summary

This section documented the MSC review of the ship structures, and provided a summary of the applicable structures criteria and review of documented structural assessments completed and approved by ABS. This section also provided a summary of the CargoMax application for hull girder strength assessment.

Based on the MSC review of the documentation available, it appears that the ship structures met all regulatory and classification society (ABS) structural requirements.

For the accident voyage, bending moments calculated using the MSC GHS computer model are approximately 13% higher amidships compared to the CargoMax values, but are still within the ABS allowable bending moment limits. The differences in calculated bending moments can be attributed to differences in the estimated lightship weight distribution.

8. Conclusions

The following provides a summary of key MSC observations and conclusions, listed by topic area:

- (1) MSC computer model, and comparison with the T&S Booklet and CargoMax stability software:
 - a. Hull hydrostatic properties compared closely when comparing the T&S Booklet and CargoMax values to the MSC computer model, with approximately 0.1% difference in calculated displacement at the full load draft. All hydrostatic properties were within the tolerance of IMO MSC.1/Circ.1229, which has been used as an objective quality standard.
 - b. Comparison of tank volumes, centers and free surface inertia values identified discrepancies with T&S Booklet and CargoMax calculated values. Using IMO MSC.1/Circ.1229 as an objective quality standard, when comparing the T&S Booklet and CargoMax values to the MSC computer model, 19 tanks were in excess of the 2% tolerance for volume, and 22 tanks were in excess of the 2% tolerance for maximum slack free surface inertia. Based on additional MSC review of EL FARO and sister vessel T&S Booklets going back to the 1970s, it appears that errors were made in the original tank geometry definition and/or in the original numerical integration. It also appears that these discrepancies in tank values would apply to all of the vessels of the PONCE DE LEON class.
- (2) Stability test, lightship calculations, and uncertainty analysis
 - a. Based on the MSC uncertainty analysis of the stability test, the uncertainty in the as-inclined GM was calculated to be approximately 0.2 feet (with 95% confidence). This means that there is a 95% confidence that the true value of GM in the as-inclined condition is within ± 0.2 feet of the value calculated in the Stability Test Report. The uncertainty in the lightship KG was calculated to be approximately 0.7 feet (with 95% confidence), and the uncertainty in the GM for the accident voyage departure condition was calculated to be approximately 0.7 feet (with 95% confidence). The last statement means that there is a 95% confidence that the true value of the accident voyage GM was within ± 0.7 feet of the calculated value.
- (3) T&S Booklet and CargoMax stability software:
 - a. The CargoMax stability software used onboard the EL FARO and for load planning by shore-side personnel was neither reviewed nor approved for assessment of loading and hull strength since there was no loading manual required for the EL FARO. However, the EL FARO CargoMax software did contain features to assess hull strength, and the vessel operators relied on these features for assessment of hull girder bending moment in load planning.

- b. The CargoMax software was neither reviewed nor approved for assessment of cargo loading and securing, including calculations required in the Cargo Securing Manual, which had been reviewed and approved by ABS. However, the EL FARO CargoMax software did contain features for assessment of cargo securing, and the vessel operators relied on these features for assessment of LO/LO container loading and securing.
- c. With the exception of recent amendments to several IMO instruments applicable to oil, chemical and gas carriers, there are no requirements for the use of onboard software for vessel stability, strength or cargo loading and securing. Under Coast Guard policy, the master must be provided with the capability to manually calculate stability. However, he may use whatever tools he wishes to assist him in his responsibility to ensure satisfactory stability. The Coast Guard will, upon request, verify that the onboard stability software produces nearly identical results to the approved stability booklet in a number of representative loading conditions. After verification, the Coast Guard will recognize the software as an adjunct to the stability booklet; however, it remains incumbent upon the master to ensure the vessel is compliant with all aspects of the stability booklet.

(4) Intact and damage stability:

- a. The MSC computer model was used to assess eight “benchmark” loading conditions defined by the MSC against intact stability criteria. The eight “benchmark” conditions included the full load departure and arrival conditions from the 1993 and 2007 T&S Booklets, a representative departure and arrival condition from August 2015 (voyage 178S), and the accident voyage (185S) departure condition and estimated condition at the time of loss of propulsion on October 1, 2015.
- b. The eight “benchmark” loading conditions all met the applicable intact stability requirements of 46 CFR 170.170 (the GM “weather” criteria), which were applicable to the EL FARO at the time of the casualty. However, it is noted that the vessel was often operated very close to the maximum load line drafts, with minimal stability margin compared to the required GM, and little available freeboard and ballast capacity, leaving little flexibility for improving stability at sea if necessary due to heavy weather or flooding.
- c. If EL FARO were constructed in 2016, she would be required to meet the righting arm criteria of Sections 2.2 and 2.3 of Part A of the 2008 IS Code. Of the eight “benchmark” conditions, only the 1997 T&S Booklet loading conditions would meet the righting arm criteria of Section 2.2. The actual operating conditions of voyage 178S and the accident voyage 185S would not meet the criteria based on limited available area (righting energy) between 30 and 40 degrees and insufficient angle of maximum righting arm. All of the eight conditions would meet the severe wind and rolling righting arm criteria of Section 2.3. In order to

fully meet the intact stability criteria of Part A of the 2008 IS Code at the full load draft, the minimum required GM would be approximately 6.8 feet, which is 2.5 feet greater than the GM of the actual departure loading condition of the accident voyage. It is noted that paragraph 2.2.3 of Part A of the 2008 IS Code provides that “alternate criteria based on an equivalent level of safety may be applied subject to the approval of the administration” if obtaining the required 25 degree angle for maximum righting arm is “not practicable.” Thus there could be permitted a relaxation of the limiting criteria for minimum angle of maximum righting arm (25 degrees), if allowed by the USCG on a case-by-case basis. In such a case the minimum required GM could be less, and could also become limited by the damage stability criteria.

- d. Despite the 2-foot increase in the load line draft resulting from the 2005-2006 conversion for carrying LO/LO containers, there was no damage stability assessment completed to verify that the EL FARO would remain limited by the intact stability criteria for all loading conditions. Damage stability assessments conducted using the applicable 1990 SOLAS probabilistic stability standards demonstrate that for load conditions with two or fewer tiers of containers, the limiting stability criteria could be the damage stability criteria instead of the intact stability criteria, and this was not reflected on the minimum required GM curves of the T&S Booklet. However, for the departure condition of the accident voyage, the limiting stability criteria was the intact stability criteria, which was properly reflected in the T&S Booklet and incorporated in the CargoMax stability software. If EL FARO were constructed in 2016, she would be required to meet the 2009 SOLAS probabilistic damage stability standards. In order to fully meet these 2009 SOLAS damage stability standards at the full load draft, the minimum required GM would be approximately 5.8 feet, which is 1.5 feet greater than the GM of the actual departure loading condition of the accident voyage.
- e. The righting arm curves for the EL FARO are generally characterized by relatively small area (righting energy) and range of stability compared to conventional cargo vessels (see Figure 5-6). These characteristics are especially significant in consideration of limited residual righting arms and righting energy with the vessel subjected to heeling forces and moments as might be experienced in heavy weather where high winds and seas can be expected. These characteristics are significant in consideration of limited residual righting arms and righting energy when subjected to flooding.

(5) Hydrostatic sinking analyses:

- a. The MSC approach to the hydrostatic sinking analyses was fundamentally based on a first-principles assessment of flooding and wind heel, focusing on the righting arms, including righting energy and range of stability considerations. Effects of free surface effects due to the floodwater in the cargo holds were included.

- b. The analyses results were highly sensitive to variation in permeability values, and a range of permeability values was used to assess impacts of the variability on the hydrostatics and stability. The evaluation of flooding required careful consideration of compartment permeability and “pocketing” effects. For permeability, this included significant variability in both overall fraction and uniformity throughout the cargo holds. This is especially important when considering containers, where permeability varies significantly depending on the assumed watertight integrity and specific locations of the containers.
- c. The analyses results were highly sensitive to variation in wind speed, especially in combination with floodwater free surface, with variability of permeability and pocketing effects considered. Single compartment flooding of Hold 3 with combined wind heel of 70-90 knot beam winds resulted in very small residual righting arms and little residual righting energy. This would suggest that it would be highly unlikely that the EL FARO could have survived even single compartment uncontrolled flooding of Hold 3, given the sea conditions. This is illustrated in Figure 6-22 through Figure 6-24. To put this into perspective in terms of overall effects on righting arms and righting energy, Figure 8-1 adds several conditions with 80 knot beam winds and flooding of Hold 3 to the curves in Figure 5-6. It is clear from the minimal residual righting energy that with combined wind and flooding, the EL FARO would have had great difficulty surviving, when also considering the significant additional heeling energy imposed by the 25-30 foot seas she was encountering.
- d. Potential sources of flooding of Hold 3 and the other cargo holds were investigated, including vulnerabilities associated with the cargo hold ventilation system. It was highlighted that the locations of the ventilation openings would likely result in at least intermittent flooding into the cargo holds, as the vessel was subject to a variable wave height on the side shell and rolled about the mean wind heel angle of around 15 degrees.
- e. Based on the MSC analyses, regardless of the sources of flooding, the free surface associated with the floodwater in multiple cargo holds combined with hurricane force winds and seas would likely have resulted in the capsizing of the vessel. The capsizing may have been slowed or temporarily arrested as containers on deck began to wash overboard, but as the vessel slowly rolled onto her port side, floodwater would have entered through the ventilation openings into all of the cargo holds and the engine room, resulting in the sinking.

(6) Ship structures:

- a. Based on the MSC review of the documentation available, the EL FARO ship structures met all regulatory and class structural requirements for strength.
- b. For the accident voyage, bending moments calculated using the MSC GHS computer model are approximately 13% higher amidships compared to the

CargoMax values, but are still within the ABS allowable bending moment limits. The differences in calculated bending moments can be attributed to differences in the estimated lightship weight distribution.

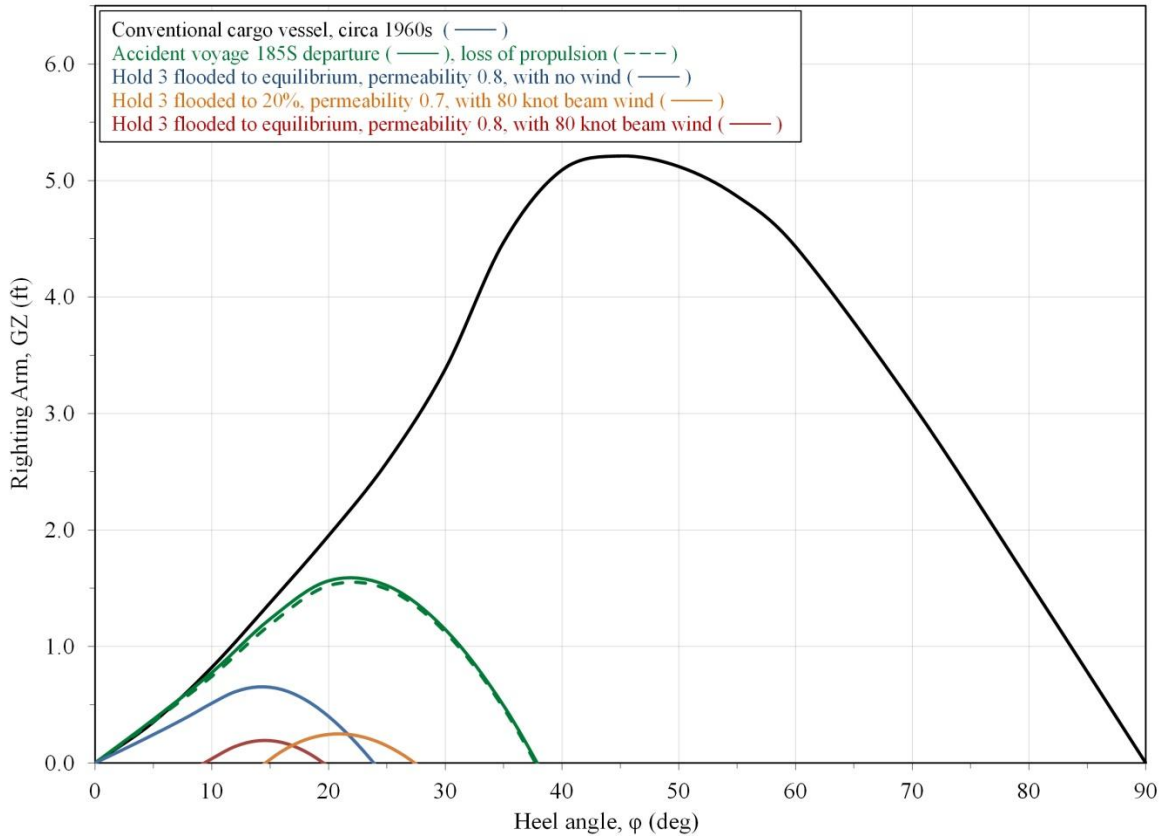


Figure 8-1: Righting arm curves for the accident voyage, with comparison to a conventional cargo vessel (conventional vessel curve reproduced from [51] with permission).

9. References

- 1 MSC Technical Review and Analysis of the SS EL FARO, O.N. 561732, Memorandum from Commandant (CG-INV) to Marine Safety Center (CG MSC), dated July 22, 2016 (MBI Exhibit 243).
- 2 SS EL FARO HECSALV Computer Model, File “Faro-10.shp”, dated March 13, 2007, Herbert-ABS Software Solutions LLC.
- 3 SS EL FARO Final Offsets, Drawing SK-647-700-407, Alt 13, dated November 12, 1969, Sun Shipbuilding (MBI Exhibit 135).
- 4 SS EL FARO General Arrangement Drawing, Drawing SSL-670-100-026, Rev 0, dated April 24, 2006, Herbert Engineering Corporation (MBI Exhibit 007).
- 5 SS EL FARO Midship Section Plan, Drawing 662-700-201, Alt E, dated October 18, 1974, Sun Shipbuilding (MBI Exhibit 244).
- 6 SS EL FARO Shell Plating Fr 20 to 87, Drawing 647-706-2, dated July 22, 1975, Sun Shipbuilding (MBI Exhibit 245).
- 7 SS EL FARO Shell Plating Fr 87 to 172, Drawing 663-706-3, dated August 9, 1974, Sun Shipbuilding (MBI Exhibit 246).
- 8 SS EL FARO Shell Plating Fr 172 to 204, Drawing 670-706-4, dated July 9, 1974, Sun Shipbuilding (MBI Exhibit 247).
- 9 SS EL FARO Combined Bulkheads Drawing (drawing numbers and dates unreadable), Sun Shipbuilding (MBI Exhibit 248). [provided by ABS]
- 10 SS EL FARO Capacity Plan, Drawing SSL-670-100-027, Alt C, dated March 3, 2006, Herbert Engineering Corporation (MBI Exhibit 133).
- 11 SS EL FARO CargoMax Printout, Revised, for accident voyage 185S, printed 11:48 on 01 Oct 2015, Tote Inc (MBI Exhibit 059).
- 12 SS EL FARO Trim and Stability Booklet, Drawing 1252-700-602, Rev E, dated February 14, 2007, Herbert Engineering Corporation (MBI Exhibit 008).
- 13 IMO MSC.1/Circ.1229, Guidelines for Approval of Stability Instruments, dated January 11, 2007.
- 14 International Association of Class Societies (IACS) Unified Requirement L5: Onboard Computers for Stability Calculations, Corr. 1, dated 2006.
- 15 SS EL FARO Floors Fr 47 to 87, Drawing 666-710-2, Alt 3, dated May 22, 1974, Sun Shipbuilding (MBI Exhibit 249).
- 16 SS EL FARO Floors Fr 88 to 172, Drawing 666-710-4, Alt 10, dated September 12, 1974, Sun Shipbuilding (MBI Exhibit 250).
- 17 SS NORTHERN LIGHTS Trim and Stability Booklet, Drawing 1252-700-602, Rev A1, dated May 6, 1993, Atlantic Marine Inc. (MBI Exhibit 251).
- 18 Transcript, U.S. Coast Guard Marine Board of Investigation ICO the Sinking of the SS El Faro Held in Jacksonville, Florida, February 20, 2016, Volume 5.
- 19 Transcript, U.S. Coast Guard Marine Board of Investigation ICO the Sinking of the SS El Faro Held in Jacksonville, Florida, February 25, 2016, Volume 9.
- 20 Transcript, U.S. Coast Guard Marine Board of Investigation ICO the Sinking of the SS El Faro Held in Jacksonville, Florida, February 18, 2016, Volume 3.
- 21 ABS Houston Letter Ref 314297 - SS EL FARO Stability Review on Behalf of the U.S. Coast Guard – NVIC 3-97 (CargoMax Version 1.21 Approval), dated February 8, 2008 (MBI Exhibit 254).

- 22 SS EL FARO Stability Test Report, date of inclining February 12, 2006, ABS approved March 22, 2006, Herbert Engineering Corporation (MBI Exhibit 139).
- 23 NORTHERN LIGHTS Conversion Preliminary Weight Estimate, Drawing 1252-700-001, Rev A2, dated November 11, 1992, JJH, Inc. (MBI Exhibit 255).
- 24 SS NORTHERN LIGHTS (EL FARO) Fixed Ballast Installation, Drawing SSL-670-100-003, dated May 24, 2005, Herbert Engineering Corporation (MBI Exhibit 257).
- 25 SS NORTHERN LIGHTS (EL FARO) Container Support Structure, Drawing SSL-670-100-001, dated June 15, 2005, Herbert Engineering Corporation (MBI Exhibit 407).
- 26 SS NORTHERN LIGHTS (EL FARO) Spar Deck Removal, Drawing SSL-670-100-024, undated, Herbert Engineering Corporation (MBI Exhibit 406).
- 27 ASTM F1321-92 (Reapproved 2004), Standard Guide for Conducting a Stability Test (Lightweight Survey and Inclining Experiment) to Determine the Light Ship Displacement and Centers of Gravity of a Vessel, ASTM International, 2004 (MBI Exhibit 194).
- 28 SS EL FARO Stability Test Procedure, Drawing SSL-670-100-10, dated December 23, 2005, ABS approved February 2, 2006, Herbert Engineering Corporation (MBI Exhibit 258).
- 29 ABS Statutory Survey Report M662652: SS EL FARO Inclining Experiment, dated February 12, 2006 (MBI Exhibit 190).
- 30 SS EL FARO Inclining Experiment Record Sheet, dated February 12, 2006, Herbert Engineering Corporation (MBI Exhibit 259).
- 31 Transcript, U.S. Coast Guard Marine Board of Investigation ICO the Sinking of the SS El Faro Held in Jacksonville, Florida, February 24, 2016, Volume 8.
- 32 Transcript, U.S. Coast Guard Marine Board of Investigation ICO the Sinking of the SS El Faro Held in Jacksonville, Florida, May 16, 2016, Volume 11.
- 33 ABS Houston Letter Ref 348013 - SS EL FARO Stability Review on Behalf of the U.S. Coast Guard – NVIC 3-97 (Trim and Stability Booklet Approval), dated May 31, 2007 (MBI Exhibit 253).
- 34 International Load Line Certificate for EL FARO, dated January 29, 2011, issued by American Bureau of Shipping (MBI Exhibit 260).
- 35 SS EL FARO Cargo Securing Manual, Procedure No. E-03(Series), Rev 0, dated December 12, 2005, Herbert Engineering Corporation (MBI Exhibit 040).
- 36 ABS Steel Vessel Rules, Part 3, Chapter 3, Appendix 3, Onboard Computers for Stability Calculations, dated July 1, 2005.
- 37 COMDTINST M16000.9, Marine Safety Manual, Volume IV (Technical), Chapter 6 (Ship Stability, Subdivision, Structures, Welding, Load Lines, and Maneuverability), Change 3 dated September 29, 2004, U.S. Coast Guard.
- 38 Transcript, U.S. Coast Guard Marine Board of Investigation ICO the Sinking of the SS El Faro Held in Jacksonville, Florida, May 19, 2016, Volume 14.
- 39 Transcript, U.S. Coast Guard Marine Board of Investigation ICO the Sinking of the SS El Faro Held in Jacksonville, Florida, May 20, 2016, Volume 15.
- 40 Transcript, U.S. Coast Guard Marine Board of Investigation ICO the Sinking of the SS El Faro Held in Jacksonville, Florida, May 23, 2016, Volume 16.
- 41 ABS Memorandum, SOLAS Probabilistic Damage Stability Analysis, submitted by Thomas Gruber to the MBI, dated May 6, 2016 (MBI Exhibit 166).
- 42 CargoMax for Windows Version 1.21 Vessel Information Book for SS EL FARO, Rev 2, dated March 13, 2007, Herbert Software Solutions Inc. (MBI Exhibit 261).

- 43 Direct Calculation of Required GM for USCG Windheel Criteria Within the CargoMax Loading Program: Implementation System and Supporting Calculations for SS EL FARO, dated April 14, 2006, Herbert Engineering Corporation (MBI Exhibit 262).
- 44 CargoMax for Windows User's Manual, 9th Edition dated September 2011, Herbert-ABS Software Solutions LLC (MBI Exhibit 263).
- 45 CargoMax for Windows Version 1.21 Vessel Information Book for SS EL FARO, Rev 1, dated October 19, 2006, Herbert Software Solutions Inc. (MBI Exhibit 256).
- 46 CargoMax Trim and Stability Summary Printout (Annotated) and Deck Log for Tuesday August 11, 2015 (Jacksonville Departure Voyage 178S), Tote Inc. (MBI Exhibit 088).
- 47 Moore, C.S., Principles of Naval Architecture Series: Intact Stability, Society of Naval Architects and Marine Engineers (SNAME), Alexandria, VA, 2010.
- 48 Henrickson, W.A., "Assessing Intact Stability," Marine Technology, Vol. 17, No. 2, April 1980, pp. 163-173.
- 49 Circular MSC.1/Circ 1281, "Explanatory Notes to the International Code On Intact Stability, 2008," December 9, 2008, International Maritime Organization (IMO).
- 50 Rahola, J., "The Judging of the Stability of Ships and their Determination of the Minimum Amount of Stability," Doctoral Thesis, University of Finland, Helsinki, 1939.
- 51 Mok, Y. and Hill, R.C., "On the Design of Offshore Supply Vessels," Marine Technology, Vol. 7, No. 3, July 1970, pp. 278-297.
- 52 Annex 2 of Resolution MSC.267(85) (MSC 85/26/Add.1), "Adoption of the International Code on Intact Stability, 2008 (2008 IS Code)", Adopted December 4, 2008, International Maritime Organization (IMO).
- 53 U.S. Supplement to ABS Rules for Steel Vessels for Vessels Certified for International Voyages (ACP Supplement), dated April 1, 2011 (USCG approval May 3, 2011), American Bureau of Shipping (MBI Exhibit 113)
- 54 SS EL FARO CargoMax Printout for Voyage 178S, from CargoMax load case file "EF178JX.LC", Tote Inc. (MBI Exhibit 264).
- 55 Tagg, R.D., Damage Survivability of Cargo Ships, SNAME Transactions, Vol. 90, 1982, pp. 26-40.
- 56 MARAD Damaged Stability Standard (MARAD Design Letter No. 3) dated August 1, 1983, reissued January 4, 1991, U.S. Department of Transportation, Washington DC.
- 57 Nickum, G.C., Subdivision and Damage Stability, in Principles of Naval Architecture Vol. 1, Stability and Strength, Society of Naval Architects and Marine Engineers, 1988
- 58 SOLAS Consolidated Edition 2001, Consolidated Text of the International Convention for the Safety of Life at Sea, 1974 and its Protocol of 1978 (articles, annexes and certificates, incorporating all amendments in effect from 1 January 2001).
- 59 IMO Resolution A.684(17), Explanatory Notes to the SOLAS Regulations on Subdivision and Damage Stability of Cargo Ships of 100 Meters in Length and Over, adopted November 6, 1991.
- 60 SOLAS Consolidated Edition 2014, Consolidated Text of the International Convention for the Safety of Life at Sea, 1974 and its Protocol of 1988 (articles, annexes and certificates, incorporating all amendments in effect from 1 July 2014).
- 61 IMO Resolution MSC.281(85), Explanatory Notes to the SOLAS Chapter II-1 Subdivision and Damage Stability Regulations, adopted December 4, 2008.

- 62 Tagg, R.D., “Comparison of Survivability between SOLAS 90/95 and SOLAS 2009 ships – A retrospective view 10 years on from the project HARDER,” Proceedings of the 14th International Ship Stability Workshop, 2014.
- 63 ABS Houston Letter Ref 7500285 – RO-RO Vessel O.N. 561732, Stability Review on Behalf of the U.S. Coast Guard (Subdivision and Damage Stability and Intact Stability), dated May 6, 1993 (MBI Exhibit 265).
- 64 Transcript, Group Chairman’s Factual Report of Investigation, Voyage Data Recorder – Audio Transcript, SS El Faro, December 12, 2016, National Transportation Safety Board (MBI Exhibit 266).
- 65 Fidele et.al., On the Prediction of Rogue Waves During Hurricane Joaquin, Technical Report, Georgia Tech School of Civil and Environmental Engineering and the Italian Ship Model Basin (INSEAN), dated October 16, 2016 (MBI Exhibit 267).
- 66 NTSB Group Chairman’s Factual Report (Meteorology Group), SS EL FARO, DCA16MM001, draft dated November 7, 2016 (MBI Exhibit 268).
- 67 Brater, E.F. and King, H.W., Handbook of Hydraulics, 6th Edition, McGraw-Hill Co., New York, 1976.
- 68 Ventilation Arrangement Holds 2A & 3, Drawing 1252-877-2A Rev A, dated December 12, 1992, JJH, Inc. (MBI Exhibit 269).
- 69 NORTHERN LIGHTS Downflooding Points Cont. (Excerpts from various ventilation system drawings), JJH, Inc. Fax Transmission dated May 10, 1993 (MBI Exhibit 270).
- 70 Final Stow Plan for EL FARO Voyage 185S, dated September 29, 2015, Tote Inc. (MBI Exhibit 069).
- 71 SS NORTHERN LIGHTS Conversion Scantling Plan, Drawing 1252-702-602, Revision A2, dated October 15, 1992, JJH, Inc. (MBI Exhibit 271).
- 72 EL FARO Hull Girder Section Modulus Analysis (Rev 11/5/2015), ABS Structures Group (MBI Exhibit 167).
- 73 ABS Statutory Survey Report M9206092: Hull and Deck Plating Thickness Gauging, dated January 29, 2011 (MBI Exhibit 272).

Appendix A: Uncertainty Analysis of the Stability Test and Departure Condition

A.1. Introduction

The MSC was requested to review the EL FARO inclining experiment and Stability Test Report, and estimate the uncertainty in the vessel's lightship KG and in the GM for the accident voyage departure condition. This Appendix provides the detailed procedure and results for the requested uncertainty analysis. The analysis is based on the documentation available for the last stability test completed on the EL FARO on February 12, 2006 [A1 through A4], and the CargoMax accident voyage departure condition loading summary [A5].

It should be noted that there is no standard accepted procedure or guidance for completing an uncertainty analysis from the results of a stability test. The procedure undertaken by the MSC is based on an application of the principles of experimental uncertainty analysis, including assessment of potential sources of measurement errors, statistical analysis, and propagation of errors. The results of the analysis are fundamentally limited based on the size and type of vessel, the stability test procedure, the type of cargo and the specific loading condition. The results obtained for the uncertainty associated with the stability test and the lightship weight and center of gravity could be considered somewhat typical of similar large deep draft vessels. The additional uncertainty associated with the vessel loading condition can vary, depending on the particular type of cargo and loading procedures.

It is often the case that vessel operators consider the calculated GM, whether calculated by hand or by stability and loading software, to be fairly precise, and then operate the vessel fairly close to the minimum required GM. It is important to recognize that the actual GM may not be precisely known and uncertainty in the calculated GM can exist. However, calculated uncertainty in KG or GM for an operating condition should not be used to calculate a probability that the vessel would not meet the stability criteria for that operating condition. There is currently no consideration for uncertainty in assessing a vessel's stability in accordance with U.S. or international standards, as discussed in Section 5 of this report.

A.2. Background

A stability test (also called an inclining experiment) is conducted to experimentally determine a vessel's lightship weight (displacement) and location of the center of gravity, most importantly the vertical position or height of the center of gravity (KG or VCG). As with any experiment, errors in the measurements or measurement system create uncertainty in the results. The term "uncertainty" has been defined in this context as "a possible value that an error may have," and the term "uncertainty analysis" refers to the process of estimating how great an effect the uncertainties in the individual measurements have on the calculated result [A6, A7].

A thorough presentation of uncertainty analysis principles and techniques applied to a wide variety of experimental applications can be found in a variety of references. An excellent historical perspective on uncertainty analysis is provided by ITTC [A8]. One of the important aspects of this history is that despite the mathematical principles all being based on the same statistical principles, there is a wide variety of fundamental approaches and nomenclature that

have been applied to uncertainty analyses over the years. Although there have been attempts to try to standardize around a single international standard with the International Standards Organization (ISO) “Guide to Expression of Uncertainty in Measurement” (ISO GUM), significant differences in techniques still exist, largely due to long-favored experimental approaches and unique experimental applications.

Most experimental uncertainty analysis techniques focus around statistical principles when an experimental measurement is repeated a large number of times, as is typically done in experimental hydrodynamics or other measurements where ensemble averaging can be used based on high sampling rates using electronic instrumentation and computer analysis. Basic statistical principles may be applied to uncertainty analysis whenever repeated measurements are made under fixed operating conditions. This is applicable to a portion of the ship inclining experiment, where a series of incremental transverse weight shifts are made and resulting angles measured. Uncertainty analysis is more difficult in engineering experiments which cannot be repeated enough times to provide useful statistical information, for reasons of cost or time [A7]. This is generally applicable to a portion of a ship inclining experiment, where only a single set of draft readings is taken to determine vessel hydrostatic properties including displacement. As will be shown in this case for the EL FARO, it is this portion of the stability test which introduces the most uncertainty in terms of the calculation of lightship KG and GM for the departure condition.

Historically for uncertainty analyses, sources of error have been considered as falling into one of two categories [A9, A10]. Systematic errors (also called bias or fixed errors) fundamentally remain constant in repeated measurements under fixed operating conditions, and may cause either a high or a low offset or bias in the estimate of the true value of the measured variable. Because the effect is constant, it is difficult to estimate or even recognize the contribution of a systematic error in an experimental measurement system, but it may be partially quantified through good modeling and calibration procedure, and in some sense by applying good engineering judgment to the experiment, in which systematic errors can be estimated from experience with similar experiments or measurement systems. Random errors (also called precision or variable errors) fundamentally are manifested as scatter of the measured data when repeated measurements are made under fixed operating conditions. Random errors arise due to measurement system resolution, environmental conditions causing random temporal and spatial variations, among other causes. Uncertainty associated with random errors may be quantified through repeated measurements under fixed operating conditions and statistical analysis.

For stability tests, there is an attempt in ASTM F1321 [A11] to specify precision of measurements taken in the inclining, but it does not address assessment of uncertainty for different error sources or quantities. Three papers were published in 1967, 1977, and 1985, which provide examples of uncertainty analyses of inclining experiments [A12, A13, A14]. The uncertainty analyses presented in those papers were based upon experience in construction and inclining operations at several large U.S. shipyards during the 1960s and 1970s, and can be considered good sources for baseline precision estimates associated with shipyard construction and inclining procedures, especially noting that the EL FARO was constructed in the mid-1970s at a large U.S. shipyard (Sun Shipbuilding). It is noted, however, that nomenclature and approach varied significantly. A modified nomenclature is adapted here for application to the EL FARO stability test.

As stated previously, uncertainty associated with random errors may be quantified through repeated measurements under fixed operating conditions and statistical analysis. A “single-sample” experiment is one in which each test point is run only once, or at most a few times [A7]. Normally it is desirable in single-sample experiments to run an auxiliary experiment in order to estimate the random component of uncertainty through statistical analysis of the auxiliary experiment. This usually takes the form of a set of independent measurements at a single representative test condition, with enough observations to establish a statistical basis which may be extended to other operating conditions. It should be noted that this is rarely done for draft measurement in an inclining experiment, so there is little statistical basis for quantifying uncertainty associated with random errors in draft readings and hydrostatic parameters. However, uncertainty in the reading of drafts may be assessed by making use of estimates of precision (for example per the guidance in ASTM F1321), and this may be applied to the results through an analysis of the propagation of the uncertainty in the measurements.

Propagation of error and uncertainty:

Consider a general functional equation of a result R which is a function of several variables [A9]

$$R = R(X_1, X_2, \dots, X_n) \quad (\text{A-1})$$

The uncertainty in the result (U_R) is given by a root sum square (RSS) equation (derived from a Taylor Series expansion [A9, A10])

$$U_R = \sqrt{\left(\frac{\partial R}{\partial X_1} U_{X_1}\right)^2 + \left(\frac{\partial R}{\partial X_2} U_{X_2}\right)^2 + \dots + \left(\frac{\partial R}{\partial X_N} U_{X_N}\right)^2} \quad (\text{A-2})$$

where U_{X_i} are the uncertainties in each of the measured variables X_i . The partial derivatives are often referred to as “sensitivity coefficients”, since they reflect how the result changes with changes in each individual variable with other variables held constant. Therefore, each term represents the contribution made by each variable. Note that the uncertainty in the result U_R is the total uncertainty and has the same units as R .

Whenever the functional equation involves products, the uncertainty can be simplified and rewritten in terms of “relative uncertainties.” For the general “product” form

$$R = X_1^a X_2^b X_3^c \dots X_N^n \quad (\text{A-3})$$

the uncertainty can be simplified and written

$$\left(\frac{U_R}{R}\right) = \sqrt{\left(a \frac{U_{X_1}}{X_1}\right)^2 + \left(b \frac{U_{X_2}}{X_2}\right)^2 + \dots + \left(n \frac{U_{X_N}}{X_N}\right)^2} \quad (\text{A-4})$$

This is in terms of relative uncertainties, which provides uncertainties as fractions (which can be converted to % by multiplying by 100). This is a convenient form as it shows clearly by each term the fraction (or %) of the total being contributed by each measured variable.

In this Appendix, for presentation clarity, the relative uncertainties will be written in a condensed or shorthand notation as

$$\hat{U}_R \equiv \left(\frac{U_R}{R} \right) \quad \hat{U}_{X_i} \equiv \left(\frac{U_{X_i}}{X_i} \right)$$

Depending on the relationship, either uncertainty result may be useful, as will be shown subsequently.

As stated previously, the term “uncertainty” has been defined as “a possible value that an error may have” [A6]. Therefore it is necessary to state to what confidence there is in any stated level of uncertainty. Indeed, the representation of any uncertainty must include the confidence level (sometimes referred to as “confidence interval” or “probability”) of the uncertainty. These confidence levels should originate with the measurement statistics, but they are often based on experience from past experiments for certain measurement systems. The confidence level remains part of the uncertainty in the data reduction or propagation. In equation form, for a C% confidence that the true value of R lies within the interval $\pm U_R$ from the calculated (estimated) value of R:

$$R_{true} = R_{estimate} \pm U_R (C\%) \quad (A-5)$$

Historically, different confidence levels have been favored for documentation by different investigators or organizations. The ISO GUM suggest using a “standard error” ($1\sigma = 68.3\%$ confidence), but it is more common in the U.S. to see the 95% confidence level used (approximately $2\sigma = 95.5\%$), or in older literature 50% or even 99.7% (3σ) have been used. However the chosen confidence level does not change the final result since U_R can be converted from one confidence level to the other as desired.

A.3. Uncertainty in the As-Inclined GM

Basic relation:

In a stability test (inclining experiment), the equation for calculating the metacentric height (GM) in the as-inclined condition is [A11]

$$GM = \frac{w \cdot a}{\Delta \cdot \tan\theta} = \left(\frac{w \cdot a}{\tan\theta} \right) \cdot \left(\frac{1}{\Delta} \right) \quad (A-6)$$

where w is the weight of the inclining weights (LT), a is the distance inclining weights are moved (ft), $\tan\theta$ is the tangent of the angle of heel induced by the movement of the inclining weights, and Δ is the vessel displacement or total weight in the as-inclined condition (LT).

The first term is determined from the slope of the “best fit” line from the plot of the applied moment ($w \cdot a$) and measured angle tangent ($\tan\theta$) for a series of sequential weight movements. The second term is determined by calculation of the displacement using the measured drafts and the hull offsets. In order to calculate the uncertainty in as-inclined GM, the uncertainty in each term must be calculated based on the experimental method, and then combined.

Equation A-6 can be rewritten in terms of the “best fit” slope and displacement:

$$GM = \left(\frac{1}{slope}\right) \cdot \left(\frac{1}{\Delta}\right) = (slope)^{-1} \cdot (\Delta)^{-1} \quad (A-7)$$

where the slope is that of the “best fit” line from the x-y plot of applied moment (independent variable, x) and measured tangent (dependent variable, y). The slope is typically calculated by computer by the method of least-squares (but was historically determined by hand from the plot by manual estimation).

Since this expression for GM in equation A-7 is a product, the uncertainty can be calculated (equation A-4)

$$\left(\frac{U_{GM}}{GM}\right) = \sqrt{\left(\frac{U_{slope}}{slope}\right)^2 + \left(\frac{U_{\Delta}}{\Delta}\right)^2} \quad (A-8)$$

where U_{GM} is the uncertainty in GM, U_{slope} is the uncertainty in slope, and U_{Δ} is the uncertainty in displacement. In shorthand notation:

$$\hat{U}_{GM} = \sqrt{\hat{U}_{slope}^2 + \hat{U}_{\Delta}^2} \quad (A-9)$$

Uncertainty in the slope:

For the EL FARO inclining experiment completed in 2006 [A1 through A4], each of seven steps or “trials” involved moving two or three inclining weights in sequence from port to starboard or starboard to port (initially, five weights were placed port and five weights were placed starboard). For each trial, three independent pendulums were used to measure the tangent of the induced angle. Thus there were 21 measurements of tangent (three in each of the seven trials) which could be used in the determination of the slope. The measurement data from the Inclining Experiment Record Sheet [A3] with additional calculation of moments and tangents are provided in Table A-1.

A “best fit” slope is easily calculated using the ordinary linear least-squares regression method using a spreadsheet calculation. In Excel this is implemented through the basic TRENDLINE function, but additional statistics on the linear least-squares fit are provided using the LINEST function, which includes calculation of the least-squares slope and intercept, along with standard error of the slope, standard error of the intercept, and additional statistics of the fit.

The ordinary linear least-squares regression assumes a linear equation of the form

$$y = mx + b \quad (\text{A-10})$$

where x is the independent variable and y is the dependent variable, m is the slope, and b is the y -intercept. For ordinary least-squares, all data points (i) are assumed to have the same error or uncertainty in y_i , and no error or uncertainty in x_i , and as a result each data point is given equal weight in the regression. Based on the ordinary least-squares regression, the slope m and intercept b are calculated [A9]

$$m = \frac{N \sum x_i y_i - \sum x_i \sum y_i}{N \sum x_i^2 - (\sum x_i)^2} \quad b = \frac{\sum x_i^2 \sum y_i - \sum x_i \sum (x_i y_i)}{N \sum x_i^2 - (\sum x_i)^2} \quad (\text{A-11})$$

where the summation is from 1 to N data points. The standard error of the estimate (predicted value of y) is

$$S_y = \sqrt{\frac{\sum (y_i - (mx_i + b))^2}{N - 2}} \quad (\text{A-12})$$

And the standard error (68.3% confidence) of the slope is

$$S_{slope} = S_m = S_y \sqrt{\frac{N}{N \sum x_i^2 - (\sum x_i)^2}} \quad (\text{A-13})$$

With $N = 21$ in the EL FARO inclining experiment, the 95% confidence uncertainty is approximately twice the standard error of the slope (actually 2.093 times the standard error, based on the t -distribution with $N-2 = 19$ degrees of freedom [A9]). Table A-2 lists the calculated slope, standard error of the slope, 95% confidence uncertainty, and 95% confidence relative uncertainty.

Trial #	Weight #	Weight (LT)	Distance Moved (ft)	Moment (ft·LT)	Trial Moment (ft·LT)	Pendulum #	Pendulum Length (in)	Pendulum Movement (in)	Tangent
1	1	18.571	88.0	1,634.3	3,286.3	1	199.38	1.52	0.00762
	3	18.772	88.0	1,652.0	3,286.3	2	203.13	1.62	0.00798
					3,286.3	3	331.50	2.56	0.00772
2	5	18.839	97.0	1,827.4	8,578.1	1	199.38	4.06	0.02036
	7	18.839	97.0	1,827.4	8,578.1	2	203.13	4.11	0.02023
	9	18.603	88.0	1,637.0	8,578.1	3	331.50	6.63	0.02000
3	3	18.772	-88.0	-1,652.0	5,098.7	1	199.38	2.53	0.01269
	5	18.839	-97.0	-1,827.4	5,098.7	2	203.13	2.44	0.01201
					5,098.7	3	331.50	4.01	0.01210
4	1	18.571	-88.0	-1,634.3	0.0	1	199.38	-0.04	-0.00020
	7	18.839	-97.0	-1,827.4	0.0	2	203.13	0.00	0.00000
	9	18.603	-88.0	-1,637.0	0.0	3	331.50	-0.04	-0.00012
5	2	18.683	-96.0	-1,793.6	-5,201.7	1	199.38	-2.40	-0.01204
	8	18.504	-88.0	-1,628.4	-5,201.7	2	203.13	-2.44	-0.01201
	10	18.348	-97.0	-1,779.8	-5,201.7	3	331.50	-3.99	-0.01204
6	4	18.884	-88.0	-1,661.8	-8,529.2	1	199.38	-3.97	-0.01991
	6	18.929	-88.0	-1,665.7	-8,529.2	2	203.13	-3.99	-0.01964
					-8,529.2	3	331.50	-6.62	-0.01997
7	2	18.683	96.0	1,793.6	-3,294.1	1	199.38	-1.55	-0.00777
	4	18.884	88.0	1,661.8	-3,294.1	2	203.13	-1.56	-0.00768
	10	18.348	97.0	1,779.8	-3,294.1	3	331.50	-2.54	-0.00766

Table A-1: Inclining measurement data with additional calculation of moments and tangents for slope calculation. Distances and moments are (+) for starboard and (-) for port.

It was stated that the ordinary least-squared regression assumes that all data points have the same error or uncertainty in y_i , and no error or uncertainty in x_i , and as a result each data point is given equal weight in the regression. However, in the more general case of unequal uncertainties in y_i (and perhaps also uncertainties in x_i), a weighted least-squares method can be applied. The foundation of this method applies a “best fit” by minimizing the sum of the weighted squared residuals (differences between the observed and calculated values) to each x_i and y_i value pair (see [A15, A16]). The weighting factors applied to each x_i and y_i are typically assigned as the inverse squares of the uncertainties in the data values of x_i and y_i . As a result, the general effect of the weighted linear least-squares method is that the fit favors the data points with smaller uncertainties at the expense of those with larger uncertainties. In general, this also reduces the standard error and uncertainty of the slope. A spreadsheet calculation implementing the method developed by Reed [A16] provides weighted least-squares results provided in Table A-2. Note that the standard error and uncertainty of the slope are significantly reduced with the weighted least-squares compared to the ordinary (unweighted) least-squares. Regardless, it will be shown that in this case the uncertainty in the slope is small compared to the uncertainty in displacement, so the resulting uncertainty in as-inclined GM is only minimally changed by the least-squares method chosen.

	Ordinary Least-Squares	Weighted Least-Squares
Slope (tangent/moment) (1/ft·LT)	2.3460×10^{-6}	2.3432×10^{-6}
Standard error of the slope, S_{slope} (1/ft·LT)	7.98×10^{-9}	1.61×10^{-9}
Uncertainty of the slope (95%), U_{slope} (1/ft·LT)	16.68×10^{-9}	3.37×10^{-9}
Relative uncertainty (95%), \hat{U}_{slope}	0.0071 (0.71%)	0.0014 (0.14%)

Table A-2: Slope, standard error of the slope, 95% confidence uncertainty of the slope, and 95% confidence relative uncertainty.

To apply the weighted least-squares method, the weighting factors are chosen as the inverse of the uncertainties in the values of moment and tangent for each data point. These are calculated based on first-order estimates of uncertainties in the individual inclining weights, distance moved, and tangent of the induced angle, based on the EL FARO Stability Test Report and Inclining Experiment Record Sheet [A2, A3]. Results are provided in Table A-3, with the methodology summarized below. Figure A-1 shows the data points, the linear fit based on the ordinary least-squares method, and error bars showing the estimated 95% confidence level uncertainties for each data point.

The uncertainty in the weight of the inclining weights has several sources. The scale used to measure the weights has an uncertainty which arises from the resolution of the scale (i.e. how precisely the scale display can be read or discerned), but also uncertainties related to the linearity and hysteresis of the scale, and the procedure for weight measurement. The EL FARO Stability Test Report and Inclining Experiment Record Sheet [A2, A3] state a scale precision of ± 750 lb or 1.5% of the full scale of 50,000 lb. It is noted however that the calibration certificate included in the ABS Surveyor’s Report [A4] appears to show an error or precision of -0.5%. However it appears that there is a bias or systematic source of error since all readings vary precisely -0.5% compared to the calibration weights and there appears to be no random error in the calibration. Additionally, the calibration certificate also shows an accuracy of $\pm 1\%$ for the calibration source, and it is possible that it was on this basis that the test engineers cited $\pm 1.5\%$ as the uncertainty stated on the Inclining Experiment Record Sheet. It is also assumed that this overall uncertainty refers to the 95% confidence uncertainty. Since there is no detail given about the scale display, it is assumed that the display resolution uncertainty is small compared to the calibration uncertainty, although for an analog display scale this may not be the case. During the EL FARO inclining, each of the 7 trials or steps involved moving 2 or 3 of the 10 inclining weights in sequence from port to starboard or starboard to port (initially, 5 weights were placed port and 5 weights were placed starboard). Weights were provided in the Inclining Experiment Record Sheet [A3]. It was also stated in the notes of the Stability Test Report that there was up to 100 lb of rain water in the padeye recess for many of the weight blocks while they were weighed, and up to 15 lb remaining during the inclining. Because the process for subtraction of this water weight was not clear, additional uncertainty should be added on this basis, but this was not included in this analysis.

Although the placement and measurement of the distance moved for each weight block can be determined precisely if high-tech methods are used (for example, using laser measurement systems), in practice common hand-measurement methods for a carefully-conducted inclining

provide an uncertainty on the order of 5/8 inch in 50 feet at 50% probability [A12]. Therefore the relative uncertainty in the distance shifted at the 95% confidence level is

$$\hat{U}_a = \left(\frac{U_a}{a}\right) = 3.0 \cdot \frac{(5/8 \text{ in})(1 \text{ ft}/12 \text{ in})}{50 \text{ ft}} = 0.003 = 0.3\% \text{ (95\%)}$$

Note that the factor 3.0 converts uncertainty at the 50% confidence level [A12] to the 95% confidence level. Note also that the relative uncertainty of the distance moved is small compared to the relative uncertainty of the weight measurement.

The moment for each weight movement is calculated as the product of the weight and distance moved. Therefore the total uncertainty in the moment for each block move is (equation A-4)

$$\left(\frac{U_{\text{moment}}}{\text{moment}}\right) = \sqrt{\left(\frac{U_w}{w}\right)^2 + \left(\frac{U_a}{a}\right)^2}$$

As an example, for weight #1 in trial #1 (see Table A-3) the calculated moment and moment uncertainty are:

$$\begin{aligned}\hat{U}_{\text{moment}} &= \left(\frac{U_{\text{moment}}}{\text{moment}}\right) = \sqrt{(0.015)^2 + (0.003)^2} = 0.0153 \\ \text{moment} &= w \cdot a = (18.571 \text{ LT})(88.0 \text{ ft}) = 1,634.3 \text{ ft} \cdot \text{LT} \\ U_{\text{moment}} &= 0.0153 \cdot 1,634.3 \text{ ft} \cdot \text{LT} = 25.0 \text{ ft} \cdot \text{LT} \text{ (95\%)}\end{aligned}$$

For each trial, the total moment is simply the sum of the moments for the weight blocks moved in that trial. Therefore the total moment uncertainty for each trial is simply the root sum square of the uncertainties of each weight moved (equation A-2).

The accuracy of measurement of the angle of induced heel is affected by a number of factors including wind, tides and currents, mooring arrangements, and movement of people and equipment (for small or tender vessels), in addition to equipment and procedural sources of error. ASTM F1321 provides guidance on test conditions and procedures for precision in measurement using pendulums, but does not provide specific guidance on assessing the uncertainty in the results of the inclining. While ASTM F1321 recommends that pendulum lengths and readings be precise to within 1/16 inch, in practice due to dynamic and procedural effects, common manual measurement methods provide uncertainty on the order of 1/8 inch [A12, A13]. The EL FARO Stability Test Report and Inclining Experiment Record Sheet [A2, A3] list pendulum lengths of 199.38 in, 203.13 in and 331.50 in. For this assessment, a practical measurement uncertainty value of 1/8 inch (at 95% confidence) is used, noting that the ASTM suggested precision of 1/16 inch, would likely only be achieved with a standard confidence (68.3%), which is equivalent to the 1/8 inch at the 95% confidence. As an example, for pendulum #1 in trial #1 (see Table A-3) the calculated tangent and uncertainty in the tangent are:

$$\tan\theta = \frac{1.52 \text{ in}}{199.38 \text{ in}} = 0.00762 \quad U_{\tan\theta} = \frac{1/8 \text{ in}}{199.38 \text{ in}} = 0.00063 \text{ (95\%)}$$

The uncertainties in moment and tangent for each of the 21 measurements are plotted as error bars in Figure A-1. Note that the relative uncertainties of the moment values at only 1.5% are much smaller compared to the relative uncertainties of the tangent values, so the error bars for the moment values are difficult to see in the figure.

The use of the linear least-squares fit for calculation of the standard error and uncertainty of the slope assumes that errors associated with each data point measurement would be normally distributed if taken many times at each particular operating condition. Therefore the calculated standard error and uncertainty of the slope includes only a random component of uncertainty. If systematic or bias errors in the measurement or measurement system exist, they are not included in the error estimate. It has been assumed in this procedure that any systematic or bias errors of the measurements of weight, distance moved and angle tangent are small and can be neglected.

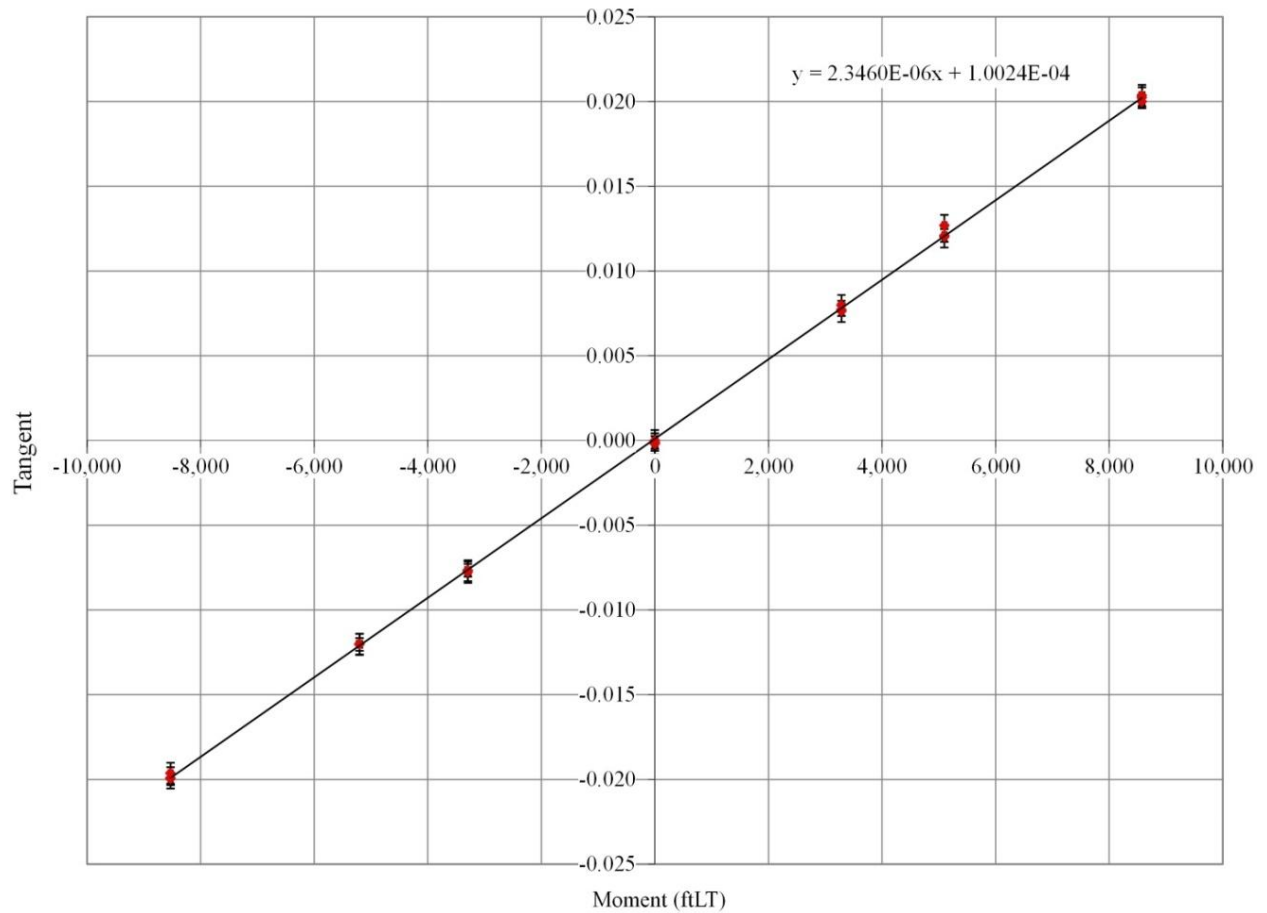


Figure A-1: Plot of moment vs. tangent data from the inclining with standard least-squares linear fit. Error bars show estimated 95% confidence level uncertainties for each data point based on separate error assessment.

Trial #	Weight #	Weight (LT)	Weight Rel Unc (1.5%)	Weight Unc (LT)	Distance Moved (ft)	Distance Rel Unc (0.3%)	Distance Unc (ft)	Moment (ft-LT)	Moment Rel Unc	Moment Unc (ft-LT)	Trial Moment (ft-LT)	Trial Moment Unc (ft-LT)	Pendulum #	Pendulum Length (in)	Pendulum Movement (in)	Pendulum Movement Unc (1/8 in)	Tangent	Tangent Unc
1	1	18.571	0.015	0.279	88.0	0.003	0.26	1,634.3	0.015	25.0	3,286.3	35.5	1	199.38	1.52	0.125	0.00762	0.00063
	3	18.772	0.015	0.282	88.0	0.003	0.26	1,652.0	0.015	25.3	3,286.3	35.5	2	203.13	1.62	0.125	0.00798	0.00062
													3	331.50	2.56	0.125	0.00772	0.00038
2	5	18.839	0.015	0.283	97.0	0.003	0.29	1,827.4	0.015	28.0	8,578.1	46.8	1	199.38	4.06	0.125	0.02036	0.00063
	7	18.839	0.015	0.283	97.0	0.003	0.29	1,827.4	0.015	28.0	8,578.1	46.8	2	203.13	4.11	0.125	0.02023	0.00062
	9	18.603	0.015	0.279	88.0	0.003	0.26	1,637.0	0.015	25.0	8,578.1	46.8	3	331.50	6.63	0.125	0.02000	0.00038
3	3	18.772	0.015	0.282	-88.0	0.003	-0.26	-1,652.0	0.015	-25.3	5,098.7	37.7	1	199.38	2.53	0.125	0.01269	0.00063
	5	18.839	0.015	0.283	-97.0	0.003	-0.29	-1,827.4	0.015	-28.0	5,098.7	37.7	2	203.13	2.44	0.125	0.01201	0.00062
													3	331.50	4.01	0.125	0.01210	0.00038
4	1	18.571	0.015	0.279	-88.0	0.003	-0.26	-1,634.3	0.015	-25.0	0.0	45.1	1	199.38	-0.04	0.125	-0.00020	0.00063
	7	18.839	0.015	0.283	-97.0	0.003	-0.29	-1,827.4	0.015	-28.0	0.0	45.1	2	203.13	0.00	0.125	0.00000	0.00062
	9	18.603	0.015	0.279	-88.0	0.003	-0.26	-1,637.0	0.015	-25.0	0.0	45.1	3	331.50	-0.04	0.125	-0.00012	0.00038
5	2	18.683	0.015	0.280	-96.0	0.003	-0.29	-1,793.6	0.015	-27.4	-5,201.7	46.0	1	199.38	-2.40	0.125	-0.01204	0.00063
	8	18.504	0.015	0.278	-88.0	0.003	-0.26	-1,628.4	0.015	-24.9	-5,201.7	46.0	2	203.13	-2.44	0.125	-0.01201	0.00062
	10	18.348	0.015	0.275	-97.0	0.003	-0.29	-1,779.8	0.015	-27.2	-5,201.7	46.0	3	331.50	-3.99	0.125	-0.01204	0.00038
6	4	18.884	0.015	0.283	-88.0	0.003	-0.26	-1,661.8	0.015	-25.4	-8,529.2	36.0	1	199.38	-3.97	0.125	-0.01991	0.00063
	6	18.929	0.015	0.284	-88.0	0.003	-0.26	-1,665.7	0.015	-25.5	-8,529.2	36.0	2	203.13	-3.99	0.125	-0.01964	0.00062
													3	331.50	-6.62	0.125	-0.01997	0.00038
7	2	18.683	0.015	0.280	96.0	0.003	0.29	1,793.6	0.015	27.4	-3,294.1	46.3	1	199.38	-1.55	0.125	-0.00777	0.00063
	4	18.884	0.015	0.283	88.0	0.003	0.26	1,661.8	0.015	25.4	-3,294.1	46.3	2	203.13	-1.56	0.125	-0.00768	0.00062
	10	18.348	0.015	0.275	97.0	0.003	0.29	1,779.8	0.015	27.2	-3,294.1	46.3	3	331.50	-2.54	0.125	-0.00766	0.00038

Table A-3: Inclining measurement data with calculation of moments and tangents, and estimated 95% confidence level uncertainties for each data point based on error assessment. Distances and moments are (+) for starboard and (-) for port.

Uncertainty in the displacement:

Assessment of the uncertainty in the calculated as-inclined displacement (U_{Δ}) requires consideration of a number of independent sources of error, since the displacement is a derived quantity based on measurement of drafts, calculation of the submerged volume from the ship's lines, and measurement of water density

$$\Delta = \gamma \cdot \nabla \tag{A-14}$$

Note that this is just an expression of Archimedes' Principle. Since this is a simple product, the relative uncertainty in as-inclined displacement can be written

$$\hat{U}_{\Delta} = \sqrt{\hat{U}_{\nabla}^2 + \hat{U}_{\gamma}^2} \tag{A-15}$$

where \hat{U}_{∇} is the relative uncertainty in displacement volume and \hat{U}_{γ} is the relative uncertainty in water density (more precisely specific weight, $\gamma = \rho g$).

Displacement volume is calculated from integration of the lines, and is therefore a function of the longitudinal, transverse and vertical dimensions of the lines or offsets, as well as the actual vessel drafts. The uncertainty in displacement volume can therefore be written

$$U_{\nabla} = \sqrt{\left(\frac{\partial \nabla}{\partial V} U_V\right)^2 + \left(\frac{\partial \nabla}{\partial d} U_d\right)^2 + \left(\frac{\partial \nabla}{\partial m} U_m\right)^2}$$

where U_V is the uncertainty in volume between the molded lines and the as-built lines, U_d is the uncertainty in drafts, and U_m is the uncertainty in (calculated) volume from the molded lines.

Note that the partial derivatives $\partial \nabla / \partial V$ and $\partial \nabla / \partial m$ are both equal to 1, and $\partial \nabla / \partial d$ is the waterplane area (A_{wp}), therefore

$$U_{\nabla} = \sqrt{(U_V)^2 + (A_{wp} \cdot U_d)^2 + (U_m)^2} \tag{A-16}$$

The uncertainty in volume between the molded lines and the as-built dimensions can be separated into differences in longitudinal, transverse, and vertical dimensions, with the uncertainty in volume being the product of these. Therefore, the relative uncertainty can be written

$$\hat{U}_V = \sqrt{\hat{U}_L^2 + \hat{U}_B^2 + \hat{U}_D^2} \tag{A-17}$$

where \hat{U}_L is the relative uncertainty in longitudinal dimension between molded and as-built lines, \hat{U}_B is the relative uncertainty in transverse dimension between molded and as-built lines, and \hat{U}_D is the relative uncertainty in vertical dimension between molded and as-built lines.

Each of these dimensions has uncertainty associated with construction tolerances plus deflection and distortion of the hull during construction. Construction tolerances may be specified but are fundamentally attributable to the construction processes, and therefore vary from shipyard to shipyard and even vessel to vessel. Typical construction tolerances given the shipyard construction processes in the 1960s and 1970s can be estimated [A12, A13] as

Length = ±1 inch per 100 ft length
 Beam = ± 1 inch
 Depth = ± ½ inch

In addition to these construction tolerances, the ship and the ways or drydock move continuously during construction due to a variety of causes including ambient temperature changes, including due to direct sunlight, progress of welding, settlement under load, tidal effects, etc. For example at Newport News in the 1960s and 1970s, the complex of ship and drydock could settle as much as ¾ in and the keel at the extreme ends could move up and down ¾ in with temperature changes and welding progress, and athwartships shifts of the vessel’s centerline due to temperature and welding of 1 in, and length changes up to ¾ in [A12].

The relative uncertainties associated with construction tolerances plus deflection and distortion can be combined as

$$\hat{U}_L = \sqrt{\hat{U}_{L1}^2 + \hat{U}_{L2}^2} \quad \hat{U}_B = \sqrt{\hat{U}_{B1}^2 + \hat{U}_{B2}^2} \quad \hat{U}_D = \sqrt{\hat{U}_{D1}^2 + \hat{U}_{D2}^2} \quad (A-18)$$

where subscript 1 refers to uncertainty due to construction tolerances and subscript 2 refers to uncertainty due to hull deflection and distortion during construction. Using the principal dimensions of the EL FARO (molded length overall, beam and depth), the associated uncertainties are

$$U_{L1} = \frac{1 \text{ in}}{100 \text{ ft}} \cdot 790.75 \text{ ft} = 7.91 \text{ in} = 0.659 \text{ ft} \text{ (95\%)}$$

$$\hat{U}_{L1} = \frac{0.659 \text{ ft}}{790.75 \text{ ft}} = 0.083\% \text{ or } 0.00083 \text{ (95\%)}$$

$$U_{L2} = 0.75 \text{ in} = 0.0625 \text{ ft} \text{ (95\%)}$$

$$\hat{U}_{L2} = \frac{(3/4 \text{ in})(1 \text{ ft}/12 \text{ in})}{790.75 \text{ ft}} = 0.008\% \text{ or } 0.00008 \text{ (95\%)}$$

$$U_{B1} = 1.0 \text{ in} = 0.0833 \text{ ft} \text{ (95\%)}$$

$$\hat{U}_{B1} = \frac{0.0833 \text{ ft}}{92.0 \text{ ft}} = 0.091\% \text{ or } 0.00091 \text{ (95\%)}$$

$$U_{B2} = 1.0 \text{ in} = 0.0833 \text{ ft} \text{ (95\%)}$$

$$\hat{U}_{B2} = \frac{0.0833 \text{ ft}}{92.0 \text{ ft}} = 0.091\% \text{ or } 0.00091 \text{ (95\%)}$$

$$U_{D1} = 0.5 \text{ in} = 0.0417 \text{ ft} \text{ (95\%)}$$

$$\hat{U}_{D1} = \frac{0.0417 \text{ ft}}{60.14 \text{ ft}} = 0.069\% \text{ or } 0.00069 \text{ (95\%)}$$

$$U_{D2} = 0.75 \text{ in} = 0.0625 \text{ ft (95\%)}$$

$$\hat{U}_{D2} = \frac{0.0625 \text{ ft}}{60.14 \text{ ft}} = 0.104\% \text{ or } 0.00104 \text{ (95\%)}$$

$$\hat{U}_L = 0.083\% = 0.00083 \text{ (95\%)}$$

$$\hat{U}_B = 0.128\% = 0.00128 \text{ (95\%)}$$

$$\hat{U}_D = 0.125\% = 0.00125 \text{ (95\%)}$$

and

$$\hat{U}_V = \sqrt{\hat{U}_L^2 + \hat{U}_B^2 + \hat{U}_D^2} = 0.00197 = 0.20\% \text{ (95\%)}$$

$$U_V = \hat{U}_V \cdot \nabla = (0.00197)(849,228 \text{ ft}^3) = 1,673 \text{ ft}^3$$

where the displacement volume has been calculated using the MSC GHS computer model for the measured drafts of the as-inclined condition.

Uncertainty in drafts comes from multiple sources, including uncertainty in measurement of the drafts during the inclining (i.e. how precisely the waterline on the draft markings can be read or discerned), uncertainty in the location of the marks relative to the baseline (i.e. vessel datum) due to layout and installation, uncertainty in the location of the marks relative to the baseline due to hull deflection or distortion during installation (due to temperature and welding and other sources), and uncertainty of the drafts due to hull deflection and trim during the inclining. These contributions are additive so the uncertainty can be written

$$U_d = \sqrt{U_{d1}^2 + U_{d2}^2 + U_{d3}^2 + U_{d4}^2} \quad (\text{A-19})$$

where U_{d1} is the uncertainty in drafts due to measurement during inclining, U_{d2} is the uncertainty in drafts due to layout and installation, U_{d3} is the uncertainty in drafts due to hull deflection and distortion during installation, and U_{d4} is the uncertainty in drafts due to hull deflection and trim during inclining.

The uncertainty in the drafts due to measurement includes a number of important factors, including the resolution of the draft markings themselves, how carefully the observer views, interpolates and averages the fluctuating waterline over the timeframe of the reading, the amplitude of local water level fluctuations due to wind, waves and currents, plus additional procedural effects such as viewing angle, proximity, etc. While ASTM F1321 suggests that draft “precision” should be to the nearest 1/8 in, Wood [A13] states an uncertainty in reading draft marks at Ingalls Shipbuilding of 0.5 in with 99% or 3σ confidence (3/8 in with 95% or 2σ confidence), and this is certainly more realistic given common practice. Shakshober and Montgomery [A12] cite uncertainty at Newport News of 1/2 in and 3/8 in for layout and installation, and hull deflection and distortion during installation, respectively. The uncertainty in drafts due to hull deflection and trim depends on how well the drafts measured and entered into the hydrostatic calculation program represent the trim and deflection of the hull in the as-inclined condition, and also whether or not the hydrostatic calculation program calculates the trimmed deflected waterline directly from the offsets or indirectly from Bonjean curves.

Methods for estimating equivalent drafts and estimating uncertainty of trimmed and deflected waterlines are provided by Shakshober and Montgomery [A12] and Hansen [A14]. However, since hull deflection and trim were accounted for in the EL FARO Stability Test Report based on direct integration of the waterlines using a parabolic curve fit, this contribution to uncertainty can be considered relatively small in this case, and is neglected. Therefore the uncertainty in drafts is

$$U_{d1} = 0.375 \text{ in} = 0.03125 \text{ ft} \text{ (95\%)}$$

$$U_{d2} = 0.5 \text{ in} = 0.0417 \text{ ft} \text{ (95\%)}$$

$$U_{d3} = 0.375 \text{ in} = 0.03125 \text{ ft} \text{ (95\%)}$$

$$U_{d4} = 0 \text{ in}$$

and

$$U_d = \sqrt{U_{d1}^2 + U_{d2}^2 + U_{d3}^2 + U_{d4}^2} = 0.73 \text{ in} = 0.0607 \text{ ft} \text{ (95\%)}$$

The waterplane area (A_{wp}) has been calculated using the MSC GHS computer model for measured drafts of the as-inclined condition as 47,879 ft².

It is noted in the Stability Test Report that only draft readings were used in the hydrostatic calculations, in lieu of combined draft and freeboard measurements or all freeboard measurements per the guidance in ASTM F1321. However, if freeboard measurements had also been used, additional uncertainty associated with location of the freeboard measurement references relative to the datum, and measurement of the freeboards themselves, would have been introduced, and would need to be added (by the root-sum-square). Based on discrepancies with freeboard references noted in the EL FARO documentation, test engineers decided not to use the freeboard measurements in the hydrostatic calculations, and therefore the freeboard uncertainties do not need to be included in this uncertainty analysis.

When computer calculations are used, the uncertainty in (calculated) volume from the molded lines (U_m) is associated with how precisely the lines are digitized, how closely the hull station spacing and placement represents the shape of the hull form, and the precision of the numerical integration technique itself (i.e. differences between Simpson's Rule and Trapezoidal Rule integrations). The International Association of Class Society (IACS) Unified Requirement L5 (Onboard Computers for Stability Calculations) [A17], sets limits on acceptable tolerances in comparing computer calculated hydrostatic parameters to approved hydrostatic values. For displacement, the acceptable tolerance is stated as 2% of the displacement. This is a likely upper bound on the variability of calculated displacement based on the molded lines, and might be used as a relative uncertainty in (calculated) volume from the molded lines at the 95% confidence level. However, a more "optimistic" estimate of 1% is used here. Using the MSC GHS computer model developed from the ship's lines, and comparing calculated displacement provided in the Stability Test Report for the as-inclined condition, the difference in displacement is 0.9% (23,715 LT from the MSC GHS computer model and 23,512 LT from the Stability Test Report). This suggests a 95% uncertainty in the calculated displacement from the lines to be at least 1%. Using this 1% value as a relative uncertainty in (calculated) volume from the molded lines

$$\hat{U}_m = 1\% = 0.01 \text{ (95\%)}$$

$$U_m = \hat{U}_m \cdot \nabla = \hat{U}_m \cdot \Delta / \gamma = (0.01)(849,228 \text{ ft}^3) = 8,492 \text{ ft}^3$$

where the displacement and specific weight are taken from the Stability Test Report.

Combining these uncertainties the uncertainty of the as-inclined displacement volume is

$$U_{\nabla} = \sqrt{(1,673 \text{ ft}^3)^2 + (47,879 \text{ ft}^2 \cdot 0.0607 \text{ ft})^2 + (8,492 \text{ ft}^3)^2} = 9,130 \text{ ft}^3$$

$$\hat{U}_{\nabla} = U_{\nabla}/\nabla = 9,130 \text{ ft}^3 / 849,228 \text{ ft}^3 = 0.0107 = 1.07\%$$

It should be noted that the largest contributor in the uncertainty in volume is due to the uncertainty in the calculated volume from the molded lines, U_m .

The final uncertainty to consider is the uncertainty in water specific gravity, specifically density or specific weight (U_{γ}) (note $\gamma = \rho g$), which is a function primarily of water temperature and salinity (assuming water to be incompressible in this case). However, specific gravity can be measured experimentally during the inclining with good accuracy using a hydrometer. Hansen [A14] and Wood [A13] cite hydrometers used in inclining experiments having relative uncertainty of 0.1% and 0.25% respectively, including both precision of reading the hydrometer and actual specific gravity variations as a function of location along the length of a ship. It should be noted however, that in estuarial flows including many bays, salinity can vary significantly depending on tides and local rain runoff, and can lead to large fluctuations in specific gravity even during the course of an inclining experiment. In the case of the EL FARO inclining at the Atlantic Marine Shipyard in Mobile Alabama, the salinity in the northern portion of Mobile Bay tends to vary only slightly with tides, and it should be considered reasonable to use a small uncertainty in specific gravity, as long as the hydrometer was used properly. For simplicity, a relative uncertainty of density of $0.0015 = 0.15\%$ is assumed here.

Therefore the relative uncertainty in the as-inclined displacement is

$$\hat{U}_{\Delta} = \sqrt{\hat{U}_{\nabla}^2 + \hat{U}_{\gamma}^2} = \sqrt{(0.0107)^2 + (0.0015)^2} = 0.0109 = 1.09\%$$

Uncertainty in GM:

The relative uncertainties in slope and displacement are combined using equation A-9. With uncertainty in slope calculated using the ordinary least-squares method:

$$\hat{U}_{GM} = \sqrt{\hat{U}_{slope}^2 + \hat{U}_{\Delta}^2} = \sqrt{(0.0071)^2 + (0.0109)^2} = 0.0130 = 1.3\% (95\%)$$

Using the calculated as-inclined GM of 18.26 ft based on the Stability Test Report, the total uncertainty in the as-inclined GM is

$$U_{GM} = 0.0130 \cdot 18.26 \text{ ft} = 0.24 \text{ ft} = 2.9 \text{ in} (95\%)$$

Using the weighted least-squares method $\hat{U}_{slope} = 0.0014$ and the uncertainty in as-inclined GM would be 0.20 ft or 2.4 in (95%).

A.4. Uncertainty in the As-Inclined KG

The ultimate goal of the inclining experiment is to determine the lightship weight and center of gravity, most importantly the height of the center of gravity (VCG or KG). The lightship KG is calculated by first finding the as-inclined KG. The as-inclined KG is easily calculated by subtracting the metacentric height from the height of the metacenter

$$KG = KM - GM \quad (\text{A-20})$$

where KM is the height of the metacenter, a hydrostatic property, which can be written

$$KM = KB + BM \quad (\text{A-21})$$

KB is the height of the center of buoyancy (the center of the displacement volume, ∇), and BM is the metacentric radius defined by

$$BM = I/\nabla \quad (\text{A-22})$$

where I is the 2nd moment of area of the waterplane area about its longitudinal centroidal axis (sometimes referred to as the transverse moment of inertia of the waterplane).

Since KG is calculated from a summation, the uncertainty in the as-inclined KG is

$$U_{KG} = \sqrt{U_{KB}^2 + U_{BM}^2 + U_{GM}^2} \quad (\text{A-23})$$

where, since BM is a product of I and ∇ , the relative uncertainty in BM is calculated

$$\hat{U}_{BM} = \sqrt{\hat{U}_I^2 + \hat{U}_\nabla^2} \quad (\text{A-24})$$

Note that the uncertainty in the as-inclined GM and relative uncertainty in displacement volume ∇ are already known, so it is only a matter of determining the uncertainty in I and KB, and both are hydrostatic properties.

The 2nd moment of area of the waterplane is calculated by integration of the waterplane area offsets

$$I = \frac{2}{3} \int_0^L y^3 dx \quad (\text{A-25})$$

where y is the transverse distance (offset) and x is the longitudinal distance. Since this is a product with an exponent (equation A-4), the relative uncertainty can be calculated

$$\hat{U}_I = \sqrt{\hat{U}_L^2 + (3\hat{U}_B)^2} \quad (\text{A-26})$$

Relative uncertainties \hat{U}_L and \hat{U}_B have already been determined, therefore

$$\hat{U}_I = \sqrt{\hat{U}_L^2 + (3\hat{U}_B)^2} = \sqrt{(0.00083)^2 + (3 \cdot 0.00128)^2} = 0.0039 = 0.39\% \text{ (95\%)}$$

and

$$\hat{U}_{BM} = \sqrt{\hat{U}_I^2 + \hat{U}_\nabla^2} = \sqrt{(0.0039)^2 + (0.0107)^2} = 0.0114 = 1.14\% \text{ (95\%)}$$

The height of the center of buoyancy KB is the vertical centroid of the displacement volume and is calculated by integration of the underwater volume to the waterline

$$KB = \int_0^{wl} A(z) dz / \nabla \quad (\text{A-27})$$

where z is the vertical distance (height) and $A(z)$ is the waterplane area. The area of the waterplane is calculated by integration of the waterplane area offsets

$$A = 2 \int_0^L y dx \quad (\text{A-28})$$

Therefore

$$\begin{aligned} \hat{U}_A &= \sqrt{\hat{U}_B^2 + \hat{U}_L^2} \\ \hat{U}_{KB} &= \sqrt{\hat{U}_A^2 + \hat{U}_D^2 + \hat{U}_\nabla^2} \end{aligned} \quad (\text{A-28})$$

and

$$\begin{aligned} \hat{U}_A &= \sqrt{(0.00128)^2 + (0.00083)^2} = 0.00153 = 0.15\% \text{ (95\%)} \\ \hat{U}_{KB} &= \sqrt{(0.00153)^2 + (0.00125)^2 + (0.0107)^2} = 0.0109 = 1.09\% \text{ (95\%)} \end{aligned}$$

From the MSC GHS computer model, for the as-inclined condition with the measured drafts, KB is 12.6 ft and BM is 31.0 ft, therefore

$$\begin{aligned} U_{KB} &= 0.0109 \cdot 12.6 \text{ ft} = 0.137 \text{ ft} \text{ (95\%)} \\ U_{BM} &= 0.0114 \cdot 31.0 \text{ ft} = 0.353 \text{ ft} \text{ (95\%)} \end{aligned}$$

Finally, the uncertainty in the as-inclined KG is

$$\begin{aligned} U_{KG} &= \sqrt{U_{KB}^2 + U_{BM}^2 + U_{GM}^2} = \sqrt{(0.137 \text{ ft})^2 + (0.353 \text{ ft})^2 + (0.237 \text{ ft})^2} = 0.45 \text{ ft} \\ &= 5.4 \text{ in} \text{ (95\%)} \\ \hat{U}_{KG} &= U_{KG}/KG = 0.45 \text{ ft}/26.02 \text{ ft} = 0.0172 = 1.7\% \text{ (95\%)} \end{aligned}$$

A.5. Uncertainty in the Lightship KG

Note: Hereafter, values applicable to the “as-inclined” condition will be given a subscript “I” and values applicable to the lightship condition will be given a subscript “L”.

The lightship weight is calculated from the as-inclined weight by adding or subtracting any changes identified in the deadweight survey using

$$\Delta_L = \Delta_I + \sum w_s + \sum w_l \quad (A-30)$$

The lightship KG_L is calculated from the as-inclined KG_I by adding or subtracting the moments of the weight changes identified in the deadweight survey using

$$KG_L = \frac{\Delta_I KG_I + \sum w_s kg_s + \sum w_l kg_l}{\Delta_L} \quad (A-31)$$

where subscript L refers to the lightship value, I refers to the as-inclined value, s refers to solid weights to be added or removed, and l refers to liquid (tank) weights to be added or removed.

Since the calculation of the lightship weight is a summation, the total uncertainty in the lightship weight can be calculated

$$U_{\Delta_L} = \sqrt{U_{\Delta_I}^2 + U_{w_s}^2 + U_{w_l}^2} \quad (A-32)$$

Since the calculation KG_L is a function including both products and sums, the total uncertainty in the lightship KG must be calculated by

$$U_{KG_L} = \sqrt{\left(\frac{\partial KG_L}{\partial \Delta_I} U_{\Delta_I}\right)^2 + \left(\frac{\partial KG_L}{\partial KG_I} U_{KG_I}\right)^2 + \left(\frac{\partial KG_L}{\partial w_s} U_{w_s}\right)^2 + \left(\frac{\partial KG_L}{\partial kg_s} U_{kg_s}\right)^2 + \left(\frac{\partial KG_L}{\partial w_l} U_{w_l}\right)^2 + \left(\frac{\partial KG_L}{\partial kg_l} U_{kg_l}\right)^2 + \left(\frac{\partial KG_L}{\partial \Delta_L} U_{\Delta_L}\right)^2}$$

Performing the required differentiations of KG_L , substituting and simplifying

$$U_{KG_L} = \sqrt{\left(\frac{KG_I}{\Delta_L} U_{\Delta_I}\right)^2 + \left(\frac{\Delta_I}{\Delta_L} U_{KG_I}\right)^2 + \left(\frac{kg_s}{\Delta_L} U_{w_s}\right)^2 + \left(\frac{w_s}{\Delta_L} U_{kg_s}\right)^2 + \left(\frac{kg_l}{\Delta_L} U_{w_l}\right)^2 + \left(\frac{w_l}{\Delta_L} U_{kg_l}\right)^2 + \left(\frac{KG_L}{\Delta_L} U_{\Delta_L}\right)^2}$$

Using this equation to perform a detailed uncertainty analysis in KG_L would be tedious in the post-analysis and require applying individual uncertainty for each weight and each vertical height for all solid weights and liquid (tank) weights in the summations. Wood [A13] takes this approach and suggests the following uncertainties be applied in the calculations

$$\hat{U}_{w_s} = 4.0\%, \quad \hat{U}_{w_l} = 2.0\%, \quad U_{kg_s} = 1.0 \text{ ft}, \quad U_{kg_l} = 0.4 \text{ ft}$$

Shakshober and Montgomery [A12] take a simplified approach and redefine the moment equation in terms of summation of individual calculated moments and then apply equivalent relative uncertainties, suggesting the following relative uncertainties be applied in the calculation

$$\begin{aligned} \hat{U}_{ws} &= 5\% \text{ (for solid weights to be added),} \\ \hat{U}_{kgs} &= 10\% \text{ (for solid weights to be added)} \\ \hat{U}_{ws} &= 10\% \text{ (for solid weights to be removed)} \\ \hat{U}_{kgs} &= 5\% \text{ (for solid weights to be removed)} \\ \hat{U}_{wl} &= \hat{U}_{\nabla} \\ \hat{U}_{kgl} &= \hat{U}_{KB} \\ &\text{(all at the 50\% confidence level)} \end{aligned}$$

The latter two assumptions are reasonable given that tank weights are based on integration of the hull offsets to obtain tank volumes, and vertical tank centers are the centroids of the tank volumes.

For simplicity and to provide a reasonable but “optimistic” engineering estimate of KG_L for this analysis, the approach taken here is to apply the approach by Shakshober and Montgomery for the liquids \hat{U}_{wl} and \hat{U}_{kgl} , but a hybrid approach for the solid weights. Based on Wood’s approach, a relative uncertainty $\hat{U}_{ws} = 4\%$ is applied for both added and removed solid weights, and for solid weights U_{kgs} is based on Wood’s suggested 1.0 ft uncertainty, but normalized based on an assumed average vertical height of 54 ft based on the deadweight survey weight accounting provided in the Stability Test Report. Thus the following weight and vertical center of gravity uncertainties are assumed

$$\begin{aligned} \hat{U}_{ws} &= 0.04 = 4.0\% \\ \hat{U}_{kgs} &= 1.0\text{ft}/54.0\text{ft} = 0.019 = 1.9\% \\ \hat{U}_{wl} &= \hat{U}_{\nabla} = 0.0107 = 1.1\% \text{ (from previous calculation)} \\ \hat{U}_{kgl} &= \hat{U}_{KB} = 0.0109 = 1.1\% \text{ (from previous calculation)} \\ &\text{(all are assumed at the 95\% confidence level)} \end{aligned}$$

The moment equation for KG_L (equation A-26) can be rewritten as

$$KG_L \Delta_L = \Delta_I KG_I + \sum w_s k g_s + \sum w_l k g_l \tag{A-33}$$

or

$$M_L = M_I + M_{sa} - M_{sr} + M_{la} - M_{lr} \tag{A-34}$$

with the following definitions:

$$\begin{aligned} M_L &= KG_L \cdot \Delta_L \\ M_I &= KG_I \cdot \Delta_I \\ M_{sa} &= \sum w_{sa} k g_{sa} \text{ (for solid weights to be added)} \\ M_{sr} &= \sum w_{sr} k g_{sr} \text{ (for solid weights to be removed)} \\ M_{la} &= \sum w_{la} k g_{la} \text{ (for liquid weights to be added)} \\ M_{lr} &= \sum w_{lr} k g_{lr} \text{ (for liquid weights to be removed)} \end{aligned}$$

Since the calculation involving the moments is now a simple summation, the total uncertainty in the lightship moment (M_L) can be calculated

$$U_{M_L} = \sqrt{U_{M_I}^2 + U_{M_{sa}}^2 + U_{M_{sr}}^2 + U_{M_{la}}^2 + U_{M_{lr}}^2} \quad (\text{A-35})$$

and the relative uncertainty in KG_L can be calculated

$$\hat{U}_{KG_L} = \sqrt{\hat{U}_{\Delta_L}^2 + \hat{U}_{M_L}^2} \quad (\text{A-36})$$

For each of the weights to be added or removed the uncertainty in each moment can be calculated from the relative uncertainty for the moment and the tabulated summation of the moment of the weights added or removed (from the Stability Test Report)

$$U_{M_{sa}} = \hat{U}_{M_{sa}} \cdot M_{sa} \quad U_{M_{sr}} = \hat{U}_{M_{sr}} \cdot M_{sr} \quad U_{M_{la}} = \hat{U}_{M_{la}} \cdot M_{la} \quad U_{M_{lr}} = \hat{U}_{M_{lr}} \cdot M_{lr}$$

Since each moment is calculated from a product of weight and vertical position, the relative uncertainty for each moment is calculated using

$$\hat{U}_{M_{sa}} = \hat{U}_{M_{sr}} = \sqrt{\hat{U}_{w_s}^2 + \hat{U}_{kg_s}^2} = \sqrt{(0.04)^2 + (0.019)^2} = 0.044 \text{ (95\%)}$$

$$\hat{U}_{M_{la}} = \hat{U}_{M_{lr}} = \sqrt{\hat{U}_{w_l}^2 + \hat{U}_{kg_l}^2} = \sqrt{(0.0107)^2 + (0.0109)^2} = 0.015 \text{ (95\%)}$$

The weights, heights, and moments of solids (dry items) and liquids to add or remove are taken from the Stability Test Report

$$w_{sa} = 11 \text{ LT}, \quad kg_{sa} = 51.47 \text{ ft}, \quad M_{sa} = 465 \text{ ftLT}$$

$$w_{sr} = 286 \text{ LT}, \quad kg_{sr} = 54.31 \text{ ft}, \quad M_{sr} = 15,524 \text{ ftLT}$$

$$w_{la} = 0 \text{ LT}, \quad kg_{la} = 0 \text{ ft}, \quad M_{la} = 0 \text{ ftLT}$$

$$w_{lr} = 3,292 \text{ LT}, \quad kg_{lr} = 12.74 \text{ ft}, \quad M_{lr} = 41,941 \text{ ftLT}$$

Therefore, the uncertainties are calculated

$$U_{M_{sa}} = \hat{U}_{M_{sa}} \cdot M_{sa} = (0.044) \cdot (465 \text{ ftLT}) = 20.5 \text{ ftLT (95\%)}$$

$$U_{M_{sr}} = \hat{U}_{M_{sr}} \cdot M_{sr} = (0.044) \cdot (15,524 \text{ ftLT}) = 683.0 \text{ ftLT (95\%)}$$

$$U_{M_{la}} = \hat{U}_{M_{la}} \cdot M_{la} = (0.0153) \cdot (0 \text{ ftLT}) = 0 \text{ ftLT (95\%)}$$

$$U_{M_{lr}} = \hat{U}_{M_{lr}} \cdot M_{lr} = (0.0153) \cdot (41,941 \text{ ftLT}) = 640.6 \text{ ftLT (95\%)}$$

and

$$M_I = KG_I \cdot \Delta_I = (26.02 \text{ ft}) \cdot (23,512 \text{ LT}) = 611,782 \text{ ftLT}$$

$$\begin{aligned}
 U_{M_I} &= \sqrt{\left(\frac{\partial M_I}{\partial KG_I} U_{KG_I}\right)^2 + \left(\frac{\partial M_I}{\partial \Delta_I} U_{\Delta_I}\right)^2} = \sqrt{(\Delta_I \cdot U_{KG_I})^2 + (KG_I \cdot U_{\Delta_I})^2} \\
 &= \sqrt{(23,512 \text{ LT} \cdot 0.447 \text{ ft})^2 + (26.02 \text{ ft} \cdot 256.3 \text{ LT})^2} \\
 &= \sqrt{(10,486 \text{ ftLT})^2 + (6,664 \text{ ftLT})^2} = 12,425 \text{ ftLT} \text{ (95\%)}
 \end{aligned}$$

The uncertainty in the lightship moment is calculated

$$\begin{aligned}
 U_{M_L} &= \sqrt{U_{M_I}^2 + U_{M_{sa}}^2 + U_{M_{sr}}^2 + U_{M_{ta}}^2 + U_{M_{tr}}^2} \\
 &= \sqrt{(12,425 \text{ ftLT})^2 + (20.5 \text{ ftLT})^2 + (683 \text{ ftLT})^2 + (0 \text{ ftLT})^2 + (640.6 \text{ ftLT})^2} \\
 &= 12,460 \text{ ftLT} \text{ (95\%)}
 \end{aligned}$$

and

$$\begin{aligned}
 M_L &= KG_L \cdot \Delta_L = (27.82 \text{ ft}) \cdot (19,943 \text{ LT}) = 554,814 \text{ ftLT} \\
 KG_L &= M_L / \Delta_L \\
 U_{\Delta_L} &= \sqrt{U_{\Delta_I}^2 + U_{w_s}^2 + U_{w_l}^2} = \sqrt{(256.3 \text{ LT})^2 + (11.9 \text{ LT})^2 + (36.5 \text{ LT})^2} \\
 &= 259.2 \text{ LT} \text{ (95\%)} \\
 \hat{U}_{\Delta_L} &= U_{\Delta_L} / \Delta_L = 259.2 \text{ LT} / 19,943 \text{ LT} = 0.0130 \text{ (95\%)} \\
 \hat{U}_{M_L} &= \frac{U_{M_L}}{M_L} = \frac{12,460 \text{ ftLT}}{554,814} \text{ ftLT} = 0.0225 \text{ (95\%)}
 \end{aligned}$$

Finally, the uncertainty in the lightship KG is

$$\begin{aligned}
 \hat{U}_{KG_L} &= \sqrt{\hat{U}_{\Delta_L}^2 + \hat{U}_{M_L}^2} = \sqrt{(0.0130)^2 + (0.0225)^2} = 0.0260 = 2.6\% \text{ (95\%)} \\
 U_{KG_L} &= \hat{U}_{KG_L} \cdot KG_L = 0.0260 \cdot 27.82 \text{ ft} = 0.72 \text{ ft} = 8.6 \text{ in} \text{ (95\%)}
 \end{aligned}$$

A.6. Uncertainty in KG and GM for the Accident Voyage

The uncertainty in the accident voyage KG and GM can be estimated by extending the above calculations, first for KG and then for GM. Note that in this case only solid and liquid weights to be added to the lightship need be considered. Table A-4 below provides the summary of the departure loading condition for the accident voyage, taken from the CargoMax loading computer printout [A5] along with calculated vertical moments and calculated relative uncertainties in weight and vertical centers. It is reasonable to reduce uncertainty in weight of the cargo from 4% to 2%, since based on the MBI hearing testimony [A18], the containers were routinely weighed as the containers were brought onto the terminal prior to being loaded onto trailers (for RO/RO cargo) or onto the container stows (for LO/LO cargo).

For an initial assessment, estimation of centers of gravity of containers and trailers is based on the CargoMax printout for the departure condition, and they are assumed to have an uncertainty in kg of 1.0 ft, but normalized separately for each dry weight category based on the respective vertical center from the CargoMax printout. This is summarized in Table A-4 below. This initial assessment will be revisited subsequently since the default kg value for LO/LO containers

is set in CargoMax as the geometric center of the container, and this potentially adds a kg-reducing (negative) bias error to the estimate.

The relative uncertainty for each moment is calculated, for example for the LO/LO containers:

$$\hat{U}_{M_{sa}(LO/LO)} = \sqrt{\hat{U}_{w_s}^2 + \hat{U}_{kg_s(LO/LO)}^2} = \sqrt{(0.01)^2 + (0.013)^2} = 0.0238 \text{ (95\%)}$$

Then the uncertainties for each moment can be calculated, for example for the LO/LO containers:

$$U_{M_{sa}(LO/LO)} = \hat{U}_{M_{sa}(LO/LO)} \cdot M_{sa}(LO/LO) = (0.0238) \cdot (528,457 \text{ ftLT}) = 12,601 \text{ ftLT (95\%)}$$

All calculated values are shown in Table A-5.

Item	Weight (LT)	Vertical Center of Gravity (ft)	Vertical Moment (ft·LT)	\hat{U}_w	\hat{U}_{kg}
Lightship	19,943.0	27.82	554,814	0.013	0.0260
Constants	171.9	52.86	9,086	0.020	0.0189
LO/LO cargo	6,862.1	77.01	528,457	0.020	0.0130
RO/RO cargo	4,183.8	38.43	160,800	0.020	0.0260
Tanks (liquids)	3,463.7	10.55	36,545	0.011	0.0109
Total departure condition	34,624.5	37.25	1,289,704		

Table A-4: Departure loading condition summary for the accident voyage, with values and calculated uncertainties for weight (w), vertical center of gravity (kg). All uncertainties are given at the 95% confidence level.

The uncertainty in the departure condition moment is calculated

$$U_{M_D} = \sqrt{U_{M_L}^2 + \Sigma(U_M^2)} = 18,501 \text{ ftLT (95\%)}$$

and

$$M_D = KG_D \cdot \Delta_D = 1,289,704 \text{ ftLT}$$

$$U_{\Delta_D} = \sqrt{U_{\Delta_L}^2 + \Sigma(U_w^2)} = 307.4 \text{ LT (95\%)}$$

$$\hat{U}_{\Delta_D} = U_{\Delta_D} / \Delta_D = 307.4 \text{ LT} / 34,624.5 \text{ LT} = 0.0089 \text{ (95\%)}$$

$$\hat{U}_{M_D} = \frac{U_{M_D}}{M_D} = \frac{18,501 \text{ ftLT}}{1,289,704 \text{ ftLT}} = 0.0143 \text{ (95\%)}$$

Finally, the uncertainty in the departure condition KG is

$$\hat{U}_{KG_D} = \sqrt{\hat{U}_{\Delta_D}^2 + \hat{U}_{M_D}^2} = 0.0169 = 1.7\% \text{ (95\%)}$$

$$U_{KG_D} = \hat{U}_{KG_D} \cdot KG_D = 0.0169 \cdot 37.25 \text{ ft} = 0.628 \text{ ft} = 7.5 \text{ in (95\%)}$$

The uncertainty in GM for the departure condition can be calculated in a similar manner to Section A.3 with

$$GM = KM - KG$$

$$KM = KB + BM$$

$$BM = I/\nabla$$

$$U_{GM} = \sqrt{U_{KB}^2 + U_{BM}^2 + U_{KG}^2}$$

$$\hat{U}_{BM} = \sqrt{\hat{U}_I^2 + \hat{U}_{\nabla}^2} \tag{A-37}$$

$$I = \frac{2}{3} \int_0^L y^3 dx$$

$$\hat{U}_I = \sqrt{\hat{U}_L^2 + (3\hat{U}_B)^2}$$

with $\hat{U}_I = 0.39\% = 0.0039$.

Item	Weight (LT)	Vertical Center of Gravity (ft)	Vertical Moment (ft·LT)	\hat{U}_w	U_w (LT)	\hat{U}_{kg}	U_{kg} (ft)	\hat{U}_M	U_M (ft·LT)
Lightship	19,943.0	27.820	554,814	0.013	259.2	0.0260	0.72	0.0225	12,460
Constants	171.9	52.859	9,086	0.020	3.4	0.0189	1.00	0.0275	250
LO/LO cargo	6,862.1	77.011	528,457	0.020	137.2	0.0130	1.00	0.0238	12,601
RO/RO cargo	4,183.8	38.434	160,800	0.020	83.7	0.0260	1.00	0.0328	5,277
Tanks (liquids)	3,463.7	10.551	36,545	0.011	38.1	0.0109	0.12	0.0155	566
Total departure condition	34,624.5	37.25	1,289,704	0.0089	307.4	0.0169	0.63	0.0143	18,501

Table A-5: Departure loading condition summary for the accident voyage, with values and calculated uncertainties for weight (w), vertical center of gravity (kg), and vertical moment (M). All uncertainties are given at the 95% confidence level.

From above, for the departure condition, $\hat{U}_{\Delta_D} = 0.0089$. For the departure on the accident voyage, the specific gravity is taken as 1.025 (salt water), but the relative uncertainty for the specific gravity depends primarily on the hydrometer precision as for the inclining, therefore

$$\hat{U}_{\nabla} = \sqrt{\hat{U}_{\Delta}^2 + \hat{U}_{\gamma}^2} = \sqrt{(0.0089)^2 + (0.0015)^2} = 0.0090 = 0.90\%$$

Therefore

$$\hat{U}_{BM} = \sqrt{\hat{U}_I^2 + \hat{U}_{\nabla}^2} = \sqrt{(0.0039)^2 + (0.0090)^2} = 0.0098 = 0.98\% \text{ (95\%)}$$

and

$$\begin{aligned} \hat{U}_{KB} &= \sqrt{\hat{U}_L^2 + \hat{U}_B^2 + \hat{U}_D^2 + \hat{U}_{\nabla}^2} \\ &= \sqrt{(0.00083)^2 + (0.00128)^2 + (0.00125)^2 + (0.0090)^2} = 0.0092 \\ &= 0.92\% \text{ (95\%)} \end{aligned}$$

From the MSC GHS computer model, for departure drafts of 26.79 ft forward, 29.69 ft midship and 32.59 ft aft, KB is 16.9 ft and BM is 25.1 ft. Therefore

$$\begin{aligned} U_{KB} &= 0.0092 \cdot 16.9 \text{ ft} = 0.155 \text{ ft} \text{ (95\%)} \\ U_{BM} &= 0.0098 \cdot 25.1 \text{ ft} = 0.246 \text{ ft} \text{ (95\%)} \end{aligned}$$

Finally, the uncertainty in GM for the departure condition is

$$\begin{aligned} U_{GM} &= \sqrt{U_{KB}^2 + U_{BM}^2 + U_{KG}^2} = \sqrt{(0.155 \text{ ft})^2 + (0.246 \text{ ft})^2 + (0.628 \text{ ft})^2} = 0.69 \text{ ft} \\ &= 8.3 \text{ in} \text{ (95\%)} \end{aligned}$$

In words, this says that there is a 95% confidence that the calculated value of GM for the departure condition lies within ± 0.69 feet of the true value of GM. In equation form this can be written (to one decimal place)

$$GM = 4.3 \pm 0.7 \text{ ft} \text{ (with 95\% confidence)}$$

A.7. Additional Considerations

Use of results from prior stability tests:

This procedure calculates the uncertainty in GM and KG based solely on the results of the 2006 stability test, and the documented vessel loading for the departure condition. It is possible in theory to incorporate the results of prior stability tests to supplement the calculations and perhaps refine the uncertainty estimate. It might be possible to estimate the 2006 weight and KG based on the weight and KG from the 1993 stability test, accounting for all of the various weights which were added or removed over the 13 year period between stability tests. If these weight changes (and their centers of gravity) were known with quantifiable uncertainty, then this could add an additional calculation on which to base a refinement of the uncertainty estimate.

However, in the case of the EL FARO for the period between the 1993 and 2006 stability tests, a significant amount of weight was added and removed. The post-inclining 1993 displacement was 15,743 LT with KG 35.59 ft [A19] and the post-inclining 2006 displacement was 19,943 LT with KG 27.82 ft [A20]. The weight changes included removal of the spar deck (estimated at 713 LT) [A21], addition of container foundations and support structure (estimated at 200-300 LT), and addition of an estimated 4,875 LT of fixed ballast in the double bottom tanks [A22], plus numerous smaller changes. This total change amounts to more than 38% of the lightship weight, which is a significant change. Additionally, the center of gravity locations of these weights could only be estimated, and therefore uncertainty in moments of the weight changes could be significant. Nevertheless, it is acknowledged that this approach could potentially provide useful information which might be considered in assessment of the uncertainty, if sufficiently detailed weight data would be available.

Container centers of gravity:

As mentioned in Section A.6, the default centers of gravity (VCG or kg) for LO/LO containers were calculated by default in CargoMax at the geometric center of the containers. It is recognized that most containers would likely contain cargo which would result in a center of gravity below the center of the container, and this would potentially suggest addition of a KG-reducing (negative) bias error adjustment to the estimate of uncertainty provided in Section A.6.

Unfortunately, there is insufficient container weight data available on which to base a rigorous analysis to calculate the magnitude of this bias error. However, an estimate of the bias error can be made for the accident voyage. Page 10 of the Trim and Stability Booklet [A20] provides curves to estimate vertical center of gravity of 40-ft containers on trailers. Unfortunately, it is unknown how these curves were developed, what limitations might be required in their use, or how much uncertainty might be built into these curves. But these curves are used in this analysis as a tool to estimate the negative bias error for the accident voyage departure condition. Using the Final Stow Plan for the accident voyage [A23], and using the weight and height of the trailers and stands annotated, these curves can be used to provide a better estimate of the center of gravity of 40-ft containers in the various LO/LO container bays. Using this approach, the centers of gravity of the LO/LO containers onboard for the accident voyage are estimated to be on average approximately 1.0 ft below the center of the container. Using the CargoMax printout for

the accident voyage and a simple moment calculation, the impact of this on the accident voyage departure condition would be approximately a 0.2 ft reduction in the departure KG (VCG) and a 0.2 ft increase in the GM. In equation form this can be written (to one decimal place)

$$GM = (4.3 + 0.2) \pm 0.7 \text{ ft} = 4.5 \pm 0.7 \text{ ft (with 95\% confidence)}$$

In the course of conducting this assessment, it was noticed that values of VCG of the trailered RO/RO cargo entered into CargoMax were all based on the default values from the Trim and Stability Book for 52,000 lb trailers, and were not appropriately adjusted (increased) for the heavier trailers being carried aboard on the accident voyage. However, KG-increasing (positive) bias errors introduced in this manner are only estimated to be on the order of 0.1-0.2 ft, and are therefore small compared to the larger 1.0 ft negative bias errors associated with the LO/LO containers.

A.8. Summary

Table A-6 below provides a summary of the calculated uncertainties. Included in the table are the key results from the uncertainty analysis of the February 12, 2006 stability test, plus results of the uncertainty analysis of the departure condition for the accident voyage.

Parameter	Measured, calculated or nominal value with units	Uncertainty with units	Relative uncertainty (%)
Slope (tangent/moment)	2.3460 x 10 ⁻⁶ 1/ftLT	16.68 x 10 ⁻⁹ 1/ftLT	0.007 (0.7%)
Molded vs. as-built volume (V)	849,229 ft ³	1,673 ft ³	0.002 (0.2%)
Vessel drafts	22.45 ft	0.061 ft	0.003 (0.3%)
Calculated molded volume (m)	849,229 ft ³	8,492 ft ³	0.01 (1%)
Displacement volume (∇)	849,229 ft ³	9,126 ft ³	0.011 (1.1%)
Specific weight, density	62.55 lb/ft ³	0.09 lb/ft ³	0.002 (0.2%)
Vessel displacement (Δ)	23,512 LT	260 LT	0.011 (1.1%)
As-inclined GM	18.26 ft	0.24 ft	0.013 (1.3%)
As-inclined KG	26.02 ft	0.45 ft	0.017 (1.7%)
Lightship KG	27.82 ft	0.72 ft	0.026 (2.6%)
Accident voyage departure KG	37.25 ft *[-0.2 ft]	0.63 ft	0.017 (1.7%)
Accident voyage departure GM	4.28 ft *[+0.2 ft]	0.69 ft	0.161 (16%)

Table A-6: Summary of results of the uncertainty analyses of the stability test and the departure condition for the accident voyage. All uncertainties are given at the 95% confidence level.

*Bracketed estimated values reflect potential bias correction, lowering KG and increasing GM due to default location of centers of gravity of LO/LO containers in CargoMax.

A.9. Appendix References

- A1 SS EL FARO Stability Test Procedure, Drawing SSL-670-100-10, dated December 23, 2005, ABS approved February 2, 2006, Herbert Engineering Corporation (MBI Exhibit 258).
- A2 SS EL FARO Stability Test Report, date of inclining February 12, 2006, ABS approved March 22, 2006, Herbert Engineering Corporation (MBI Exhibit 139).
- A3 SS EL FARO Inclining Experiment Record Sheet, dated February 12, 2006, Herbert Engineering Corporation (MBI Exhibit 259).
- A4 ABS Statutory Survey Report M662652 – SS EL FARO Inclining Experiment, dated February 12, 2006 (MBI Exhibit 190).
- A5 SS EL FARO CargoMax Printout, Voyage No. 185, printed 11:48 on 01 Oct 2015, Tote Inc (MBI Exhibit 059).
- A6 Kline, S. J. and McClintock, F. A., “Describing Uncertainties in Single-Sample Experiments”, ASME Mechanical Engineering, Vol. 75, No. 1, 1953, pp. 3-8.
- A7 Moffat, R. J., “Describing the Uncertainties in Experimental Results”, Experimental Thermal and Fluid Science, Vol. 1, No. 1, 1988, pp. 3-17.
- A8 ITTC (International Towing Tank Conference), “The Specialist Committee on Uncertainty Analysis: Final Report and Recommendations to the 25th ITTC”, Proceedings of the 25th ITTC, Fukuoka, Japan, 2008, pp. 433-471.
- A9 Coleman, H.W. and Steele, W.G., Experimentation and Uncertainty Analysis for Engineers, John Wiley and Sons, New York, 1999.
- A10 Figliola, R.S. and Beasley, D.E., Theory and Design for Mechanical Measurements, 5th Edition, John Wiley and Sons, Hoboken, NJ, 2011.
- A11 ASTM F1321-92 (Reapproved 2004), Standard Guide for Conducting a Stability Test (Lightweight Survey and Inclining Experiment) to Determine the Light Ship Displacement and Centers of Gravity of a Vessel, ASTM International, 2004 (MBI Exhibit 194).
- A12 Shakshober, M.C. and Montgomery, J.B., “Analysis of the Inclining Experiment,” presented at the meeting of the Hampton Roads Section of the Society of Naval Architects and Marine Engineers, February 1967.
- A13 Wood, N.L., “Inclining Experiment Uncertainty Analysis,” Proceedings of the 36th Annual Conference of the Society of Allied Weight Engineers, San Diego, CA, May 1977.
- A14 Hansen, E.O., “An Analytic Treatment of the Accuracy of the Results of the Inclining Experiment,” Naval Engineer’s Journal, American Society of Naval Engineers, May 1985, pp. 97-115.
- A15 Reed, G.C., Linear Least-Squares Fits with Errors in Both Coordinates, American Journal of Physics, 57 (7), July 1989, pp. 642-646.
- A16 Reed, G.C., A Spreadsheet for Linear Least-Squares Fitting with Errors in Both Coordinates, Physics Education, 45 (1), January 2010, pp. 93-96.
- A17 International Association of Class Societies (IACS) Unified Requirement L5: Onboard Computers for Stability Calculations, Corr. 1, 2006.
- A18 Transcript, U.S. Coast Guard Marine Board of Investigation ICO the Sinking of the SS El Faro Held in Jacksonville, Florida, February 20, 2016, Volume 5.
- A19 SS NORTHERN LIGHTS Trim and Stability Booklet, Drawing 1252-700-602, Rev A1, dated May 6, 1993, Atlantic Marine Inc. (MBI Exhibit 251).

- A20 SS EL FARO Trim and Stability Booklet, Drawing 1252-700-602, Rev E, dated February 14, 2007, Herbert Engineering Corporation (MBI Exhibit 008).
- A21 SS NORTHERN LIGHTS (EL FARO) Spar Deck Removal, Drawing SSL-670-100-024, undated, Herbert Engineering Corporation (MBI Exhibit 406).
- A22 SS NORTHERN LIGHTS (EL FARO) Fixed Ballast Installation, Drawing SSL-670-100-003, dated May 24, 2005, Herbert Engineering Corporation (MBI Exhibit 257).
- A23 Final Stow Plan for EL FARO Voyage 185S, dated September 29, 2015, Tote Inc. (MBI Exhibit 069).

Appendix B: SOLAS Probabilistic Damage Stability Analysis

Next Page

01/05/17 15:56:26
GHS 15.00

USCG - MSC, Washington, D.C.
ELFARO321

Page 1
RUN1

Damage Stability Analysis
GHS DAMSTAB2 Wizard version 13.38S

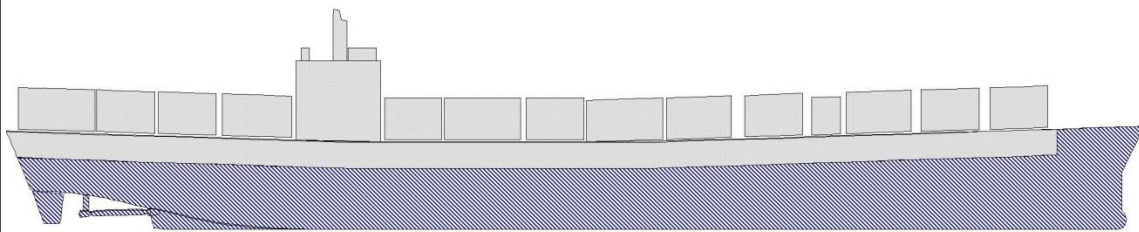
Probabilistic Damage

PORT-side Probabilistic Cargo old SOLAS Reg 25

Deepest draft (ds)

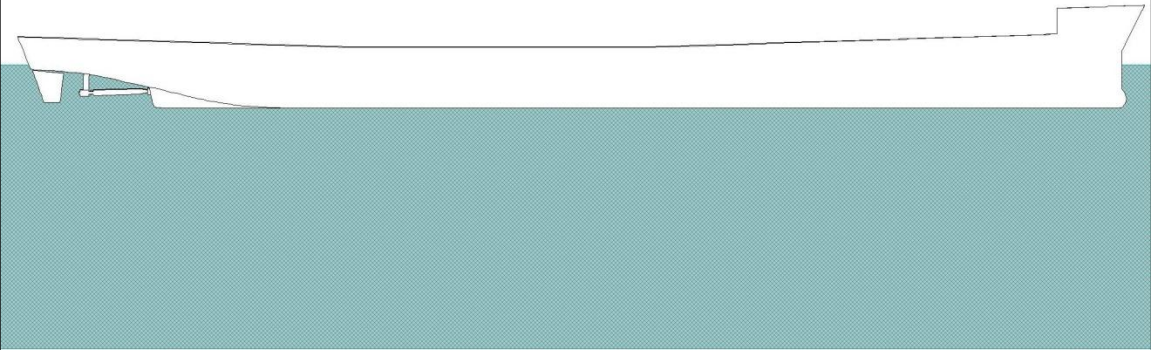
Condition Graphic

Outboard Profile View



01/05/17 15:56:26 GHS 15.00		USCG - MSC, Washington, D.C. ELFARO321			Page 2 RUN1
DIVISION definitions					
Division	Fwd End	Aft End	Wing	HBhd	Parts
1	20.59f	40.00a		51.43	BOSUNSTORES.C CHNLKRFP.C FOREPKTK.C
2	40.00a	68.42a			DTNO1A.C
3	68.42a	99.67a			DTNO1BP-SLOP.P
4	99.67a	212.42a			DBNO1P.P HOLDA.P
5	212.42a	325.17a	23.94		DBNO2IP.P DB2OP.P
			24.00		HOLDB.S HOLDA.P
6	325.17a	415.92a	26.75		DBNO2AIP.P DB2AOP.P
					HOLDC.C
7	415.92a	528.67a	26.73		DBNO3IP.P DB3OP.P
					HOLDD.C VOIDD.C
8	528.67a	613.92a	13.55		DBNO4P.P LO_SUMP.C
			20.80		ENGINEERROOM.C
9	613.92a	638.67a	22.05		DISTWTR.P HOLDF3RD.P
					DBNO4P.P LO_SUMP.C
					ENGINEERROOM.C DTAFTP.P
10	638.67a	668.92a	20.05		HOLDF3RD.P
					DTAFTP.P FOSETT.C
					HOLDF3RD.P
11	668.92a	694.75a	16.75		STERNTCOMP.C
					DTAFTP.P AFTPEAKCL.C
12	694.75a	726.75a	14.85		HOLDF3RD.P
					AFTPEAKCL.C
13	726.75a	758.75a	5.90	37.50	AFTPEAKP.P HOLDF3RD.P
					AFTPEAKCL.C
					AFTPEAKP.P
					STEERINGGEAR.C
Distances in FEET.					

01/05/17 15:56:26 GHS 15.00		USCG - MSC, Washington, D.C. ELFARO321			Page 3 RUN1	
Downflooding Points						
	Critical Points		LCP	TCP	VCP	Tank
(1)	H1-EF-L	FLOOD	102.40a	25.50	64.60	HOLDA.P
(2)	H1-EA-L	FLOOD	193.20a	35.50	61.50	HOLDA.P
(3)	H2-EF-BA	FLOOD	228.90a	45.20	58.60	HOLDB.S
(4)	H2-EA-BA	FLOOD	311.40a	45.50	56.50	HOLDB.S
(5)	H2A-EF-BA	FLOOD	341.70a	45.70	55.90	HOLDC.C
(6)	H2A-EA-BA	FLOOD	402.20a	45.80	55.90	HOLDC.C
(7)	H3-EF-BA	FLOOD	435.20a	46.00	55.90	HOLDD.C
(8)	H3-EA-BA	FLOOD	501.20a	46.00	55.90	HOLDD.C
(9)	H5-EF-BA	FLOOD	674.40a	44.70	61.30	HOLDF3RD.P
Distances in FEET.						

01/05/17 15:56:26 GHS 15.00	USCG - MSC, Washington, D.C. ELFARO321	Page 4 RUN1
WEIGHT STATUS		
Trim: 0.00 deg., Heel: zero		
Part	Weight(LT)	LCG TCG VCG
WEIGHT	34,646.44	391.49a 0.00 38.04
Distances in FEET.		
Draft at LCF: 30.109		
Draft at mid subdivision length: 30.109		
Condition Graphic - Draft: 30.11 @ 0.00 Trim: 0.00 deg. Heel: zero		
Profile View		
		
Plan View		
		

01/05/17 15:56:26 GHS 15.00	USCG - MSC, Washington, D.C. ELFARO321	Page 5 RUN1		
PERMEABILITY SETTINGS				
Name	Description	Flooded	Normal	Cubic FEET
DBNO1P.P		0.9500	0.9500	11,262.4
DBNO1S.S		0.9500	0.9500	11,262.4
DBNO2IP.P		0.9500	0.9500	14,784.8
ELPITDB.S		0.9500	0.7500	913.3
DBNO2IS.S		0.9500	0.9500	13,628.0
DBNO2AIP.P		0.9500	0.9500	12,129.0
DBNO2AIS.S		0.9500	0.9500	12,129.0
DBNO3IP.P		0.9500	0.9500	15,047.0
DBNO3IS.S		0.9500	0.9500	15,047.0
LO_SETT.P		0.9500	0.9800	630.6
LO_STOR.S		0.9500	0.9800	490.5
POTWTR.S		0.9500	0.9800	2,735.4
DISTWTR.P		0.9500	0.9800	3,224.8
LO_SUMP.C		0.9500	0.9800	551.9
LO_GRAV.C		0.9500	0.9800	539.0
DO.P		0.9500	0.9800	679.1
FOSETT.C		0.9500	0.9800	10,299.4
FWDRAMP.P		0.7000	0.7000	14,972.2
AFTRAMP.P		0.7000	0.7000	11,686.0
HOLDA.P		0.7000	0.8000	193,548.9
FWDRAMFLOW.P		0.7000	1.0000	16,851.5
HOLDB.S		0.7000	0.8000	263,376.9
HOLDC.C		0.7000	0.8000	232,601.3
VOIDD.C		0.9500	1.0000	10,979.1
HOLDD.C		0.7000	0.8000	277,146.9
HOLDF3RD.P		0.7000	0.8000	140,035.7
ERRAMP.P		0.7000	1.0000	11,501.5
ENGINEERROOM.C		0.8500	0.8500	212,361.0
DTNO1A.C		0.9500	0.9800	20,210.9
DTNO1BP-SLOP.P		0.9500	0.9800	16,973.2
DTNO1BS.S		0.9500	0.9800	16,973.2
DTAFTP.P		0.9500	0.9800	9,393.8
DTAFTS.S		0.9500	0.9800	9,393.8
CHNLKRFP.C		0.9500	1.0000	3,209.8
FOREPKTK.C		0.9500	0.9800	15,430.6
STEERINGGEAR.C		0.9500	0.9500	25,527.3
BOSUNSTORES.C		0.6000	0.9000	22,696.7
AFTPEAKCL.C		0.9500	0.9500	28,780.5
AFTPEAKP.P		0.9500	0.9500	4,150.2
AFTPEAKS.S		0.9500	0.9500	4,150.2
COFF.P		0.9500	1.0000	401.7
DBNO4P.P		0.9500	0.9800	3,932.2
DBNO4S.S		0.9500	0.9800	3,932.2
DB2OP.P		0.9500	0.9800	9,394.4
DB2OS.S		0.9500	0.9800	9,394.4
DB2AOP.P		0.9500	0.9800	13,461.6
DB2AOS.S		0.9500	0.9800	13,461.6
DB3OP.P		0.9500	0.9800	13,086.5
DB3OS.S		0.9500	0.9800	13,086.5
SECONDDECK.C		0.7000	0.9800	1,082,915.5
STERNTCOMP.C			0.9000	6,776.8

01/05/17 15:56:26 GHS 15.00	USCG - MSC, Washington, D.C. ELFARO321							Page 6 RUN1		
PROBABILISTIC DAMAGE STABILITY										
Cargo Vessel Version										
Subdivision length: 788.30			Terminals: 20.59f, 767.71a							
Breadth: 96.00			Draft: 30.11			Hmax: 53.04				
Divisions	P	Smin	P*S*V	A	Depth	Trim	Heel	Range	MaxRA	
None	0.00000	1.000	0.000	0.000	30.11	0.00	0.00	29.22	1.28	
1	0.06159	1.000	0.057	0.057	31.30	0.14 f	0.00	28.83	1.28	
1+u1	0.06159	1.000	0.004	0.062	31.30	0.14 f	0.00	28.83	1.28	
2	0.00734	1.000	0.007	0.069	31.10	0.11 f	0.00	28.87	1.27	
3	0.00882	1.000	0.009	0.078	30.89	0.09 f	0.44 p	28.43	1.25	
4	0.09356	1.000	0.094	0.171	40.40	1.09 f	1.64 p	22.64	0.66	
5	0.06620	0.955	0.063	0.235	41.13	1.01 f	4.36 p	18.25	0.36	
5+i1	0.00005	0.000	0.000	0.235	37.94	6.32 f	179.58 p	0.00		
5+i1+i2	0.02731	0.000	0.000	0.235	43.49	6.84 f	179.32 p	0.00		
6	0.04815	0.912	0.044	0.278	35.37	0.33 f	6.98 p	16.63	0.37	
6+i1	0.01545	0.883	0.014	0.292	35.76	0.36 f	7.81 p	15.61	0.35	
7	0.05740	0.905	0.052	0.344	31.64	0.28 a	5.76 p	16.38	0.40	
7+i1	0.02053	0.867	0.018	0.362	31.74	0.30 a	6.77 p	15.05	0.38	
8	0.01965	0.185	0.004	0.365	23.98	1.42 a	5.27 s	5.57	0.04	
8+i1	0.00723	0.185	0.001	0.367	23.98	1.42 a	5.27 s	5.57	0.04	
8+i1+i2	0.01144	0.185	0.002	0.369	23.98	1.42 a	5.27 s	5.57	0.04	
9	0.00300	0.000	0.000	0.369	-36.56	3.40 a	179.73 p	0.00		
9+i1	0.00022	0.000	0.000	0.369	-36.86	3.47 a	179.68 p	0.00		
10	0.00373	0.996	0.004	0.373	28.99	0.18 a	6.35 p	19.84	0.51	
10+i1	0.00063	0.988	0.001	0.373	28.46	0.29 a	6.21 p	19.53	0.51	
11	0.00228	0.996	0.002	0.376	28.99	0.18 a	6.35 p	19.84	0.51	
11+i1	0.00064	0.946	0.001	0.376	27.18	0.51 a	6.37 p	17.91	0.44	
12	0.00262	1.000	0.003	0.379	29.52	0.11 a	1.51 p	25.59	0.61	
12+i1	0.00135	1.000	0.001	0.380	27.64	0.45 a	2.36 p	22.94	0.54	
13	0.00112	1.000	0.000	0.380	30.02	0.02 a	0.52 p	28.67	1.22	
13+i1	0.00235	1.000	0.001	0.381	28.74	0.25 a	0.72 p	28.26	1.24	
13+u1	0.00112	1.000	0.001	0.382	30.02	0.02 a	0.52 p	28.63	1.20	
13+u1+i1	0.00235	1.000	0.002	0.384	28.74	0.25 a	0.72 p	28.08	1.20	
1-division damage:				0.384	Probability of damage:					0.463
1+2	0.02990	1.000	0.028	0.411	32.35	0.25 f	0.00	28.45	1.28	
1+2+u1	0.02990	1.000	0.002	0.413	32.35	0.25 f	0.00	28.45	1.28	
2+3	0.01392	1.000	0.014	0.427	31.94	0.21 f	0.46 p	28.02	1.23	
3+4	0.03697	1.000	0.037	0.464	41.96	1.27 f	2.64 p	20.39	0.53	
4+5	0.04187	0.000	0.000	0.464	43.58	6.87 f	179.43 p	0.00		
4+5+i1	0.00004	0.000	0.000	0.464	43.58	6.87 f	179.43 p	0.00		
4+5+i1+i2	0.03434	0.000	0.000	0.464	50.20	7.49 f	179.16 p	0.00		
5+6	0.04035	0.000	0.000	0.464	13.37	3.56 f	179.95 p	0.00		
5+6+i1	0.00004	0.000	0.000	0.464	642.07	90.00 f	0.98 p	0.00	0.00	
5+6+i1+i2	0.03161	0.000	0.000	0.464	559.06	62.16 f	176.96 p	0.00		
6+7	0.03928	0.000	0.000	0.464	-8.46	0.93 f	180.00 s	0.00		
6+7+i1	0.02727	0.000	0.000	0.464	-8.46	0.93 f	180.00 s	0.00		
7+8	0.02045	0.000	0.000	0.464	-91.49	22.71 a	179.04 p	0.00		
7+8+i1	0.00722	0.000	0.000	0.464	-119.14	35.61 a	178.31 p	0.00		
continued next page										

01/05/17 15:56:26		USCG - MSC, Washington, D.C.						Page 7		
GHS 15.00		ELFARO321						RUN1		
Divisions	P	Smin	P*S*V	A	Depth	Trim	Heel	Range	MaxRA	
7+8+i1+i2	0.02462	0.000	0.000	0.464	-120.04	36.10a	178.31p	0.00		
8+9	0.00694	0.000	0.000	0.464	-36.80	3.45a	179.68p	0.00		
8+9+i1	0.00239	0.000	0.000	0.464	-37.23	3.55a	179.53p	0.00		
8+9+i1+i2	0.00699	0.000	0.000	0.464	-37.23	3.55a	179.53p	0.00		
9+10	0.00391	0.000	0.000	0.464	-36.56	3.40a	179.73p	0.00		
9+10+i1	0.00266	0.000	0.000	0.464	-39.51	4.02a	179.65p	0.00		
10+11	0.00334	0.996	0.003	0.468	28.99	0.18a	6.35p	19.84	0.51	
10+11+i1	0.00290	0.941	0.003	0.470	26.55	0.64a	6.01p	17.70	0.44	
11+12	0.00291	0.925	0.003	0.473	28.59	0.23a	8.07p	17.10	0.42	
11+12+i1	0.00302	0.858	0.003	0.476	26.68	0.58a	8.41p	14.73	0.35	
12+13	0.00160	1.000	0.001	0.476	29.52	0.11a	1.51p	25.59	0.61	
12+13+i1	0.00475	1.000	0.002	0.478	27.64	0.45a	2.36p	22.94	0.54	
12+13+u1	0.00160	1.000	0.001	0.479	29.52	0.11a	1.51p	24.06	0.57	
12+13+u1+i1	0.00475	1.000	0.003	0.482	27.64	0.45a	2.36p	20.91	0.47	
2-division damage:				0.098	Probability of damage:				0.389	
1+2+3	0.02208	1.000	0.021	0.503	33.25	0.35 f	0.48p	27.54	1.23	
1+2+3+u1	0.02208	1.000	0.002	0.504	33.25	0.35 f	0.48p	27.54	1.23	
2+3+4	0.02196	0.936	0.021	0.525	44.11	1.52 f	2.87p	17.54	0.44	
3+4+5	0.00000	0.000	0.000	0.525	56.07	8.07 f	179.20p	0.00		
3+4+5+i1	0.00000	0.000	0.000	0.525	56.07	8.07 f	179.20p	0.00		
3+4+5+i1+i2	0.00189	0.000	0.000	0.525	66.78	9.09 f	178.87p	0.00		
4+5+6	0.00000	0.000	0.000	0.525	532.75	58.66 f	177.62p	0.00		
4+5+6+i1	0.00000	0.000	0.000	0.525	556.43	61.92 f	177.17p	0.00		
4+5+6+i1+i2	0.00326	0.000	0.000	0.525	584.97	66.20 f	176.61p	0.00		
5+6+7	0.00049	0.000	0.000	0.525	53.00	6.70 f	177.48p	0.00		
5+6+7+i1	0.00000	0.000	0.000	0.525	SUNK					
5+6+7+i1+i2	0.00556	0.000	0.000	0.525	SUNK					
6+7+8	0.00000	0.000	0.000	0.525	-36.56	75.43a	177.46p	0.00		
6+7+8+i1	0.00000	0.000	0.000	0.525	SUNK					
6+7+8+i1+i2	0.00248	0.000	0.000	0.525	SUNK					
7+8+9	0.00100	0.000	0.000	0.525	-112.85	31.89a	178.26p	0.00		
7+8+9+i1	0.00032	0.000	0.000	0.525	-133.28	44.26a	177.50p	0.00		
7+8+9+i1+i2	0.00239	0.000	0.000	0.525	-133.28	44.26a	177.50p	0.00		
8+9+10	0.00550	0.000	0.000	0.525	-36.80	3.45a	179.68p	0.00		
8+9+10+i1	0.00204	0.000	0.000	0.525	-39.92	4.11a	179.50p	0.00		
8+9+10+i1+i2	0.00646	0.000	0.000	0.525	-39.92	4.11a	179.50p	0.00		
9+10+11	0.00201	0.000	0.000	0.525	-36.56	3.40a	179.73p	0.00		
9+10+11+i1	0.00219	0.000	0.000	0.525	-45.80	5.35a	179.63p	0.00		
10+11+12	0.00249	0.925	0.002	0.527	28.59	0.23a	8.07p	17.10	0.42	
10+11+12+i1	0.00322	0.854	0.003	0.530	26.07	0.70a	7.97p	14.58	0.35	
11+12+13	0.00097	0.925	0.000	0.530	28.59	0.23a	8.07p	17.10	0.42	
11+12+13+i1	0.00322	0.858	0.001	0.531	26.68	0.58a	8.41p	14.73	0.35	
11+12+13+u1	0.00097	0.878	0.001	0.531	28.59	0.23a	8.07p	15.43	0.38	
11+12+13+u1+i1	0.00322	0.705	0.002	0.533	26.60	0.58a	8.72p	12.13	0.27	
3-division damage:				0.051	Probability of damage:				0.090	
1+2+3+4	0.01862	0.844	0.015	0.548	46.68	1.82 f	3.10p	14.26	0.34	
continued next page										

01/05/17 15:56:26 GHS 15.00		USCG - MSC, Washington, D.C. ELFARO321						Page 8 RUN1		
Divisions	P	Smin	P*S*V	A	Depth	Trim	Heel	Range	MaxRA	
1+2+3+4+u1	0.01862	0.843	0.001	0.549	46.68	1.82f	3.10p	14.22	0.34	
2+3+4+5	0.00000	0.000	0.000	0.549	87.62	11.16f	179.07p	0.00		
2+3+4+5+i1	0.00000	0.000	0.000	0.549	87.62	11.16f	179.07p	0.00		
2+3+4+5+i1+										
i2	0.00080	0.000	0.000	0.549	121.02	14.43f	178.62p	0.00		
7+8+9+10	0.00001	0.000	0.000	0.549	-112.85	31.89a	178.26p	0.00		
7+8+9+10+i1	0.00000	0.000	0.000	0.549	-144.21	55.62a	177.46p	0.00		
7+8+9+10+										
i1+i2	0.00137	0.000	0.000	0.549	-144.21	55.62a	177.46p	0.00		
8+9+10+11	0.00261	0.000	0.000	0.549	-36.80	3.45a	179.68p	0.00		
8+9+10+11+										
i1	0.00091	0.000	0.000	0.549	-46.33	5.48a	179.48p	0.00		
8+9+10+11+										
i1+i2	0.00362	0.000	0.000	0.549	-46.33	5.48a	179.48p	0.00		
9+10+11+12	0.00149	0.000	0.000	0.549	-37.31	3.55a	179.52p	0.00		
9+10+11+12+										
i1	0.00208	0.000	0.000	0.549	-46.86	5.59a	179.41p	0.00		
10+11+12+13	0.00082	0.925	0.000	0.549	28.59	0.23a	8.07p	17.10	0.42	
10+11+12+										
13+i1	0.00285	0.854	0.001	0.550	26.07	0.70a	7.97p	14.58	0.35	
10+11+12+										
13+u1	0.00082	0.878	0.000	0.550	28.59	0.23a	8.07p	15.43	0.38	
10+11+12+										
13+u1+i1	0.00285	0.650	0.001	0.552	25.50	0.81a	8.16p	11.44	0.24	
4-division damage:				0.018	Probability of damage:				0.035	
7+8+9+10+11	0.00000	0.000	0.000	0.552	-112.85	31.89a	178.26p	0.00		
7+8+9+10+										
11+i1	0.00000	0.000	0.000	0.552	-142.25	67.52a	177.46p	0.00		
7+8+9+10+										
11+i1+i2	0.00052	0.000	0.000	0.552	-142.25	67.52a	177.46p	0.00		
8+9+10+11+										
12	0.00118	0.000	0.000	0.552	-37.60	3.61a	179.45p	0.00		
8+9+10+11+										
12+i1	0.00039	0.000	0.000	0.552	-47.41	5.72a	179.26p	0.00		
8+9+10+11+										
12+i1+i2	0.00236	0.000	0.000	0.552	-47.41	5.72a	179.26p	0.00		
9+10+11+12+										
13	0.00040	0.000	0.000	0.552	-37.31	3.55a	179.52p	0.00		
9+10+11+12+										
13+i1	0.00149	0.000	0.000	0.552	-46.86	5.59a	179.41p	0.00		
9+10+11+12+										
13+u1	0.00040	0.000	0.000	0.552	-42.72	4.65a	179.52p	0.00		
9+10+11+12+										
13+u1+i1	0.00149	0.000	0.000	0.552	-54.48	7.43a	179.38p	0.00		
5-division damage:				0.000	Probability of damage:				0.006	
Attained index in this condition:				0.552	Total probability of damage:				0.983	
Required index:				0.602						
Distances in FEET.								Angles in deg.		

01/05/17 15:56:26 GHS 15.00	USCG - MSC, Washington, D.C. ELFARO321 ===== Summary Data =====	Page 9 RUN1
Calculation method: SDIC Condition name: Deepest draft (ds) (code 2) Damage side: Port		
Displacement: 34646.4 LONG TONS Trim: 0.00 degrees VCG: 38.045 FEET Free surface moment: 0.0 LONG TONS-FEET Environment: 1.025		
Attained index: 0.552 Overall Required index: 0.602		

12/14/16 12:02:00
GHS 15.00

USCG - MSC, Washington, D.C.
ELFARO321

Page 1
RUN2

Damage Stability Analysis
GHS DAMSTAB2 Wizard version 13.38S

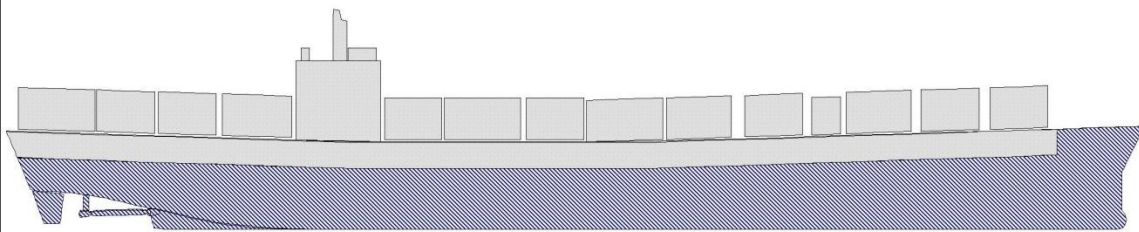
Probabilistic Damage

PORT-side Probabilistic Cargo old SOLAS Reg 25

Light-service draft (dl)

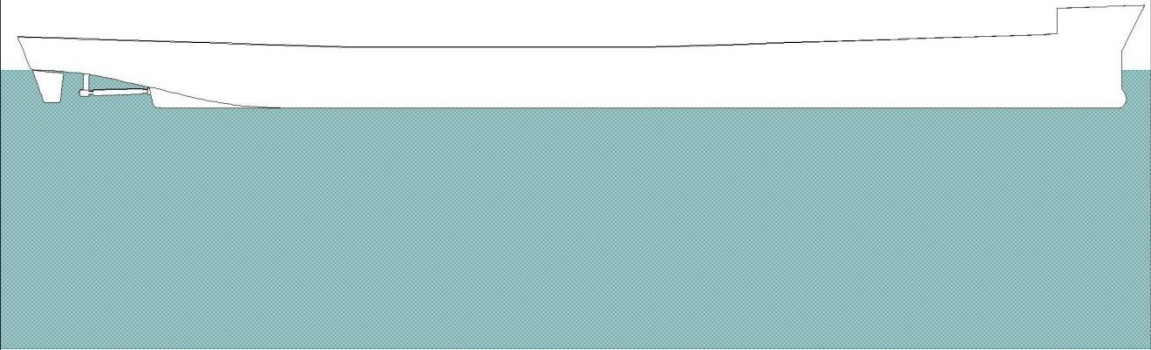

Condition Graphic

Outboard Profile View



12/14/16 12:02:00 GHS 15.00	USCG - MSC, Washington, D.C. ELFARO321				Page 2 RUN2
DIVISION definitions					
Division	Fwd End	Aft End	Wing	HBhd	Parts
1	20.59f	40.00a		51.43	BOSUNSTORES.C CHNLKRFP.C FOREPKTK.C
2	40.00a	68.42a			DTNO1A.C
3	68.42a	99.67a			DTNO1BP-SLOP.P
4	99.67a	212.42a			DBNO1P.P HOLDA.P
5	212.42a	325.17a	23.94		DBNO2IP.P DB2OP.P
			24.00		HOLDB.S HOLDA.P
6	325.17a	415.92a	26.75		DBNO2AIP.P DB2AOP.P
					HOLDC.C
7	415.92a	528.67a	26.73		DBNO3IP.P DB3OP.P
					HOLDD.C VOIDD.C
8	528.67a	613.92a	13.55		DBNO4P.P LO_SUMP.C
			20.80		ENGINEERROOM.C
9	613.92a	638.67a	22.05		DISTWTR.P HOLDF3RD.P
					DBNO4P.P LO_SUMP.C
					ENGINEERROOM.C DTAFTP.P
10	638.67a	668.92a	20.05		HOLDF3RD.P
					DTAFTP.P FOSETT.C
					HOLDF3RD.P
11	668.92a	694.75a	16.75		STERNTCOMP.C
					DTAFTP.P AFTPEAKCL.C
12	694.75a	726.75a	14.85		HOLDF3RD.P
					AFTPEAKCL.C
13	726.75a	758.75a	5.90	37.50	AFTPEAKP.P HOLDF3RD.P
					AFTPEAKCL.C
					AFTPEAKP.P
					STEERINGGEAR.C
Distances in FEET.					

12/14/16 12:02:00 GHS 15.00		USCG - MSC, Washington, D.C. ELFARO321			Page 3 RUN2	
Downflooding Points						
	Critical Points		LCP	TCP	VCP	Tank
(1)	H1-EF-L	FLOOD	102.40a	25.50	64.60	HOLDA.P
(2)	H1-EA-L	FLOOD	193.20a	35.50	61.50	HOLDA.P
(3)	H2-EF-BA	FLOOD	228.90a	45.20	58.60	HOLDB.S
(4)	H2-EA-BA	FLOOD	311.40a	45.50	56.50	HOLDB.S
(5)	H2A-EF-BA	FLOOD	341.70a	45.70	55.90	HOLDC.C
(6)	H2A-EA-BA	FLOOD	402.20a	45.80	55.90	HOLDC.C
(7)	H3-EF-BA	FLOOD	435.20a	46.00	55.90	HOLDD.C
(8)	H3-EA-BA	FLOOD	501.20a	46.00	55.90	HOLDD.C
(9)	H5-EF-BA	FLOOD	674.40a	44.70	61.30	HOLDF3RD.P
Distances in FEET.						

12/14/16 12:02:00 GHS 15.00	USCG - MSC, Washington, D.C. ELFARO321	Page 4 RUN2
WEIGHT STATUS		
Trim: 0.00 deg., Heel: zero		
Part	Weight(LT)	LCG TCG VCG
WEIGHT	28,673.26	384.83a 0.00 38.55
Distances in FEET.		
Draft at LCF: 26.026		
Draft at mid subdivision length: 26.026		
Condition Graphic - Draft: 26.03 @ 0.00 Trim: 0.00 deg. Heel: zero		
Profile View		
		
Plan View		
		

12/14/16 12:02:00 GHS 15.00	USCG - MSC, Washington, D.C. ELFARO321	Page 5 RUN2		
PERMEABILITY SETTINGS				
Name	Description	Flooded	Normal	Cubic FEET
DBNO1P.P		0.9500	0.9500	11,262.4
DBNO1S.S		0.9500	0.9500	11,262.4
DBNO2IP.P		0.9500	0.9500	14,784.8
ELPITDB.S		0.9500	0.7500	913.3
DBNO2IS.S		0.9500	0.9500	13,628.0
DBNO2AIP.P		0.9500	0.9500	12,129.0
DBNO2AIS.S		0.9500	0.9500	12,129.0
DBNO3IP.P		0.9500	0.9500	15,047.0
DBNO3IS.S		0.9500	0.9500	15,047.0
LO_SETT.P		0.9500	0.9800	630.6
LO_STOR.S		0.9500	0.9800	490.5
POTWTR.S		0.9500	0.9800	2,735.4
DISTWTR.P		0.9500	0.9800	3,224.8
LO_SUMP.C		0.9500	0.9800	551.9
LO_GRAV.C		0.9500	0.9800	539.0
DO.P		0.9500	0.9800	679.1
FOSETT.C		0.9500	0.9800	10,299.4
FWDRAMP.P		0.7000	0.7000	14,972.2
AFTRAMP.P		0.7000	0.7000	11,686.0
HOLDA.P		0.7000	0.8000	193,548.9
FWDRAMFLOW.P		0.7000	1.0000	16,851.5
HOLDB.S		0.7000	0.8000	263,376.9
HOLDC.C		0.7000	0.8000	232,601.3
VOIDD.C		0.9500	1.0000	10,979.1
HOLDD.C		0.7000	0.8000	277,146.9
HOLDF3RD.P		0.7000	0.8000	140,035.7
ERRAMP.P		0.7000	1.0000	11,501.5
ENGINEERROOM.C		0.8500	0.8500	212,361.0
DTNO1A.C		0.9500	0.9800	20,210.9
DTNO1BP-SLOP.P		0.9500	0.9800	16,973.2
DTNO1BS.S		0.9500	0.9800	16,973.2
DTAFTP.P		0.9500	0.9800	9,393.8
DTAFTS.S		0.9500	0.9800	9,393.8
CHNLKRFP.C		0.9500	1.0000	3,209.8
FOREPKTK.C		0.9500	0.9800	15,430.6
STEERINGGEAR.C		0.9500	0.9500	25,527.3
BOSUNSTORES.C		0.6000	0.9000	22,696.7
AFTPEAKCL.C		0.9500	0.9500	28,780.5
AFTPEAKP.P		0.9500	0.9500	4,150.2
AFTPEAKS.S		0.9500	0.9500	4,150.2
COFF.P		0.9500	1.0000	401.7
DBNO4P.P		0.9500	0.9800	3,932.2
DBNO4S.S		0.9500	0.9800	3,932.2
DB2OP.P		0.9500	0.9800	9,394.4
DB2OS.S		0.9500	0.9800	9,394.4
DB2AOP.P		0.9500	0.9800	13,461.6
DB2AOS.S		0.9500	0.9800	13,461.6
DB3OP.P		0.9500	0.9800	13,086.5
DB3OS.S		0.9500	0.9800	13,086.5
SECONDDECK.C		0.7000	0.9800	1,082,915.5
STERNTCOMP.C			0.9000	6,776.8

12/14/16 12:02:00 GHS 15.00	USCG - MSC, Washington, D.C. ELFARO321							Page 6 RUN2		
PROBABILISTIC DAMAGE STABILITY										
Cargo Vessel Version										
Subdivision length: 788.30			Terminals: 20.59f, 767.71a							
Breadth: 96.00			Draft: 26.03			Hmax: 48.96				
Divisions	P	Smin	P*S*V	A	Depth	Trim	Heel	Range	MaxRA	
None	0.00000	1.000	0.000	0.000	26.03	0.00	0.00	33.92	1.55	
1	0.06159	1.000	0.062	0.062	27.29	0.15 f	0.00	33.54	1.57	
2	0.00734	1.000	0.007	0.069	26.98	0.11 f	0.00	33.60	1.56	
3	0.00882	1.000	0.009	0.078	26.73	0.08 f	0.41 p	33.20	1.58	
4	0.09356	1.000	0.094	0.171	35.36	1.04 f	1.77 p	27.79	1.20	
5	0.06620	1.000	0.066	0.237	35.97	0.99 f	9.16 p	20.14	0.51	
5+i1	0.00005	0.000	0.000	0.237	16.84	4.59 f	179.87 p	0.00		
5+i1+i2	0.02731	0.000	0.000	0.237	18.10	4.71 f	179.72 p	0.00		
6	0.04815	1.000	0.048	0.286	30.40	0.32 f	10.81 p	20.21	0.58	
6+i1	0.01545	0.981	0.015	0.301	30.80	0.35 f	11.44 p	19.24	0.60	
7	0.05740	1.000	0.057	0.358	26.96	0.27 a	8.42 p	22.30	0.66	
7+i1	0.02053	1.000	0.021	0.379	27.05	0.29 a	9.32 p	21.01	0.71	
8	0.01965	1.000	0.020	0.398	21.69	1.04 a	1.97 s	25.73	0.52	
8+i1	0.00723	1.000	0.007	0.406	21.54	1.06 a	4.37 p	23.32	0.48	
8+i1+i2	0.01144	1.000	0.011	0.417	21.51	1.07 a	4.24 p	23.46	0.48	
9	0.00300	0.886	0.003	0.420	20.98	1.08 a	10.46 p	15.68	0.34	
9+i1	0.00022	0.864	0.000	0.420	20.82	1.12 a	10.86 p	15.05	0.33	
10	0.00373	1.000	0.004	0.424	25.57	0.08 a	3.87 p	29.46	1.30	
10+i1	0.00063	1.000	0.001	0.424	24.76	0.23 a	3.91 p	28.88	1.34	
11	0.00228	1.000	0.002	0.427	25.57	0.08 a	3.87 p	29.46	1.30	
11+i1	0.00064	1.000	0.001	0.427	24.72	0.23 a	4.34 p	28.36	1.26	
12	0.00262	1.000	0.003	0.430	26.02	0.00	0.04 p	33.42	1.21	
12+i1	0.00135	1.000	0.001	0.431	25.36	0.12 a	0.08 p	32.85	1.19	
13	0.00112	1.000	0.001	0.432	26.02	0.00	0.04 p	33.85	1.52	
13+i1	0.00235	1.000	0.001	0.433	25.36	0.12 a	0.08 p	33.72	1.54	
13+u1	0.00112	1.000	0.001	0.433	26.02	0.00	0.04 p	33.83	1.52	
13+u1+i1	0.00235	1.000	0.001	0.435	25.36	0.12 a	0.08 p	33.69	1.54	
1-division damage:				0.435	Probability of damage:					0.463
1+2	0.02990	1.000	0.030	0.464	28.31	0.27 f	0.00	33.19	1.58	
2+3	0.01392	1.000	0.014	0.478	27.74	0.20 f	0.43 p	32.82	1.58	
3+4	0.03697	1.000	0.037	0.515	36.79	1.21 f	2.68 p	25.84	1.07	
4+5	0.04187	0.000	0.000	0.515	19.40	4.85 f	179.67 p	0.00		
4+5+i1	0.00004	0.000	0.000	0.515	19.40	4.85 f	179.67 p	0.00		
4+5+i1+i2	0.03434	0.000	0.000	0.515	21.12	5.02 f	179.47 p	0.00		
5+6	0.04035	0.000	0.000	0.515	-1.21	2.56 f	179.74 s	0.00		
5+6+i1	0.00004	0.000	0.000	0.515	61.58	8.66 f	178.43 p	0.00		
5+6+i1+i2	0.03161	0.000	0.000	0.515	75.17	9.97 f	177.97 p	0.00		
6+7	0.03928	0.000	0.000	0.515	-13.20	1.15 f	180.00 s	0.00		
6+7+i1	0.02727	0.000	0.000	0.515	-13.19	1.15 f	180.00 s	0.00		
7+8	0.02045	0.000	0.000	0.515	-44.85	5.15 a	179.60 p	0.00		
7+8+i1	0.00722	0.000	0.000	0.515	-46.71	5.63 a	178.96 p	0.00		
7+8+i1+i2	0.02462	0.000	0.000	0.515	-46.82	5.66 a	178.94 p	0.00		
8+9	0.00694	0.864	0.006	0.521	20.82	1.12 a	10.86 p	15.05	0.33	
continued next page										

12/14/16 12:02:00		USCG - MSC, Washington, D.C.						Page 7		
GHS 15.00		ELFARO321						RUN2		
Divisions	P	Smin	P*S*V	A	Depth	Trim	Heel	Range	MaxRA	
8+9+i1	0.00239	0.702	0.002	0.523	20.57	1.14a	12.21p	12.70	0.25	
8+9+i1+i2	0.00699	0.702	0.005	0.528	20.57	1.14a	12.21p	12.70	0.25	
9+10	0.00391	0.886	0.003	0.531	20.98	1.08a	10.46p	15.68	0.34	
9+10+i1	0.00266	0.886	0.002	0.534	20.98	1.08a	10.46p	15.68	0.34	
10+11	0.00334	1.000	0.003	0.537	25.57	0.08a	3.87p	29.46	1.30	
10+11+i1	0.00290	1.000	0.003	0.540	23.61	0.44a	4.31p	27.58	1.29	
11+12	0.00291	1.000	0.003	0.543	25.52	0.08a	4.14p	29.03	1.22	
11+12+i1	0.00302	1.000	0.003	0.546	24.58	0.25a	4.94p	27.47	1.16	
12+13	0.00160	1.000	0.001	0.547	26.02	0.00	0.04p	33.42	1.21	
12+13+i1	0.00475	1.000	0.002	0.549	25.36	0.12a	0.08p	32.85	1.19	
12+13+u1	0.00160	1.000	0.001	0.550	26.02	0.00	0.04p	33.32	1.21	
12+13+u1+i1	0.00475	1.000	0.002	0.552	25.36	0.12a	0.08p	32.56	1.18	
2-division damage:				0.118	Probability of damage:				0.389	
1+2+3	0.02208	1.000	0.022	0.574	29.14	0.37f	0.46p	32.35	1.60	
2+3+4	0.02196	1.000	0.022	0.596	38.80	1.45f	2.82p	24.47	0.97	
3+4+5	0.00000	0.000	0.000	0.596	24.16	5.34f	179.38p	0.00		
3+4+5+i1	0.00000	0.000	0.000	0.596	24.16	5.34f	179.38p	0.00		
3+4+5+i1+i2	0.00189	0.000	0.000	0.596	26.70	5.58f	179.13p	0.00		
4+5+6	0.00000	0.000	0.000	0.596	67.17	9.22f	178.46p	0.00		
4+5+6+i1	0.00000	0.000	0.000	0.596	75.53	10.02f	178.11p	0.00		
4+5+6+i1+i2	0.00326	0.000	0.000	0.596	98.41	12.25f	177.52p	0.00		
5+6+7	0.00049	0.000	0.000	0.596	5.75	2.78f	179.73s	0.00		
5+6+7+i1	0.00000	0.000	0.000	0.596	593.97	64.60f	174.75p	0.00		
5+6+7+i1+i2	0.00556	0.000	0.000	0.596	624.26	69.22f	173.95p	0.00		
6+7+8	0.00000	0.000	0.000	0.596	-64.17	12.99a	177.46p	0.00		
6+7+8+i1	0.00000	0.000	0.000	0.596	-86.15	22.88a	175.95p	0.00		
6+7+8+i1+i2	0.00248	0.000	0.000	0.596	-87.41	23.44a	175.95p	0.00		
7+8+9	0.00100	0.000	0.000	0.596	-46.85	5.62a	178.85p	0.00		
7+8+9+i1	0.00032	0.000	0.000	0.596	-49.12	6.22a	178.15p	0.00		
7+8+9+i1+i2	0.00239	0.000	0.000	0.596	-49.12	6.22a	178.15p	0.00		
8+9+10	0.00550	0.864	0.005	0.601	20.82	1.12a	10.86p	15.05	0.33	
8+9+10+i1	0.00204	0.735	0.002	0.603	20.12	1.25a	11.10p	13.40	0.26	
8+9+10+i1+i2	0.00646	0.735	0.005	0.607	20.12	1.25a	11.10p	13.40	0.26	
9+10+11	0.00201	0.886	0.002	0.609	20.98	1.08a	10.46p	15.68	0.34	
9+10+11+i1	0.00219	0.793	0.002	0.611	17.37	1.86a	5.95p	15.41	0.27	
10+11+12	0.00249	1.000	0.002	0.613	25.52	0.08a	4.14p	29.03	1.22	
10+11+12+i1	0.00322	1.000	0.003	0.617	23.36	0.48a	5.21p	26.38	1.19	
11+12+13	0.00097	1.000	0.000	0.617	25.52	0.08a	4.14p	29.03	1.22	
11+12+13+i1	0.00322	1.000	0.002	0.619	24.58	0.25a	4.94p	27.47	1.16	
11+12+13+u1	0.00097	1.000	0.000	0.619	25.52	0.08a	4.14p	28.81	1.20	
11+12+13+u1+i1	0.00322	1.000	0.002	0.621	24.58	0.25a	4.94p	27.15	1.12	
3-division damage:				0.068	Probability of damage:				0.090	
1+2+3+4	0.01862	1.000	0.019	0.639	41.25	1.74f	2.96p	22.84	0.86	
2+3+4+5	0.00000	0.000	0.000	0.639	31.14	6.05f	179.30p	0.00		
2+3+4+5+i1	0.00000	0.000	0.000	0.639	31.14	6.05f	179.30p	0.00		
2+3+4+5+i1+i2	0.00080	0.000	0.000	0.639	34.69	6.39f	179.03p	0.00		
continued next page										

12/14/16 12:02:00 GHS 15.00		USCG - MSC, Washington, D.C. ELFARO321							Page 8 RUN2	
Divisions	P	Smin	P*S*V	A	Depth	Trim	Heel	Range	MaxRA	
7+8+9+10	0.00001	0.000	0.000	0.639	-46.85	5.62a	178.85p	0.00		
7+8+9+10+i1	0.00000	0.000	0.000	0.639	-53.65	7.38a	177.99p	0.00		
7+8+9+10+										
i1+i2	0.00137	0.000	0.000	0.639	-53.65	7.38a	177.99p	0.00		
8+9+10+11	0.00261	0.864	0.002	0.642	20.82	1.12a	10.86p	15.05	0.33	
8+9+10+11+										
i1	0.00091	0.617	0.001	0.642	17.19	1.88a	7.49p	12.58	0.20	
8+9+10+11+										
i1+i2	0.00362	0.617	0.002	0.644	17.19	1.88a	7.49p	12.58	0.20	
9+10+11+12	0.00149	0.649	0.001	0.645	20.44	1.14a	12.58p	12.00	0.23	
9+10+11+12+										
i1	0.00208	0.521	0.001	0.646	16.94	1.91a	8.14p	11.14	0.16	
10+11+12+13	0.00082	1.000	0.000	0.647	25.52	0.08a	4.14p	29.03	1.22	
10+11+12+										
13+i1	0.00285	1.000	0.001	0.648	23.36	0.48a	5.21p	26.38	1.19	
10+11+12+										
13+u1	0.00082	1.000	0.000	0.649	25.52	0.08a	4.14p	28.81	1.20	
10+11+12+										
13+u1+i1	0.00285	1.000	0.001	0.650	23.36	0.48a	5.21p	25.98	1.12	
4-division damage:				0.029	Probability of damage: 0.035					
7+8+9+10+11	0.00000	0.000	0.000	0.650	-46.85	5.62a	178.85p	0.00		
7+8+9+10+										
11+i1	0.00000	0.000	0.000	0.650	-64.92	10.59a	177.82p	0.00		
7+8+9+10+										
11+i1+i2	0.00052	0.000	0.000	0.650	-64.92	10.59a	177.82p	0.00		
8+9+10+11+										
12	0.00118	0.616	0.001	0.651	20.29	1.18a	12.79p	11.53	0.22	
8+9+10+11+										
12+i1	0.00039	0.333	0.000	0.651	16.75	1.93a	9.48p	8.18	0.09	
8+9+10+11+										
12+i1+i2	0.00236	0.333	0.001	0.652	16.75	1.93a	9.48p	8.18	0.09	
9+10+11+12+										
13	0.00040	0.649	0.000	0.652	20.44	1.14a	12.58p	12.00	0.23	
9+10+11+12+										
13+i1	0.00149	0.521	0.000	0.652	16.94	1.91a	8.14p	11.14	0.16	
9+10+11+12+										
13+u1	0.00040	0.179	0.000	0.652	19.82	1.21a	14.79p	4.85	0.04	
9+10+11+12+										
13+u1+i1	0.00149	0.000	0.000	0.652	-45.31	4.30a	179.45p	0.00		
5-division damage:				0.002	Probability of damage: 0.006					
8+9+10+11+										
12+13	0.00005	0.616	0.000	0.652	20.29	1.18a	12.79p	11.53	0.22	
8+9+10+11+										
12+13+i1	0.00000	0.333	0.000	0.652	16.75	1.93a	9.48p	8.18	0.09	
8+9+10+11+										
12+13+i1+										
i2	0.00092	0.333	0.000	0.652	16.75	1.93a	9.48p	8.18	0.09	
8+9+10+11+										
12+13+u1	0.00005	0.098	0.000	0.652	19.54	1.25a	15.47p	3.15	0.02	
continued next page										

12/14/16 12:02:00 GHS 15.00		USCG - MSC, Washington, D.C. ELFARO321						Page 9 RUN2	
Divisions	P	Smin	P*S*V	A	Depth	Trim	Heel	Range	MaxRA
8+9+10+11+ 12+13+u1+ i1	0.00000	0.000	0.000	0.652	-45.63	4.38a	179.30p	0.00	
8+9+10+11+ 12+13+u1+ i1+i2	0.00092	0.000	0.000	0.652	-45.63	4.38a	179.30p	0.00	
6-division damage:				0.000	Probability of damage: 0.001				
Attained index in this condition:				0.652	Total probability of damage: 0.984				
Required index:				0.602					
Distances in FEET.								Angles in deg.	